PHYSICAL INACTIVITY-INDUCED DYSREGULATION OF SKELETAL MUSCLE AND ADIPOSE TISSUE METABOLISM

A Dissertation
presented to
the Faculty of the Graduate School
University of Missouri-Columbia

In Partial Fulfillment
Of the Requirements for the Degree

Doctor of Philosophy

by

DAVID S KUMP

Frank W. Booth, Dissertation Supervisor
MAY 2005

The undersigned, appointed by the Dean of the Graduate School, have examined the dissertation entitled

PHYSICAL INACTIVITY-INDUCED DYSREGULATION OF SKELETAL MUSCLE AND ADIPOSE TISSUE METABOLISM

Presented by David S Kump

a candidate for the degree of Doctor of Philosophy

and hereby certify that in their opinion it is worthy of acceptance.

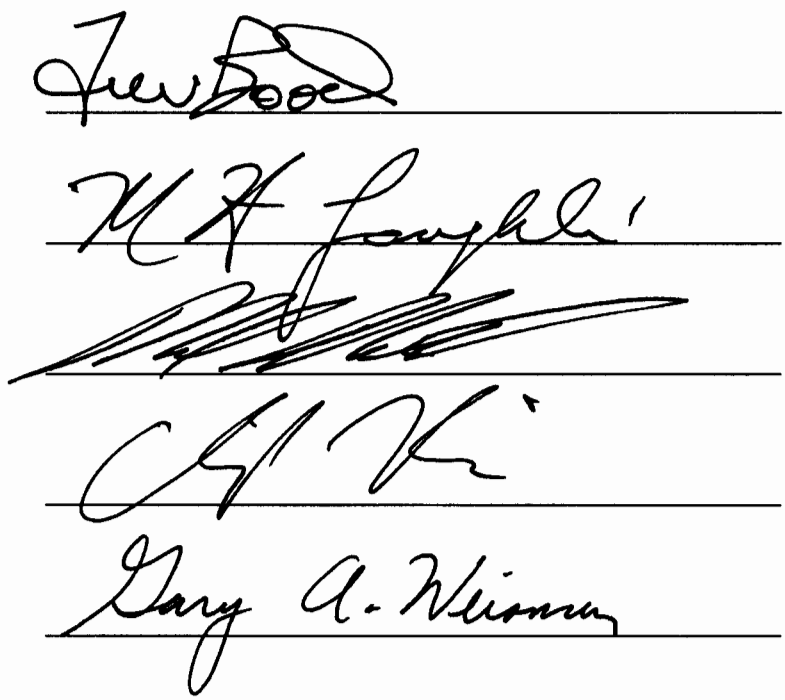

Acknowledgments

A dissertation cannot be completed alone. It would be impossible to acknowledge each individual that has contributed in some way. The staff and faculty of the Department of Medical Pharmacology and Physiology and the Department of Biomedical Sciences have been most helpful in taking care of many of the little things associated with everyday academic life. David Stock and Ron Marshall have helped in caring for animals and have prepared hundreds of cages and water bottles for me. Dr. John Holloszy permitted me to learn the 2-deoxyglucose uptake assay in his laboratory from two of his postdoctoral fellows, Drs. Lori Nolte and Jon Fischer. Dr. Holloszy also made several helpful comments early in the experimental design, as did Dr. Espen Spangenburg. My committee of Drs. Chris Hardin, Harold Laughlin, Mark Milanick, Gary Weisman, and formerly Michael Sturek has been extremely supportive, and their comments have strengthened my dissertation. Dr. Richard Madsen has provided invaluable statistical advice, and Dr. Boyd O'Dell permitted the use of the Coulter counter in his laboratory. I appreciate the help and support I have received from all of the members of the Booth lab, and want to especially recognize the contributions of Tsghe Abraha, whose inestimable technical and laboratory skills furthered my research. I thank the American Heart Association and those who give generously to it, as my research for these last two years has been partly funded

by an American Heart Association (Heartland chapter; 0135202Z) pre-doctoral fellowship.

There are not words to express the gratitude that I owe to Dr. Booth for allowing me to study with him for these last 5+ years. His passion and energy are infectious, and I am a better person in all aspects of life because of association with him. I appreciate his willingness to let me explore ideas and make decisions. His patience, guidance, support, and leadership have helped me develop into a better scientist.

Finally, it would not have been possible to pursue my doctoral degree without the love and support of my sweetheart Jennifer and our four children. Jennifer has served as our primary bread-winner and homemaker and has often been with the children alone as I have spent time in the laboratory, but has always been 100% supportive of me. I am thankful to be able to continue to receive that support in my future pursuits.

Table of Contents

ACKNOWLEDGMENTS ..... **II**

TABLE OF CONTENTS ..... **IV**

LIST OF TABLES ..... **XIV**

LIST OF FIGURES ..... **XV**

LIST OF ABBREVIATIONS ..... **XVIII**

ABSTRACT ..... **XX**

CHAPTER 1: INTRODUCTION **1**

INACTIVITY AND INSULIN RESISTANCE TO GLUCOSE UPTAKE 2

Insulin resistance to glucose uptake is associated with modern chronic diseases. *2*

Epidemiological studies demonstrate a strong independent relationship between physical inactivity and glucose intolerance *2*

Insulin sensitivity is lower in sedentary subjects than in physically trained subjects. *3*

Cumulative effects of repeated daily exercise training bouts have a larger impact on insulin sensitivity than the residual effects of a single exercise bout. *5*

Exercise-trained individuals who stop exercising show impaired indices of insulin action. *8*

ACTIVITY-RELATED CHANGES IN INSULIN SIGNALING 10

Insulin signaling with activity and inactivity in humans *11*

Activity-related changes in glucose uptake in animals *16*

Activity-related changes in skeletal muscle insulin signaling in animals. *19*

Glucose uptake into skeletal muscle and insulin signaling decrease upon training cessation *21*
OBESITY AND PHYSICAL INACTIVITY 24
Adiposity with cessation of physical training in humans *24*
Adiposity with cessation of physical training in animals *25*
Potential mechanisms governing the increase in fat mass upon reduced physical activity *26*
SPECIFIC AIMS 35
CHAPTER 2: EXPERIMENTAL DESIGN 38
BASIS OF THE EXPERIMENTAL DESIGN 38
DESCRIPTION OF THE EXPERIMENTAL GROUPS 39
HANDLING AND SACRIFICE OF ANIMALS 40
JUSTIFICATION OF THE DESIGN 40
Rat strain *40*
Rat gender *41*
Age to start running *42*
Duration of voluntary wheel training *42*
Duration of wheel lock/reduced physical activity *42*
Assignment of experimental groups *43*
Selection of exercise training model *44*
Protocols when access to running wheels is ended and prior to sacrifice ... *45*
Selection of the epitrochlearis muscle *46*
Selection of epididymal fat *46*
CHAPTER 3: ESTABLISHMENT OF METHODS 48
MEASUREMENT OF RUNNING ACTIVITY 48
RADIOACTIVITY 49
Counting of ^{125}I *49*
Counting of ^{3}H *49*
Dual label counting of ^{3}H and ^{14}C *50*

ASSAYS INVOLVING THE EPITROCHLEARIS MUSCLE 51
2-deoxyglucose uptake *51*
Insulin binding *54*
Immunoblotting *54*
Immunoprecipitation of the insulin receptor β-subunit *56*
Citrate synthase activity *57*
Glycogen content *57*
ASSAYS PERFORMED ON PLASMA 57
ASSAYS PERFORMED ON EPIDIDYMAL FAT 58
Adipocyte isolation *58*
Counting and sizing fat cells *58*
Immunoblotting *59*
2-Deoxyglucose uptake *59*
Enzyme activities *60*
Real-time polymerase chain reaction (PCR) *60*

CHAPTER 4: ALTERATIONS IN INSULIN RECEPTOR SIGNALING IN THE RAT EPITROCHLEARIS MUSCLE UPON CESSATION OF VOLUNTARY EXERCISE 62

INTRODUCTION 62
METHODS 64
Materials *64*
Animal protocol *65*
2-Deoxyglucose uptake *66*
Insulin binding *68*
Immunoblots and immunoprecipitations *68*
Citrate synthase activity *71*
Glycogen concentration *71*
Statistics *72*
RESULTS 73
2-Deoxyglucose uptake *73*

Insulin binding, insulin receptor protein level, and insulin receptor tyrosine phosphorylation *74*
PTP1B, SHP2, and PKCθ *76*
Akt, citrate synthase activity, glycogen concentration, and GLUT4 ..... *78*
DISCUSSION 79

CHAPTER 5: LOWER MUSCLE MASS IN RATS WITHOUT RUNNING WHEELS: GROWTH AND FOOD INTAKE COMPARISONS. 85

INTRODUCTION 85
METHODS 86
Animal protocol *86*
Statistics *88*
RESULTS 90
Running activity *90*
Growth rate *91*
Food intake *95*
Skeletal and left ventricular muscle mass *98*
DISCUSSION 99
Growth rate and food intake *99*
Skeletal muscle mass *101*
Clinical relevance *103*
Summary *104*

CHAPTER 6: SUSTAINED RISE IN TRIACYLGLYCEROL SYNTHESIS PRECEDES INCREASED EPIDIDYMAL FAT MASS WHEN RATS CEASE VOLUNTARY WHEEL RUNNING 105

INTRODUCTION 105
METHODS 106
Materials *106*
Animal protocol *107*
Adipocyte isolation *109*

Adipocyte size and number *109*
Cellular lipid content *110*
2-Deoxyglucose uptake *111*
Triacylglycerol synthesis *111*
Immunoblots *113*
Plasma assays *113*
Statistics *114*
RESULTS 114
Adipose mass and cellularity *114*
Plasma analytes *116*
2-Deoxyglucose uptake *117*
Triacylglycerol synthesis *117*
Immunoblots *118*
DISCUSSION 118
Epididymal adipose tissue mass and cellularity *119*
Plasma triacylglycerol *121*
2-Deoxyglucose uptake into isolated epididymal adipocytes *122*
Epididymal fat triacylglycerol synthesis *122*
PPARγ and C/EBPα protein levels *125*
Food intake *126*
Clinical significance *126*
Conclusion *128*

CHAPTER 7: INCREASED GLYCEROL-3-PHOSPHATE ACYLTRANSFERASE PROTEIN LEVEL AND ENZYME ACTIVITY IN RAT EPIDIDYMAL FAT UPON CESSATION OF WHEEL RUNNING 129

INTRODUCTION 129
METHODS 131
Materials *131*
21 days of voluntary running *132*
One-day (acute) physical activity *132*

Enzyme activity *135*
Immunoblots *136*
Real-time PCR *137*
Statistics *137*
RESULTS 138
Triacylglycerol synthesis following one-day (acute) physical activity *138*
GPAT and DGAT enzyme activities upon cessation of 21 days of voluntary running *140*
Mitochondrial GPAT protein level *141*
Mitochondrial GPAT mRNA upon cessation of 21 days of voluntary running *141*
SREBP-1, nuclear factor Y-β, CBP, and Sp1 protein levels *143*
AMPK Thr^{172} phosphorylation *143*
Casein kinase II-α *147*
DISCUSSION 147
More than a single day of physical activity is needed to produce the physical inactivity-induced overshoot in triacylglycerol synthesis. *148*
Mitochondrial GPAT activity and protein increase, but its mRNA does not change *149*
Post-transcriptional regulation of mitochondrial GPAT activity *153*
Summary and conclusions *155*

CHAPTER 8: DISCUSSION 157

CHAPTER 9: REFERENCES 161

APPENDIX A: PRELIMINARY DATA: 2-D GEL PROTEOMIC ANALYSIS OF PROTEINS SECRETED BY ADIPOSE TISSUE AND SKELETAL MUSCLE AND THE EFFECT OF REDUCED PHYSICAL ACTIVITY 195

INTRODUCTION 195
METHODS 196
Conditioning media with adipose tissue fragments *196*

Conditioning media with epitrochlearis or split soleus muscle *197*
Lactate dehydrogenase (LDH) activity *197*
RESULTS AND DISCUSSION 198

APPENDIX B: PRELIMINARY DATA: THE EFFECT OF 83 WEEKS OF VOLUNTARY WHEEL RUNNING ON ADIPOSE CELLULARITY IN FEMALE RATS 200

APPENDIX B: PRELIMINARY DATA: THE EFFECT OF 83 WEEKS OF VOLUNTARY WHEEL RUNNING ON ADIPOSE CELLULARITY IN FEMALE RATS 201

METHODS 201
RESULTS 203
RESULTS 204
CONCLUSIONS 205

APPENDIX C: DETAILED PROTOCOLS 207

2-DOG TRANSPORT IN ISOLATED SKELETAL MUSCLE 207
Protocol *207*
Solutions *217*
INSULIN BINDING IN EPITROCHLEARIS MUSCLE 221
Protocol *221*
Solutions *225*
EPITROCHLEARIS HOMOGENIZATION PROTOCOL/BRADFORD ASSAY 228
Protocol *228*
Bradford assay *230*
Aliquot samples *234*
Solutions *235*
SDS-PAGE/IMMUNOBLOT 240
SDS-PAGE Protocol *240*
Transfer *249*
Immunoblotting *252*

Stripping protocol *253*
Solutions *255*
Protocols for different antibodies for use on immunoblots for epitrochlearis muscle *266*
Protocols for different antibodies for use on immunoblots for epididymal fat *270*
IMMUNOPRECIPITATION PROTOCOL FOR THE INSULIN RECEPTOR B-SUBUNIT 273
Notes *273*
Protocol *273*
Solutions *276*
RUBPS GEL STAINING 283
Protocol *283*
Solutions *284*
CITRATE SYNTHASE ACTIVITY ASSAY 286
Protocol *286*
Solutions *289*
GLYCOGEN ASSAY 291
Protocol *291*
Solutions *296*
ISOLATION OF RAT PRIMARY ADIPOCYTES 298
Protocol *298*
Solutions *303*
OIL RED O STAINING OF PRIMARY ADIPCOYTES 304
Protocol *304*
Solutions *306*
CELL VIABILITY ASSAY FOR PRIMARY ADIPOCYTES 307
2-DEOXYGLUCOSE UPTAKE IN PRIMARY RAT ADIPOCYTES 308
Protocol *308*
Solutions *315*
CELLULARITY PROTOCOL FOR ISOLATED ADIPOCYTES 318

Protocol on day of sacrifice *318*
Preparation of the sample for counting and sizing *318*
Solutions *320*
COULTER COUNTER PROTOCOL FOR COUNTING AND SIZING FIXED ADIPOCYTES .. 321
Protocol *321*
Use of the Coulter counter *322*
Solutions *330*
COULTER COUNTER DATA ANALYSIS 330
LIPID CONTENT PROTOCOL 332
Protocol *332*
Solutions *333*
HOMOGENIZATION OF FAT 334
Protocol *334*
Alternative fat cake protocol *337*
Solutions *338*
CB-X PROTEIN ASSAY 342
PALMITIC ACID INCORPORATION INTO TRIACYLGLYCEROL 343
Protocol *343*
Solutions *349*
GLYCEROL-3-PHOSPHATE ACYLTRANSFERASE ACTIVITY 357
Protocol *357*
Solutions *363*
DIACYLGLYCEROL ACYLTRANSFERASE ACTIVITY 371
Protocol *371*
Solutions *376*
CONDITIONING MEDIA WITH ADIPOSE TISSUE FRAGMENTS 384
Protocol *384*
Solutions *386*
CONDITIONING MEDIA WITH MUSCLE 388
Protocol *388*

Solutions *390*
LDH ACTIVITY (TYPE H) 391
Protocol *391*
Solutions *393*
LDH ACTIVITY (TYPE M) 395
Protocol *395*
Solutions *397*
PREPARATION OF PLASMA OR SERUM 399
PLASMA TRIACYLGLYCEROL AND GLYCEROL 399
PLASMA GLUCOSE 401
PLASMA FREE FATTY ACIDS 402
PLASMA INSULIN 403
VITA 406

List of Tables

Table 1. Directional changes in groups having wheels locked for 29 or 53 hours and in sedentary group relative to 5 hours of wheel lock. 81

Table 2. Comparison of body mass, growth, running activity and food intake variables across all groups..... 91

List of Figures

Figure 1. Experimental design. 39

Figure 2. Energy spectra for ^{3}H and ^{14}C 50

Figure 3. Quench-efficiency curves for dual scintillation counting of ^{3}H and ^{14}C…. 50

Figure 4. Insulin binding preliminary control experiments. 54

Figure 5. Example of linearity with immunoblotting technique. 55

Figure 6. Linearity of lipid content assay with packed cell volume. 58

Figure 7. Lineweaver-Burk plot of triacylglycerol synthesis with variable ATP concentration. 60

Figure 8. Effect of reduced physical activity on 2-deoxyglucose uptake into isolated epitrochlearis muscle under basal, submaximal insulin, and maximal insulin-stimulated conditions. 73

Figure 9. Effect of decreased physical activity on descriptive indices of the insulin receptor and its activation in epitrochlearis muscle..... 75

Figure 10. Effect of decreased physical activity on negative regulators of insulin receptor activation in epitrochlearis muscle. 76

Figure 11. Effect of reduced physical activity on the interaction of PTP1B, SHP2, and PKCθ with IRβ. 78

Figure 12. Biochemical adaptations to decreased physical activity in the epitrochlearis muscle. 80

Figure 13. Running activity and relationship to initial body mass. 92

Figure 14. Growth characteristics. 94

Figure 15. Relationship between 21-day total running distance and fold-increase in body mass. 95

Figure 16. Food consumption. 97

Figure 17. Skeletal muscle mass increases with voluntary wheel running. 99

Figure 18. Adipose mass and cellularity. 115

Figure 19. Effect of reduced physical activity on various plasma analytes. 117

Figure 20. 2-Deoxyglucose uptake into isolated epididymal adipocytes. 118

Figure 21. Effect of reduced physical activity on triacylglycerol synthesis in epididymal fat. 118

Figure 22 The effect of voluntary wheel running on PPARγ and C/EBPα protein levels in epididymal fat. 119

Figure 23. Triacylglycerol synthesis in epididymal fat homogenates following one-day (acute) physical activity. 139

Figure 24. GPAT and DGAT activities in epididymal fat homogenates upon cessation of 21 days of voluntary wheel running. 141

Figure 25. Mitochondrial GPAT protein level in epididymal fat upon cessation of 21 days of voluntary wheel running and following one-day (acute) physical activity. 142

Figure 26. 18S and mitochondrial GPAT mRNA expression upon cessation of 21 days of voluntary wheel running. 142

Figure 27. Protein levels of SREBP-1, CBP, nuclear factor Y-β, and Sp1 upon cessation of 21 days of voluntary wheel running. 144

Figure 28. AMPK-α Thr172 phosphorylation, total AMPK-α protein levels, ratio of AMPK-α Thr172 phosphorylation to total AMPK-α protein, and acetyl coenzyme A carboxylase Ser79 phosphorylation. 145

Figure 29. Casein kinase II-α protein levels upon cessation of 21 days of voluntary wheel running. 147

Figure 30. LDH activity over time in media conditioned by skeletal muscle or epididymal adipose tissue fragments. 198

Figure 31. Protein concentration over time in media conditioned by skeletal muscle or epididymal adipose tissue fragments. 198

Figure 32. Protein concentration in media conditioned by split soleus..... 199

Figure 33. 2-D gel of soleus-conditioned media..... 200

Figure 34. Weekly running distance for 83 weeks for female rats with voluntary running wheels..... 201

Figure 35. Growth curve of female rats with or without running wheels. 202

Figure 36. Absolute and relative food consumption in female rats with or without running wheels..... 203

Figure 37. Ovarian fat mass and cellularity in female rats with or without 83 weeks of running wheel access. 204

List of Abbreviations

AMPK-α, adenosine 5'-monophosphate-activated kinase-α

ANOVA, analysis of variance

ATP, adenosine 5'-triphosphate

BM, body mass

BSA, bovine serum albumin

C/EBPα, CCAAT/enhancer binding protein-α

CBP, cyclic AMP enhancer element binding protein

DGAT, 1,2-Diacylglycerol:acyl coenzyme A acyltransferase

DNA, deoxyribonucleic acid

dpm, disintegrations per minute

EDTA, ethylenediaminetetraacetic acid tetrasodium dehydrate

EGTA, ethylene glycol-bis-N,N,N',N'-tetraacetic acid

FBN, Fischer 344 X Brown Norway F1 generation hybrid rat strain

GLUT1, glucose transporter 1

GLUT4, glucose transporter 4

GPAT, acyl coenzyme A:glycerol-*sn*-3-phosphate acyltransferase, or glycerol-3-phosphate acyltransferase

HBS, HEPES-buffered saline

HEPES, (N-[2-hydroxyethyl]popeerazine-N'-[2-ethanesulfonic acid])

HRP, horseradish peroxidase

IB, immunoblot

IP, immunoprecipitation

IRS, insulin receptor substrate

IRβ, insulin receptor β-subunit

KHB, Krebs-Henseleit buffer

KRHB, Krebs-Ringer-HEPES buffer

LDH, lactate dehydrogenase

mRNA, messenger ribonucleic acid

NAD^+, β-nicotinamide adenine dinucleotide

NADH, β-nicotinamide adenine dinucleotide, reduced form

PBS, phosphate-buffered saline

PCR, polymerase chain reaction

PI3K, phosphoinositide-3 kinase

PPARγ, peroxisome proliferators-activated receptor-γ

PTP1B, protein tyrosine phosphatase 1B

RNA, ribonucleic acid

SEM, standard error of the mean

SHP2, src homology phosphatase-2

SREBP-1, sterol regulatory element binding protein-1

VRW, voluntary running wheels

VWR, voluntary wheel running

PHYSICAL INACTIVITY-INDUCED DYSREGULATION OF SKELETAL MUSCLE AND ADIPOSE TISSUE METABOLISM

David S Kump

Dr. Frank W. Booth, Dissertation Supervisor

ABSTRACT

There has been a precipitous decline in the daily physical activity in humans that has been accompanied by an epidemic rise in the incidence of obesity and type II diabetes. This rapid decline in physical activity in humans was simulated using a rat model where male rats that were physically active on voluntary running wheels for 21 days had their running wheels locked for 5-53 hours. During this time frame (between 5 and 53 hours of reduced physical activity), there is decreased insulin sensitivity in the epitrochlearis muscle, an increase in the mass of the epididymal and omental fat depots, and an increase in the size of epididymal adipocytes. In the epitrochlearis muscle, there was a decrease in multiple descriptive indices of insulin receptor activation that was associated with the decreased insulin sensitivity. In epididymal fat, there was an increase in triacylglycerol synthesis above that of animals that did not have access to running wheels; this was paralleled by an increase in the enzyme

activity of mitochondrial glycerol-3-phosphate acyltransferase (GPAT), a key regulatory point in the triacylglycerol synthesis pathway. An increase in mitochondrial GPAT protein is at least partly responsible for the increased enzyme activity. These studies provide a seminal foundation of mechanistic insights on how reduced physical activity elicits physiological changes that are commonly associated with common modern chronic diseases.

Chapter 1: Introduction

Throughout history, humans have been physically active. In recent decades, there has been a precipitous decline in the amount of daily physical activity (22; 30; 71; 182). This decline has been accompanied by an epidemic increase in type II diabetes (216), obesity (82; 225), and some site-specific cancers (174); the relationship between physical inactivity and these modern chronic diseases has been extensively reviewed (22; 23; 238). Despite a preponderance of epidemiological evidence supporting a cause-and-effect connection between decreased physical inactivity and chronic disease, a molecular link has proved elusive. The studies detailed in this paper begin to uncover some of the biochemical and cellular mechanisms by which a decrease in physical inactivity can produce decreased skeletal muscle insulin sensitivity and increased intraabdominal fat, two hallmark characteristics common to physical inactivity, insulin resistance, and obesity (109; 168; 189; 267).

INACTIVITY AND INSULIN RESISTANCE TO GLUCOSE UPTAKE

Insulin resistance to glucose uptake is associated with modern chronic diseases.

Insulin resistance occurs when physiological levels of insulin produce a subnormal response (140); it is commonly associated with sedentary lifestyle and obesity, and it increases the risk of the chronic health disorders hypertension, dyslipidemia, endothelial dysfunction, and cardiovascular disease (230), and has been suggested as an independent risk factor for cardiovascular disease (1). Using 1988-1994 NHANES data, one study indicates that at least 25% of the U.S. population is already suffering from these chronic health disorders in conjunction with insulin resistance (85). Insulin resistance to glucose uptake is a necessary precursor to type II diabetes (1; 16) and the strongest risk factor for predicting future occurrence of type II diabetes (298). There is a particularly strong relationship between intraabdominal fat and insulin resistance (34; 63; 88; 91; 141; 214; 228; 287; 294).

Epidemiological studies demonstrate a strong independent relationship between physical inactivity and glucose intolerance.

A sedentary lifestyle impairs insulin-stimulated glucose uptake. This concept is supported by a number of epidemiological and clinical studies demonstrating a clear relationship between physical inactivity and indices of

insulin-stimulated glucose disposal. Epidemiological evidence includes a strong correlation between self-reported hours of *in*activity and an index of insulin resistance [product of fasting insulin and glucose; (99)]. Another study indicated that low habitual physical activity in Pima Indians is predictive of future glucose intolerance (161). In Mauritius, glucose intolerance was increased with self-reported inactivity, and physical inactivity was a strong independent predictor of glucose intolerance even after controlling for body mass index, waist-to-hip ratio, age, and family history of type II diabetes (222). These results were confirmed by a large cross-sectional study reporting significantly impaired insulin sensitivity measured during an intravenous glucose tolerance test in individuals that were not involved in regular vigorous or non-vigorous physical activity; this relationship remained significant after controlling for percent body fat and fat distribution (183). Because these latter two studies controlled for body fat, it indicates that the deleterious effect of physical inactivity on insulin action and glucose tolerance is largely independent of alterations in the amount or distribution of body fat.

Insulin sensitivity is lower in sedentary subjects than in physically trained subjects.

- Using the hyperinsulinemic, euglycemic clamp technique, Kirwan *et al*. (152) showed that aerobically trained young men and women had an ~35% greater glucose disposal rate than sedentary subjects.
- Regular vigorous exercise (average of 8 miles/day running or 19 miles/day of cycling during the previous 11 years) prevented the

deterioration of glucose tolerance and insulin sensitivity with aging in 60-year-old masters athletes (256). Compared to the 60-year-old athletes, the total area under the insulin curve during an oral glucose tolerance test was 2.5-fold greater in untrained 28-year-old men, while the glucose area under the curve was the same. In a comparison among 60-year-old men, the total area under the insulin curve during a glucose tolerance test was 6-fold higher in 62-year-old untrained non-lean men and 2.5-fold higher in 61-year-old untrained lean men than in the 60-year-old masters athletes. Both untrained 60^{+}-year-old groups had twice the area under the glucose tolerance curve than did the masters athletes (256).

- Older (50-80 years old) and younger (21-35 years old) endurance-trained subjects had approximately twice the insulin sensitivity as age-matched sedentary counterparts. When the age groups were subdivided into smaller groups that were matched for percent body fat, this relationship remained unchanged (47).
- The amount of glucose infused to maintain euglycemia during the last thirty minutes of a two-hour hyperinsulinemic, euglycemic clamp increased 26% following seven days of training on a cycle ergometer in young subjects as compared to their sedentary values prior to training. Fasting insulin and glucose did not differ (128).

- Previously sedentary young (20-37 years old) subjects who underwent seven days of exercise training improved their insulin sensitivity 33% as measured by an intravenous glucose tolerance test (313).
- When previously sedentary 50-70-yr-old men exercised seven days on cycle ergometer, insulin action, the M-value (the ratio of whole body glucose disposal to steady state insulin levels) increased 33% during a hyperinsulinemic, euglycemic clamp (278).
- A 6-week exercise-training program improved whole-body insulin sensitivity (hyperglycemic-hyperinsulinemic clamp technique) by 40 % in both the adult children of parents with type II diabetes and normal subjects (223).

Cumulative effects of repeated daily exercise training bouts have a larger impact on insulin sensitivity than the residual effects of a single exercise bout.

There is a well-documented transient increase in skeletal muscle glucose uptake that occurs following a single bout of exercise [reviewed in (96)]. This increase is accompanied by an increase in sensitivity to insulin as shown by glucose tolerance tests or hyperinsulinemic, euglycemic clamps (20; 65; 185; 186; 237). This raises the question of whether increases in insulin sensitivity with exercise training are due to the effect of the last exercise bout or whether there is an effect of exercise training. The literature reviewed below supports the notion

that exercise-trained individuals have an increased insulin sensitivity that is independent of the acute effect of the last exercise bout:

- Twelve hours following the end of an exercise bout, trained subjects had a 2-fold greater glucose clearance than untrained subjects as measured by the euglycemic clamp technique. Sixty hours following the exercise bout, the trained subjects had a 29% greater glucose clearance. Fasting plasma insulin doubled at the seventh day of detraining from the values at 12- and 60-hours post-exercise (33).
- Young *et al*. (312) showed that the insulin area under the curve for a single bout of exercise in aerobically trained individuals did not differ whether the exercise bout was performed 14 or 40 hours prior to an oral glucose tolerance test, whereas in non-trained subjects the insulin area under the curve doubled from 14 to 40 hrs post exercise. The authors (312) wrote that this finding suggests that the cumulative effects of regularly performed exercise are more important than the residual effects of any single exercise bout in maintaining the improved glucose tolerance and enhanced insulin sensitivity associated with the trained state.
- Endurance-trained subjects who stopped exercising for 10 days had greater plasma glucose and insulin levels during a glucose tolerance test. Although one bout of exercise improved their insulin sensitivity, the sum and pattern of the insulin responses did not return to the trained level, indicating that regularly performed exercise had a greater

effect on lowering the insulin response to a glucose load than did a single bout of exercise (96; 111).

- In a novel study (60), young male subjects trained one leg on a cycle ergometer for six weeks, after which a three-step hyperinsulinemic, euglycemic clamp was performed in conjunction with measurement of arteriovenous differences across the thigh. Sixteen hours following the last exercise bout, there was no difference in glucose uptake between the trained and untrained leg under basal conditions. Under both physiological and maximally effective insulin concentrations, glucose uptake in the trained leg was significantly higher. Following six days of no exercise, the subjects exercised their untrained leg sixteen hours prior to repeating the glucose clamp. Interestingly, glucose uptake in the trained leg did not differ following six days of inactivity, nor did glucose uptake in the untrained leg increase despite having exercised sixteen hours prior. This study shows four things: 1) skeletal muscle glucose uptake remains at trained levels for at least six days following the onset of inactivity, 2) one bout of exercise is insufficient to increase insulin-stimulated glucose uptake at sixteen hours post-exercise, 3) in regards to insulin-stimulated glucose uptake, the muscular adaptation to training only occurs in the trained muscle, and 4) the effects of repeatedly performed exercise are greater than the effects of a single exercise bout.

In sum, these studies show that once the acute effect of exercise has dissipated, insulin sensitivity in trained subjects remains higher than in untrained subjects. This provides evidence for a training effect of enhanced insulin sensitivity from repeated bouts of exercise that is independent of the increased insulin sensitivity following a single exercise bout, i.e. habitual exercise results in a persistent increase in insulin-stimulated glucose disposal, whereas a single bout does not. In terms of physical inactivity lasting for days, this means that decreases in insulin-stimulated glucose uptake that occur with the onset of physical inactivity in trained individuals are due to the cessation of exercise training and not to the disappearance of an effect from the last training bout.

Exercise-trained individuals who stop exercising show impaired indices of insulin action.

- The areas under the glucose and insulin curves during an oral glucose tolerance test increased 65% and 73%, respectively, in endurance-trained men 7 days after ending training (8).
- 14 days after ceasing either endurance- or resistance-oriented training, insulin sensitivity during an oral glucose tolerance test decreased 24% and 16%, respectively, without any change in total GLUT-4 protein content in human skeletal muscle (129).
- Endurance-trained triathletes had a lower area under the insulin curve than untrained subjects, but following 10 days of inactivity, the area

under the curve had significantly decreased to the level of the untrained subjects (184).

- 10 days of no exercise caused 28-year-old endurance-trained subjects to have increased areas under the glucose and insulin curves during an oral glucose tolerance test. Maximal oxygen consumption, body mass, and skinfold measurements did not change during the 10 days of physical inactivity (111).
- Masters athletes (average age of 61) split into two response groups for glucose tolerance after 10 days of detraining. Ten of the masters athletes retained glucose tolerance by increasing the area under the insulin curve by 67% during an oral glucose tolerance test. Four other of the masters athletes had a doubling of the areas under both the glucose and insulin curves during an oral glucose tolerance test; two of them achieved clinical data sufficient to be classified as having pre-diabetes (244). This provides strong evidence that in some older individuals, short-term physical inactivity can initiate a clinical diagnosis.
- Fourteen hours after exercise, trained male athletes had a 54% higher glucose disposal rate than a sedentary group, but 38 hours, 86 hours, or 6 days following the last exercise bout, glucose disposal decreased so that it was no longer greater than the sedentary group (212).
- Endurance-trained subjects who stopped exercising for 10 days showed a decrease in glucose disposal rate at physiological insulin

levels, but not at maximally effective insulin levels relative to 15 hours following the last training bout (151).

- Endurance-trained subjects underwent a hyperinsulinemic, euglycemic clamp both 15 hours and 5 days following the last exercise bout. Insulin required for 50% of the maximal glucose uptake increased ~23% following 5 days of inactivity to levels similar to sedentary subjects. However, in response to a concentration of insulin that was close to maximum effectiveness, glucose uptake did not change and was higher than that found in sedentary subjects (186; 187).

The results of these last 2 studies (186; 187) show that insulin sensitivity decreases to sedentary levels in as little as 5 days following the cessation of training. The latter three studies (151; 186; 187) also provide some evidence that the initial decrease in insulin-stimulated glucose disposal might occur with physiological insulin concentrations, but not with maximally effective insulin concentrations.

ACTIVITY-RELATED CHANGES IN INSULIN SIGNALING

The preceding sections summarize evidence that the onset of physical inactivity in previously active individuals causes a decline in insulin-stimulated glucose disposal. Despite the clear relationship between physical inactivity, insulin resistance, and disease, there are few studies examining the cellular changes by which physical inactivity might signal decreased insulin-stimulated glucose disposal.

Insulin signaling with activity and inactivity in humans

OVERVIEW OF INSULIN SIGNALING TO GLUCOSE UPTAKE. Glucose clearance in response to insulin occurs by increasing glucose uptake into insulin-sensitive tissues and by suppressing hepatic glucose output. Although increased hepatic glucose output can delay glucose clearance, glucose removal is more important quantitatively for glucose clearance (15; 58; 142). Muscle and fat are quantitatively the major insulin-sensitive tissues that increase uptake of blood glucose in response to insulin, with skeletal muscle estimated to account for 75-95% of insulin-stimulated glucose disposal (15; 58; 142). Thus, skeletal muscle is the primary tissue for insulin-mediated blood glucose disposal. In type II muscle, glucose uptake to the cell's interior is rate-limiting for glucose uptake (104; 231).

Insulin signaling to glucose uptake into skeletal muscle and adipose tissue begins with insulin binding to its cognitive heterodimer receptor on the external α subunit, inducing autophosphorylation of multiple tyrosine residues on the intracellular β subunit. A phosphorylation cascade then proceeds, with the insulin receptor phosphorylating insulin receptor substrate (IRS, primarily IRS-1 in muscle). IRS-1 phosphorylates phosphoinositide-3 kinase (PI3K), resulting in the phosphorylation of Akt, protein kinase C-ξ, and protein kinase C-λ. Although intermediate steps remain unknown, this cascade results in the translocation of the insulin-sensitive glucose transporter GLUT4 (glucose transporter-4) from an intracellular vesicular pool to the t-tubules and sarcolemma. Insulin-stimulated

glucose transport increases in direct proportion to the amount of GLUT4 protein found at the cell surface in skeletal muscle. In skeletal muscle in the absence of insulin, only the GLUT1 glucose transporter is found at the cell surface and is responsible for basal glucose uptake (206; 303). There is also an additional IRS-independent pathway that appears to be responsible for the docking and fusion of the GLUT4-containing vesicles, but the details of this pathway are still being elucidated (249).

INSULIN SIGNALING IN SKELETAL MUSCLE IS ENHANCED WITH EXERCISE TRAINING. It is well established that contractile activity in skeletal muscle stimulates GLUT4 translation to the cell surface membrane independent of proximal insulin signaling, leading to increased glucose uptake in both trained and untrained individuals [reviewed in (96)]. As previously explained (see Inactivity and Insulin Resistance to Glucose Uptake), once this acute response to exercise disappears, there is a persistent increase in insulin sensitivity in exercise-trained individuals that does not occur in untrained individuals. Because the studies reported herein deal primarily with the effect of chronic physical activity as opposed to acute physical activity, only those studies that are concerned with insulin signaling during the persistent increase in insulin sensitivity will be reviewed.

The mechanisms that cause the improvement in insulin-stimulated glucose disposal in exercise-trained individuals are likely multifaceted. Suggestions include an increase in the number and function of glucose transporters, increased muscle capillary density (which will increase glucose and

insulin delivery to the muscle), increased muscle enzyme activity and muscle oxidative capacity, increased GLUT4 translocation, and enhanced insulin signaling (96; 153; 223). Most of the aforementioned possible mechanisms (capillary density, muscle oxidative capacity, muscle enzyme activity) are longer term adaptations that would require days to occur (122; 192; 193; 250), distinguishing them from the acute and immediate post-exercise increase in insulin sensitivity. Several studies have examined the alterations in insulin signaling that occur with exercise training:

- Nine days of endurance training in previously sedentary men aged 29 yrs did not increase insulin receptor or IRS-1 mRNA levels at 3 hours post-exercise, but did increase the mRNA levels for the p85α subunit of PI3K (293).
- A longer term exercise program in which the subjects ran 47 km/week for more than two months resulted in decreases of 44%, 57%, and 70% in insulin receptor, IRS-1, and IRS-2 protein levels, respectively in the vastus lateralis muscle in trained vs. untrained subjects (314). It is unknown whether there is enhanced signaling through the insulin receptor. In reference to this data, Zierath (319) concluded that improvements in insulin action that occur with exercise training are due to "…more efficient signaling".
- In support of Zierath's conclusion (319), 7 days of training increased insulin-stimulated autophosphorylation of the insulin receptor by 40% in vastus lateralis biopsies at both physiological and maximally

effective insulin concentrations; the increased insulin receptor autophosphorylation was associated with enhanced insulin sensitivity (313). Youngren *et al.* (313) comment that the exact mechanisms whereby insulin receptor signaling is improved with exercise remain unknown.

- After 7 days of exercise training in previously sedentary men (average age 58), phosphotyrosine-associated PI3K activity and Akt activity were unchanged at ~16 hours following the last exercise session compared to pre-training values, despite increased insulin action on whole body glucose uptake (278).
- 7 days of cycle ergometer training in previously sedentary young men resulted in a 3.1-fold increase in insulin-stimulated vastus lateralis phosphotyrosine-associated PI3K activity at ~16 hours following the last exercise bout relative to pre-training levels. Basal PI3K activity was unaffected by exercise (128). The reason for the difference with the previous study (278) is unclear, but may be due to differences in the age of the subjects.
- Individuals with a high level of physical conditioning had greater insulin-stimulated IRS-1-associated PI3K activation in skeletal muscle during hyperinsulinemia; this increase was positively correlated with an increase in insulin-stimulated glucose disposal (152).

Much attention has been given to GLUT4. Several studies show that total GLUT4 (both cell surface and intracellular) protein level in skeletal muscle

increases with exercise training. It is higher in endurance-trained than in sedentary middle-aged men (127), and it increases in both normal subjects (61; 129; 201) and those with impaired glucose tolerance (132) in response to exercise training. When measured at 48 hours post-exercise in trained men, total GLUT4 protein level was twice as high as in untrained men (314). With the onset of physical inactivity, total GLUT4 protein decreases toward sedentary levels. However, not all sources agree on the time course of a decrease in GLUT4 protein with the cessation of exercise training:

- In young endurance-trained triathletes, total GLUT4 protein level was ~2.5-fold higher in vastus lateralis muscle biopsies relative to untrained subjects, but following 10 days of inactivity in the athletes, there was no difference. This decrease in total GLUT4 protein corresponded to an increase under the insulin curve during an oral glucose tolerance test (184).
- Six weeks of treadmill exercise led to a 1.4- and 1.7-fold increase in GLUT4 protein level in the soleus and red vastus lateralis in previously untrained individuals; this increase had reversed to near pre-training values after 7 days without exercise (201).
- In 48-year-old previously sedentary subjects trained for 12 weeks, 14 days of no exercise resulted in a decrease in muscle total GLUT4 protein level of 71% and a decrease in the insulin sensitivity index of 54% from the trained values. Subjects who maintained 50% of their

previous training level for the 14 days did not show a decrease from the trained level (130).

- In contrast, Houmard *et al*. (129) studied both endurance-trained and strength-trained subjects both during training and following 14 days without training. The area under the insulin curve increased during an oral glucose tolerance test for both groups, but there was no change in total GLUT4 protein level for either group even after fourteen days of inactivity.
- Another study also shows a slower rate of decline: following 6 days of no exercise in previously endurance-trained subjects, muscle total GLUT4 protein levels had decreased 17% from their trained values and glucose disposal rates had decreased 29% and 14% at submaximal and maximal insulin infusions during hyperinsulinemic glycemic clamps from their trained values (291).

Although the latter two studies (129; 291) disagree with the previous two (130; 184), these studies demonstrate that with the onset of inactivity, a decrease in insulin action on glucose uptake may take place despite the maintenance of total GLUT4 protein, indicating a defect at some other point in the insulin signaling pathway to glucose uptake.

Activity-related changes in glucose uptake in animals

Like humans, exercise-trained rats also have improved insulin sensitivity that is rapidly lost with the onset of physical inactivity. Effects of exercise training

in animal models will be emphasized in those studies using voluntary running wheels for exercise training of rats:

VOLUNTARY WHEEL RUNNING

- A study by Mondon *et al*. (190) compared insulin sensitivity of perfused liver and hindlimb muscle from rats following 3 to 4 months of voluntary wheel running. Insulin-stimulated glucose clearance by the liver in the fed state was 65% lower in trained rats relative to sedentary controls, and it was >50% lower in the fasted state. In contrast, glucose clearance by hindlimb muscle in the fed state was increased 17% with no insulin and increased 43% with a physiological insulin concentration (40 μU/ml). In the fasted state, basal glucose clearance by hindlimb muscle was increased 57% with no insulin and 97% at a physiological insulin concentration. These findings led the authors to state "…skeletal muscle…is the organ primarily responsible for the increased sensitivity to insulin-induced glucose uptake with exercise training and that this response is enhanced after overnight fasting" (190).
- After 5 weeks of voluntary wheel running, maximal insulin stimulated glucose transport into the epitrochlearis muscle and total muscle GLUT4 protein level were increased 63% and 51%, respectively, compared to sedentary controls while basal transport (no insulin) was unchanged (241).

- After 3 weeks of voluntary wheel running, both submaximal and maximal insulin-stimulated 2-deoxyglucose transport rates into the epitrochlearis muscle were significantly enhanced by 71 and 70%, respectively, compared with those of sedentary controls (121).
- Studies using unilateral electrical stimulation of rat hindlimb muscle show that the increase in insulin-stimulated 2-deoxyglucose and 3-*O*-methylglucose transport in muscle are isolated to the contracting limb (236), suggesting that local contractile activity is responsible for the exercise-induced increases in insulin-stimulated glucose uptake.

ACUTE EXERCISE

- Basal (non-insulin-stimulated) 3-*O*-methylglucose transport into the rat epitrochlearis muscle was increased at 3, but not 16, hours following an acute bout of swimming (37). Ren *et al*. (232) interpreted these findings to imply that 16 hours post-exercise is long enough for the acute effects of exercise (i.e., basal glucose transport in the absence of added insulin) to wear off on muscle glucose transport.
- Insulin-stimulated 3-*O*-methylglucose transport was increased 60% and 103% into the epitrochlearis muscle 16 hours after a 6-hour swimming bout performed for 1 or 2 days, respectively (232).
- Sixteen hours after an acute swimming bout, insulin-stimulated 3-*O*-methylglucose transport was increased into the epitrochlearis muscle (45).

TRAINED BY FORCED SWIMMING OR FORCED TREADMILL RUNNING

- Maximal insulin-stimulated 3-*O*-methylglucose transport into fast muscle during hindlimb perfusion was increased at 24, but not at 48, hours following the last bout of forced treadmill-exercise after 12 weeks of training while total GLUT4 protein level in these rat fast muscles was increased at both 24 and 48 hrs (79).
- Sixteen hours after either an acute swimming bout or 5 days of swim training, insulin-stimulated 3-*O*-methylglucose transport was increased into the epitrochlearis muscle (45).

Activity-related changes in skeletal muscle insulin signaling in animals.

As with humans, exercise training in animals leads to enhanced insulin signaling.

INSULIN BINDING. Insulin binding to its receptor was increased in plasma membranes of mouse soleus, plantaris, and extensor digitorum longus muscles (21), in the mouse soleus muscle 24 hours post-exercise following 6 weeks of treadmill training (276), and in the biceps femoris muscle of exercise-trained rats (252).

INSULIN RECEPTOR AND IRS. The epitrochlearis muscles in ad libitum-fed rats were studied 16 hrs after a 6-hour swim in groups in which this was the only exercise bout (1-day) or in which 5 days of swimming constituted the training period (45). The authors found that: 1) Insulin receptor β-subunit protein

concentration increased in 1- and 5-day groups while insulin-stimulated IR tyrosine phosphorylation increased only in the 5-day group; 2) IRS-1 protein level decreased and PI 3-kinase activity in a polyclonal anti-IRS-1 antibody immunoprecipitate increased; 3) increases in IRS-2 protein level and PI3K activity in a polyclonal anti-IRS-2 antibody immunoprecipitate occurred in the 1-day, but not in the 5-day, group; and 4) 5 days of exercise led to a 3-fold increase in insulin-stimulated Akt phosphorylation.

TOTAL GLUT4 PROTEIN LEVEL IN EPITROCHLEARIS MUSCLE DURING VOLUNTARY RUNNING COMPARED TO AGE-MATCHED SEDENTARY CONTROLS.

- ***One week of voluntary wheel running.*** Total GLUT4 protein level was unchanged, but submaximal and maximal insulin-stimulated 2-deoxyglucose transport rates were 43 and 31% greater, respectively (121), demonstrating a transient dissociation between insulin-stimulated glucose transport and total GLUT4 protein level.
- ***Two weeks of voluntary wheel running.*** After 2 weeks of running, total GLUT4 protein level was 24% greater in epitrochlearis muscles from trained rats and submaximal and maximal insulin-stimulated 2-deoxyglucose transport rates were 86 and 57% greater, respectively (121).
- ***Three weeks of voluntary wheel running.*** Total GLUT4 protein level was 54% greater and 2-deoxyglucose transport stimulated by

submaximal and maximal doses of insulin were 71 and 70% greater, respectively (121).

- ***Five weeks of voluntary wheel running.*** Total GLUT4 protein level and 2-deoxyglucose transport increased 50% and 63%, respectively, with no change in the GLUT1 glucose transporter or in muscle fiber type composition (241).
- ***Six months of voluntary wheel running.*** Total GLUT4 protein level increased 45% relative to sedentary rats (98).

In addition, insulin-stimulated translocation of GLUT4 to the cell surface is increased at 16 hours post-exercise in swim-trained rats relative to a sedentary group (232).

Glucose uptake into skeletal muscle and insulin signaling decrease upon training cessation

SWIM TRAINING IN RATS

- Eighteen hours and 42 hours after 5 days of swim-training, maximal insulin-stimulated 2-deoxyglucose transport was 85% and 51% higher, respectively, in isolated epitrochlearis muscles from trained rats compared with age-matched controls, and GLUT4 protein level was 87 and 52% higher, respectively (143). Ninety hours after 5 days of training, there were no significant differences in maximal insulin-stimulated 2-deoxyglucose transport or total GLUT4 protein level in epitrochlearis muscle between trained or sedentary control rats. In this

study they showed a significant correlation of 0.98 between maximal insulin-stimulated 2-deoxyglucose transport and total GLUT4 protein level.

- After 5 days or 5 weeks of swim training, total GLUT4 protein level and insulin-stimulated glucose transport into the epitrochlearis muscle increased approximately 2-fold 16 hours following the last exercise bout. At 40 hours after the last exercise bout, these increases had completely reversed to the untrained level. In contrast, citrate synthase and hexokinase activities were unchanged 40 hours after 5 days of exercise (125).
- Total GLUT4 protein levels in epitrochlearis muscles from rats subjected to 5 days or 5 weeks of swim training had a 25-35% increase content when assessed at 24 hours post-training, but these decreases were reversed at 48 hours post-training (233). Insulin-stimulated 2-deoxyglucose transport into isolated epitrochlearis muscle was only determined in the 5-day swim trained rats and was enhanced by 62% in muscles 24, but not 48, hrs after the last swim bout.

FORCED TREADMILL TRAINING IN RATS

Treadmill run-training for 5 weeks produced a 35% increase in total GLUT4 protein level in the epitrochlearis muscle at 24, but not 48, hours after the last exercise bout (233).

Voluntary wheel running

- All aforementioned reports investigating the effects of detraining used the isolated epitrochlearis muscle *in vitro*. A longer duration in the maintenance of the training effect was found in an *in vivo* model. Thirty minutes after insulin (90 nmol/rat, intraperitoneal) or saline injection, the total number of skeletal muscle cell surface glucose transporters, total muscle homogenate and cell surface GLUT4 protein, and rates of cell surface vesicle D-facilitated glucose transport were higher in rats trained for 6 weeks by voluntary running wheels immediately after exercise training and did not decrease significantly during the 5 days after cessation of training (95; 233). Reasons that insulin sensitivity may remain higher longer *in vivo* likely include increased capillary density in the trained muscle, allowing increased delivery of insulin and glucose.
- Total GLUT4 protein level in triceps muscle remained high following training for a longer period of time when rats were trained on voluntary running wheels (95; 233) as compared to the epitrochlearis following swimming or treadmill exercise (125; 233). According to Reynolds *et al*. (233), this disparity may be due to the stress associated with the forced exercise of laboratory rats and concluded that future studies examining the effect of detraining on skeletal muscle GLUT4 level after voluntary exercise training are warranted.

OBESITY AND PHYSICAL INACTIVITY

Obesity is rapidly becoming a leading healthcare problem worldwide [reviewed in (264)]. In 1991, obesity and physical inactivity contributed to approximately 300,000 deaths annually, and they accounted for nearly 10% of health care expenditures in the United States (188); in 2005, these figures are likely to be much higher as obesity prevalence continues to skyrocket (81; 82). There is a well-established relationship between obesity and insulin resistance (88; 91; 228; 275; 290; 294); this is particularly true for intraabdominal obesity (34; 63; 88; 91; 141; 214; 228; 287; 294). Because less physically active individuals expend less energy, it is not surprising that there is a strong relationship between low levels of physical activity and obesity (70; 131; 251; 260; 270; 301). In particular, regular physical activity protects against increases in intraabdominal fat (31; 214; 251). Studies in both humans and animals (reviewed below) demonstrate that when physical training ceases, there is a resultant increase in adiposity.

Adiposity with cessation of physical training in humans

- 2 months following the competitive season for trained young and older male competitive cyclists, body fat as determined from skin caliper measurements had an absolute increase of >5% (92).
- Highly trained endurance rowers who ceased training increased their relative fat mass by 31%, 47%, and 70% after 5, 29, and 52 weeks of

no training, respectively, as determined by bioelectrical impedance (224).

- Female swimmers who stopped training for 2 months experienced a mean body mass increase of 4.8 kg of which 4.3 kg was fat mass (3).
- Young women who underwent 16 weeks of aerobic training demonstrated a 13% decrease in percent body fat, but 6 weeks after stopping training, body fat had increased back to pre-training levels (170).
- Cessation of physical training for 4 weeks in obese 7-11-year-olds led to an increase of percent body fat as determined by bioelectrical impedance (100).

Adiposity with cessation of physical training in animals

- Booth *et al*. (24) reported that 8 weeks after ending an 8-week treadmill training program, the mean diameter of epididymal adipocytes was 25% larger than rats that continued to train, but were not different from untrained rats.
- Total carcass fat was 70% greater at 2 weeks following a 6-week treadmill training program in rats relative to 18-21 hours following the last exercise bout. During this same 2-week time frame, total carcass fat increased just 18% in sedentary groups (7).
- In rats trained on a treadmill for 6 weeks, 2 weeks of regular sedentary cage activity resulted in a 41% increase in epididymal fat pad mass

and a 24% increase in carcass fat content relative to an untrained group (68).

- When rats underwent voluntary wheel running for 8 weeks, removal of the wheel for 1 week resulted in a 67% increase in epididymal fat pad mass and a 23% increase in adipocyte diameter (165).
- Craig *et al*. (54) showed a 53% increase in parametrial adipocyte volume just 4 days after ending a 10-week swim training program.
- In a novel study, Stern and Johnson (266) demonstrated that rat pups that were given initial access to running wheels during weaning and have the wheels removed at 8 weeks of age have 67% greater fat in three different pads and 107% greater amount of lipid per cell at 16 weeks of age than sedentary control rats, despite being only 75% and 48%, respectively, of the values of the sedentary controls at 8 weeks of age.

Potential mechanisms governing the increase in fat mass upon reduced physical activity

That adiposity should increase upon the cessation of physical training should not be surprising. During the regular cycles of physical activity, adipose triacylglycerol would undergo lipolysis, and fatty acids would be released to provide energy substrate for the working muscle. During periods of physical inactivity, it is logical that there should be mechanisms that would serve to replenish adipose tissue triacylglycerol stores. Such adaptations would be

critical for survival in the natural world (22). Triacylglycerol in adipose tissue could be increased either through enhanced uptake of triacylglycerol from the plasma, enhanced *de novo* synthesis of triacylglycerols from glucose and fatty acids, or decreased lipolysis. Thus, increased adiposity might result from any mechanisms that 1) increase the supply of triacylglycerol, glucose, or fatty acids, 2) increase their uptake into the cell and/or subsequent incorporation into triacylglycerol, or 3) decrease the rate of lipolysis. A number of studies have examined the effect of reducing physical activity on a number of these potential mechanisms. These studies have primarily used animal models.

PLASMA TRIACYLGLCYEROL

- The plasma triacylglycerol response to an oral fat tolerance test was performed 15 and 60 hours following the last bout of 13 weeks of running training in sedentary young men and women. In response to the fat load, the area under the plasma triacylglycerol curve was increased 37% at 60 hours relative to 15 hours (116).
- Sixty hours and 6.5 days after endurance-trained individuals stopped training, the area under the plasma triacylglycerol curve during an oral fat tolerance test increased 35% and 42% at 60 hours and 6.5 days, respectively, relative to 15 hours post-exercise. Fasting plasma triacylglycerol increased 28-29% at 60 hours and 6.5 days, relative to 15 hours post-exercise (105).

- Highly trained endurance rowers who ceased training experienced an increase in fasting plasma triacylglycerol of 43%, 86%, and 129% after 5, 29, and 52 weeks of no training, respectively (224).
- Plasma triacylglycerol in rats increased 48% from 24 to 72 hours following the last bout of 6 weeks of treadmill training (6).
- Following 10 weeks of treadmill training, serum triacylglycerol in trained rats increased 44% and 76% after 3 and 5 weeks, respectively, following the decrease in physical activity (112).

LIPOPROTEIN LIPASE ACTIVITY

- In rats that were sacrificed 24 hours following 6 weeks of treadmill training, lipoprotein lipase activity in epididymal fat was only 30% of the untrained group, but increased 104%, 70%, and 131% at 60, 72, and 84 hours, respectively, so that it was now 16%, 50%, and 71% greater than a time-matched untrained group. Similar results were also observed in retroperitoneal fat. In addition, plasma insulin values, which were only 49% of the untrained group at 24 hours post-training, rose 119% and 161% at 48 and 72 hours post-training, respectively, so that plasma insulin was now higher than the untrained group (6).
- When rats underwent voluntary wheel running for 8 weeks, removal of the wheel for 1 week resulted in a 155% increase in epididymal fat lipoprotein lipase activity (165).

GLUCOSE UPTAKE

- In rats sacrificed 24 hours after either 6 or 22 months of exposure to a voluntary running wheel, insulin-stimulated 2-deoxyglucose uptake into epididymal adipocytes was at least 2-fold greater than a pair-fed group with regular sedentary cage activity (53).
- 44 hours following 6 weeks of treadmill training, insulin-stimulated 3-*O*-methylglucose transport was increased 55% and basal transport was increased 78% relative to an untrained control group (297).
- Insulin-stimulated glucose uptake into adipocytes has been shown to increase in response to exercise training for 1-9 days following the last training bout (54).

FATTY ACID SYNTHESIS

- 44 hours following a 6-week treadmill training program, insulin-induced incorporation of glucose into fatty acids and triacylglycerol in isolated epididymal adipocytes was greatly enhanced as evidenced by a dose-response curve, with a greater than 8-fold increase at maximal insulin levels relative to an untrained group (297), although the relative contribution of *de novo* fatty acid synthesis or the incorporation of the fatty acid into triacylglycerol cannot be ascertained. This study also demonstrated a 4.5-fold increase in glucose oxidation, thus suggesting that decreased substrate oxidation in fat does not contribute to a reduced physical activity-induced increase in fat mass.

- In rats trained on a treadmill for 6 weeks, 2 weeks of regular sedentary cage activity resulted in a 142% greater fatty acid synthase activity in epididymal fat relative to a group that did not receive training. In this same study, relative to the untrained group, the group with 2 weeks of reduced physical training had a 51%, 203%, and 281% greater activity of the lipogenic enzymes glucose-6-phosphate dehydrogenase, citrate cleavage enzyme, and malic enzyme, respectively (68).
- 2 weeks following a 6-week treadmill training program, incorporation of tritiated H_2O into fatty acids in retroperitoneal adipose tissue increased 181% relative to 18 hours after the last exercise bout (7).
- In hamsters that had access to voluntary running wheels for 5 weeks, fatty acid synthase activity in adipose tissue was 34% higher than in a group with regular sedentary cage activity. After being denied access to the running wheels for 8 days, fatty acid synthase activity had risen 39% so that it was now 86% greater than the sedentary group. Forty-one days after cessation of wheel running, fatty acid synthase activity remained 43% higher than the sedentary group (284).

TRIACYLGLYCEROL SYNTHESIS

- Askew *et al*. (11) showed that 24 hours following the last bout of a 12-week treadmill training program, esterification into glycerolipids, including diacylglycerol and triacylglycerol, was 23% higher in the epididymal adipose tissue of trained rats relative to a sedentary group.

In addition, epididymal adipose tissue of trained rats had 57% higher glucose-6-phosphate dehydrogenase activity. Glucose-6-phosphate dehydrogenase provides NADPH, which is essential to the synthesis of fatty acids (205; 246).

- In a similar study, glycerolipid synthesis in epididymal fat increased 59% 24 hours after the last exercise bout following 12 weeks of treadmill training in rats relative to an untrained group (12).
- As described above under “Fatty Acid Synthesis”, incorporation of glucose into triacylglycerol is increased 44 hours after 6 weeks of treadmill training (297). While triacylglycerol synthesis may be increased, it cannot be separated from *de novo* fatty acid synthesis.

LIPOLYSIS

- Following a 20-week aerobic training program in young men and women, epinephrine-stimulated lipolysis in suprailiac fat biopsies had increased relative to pre-training levels, but 50 days following the end of the training program, lipolysis had decreased to the pre-training level (64).
- 24 hours after the last activity bout following 9 weeks of treadmill training, trained rats had an upward shift in an isoproterenol dose-response curve for lipolysis in isolated epididymal adipocytes relative to an untrained group while basal lipolysis was unchanged (135).

- At least 24 hours following 9 weeks of treadmill training, trained rats demonstrated a higher degree of basal and epinephrine-stimulated lipolysis and a greater degree of lipolytic inhibition by insulin than an untrained group as determined by dose-response curves in isolated epididymal adipocytes (272).
- There is a leftward shift in dose-response curve for epinephrine-induced lipolysis in isolated parametrial adipocytes from rats sacrificed 44 hours following the last bout of a 6-week treadmill training program relative to a sedentary group, indicating enhanced lipolysis (297).
- Rats sacrificed 48 hours following the last bout of 9 weeks of treadmill training had a 133% greater isoproterenol-stimulated lipolysis in epididymal fat relative to an untrained group, whereas basal lipolysis was not different (144).
- Rats trained on a treadmill for 13 weeks had an ~60% higher rate of epinephrine-stimulated lipolysis in isolated epididymal adipocytes than an untrained group when sacrificed 48 hours after the last training bout (13).
- At least 24 hours following 15 weeks of treadmill training, there was a leftward shift in the dose-response curve for isoproterenol-induced lipolysis in isolated parametrial adipocytes from trained relative to sedentary rats, indicating an increased sensitivity of lipolysis to isoproterenol (259).

- 48 hours following a 10-week swim training program, epinephrine stimulated a higher degree of lipolysis in trained rats relative to an untrained group as determined by microdialysis in retroperitoneal, parametrial, mesenteric, and subcutaneous adipose tissue (75).
- 2-3 days following 7-11 weeks of swim training, trained rats had a 46% and 33% greater degree of epinephrine-stimulated lipolysis in isolated epididymal adipocytes than untrained and pair-fed untrained controls, respectively; basal lipolysis was 42% and 27% greater in the trained rats than in the untrained and pair-fed untrained groups, respectively. Isolated parametrial adipocytes also exhibited both greater basal and epinephrine-stimulated lipolysis. In addition, parametrial adipocytes demonstrated a greater level of lipolysis in response to theophylline, dibutyryl cyclic AMP, and adrenocoritotrophic hormone (32).
- 3 days following 6 weeks of swim training, there was an upward shift in the epinephrine dose-response curve for lipolysis in isolated retroperitoneal adipocytes for trained rats relative to an untrained group while basal lipolysis was unchanged (283).
- 40 hours following 18 weeks of swim training, the enzyme activity and protein level of hormone-sensitive lipase, which is the rate-limiting enzyme for lipolysis (309), increased in both the retroperitoneal and mesenteric adipose tissue of trained rats relative to an untrained group (76).

SUMMARY OF MECHANISMS INCREASING FAT STORAGE WITH REDUCED PHYSICAL ACTIVITY. The above studies indicate that, when there is reduced physical activity following a period of exercise training, there are several mechanisms that are enhanced that would support increasing fat (triacylglycerol) storage in adipose tissue. 1. Increased plasma triacylglycerol (6; 105; 112; 116; 224) would increase the supply for the adipose triacylglycerol pool. 2. Increased lipoprotein lipase activity (6; 165) would increase the uptake of triacylglycerol. 3. Increased glucose uptake (53; 54; 297) would supply increased substrate for *de novo* fatty acid synthesis and triacylglycerol synthesis. 4. Increased fatty acid synthase activity (7; 68; 284; 297) would accelerate the conversion of glucose or other substrates to fatty acids and subsequent incorporation into triacylglycerol synthesis. 5. Increased triacylglycerol synthesis (11; 12; 297) would accelerate the rate at which new triacylglycerol is synthesized. 6. The activity of other lipogenic enzymes, such as glucose-6-phosphate dehydrogenase, citrate cleavage enzyme, and malic enzyme (11; 68) may also be increased following the cessation of exercise training and could contribute to increased fat mass. 7. After the end of exercise training, basal, epinephrine-stimulated, or isoproterenol-stimulated lipolysis are either unchanged or increased (13; 32; 64; 75; 76; 135; 144; 259; 272; 283; 297). While this would not suggest a role for decreased lipolysis in the reduced physical activity-induced increases in adiposity, at least one study (272) indicates that the suppression of lipolysis by insulin may be enhanced following cessation of exercise training. Moreover, Askew *et al*. (11) also estimate that the re-esterification of lipolysis-released fatty acid into

triacylglycerol is increased 2-fold by exercise training. Thus, it is possible that a greater inhibition of lipolysis by insulin or enhanced re-esterification of fatty acids into triacylglycerol could contribute to an increase in fat mass with reduced physical activity. Despite the numerous studies detailing biochemical changes upon exercise cessation, there is a lack of studies examining the mechanistic basis for the biochemical observations.

SPECIFIC AIMS

The numerous studies cited in the introduction support the idea that 1) physical inactivity contributes to increased insulin resistance (decreased insulin sensitivity) and intraabdominal adiposity, and 2) reduced physical activity in previously highly active humans or animals results in decreased insulin sensitivity and increases in intraabdominal fat. Thus, a reduction in physical activity in trained humans or animals parallels the changes observed in society as physical activity has declined, i.e. reduced insulin sensitivity [as determined by rising rate of type II diabetes (216)] and increased obesity (82; 225). In the studies detailed in this paper, I have taken advantage of this observation by allowing rats access to voluntary running wheels for 3 weeks, then locking the wheels for 1-2 days (see Chapter 2). The specific aims for each chapter are outlined below.

SPECIFIC AIMS FOR CHAPTER 4. To better understand the mechanisms underlying the decline in insulin-stimulated glucose uptake into skeletal muscle that occurs with reduced physical activity, the Specific Aims for Chapter 4 were 1) to determine the time course of decline of insulin-stimulated glucose uptake

into the epitrochlearis muscle upon reduced physical activity and 2) to determine whether any changes in insulin signaling accompany the decline.

SPECIFIC AIMS FOR CHAPTER 5. Changes in growth and/or food intake might contribute to any changes in muscle glucose uptake (Chapter 4) or adiposity (Chapter 6). In addition, in preliminary studies, I observed that rats with access to running wheels grew at a faster rate than those with regular sedentary cage activity. Therefore, the Specific Aims for Chapter 5 were 1) to determine the growth rate and food intake of rats with access to running wheels, 2) to determine whether growth rate or food intake were altered by a reduction in physical activity, and 3) to determine whether increased muscle mass in rats with running wheel access is associated with their accelerated growth rate.

SPECIFIC AIMS FOR CHAPTER 6. The Specific Aims for Chapter 6 were 1) to determine if the decline in muscle glucose uptake upon reduced physical activity (Chapter 4) was associated with an increase in epididymal fat mass or adipocyte size and 2) to determine whether changes in plasma triacylglycerol levels, glucose uptake, or triacylglycerol synthesis were associated with any potential increase in fat mass or adipocyte size with a reduction in physical activity.

SPECIFIC AIMS FOR CHAPTER 7. Based on findings from Chapter 6, the Specific Aims for Chapter 7 were 1) to determine if acute physical activity was sufficient to increase triacylglycerol synthesis above regular sedentary cage activity levels 10 hours following the end of the activity, 2) to determine whether decreased glycerol-3-phosphate acyltransferase or diacylglycerol acyltransferase enzyme activity was related to the suppression of triacylglycerol synthesis at 5

hours or the enhancement of triacylglycerol synthesis at 10, 29, or 53 hours of reduced physical activity following 3 weeks of voluntary wheel running, and 3) to determine mechanisms that might contribute to any potential change in glycerol-3-phosphate acyltransferase or diacylglycerol acyltransferase enzyme activities. Parts of the studies reported in this paper have either been previously published (163), are in press (162), or a manuscript is in preparation (164).

Chapter 2: Experimental Design

BASIS OF THE EXPERIMENTAL DESIGN

A sedentary lifestyle contributes to the pathophysiology of many modern chronic diseases in humans [reviewed in (22; 23; 238)]. Because the etiology of these diseases, including decreased insulin sensitivity and increased adiposity, is slow in developing, it can be difficult to detect potential mechanisms, as there may be only relatively small differences that account for the onset of the disease. However, a short-term reduction in physical activity in highly physically active humans or animals exhibits a similar phenotype for decreased insulin sensitivity and increased intraabdominal fat as that observed in less active humans or animals (see Chapter 1). Because the phenotypic changes occur more abruptly when physical activity is reduced, reducing the physical activity of highly physically active animals may provide a model for studying the mechanisms underlying the physical inactivity-related insulin resistance and obesity. In this paper, I have employed an animal model where rats are permitted unrestricted access to voluntary running wheels for 21 days, after which the running wheels were locked by tying the wheels with wire. The experimental design is outlined in Figure 1.

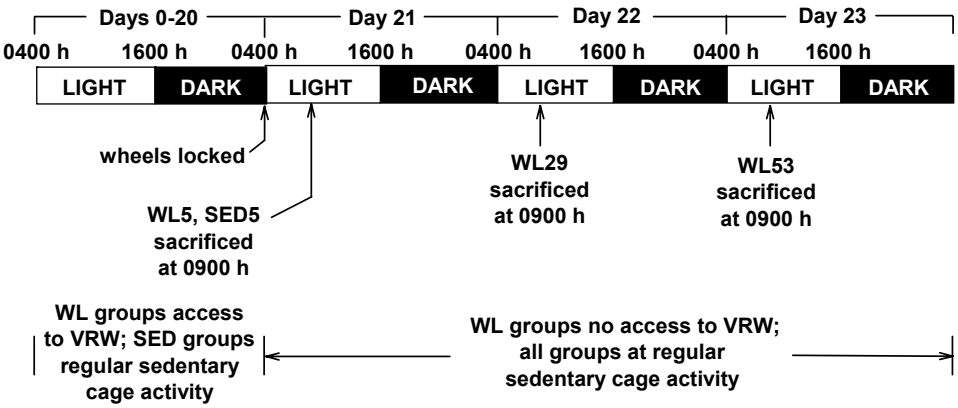

Figure 1. Experimental design.

The top two lines represent the time line. The bar represents the light:dark cycle. Preliminary studies showed that >99% of the running occurred during the dark cycle (data not shown). Wheel lock (WL) groups were given access to voluntary running wheels (VRW) at the start of day 0. Groups with regular sedentary cage activity (SED) were housed without VRW. For WL groups, wheels were locked at 0400 h on day 21 (bottom lines); arrows pointing to bar indicate the time of sacrifice. Access to food was denied at 0400 on the day of sacrifice for a given group. See text for more detail.

DESCRIPTION OF THE EXPERIMENTAL GROUPS

WHEEL-LOCK 5, 10, 29, AND 53 (WL5, WL10, WL29, AND WL53). 4-week-old rats are given unrestricted access to voluntary running wheels for 21 days, then the wheels are locked for 5 (WL5), 10 (WL10), 29 (WL29), or 53 (WL53) hours. WL5, WL29, and WL53 groups are included in all studies. Based on preliminary data (data not shown), WL10 groups were included for studies involving triacylglycerol synthesis.

REGULAR SEDENTARY CAGE ACTIVITY 5 AND 10 (SED5 AND SED10). 4-week-old rats are housed in individual cages of the same dimensions as for wheel-lock groups for 21 days, then SED5 is sacrificed at the same time as WL5, and SED10 is sacrificed at the same time as WL10. The SED5 group is included in all studies. Based on preliminary data (data not shown), the SED10 group was included for studies involving triacylglycerol synthesis.

HANDLING AND SACRIFICE OF ANIMALS

Fischer 344 X Brown Norway F1 generation male rats (Harlan, Indianapolis, Indiana) arrived at 21 to 23 days of age and were housed 6-8 animals per cage. Following one week of acclimatization, they were randomly placed into individual cages with or without a voluntary running wheel. During this time, food intake was measured daily; the animals had unrestricted access to standard rat chow throughout the experiment. Bicycle computers were attached to the wheels and used to monitor daily running distance, average running speed, and total running duration. Body mass was obtained weekly on the same day at the beginning of the light cycle. To minimize the amount of handling, the animals were supplied with fresh water and a cage containing fresh bedding weekly when they were weighed. At the time of sacrifice, the rats were anesthetized with 60 mg pentobarbital per kg body mass. When the animals were under anesthesia to the depth where there no pinch reflex exists, surgeries were performed and the animals exsanguinated. More detail on the handling and sacrifice of animals is described in the Methods sections of Chapters 4, 5, 6, and 7.

JUSTIFICATION OF THE DESIGN

Rat strain

Fischer 344 x Brown Norway F1 hybrid rats (FBN) were used in the experiments. The selection of this strain was made for several reasons: 1)

based on preliminary data (data not shown), FBN exhibit a training effect following 21 days of voluntary wheel running, including an increase in insulin-stimulated 2-deoxyglucose uptake; 2) in my hands, FBN had a significantly greater daily running distance than male Sprague-Dawley or Wistar rats of the same age (data not shown); 3) FBN have previously been used for exercise-induced changes in epitrochlearis glucose uptake (35); 4) Dr. Booth's lab has used this strain for microarray experiments in an aging study (217; 218; 220); thus, any future experiments arising from the current research could benefit from gene comparisons to the same strain; and 5) future research in Dr. Booth's lab may involve a study of aging and insulin resistance, and the FBN rat strain has been shown to be a good model for such a study (166).

Rat gender

Male rats have been used for the experiments in the current studies because 1) insulin-stimulated glucose uptake and voluntary running activity both oscillate with the estrous cycle in females (5); as it was desirable to have the animals run approximately the same distance each night, the use of males eliminates the variability in running associated with the estrous cycle and the potentially confounding effects of the estrous cycle on changes in glucose uptake with reduced physical activity, and 2) male rats show exercise training-related increases in insulin-stimulated glucose uptake [(241), and preliminary data not shown].

Age to start running

Rats were provided access to voluntary running wheels beginning at 28 to 30 days of age for 2 reasons: 1) rats of this age have a considerably higher running activity than do older rats [data not shown, see also Chapter 5, Fig. 13 (p. 92) and Table 2 (p. 91) and Chapter 7 (p. 132)] at the end of the experimental duration, the rats weighed less than 250 g (see Chapter 5); rats of this body mass have previously been used successfully to determine glucose uptake in isolated epitrochlearis without impairments in diffusion due to muscle size (35).

Duration of voluntary wheel training

Rats with access to voluntary running wheels (WL5, WL10, WL29, and WL53) had access to the wheels for 21 days. This time point was chosen because 1) preliminary data (not shown) and previous reports (190; 241) indicate running activity plateaus after this time point and 2) rats are still small enough (<250 g) at this point to permit successful use of the epitrochlearis (see Age to Start Running).

Duration of wheel lock/reduced physical activity

WL5: Two stimuli (an acute effect lasting less than 16 hrs after a single exercise bout by previously non-exercised rats, and a chronic effect lasting less than 48 hours after the last exercise bout by rats who have had many daily bouts preceding the last exercise bout, i.e., trained) increase insulin-stimulated glucose

uptake into skeletal muscle [reviewed in (96)]. In order to study the training effect only, sufficient time must pass for the acute exercise effect to dissipate. My preliminary data (data not shown) showed that with voluntary wheel running, the acute exercise effect (using the disappearance of enhanced basal glucose uptake as an index of the acute exercise effect) has worn off by the 5th hour of wheel lock. Because at 5 hours post-wheel lock only the training effect from multiple activity bouts is evident, this time point was chosen.

WL29 AND WL53: These time points were chosen based on previous literature showing that 40-48 hours following the last bout of exercise (swim training or treadmill running) in trained rats, insulin-stimulated 2-deoxyglucose uptake into the epitrochlearis muscle had returned to the levels of the sedentary groups (125; 233). Using a voluntary running model, my preliminary data showed that 53 hours following wheel lock, insulin-stimulated glucose uptake into the epitrochlearis muscle had decreased to the level of SED5 (data not shown).

Assignment of experimental groups

After the 1-week acclimatization, the animals were randomly divided into the experimental groups and separated into individual cages. The WL5, WL10, WL29, and WL53 groups were given access to voluntary running wheels (Fig. 1, p. 39), and the SED5 and SED10 groups were housed in cages of the same dimensions without a running wheel so that they only have regular sedentary cage activity.

Selection of exercise training model

There are three general models of exercise in rats: swimming, treadmill running, and voluntary wheel running. I have chosen the voluntary running model for several reasons: 1) voluntary running most closely approximates the manner in which humans have historically engaged in physical activity in that rats engage in voluntary physical activity during waking hours (i.e., night) on an intermittent basis (243); swimming and treadmill running are both forced forms of activity that generally take place during the light cycle when rats are not normally physically active; 2) rats on running wheels run at high speeds [(14; 101), and preliminary data not shown] required to recruit all muscle fiber types (10; 69; 273) without the potentially confounding effects of forced exercise (83; 243), and 3) voluntary running results in increases in insulin-stimulated glucose uptake into epitrochlearis muscle [(121; 241), and preliminary data not shown]. One drawback of the voluntary running model is the inability to determine the exact length of time (minutes) following the last bout of activity; this is due to the method of monitoring running activity using a bicycle computer, which will provide information on the total amount of running, but not on the pattern of activity. However, it was felt that the advantages far outweigh this disadvantage. In Chapter 6, when a more precise length of time following the activity was desired, a treadmill running protocol was used.

Protocols when access to running wheels is ended and prior to sacrifice

After 21 days of access to the running wheels, the wheels were locked at the start of the light cycle for WL5, WL10, WL29, and WL53. Five hours later, the SED5 and WL5 groups were sacrificed. The SED10, WL10, WL29, and WL53 groups remained in their cages. WL10 and SED10 were sacrificed 10 hours after the start of the light cycle (or 10 hours after the running wheels were locked). WL29 was sacrificed 1 day later at 5 hours after the start of the light cycle, so that the running wheels had been locked for 29 hours, and WL53 was sacrificed 2 days after the running wheels were locked at 5 hours after the start of the light cycle, so that the running wheels had been locked for 53 hours. At the start of the light cycle on the day of sacrifice for all groups, food was removed so that the animals did not eat for 5 hours prior to sacrifice, eliminating any potentially confounding effects of a last meal while avoiding increases in insulin-stimulated glucose transport that occur with fasting. This also allowed us to study the animals in a postprandial state, which is the most common condition in modern humans. Preliminary experiments showed that during the first 5 hours of the light cycle, the rats ingest <0.1% of their normal daily food intake with no difference between groups (data not shown). Preliminary data also showed that the animals are not active on their wheels during this time (data not shown). Because the animals do not normally eat or exercise during this time, they were studied in as close to their biologically normal state as possible.

Selection of the epitrochlearis muscle

The epitrochlearis muscle was selected because 1) it is commonly used in incubation experiments because its small thickness (197; 198) is not limiting to diffusion of oxygen and 2-deoxyglucose, allowing rapid equilibration between the incubation medium and the extracellular space (115); this is also important as hypoxia *per se* increases both basal and insulin-stimulated glucose transport (36); 2) it exhibits biochemical adaptations to exercise training during wheel running (121; 125; 241); 3) it shows basal and insulin-stimulated glucose transport is specific to glucose transporters as evidenced by nearly complete (99%) inhibition in the presence of cytochalasin B (311); 4) it is composed predominantly of fast fibers (60-65% type IIb, 20% type IIa, and 15% type I (197), which develop increases in insulin sensitivity with voluntary wheel running while the predominately slow soleus muscle does not (54) and data not shown); and 5) is composed of 85% fast fibers; increasing percentages of type II fibers in human skeletal muscle are associated with an increased prevalence of obesity and type II diabetes (118; 119; 277), conditions associated with increased insulin resistance (see Chapter 1).

Selection of epididymal fat

Epididymal fat was selected because it 1) is located within the abdominal cavity; 2) is large enough that it provides enough tissue for subsequent biochemical experiments, whereas other fat depots such as the omental,

mesenteric, or perirenal are too small in the size of rat being used to provide sufficient tissue for biochemistry; 3) is easy to dissect out, making it possible to sacrifice all animals within a shorter period of time and decreasing the possibility of a time effect on any measured variable; and 4) has commonly been used in experiments of physical activity and inactivity (see Chapter 1), making possible any potential comparison of results with the published literature.

Chapter 3: Establishment of Methods

This chapter reports how the different methods employed in collecting the data were established, developed, and/or verified. Detailed protocols can be found in Appendix C.

MEASUREMENT OF RUNNING ACTIVITY

Running activity was measured by securing a magnet from a bicycle computer to the side of the running wheel. The magnet sensor was then secured on the side of the cage to count the revolutions of the wheel. Each computer was set to the circumference of the wheel for accurate counting of wheel running activity. The circumference was determined by measuring the inner diameter of three separate wheels in triplicate and taking the mean measurement, which was calculated to be 1,062 cm. The computers calculate and can display the daily running distance and duration of running (computers were reset to 0 each day), mean running speed, maximum running speed, and total distance. Each variable was recorded each day, except for total distance, which was recorded weekly when the animals were weighed. Daily running distance and time were used for measurement of running activity. Mean running speed was checked to ensure that it did not exceed more than 8 km/h, as values higher than this indicate that the magnet was sometimes counting 2 revolutions on each turn of the wheel (my

observations). Total distance was used to ensure that daily running activity was accurately recorded.

RADIOACTIVITY

Counting of ^{125}I

Samples using ^{125}I as a measure were counted in a gamma counter at 100% efficiency.

Counting of ^{3}H

Samples using ^{3}H as the only radioisotope were counted on a scintillation counter. Efficiency for each sample was corrected for quench, which was measured by the scintillation counter using an internal standard. The correction was made according to a quench-efficiency curve, which was plotted according to established methods (159). Briefly, ^{3}H containing a known quantity of disintegrations per minute (dpm) was placed in vials containing scintillation fluid with incremental increases in the degree of quench. The amount of quench and the efficiency of counting for each sample were plotted (data not shown), and a third-degree polynomial equation fitting the plot was calculated: efficiency = $-1.97740 \times 10^{-6}x^3 + 0.000419970x^2 - 0.0313087x + 1.44383$, where x = quench (as calculated by the scintillation counter). This equation was used to calculate the dpm in all subsequent experiments. In addition, 10 vials containing no

radioactivity were counted, and the mean counts were used as background and subtracted from counts in all experiments.

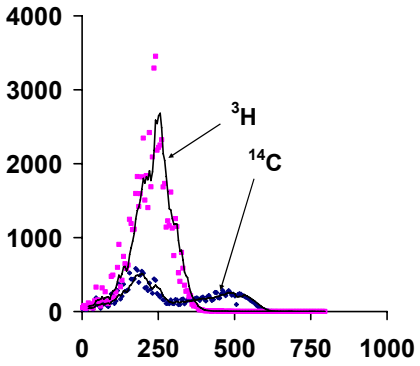

Figure 2. Energy spectra for ^{3}H and ^{14}C.

Dual label counting of ^{3}H and ^{14}C

In experiments for muscle 2-deoxyglucose uptake, triacylglycerol synthesis, and diacylglycerol acyltransferase enzyme activity, dual label counting with both ^{3}H and ^{14}C was used according to published guidelines (27; 159). To determine how to set windows on the counter so that the lower energy ^{3}H was virtually excluded from being counted in the higher energy channel, the energy spectra was determined for each isotope (Fig. 2). Quench-efficiency curves were determined for each isotope in each of the established windows (Fig. 3), and the calculated third-degree polynomial equation was used for determining the efficiency of counting for the isotopes in each window based on the quench number:

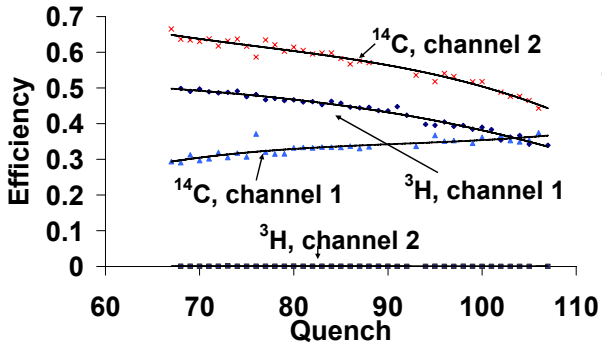

Figure 3. Quench-efficiency curves for dual scintillation counting of ^{3}H and ^{14}C.

Channel 1:

^{3}H efficiency = $-1.26906 \times 10^{-6}x^3 + 2.47812^{-4}x^2 - 0.0175312x + 1.07922$

^{14}C efficiency = $-1.64141 \times 10^{-4}x^3 + 0.00443994x^2 - 0.395374x + 11.9612$

Channel 2:

^{3}H efficiency = $-5.71639 \times 10^{-9}x^3 + 1.90256 \times 10^{-6}x^2 - 2.16942 \times 10^{-4}x +$ 0.0864043

^{14}C efficiency = $-3.02032 \times 10^{-5}x^3 + 0.00838125x^2 - 0.774969x + 24.4592$

where x = quench (as calculated by the scintillation counter). The average background was also determined for each isotope in the separate windows.

ASSAYS INVOLVING THE EPITROCHLEARIS MUSCLE

2-deoxyglucose uptake

2-Deoxyglucose uptake into the epitrochlearis muscle was measured according to procedures established in the lab of Dr. John Holloszy (Washington University, St. Louis, Missouri). Using the technique of his laboratory, I measured 2-deoxyglucose uptake in male Wistar rats (125-150 g). Measured values were a basal 2-deoxyglucose transport rate of 0.653 ± 0.047 µmol/ml/20 min (ml is intracellular space) and 2000 µU/ml insulin-stimulated transport rate of 1.631 ± 0.134 µmol/ml/20 min (n=4) for the epitrochlearis muscle. These values are similar to those published by Han *et al*. (102) of ~0.5 µmol/ml/20 min for basal 2-deoxyglucose transport and ~2.0 µmol/ml/20 min for 2000 µU/ml insulin-stimulated transport in epitrochlearis from male Wistar rats of similar size. These

values also agree with other published values in epitrochlearis muscle from rats of the same size, strain, and gender (149; 150; 204). I have also verified this technique in split soleus muscle (data not shown). The intracellular space was calculated using water content values of 0.80 for the epitrochlearis (37). 2-deoxyglucose uptake was expressed as μmol/ml intracellular space/20 min (103; 143; 233).

Insulin concentrations used were based on the work of Young *et al*. (310). That 2,000 μU/ml achieved maximal 2-deoxyglucose uptake was verified by incubating the contralateral epitrochlearis muscles from the same animal in either 2,000 μU/ml or 10,000 μU/ml. There was no further increase in 2-deoxyglucose uptake at the higher insulin concentration (data not shown). The 2-deoxyglucose concentration of 2 mM used for the experiment is well below the Km of 12 mM for 2-deoxyglucose transport; insulin or exercise both increase the V_{max} for 2-deoxyglucose uptake but do not affect the Km (103). I also verified that the assay was linear with time by incubating the contralateral epitrochlearis muscles from two separate animals for either 20 minutes or 40 minutes with the [^{3}H]2-deoxyglucose. 2-deoxyglucose uptake per minute between contralateral muscles of the same animal was not different (data not shown). This also demonstrated that 2-deoxyglucose uptake was reproducible between contralateral muscles from the same animal.

After verifying the technique, it was necessary to make some changes to the assay. Because of concerns that glucose in the incubation media would increase muscle glycogen storage in the trained animals, and because glycogen

concentration *per se* can affect glucose uptake (117; 126; 137), I desired to replace the glucose with acetate as an energy substrate as described (37; 311). When tested between the contralateral muscles of two separate animals, there was no difference in maximal (2,000 μU/ml) insulin-stimulated 2-deoxyglucose uptake between inclusion of glucose or acetate as the energy substrate (data not shown). Also, because I desired to use the same muscles for both 2-deoxyglucose uptake as well as immunoblot analysis, I tested whether cutting the muscle into sections crosswise would change the outcome of the experiment. When epitrochlearis muscles (n=4) were cut crosswise into sections approximately 1/3 and 2/3 the size of the original muscle following the incubation, there was no difference between the values (data not shown). Finally, because I desired to measure insulin receptor phosphorylation, I desired to decrease the experimental incubation times, as the phosphorylation of the insulin receptor can be transitory (304). When contralateral muscles from two separate animals were subjected to two separate incubation protocols [one as described by Han *et al*. (102), and the other as described in Chapter 4 (p. 66), there was no difference in the 2-deoxyglucose uptake values (data not shown). I verified that insulin receptor phosphorylation could be detected following incubation with submaximal (60 μU/ml) insulin with the revised protocol (40 minutes total incubation in presence of insulin), but it was much lower in the former protocol [(102); 90 minutes total incubation in presence of insulin] with the longer incubation times (data not shown). These experiments led to the current protocol described in Chapter 4.

Insulin binding

For insulin binding experiments, the number of washes necessary to eliminate unbound [^{125}I]insulin from the epitrochlearis muscle was determined (Fig. 4B; n=3 for each time point). The time course of binding (Fig. 4A; n=3 for each time point) and linearity with insulin concentration (data not shown) were also determined. The assay was found to be reproducible in contralateral epitrochelaris muscles from 3 different rats (11% coefficient of variation).

Immunoblotting

Immunoblotting was performed according to established procedures in the Booth laboratory (see Appendix C). Most antibodies worked well with the procedure with minor adaptations. When necessary, the number of washes, the blocking buffer, or antibody dilution buffer were adjusted in order to improve results. The correct band representing the protein of interest was identified using several methods, depending on the antibody: 1) it was verified that the band was at the appropriate molecular mass, 2) positive or negative controls were used, 3) inhibitory peptides were used, and/or 4) another primary antibody was used. Using a combination of these verification techniques, it

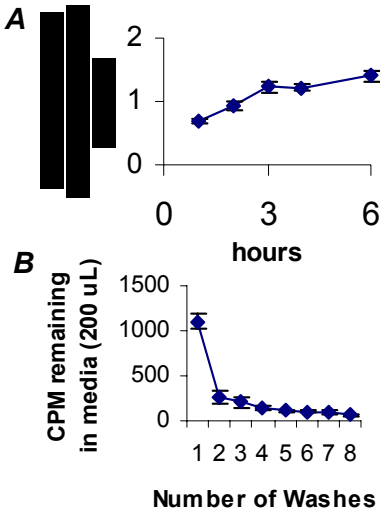

Figure 4. Insulin binding preliminary control experiments.
(*A*) Linearity of insulin binding with time and (*B*) disappearance of radioactivity with number washes in insulin binding experiment.

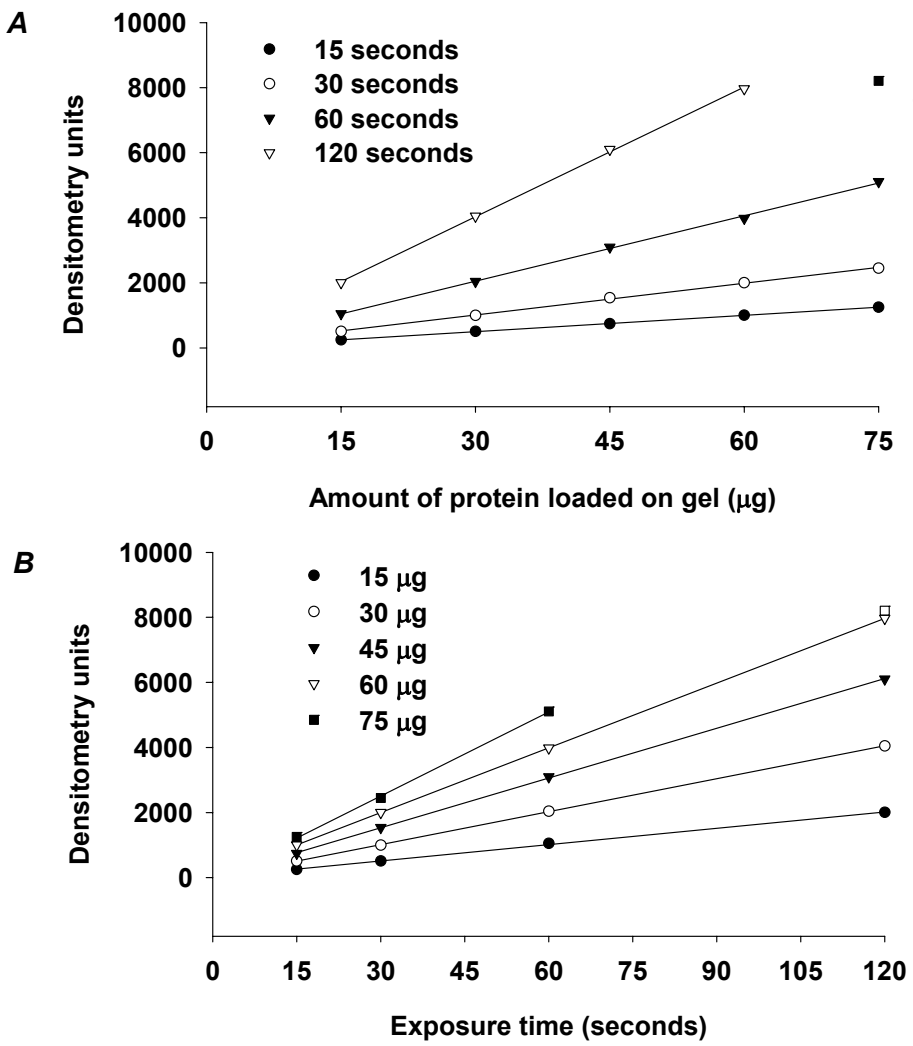

Figure 5. Example of linearity with immunoblotting technique.
Linearity of detection of PKC-θ by immunoblot with respect to (*A*) the time of exposure of film to the enhanced chemiluminescent agent-treated blot or (*B*) the amount of protein loaded on the gel. The 120 second exposure at 75 μg of protein is not presented because it was not linear with the other points, as the signal had begun to plateau. All lines are regression lines.

was possible to positively identify all but one protein of interest (leukocyte antigen-related protein). Blots were commonly stripped and re-probed for a separate protein. The stripping protocols were verified by two methods: 1) blots were exposed to an enhanced chemiluminescent reaction to verify removal of the secondary antibody, and 2) blots were subsequently re-probed with only secondary antibody to verify stripping of the primary antibody. This also established whether there were non-specific bands due to binding of the

secondary antibody. Experiments showed that blots could be re-probed at least 8 times without affecting the quality of the results (data not shown). For each antibody, it was verified that the signal was linear with respect to the amount of protein loaded on the gel and the time of exposure of the blot to film (example shown in Fig. 5).

Immunoprecipitation of the insulin receptor β-subunit

Immunoprecipitation of the β-subunit of the insulin receptor was executed for two reasons: 1) to detect the tyrosine phosphorylation status of the receptor and 2) to detect interacting proteins. Under a standard procedure for immunoprecipitation, it was possible to recover ~70% of the protein from epitrochlearis muscle homogenates (determined by running on gel in parallel with post-immunoprecipitation homogenate and corrected for the amount of protein in the original homogenate; data not shown). While phosphorylation was readily detectable in these samples, there were very few interacting proteins that were co-immunoprecipitated, as determined by fluorescent staining of the gel with ruthenium II tris (bathophenanthroline disulfonate) (227). By sequentially changing the composition of the immunoprecipitation buffer (primarily by adjusting the types and concentration of detergents), it was possible to maintain the protein:protein interactions and increase the number of detectable bands in the fluorescent-stained gels of the immunoprecipitates (data not shown), although this resulted in <30% recovery of the insulin receptor β-subunit (data not shown). Rabbit immunoglobulin G was used in lieu of the rabbit anti-insulin

receptor β-subunit antibody during the immunoprecipitation as a negative control. The only bands detected on the gel with negative control were the subunits of the immunoglobulin G (data not shown).

Citrate synthase activity

The citrate synthase activity assay was linear with respect to the amount of protein (data not shown). As it was possible to use the spectrophotometer to measure the reaction every 15 seconds, it was verified that each sample was linear over the time course of the assay. The values were within the range of published values (121; 233; 234).

Glycogen content

Glycogen content values in preliminary experiments were similar to published values (121; 234).

ASSAYS PERFORMED ON PLASMA

Assays for insulin (4.9%, 7.3%), triacylglycerol (8.9%, 12.2%), glycerol (6.9%, 12.1%), glucose (8.6%, 13.4%), and free fatty acids (1.9%, 3.9%) were all found to have acceptable rates of reproducibility. Values are the intraassay and interassay coefficients of variation, respectively. For data collection, all samples for each assay were run on the same day. All assays were shown to be linear with respect to the concentration of a standard (data not shown).

ASSAYS PERFORMED ON EPIDIDYMAL FAT

Adipocyte isolation

The purity of isolated primary adipocytes was >99% as determined by oil red O staining (data not shown). Primary skeletal muscle satellite precursor cells, kindly provided by Dr. Shuichi Machida, were used as a negative control and exhibited no staining. The viability of the isolated adipocytes was assessed by trypan blue exclusion (data not shown).

Counting and sizing fat cells

Calibration of the Coulter counter was performed with 43-μm diameter beads as per the manufacturer's recommendations. Reproducibility of the size and number of adipocytes was found to have a coefficient of variation of 10.1% and 9.2%, respectively (n=4). The amount of background was calculated after running samples on the Coulter counter. Background within the size range of the cells was not different when compared after running the first, fifth, or tenth samples within a given experiment. Therefore, the average background counts from several readings were determined and subtracted from all samples. The degree of coincidence, defined as the statistical probability of more than

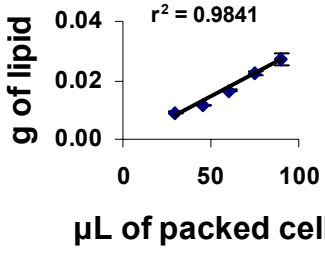

Figure 6. Linearity of lipid content assay with packed cell volume.
The mass of lipid is linear with respect to the volume of packed isolated adipocytes from which the lipid was extracted. When expressed as g of lipid per ul of packed cells, there was no significant difference between any of the points.

one cell entering the aperture at the same time, was calculated to be <5%, which is considered to be acceptable. Determination of the amount of lipid per cell was linear with the volume of packed isolated adipocytes (Fig. 6), and was not different when expressed as amount of lipid per cell.

Immunoblotting

Procedures for establishment of immunoblotting techniques for epididymal fat are the same as those reported above for epitrochlearis muscle. The secondary antibody used detected a non-specific band in fat at ~120 kD. To avoid problems with detection of full-length sterol regulatory element binding protein-1 at 125 kD, these gels were run 45 minutes longer after the dye front ran off the gel to increase separation of the proteins.

2-Deoxyglucose uptake

Insulin concentrations for 2-deoxyglucose uptake into primary isolated adipocytes were determined by constructing an insulin dose-response curve (data not shown). Cytochalasin B concentration to completely inhibit carrier-mediated uptake was determined (data not shown). The number of washes to completely remove media-associated radioactivity from the incubated cells was determined experimentally, both in the presence and absence of cytochalasin B (data not shown). The assay was found to be linear with respect to time and the volume of packed cells used for the assay (data not shown).

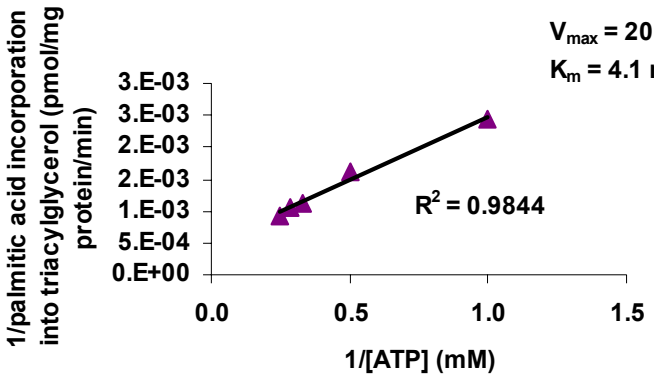

Figure 7. Lineweaver-Burk plot of triacylglycerol synthesis with variable ATP concentration.

Enzyme activities

For triacylglycerol synthesis, glycerol-3-phosphate acyltransferase activity, and diacylglycerol acyltransferase activity, Lineweaver-Burk plots were determined for each co-factor and substrate in each assay (see example in Fig. 7). These plots were used to compute the concentrations needed to maintain each component within the saturation range. Each assay was also checked for linearity with respect to the amount of protein and time (data not shown). For glycerol-3-phosphate activity, both 4 mM and 2 mM N-ethylmaleimide inhibited the total activity by about 75%, showing that 2 mM N-ethylmaleimide was sufficient to completely inhibit the microsomal isoform.

Real-time polymerase chain reaction (PCR)

Purity of isolated RNA was verified both by spectrophotometrically determining the 280:260 nm light absorbance ratio and by inspecting the ratio of 28S and 18S ribosomal RNA on a 1% agarose gel. When the primers for the real-time PCR were checked by running standard PCR with the primers under

the same conditions as for the real-time reaction, it yielded only one product at the appropriate base size when viewed on a 3% agarose gel (data not shown), demonstrating the appropriateness of the primers; RNA not subjected to complimentary DNA synthesis was used as a negative control and yielded no bands, demonstrating that the samples were not contaminated with DNA. The mitochondrial GPAT probe and the 18S probe were both found to be linear with respect to the amount of cDNA, and the slopes of the two probes were linear, demonstrating that 18S is an appropriate normalization control for the mitochondrial GPAT if there are no differences between experimental groups (see Chapter 7). Using RNA as a negative control for real-time PCR yielded no amplification of either mitochondrial GPAT or 18S mRNA.

Chapter 4: Alterations in Insulin Receptor Signaling in the Rat Epitrochlearis Muscle upon Cessation of Voluntary Exercise

INTRODUCTION

Insulin resistance to glucose uptake occurs when there is a reduction in glucose clearance from the blood in response to a physiological level of insulin (decreased insulin sensitivity; (140; 295). The relevance of insulin resistance to health is highlighted by several important associations. Insulin resistance, in itself, increases the risk of hypertension, dyslipidemia, and endothelial dysfunction (230). In addition, insulin resistance is the first measurable defect in the development of type II diabetes (208), and it is a potent predictor of coronary heart disease (1). Thus, impaired insulin sensitivity/insulin resistance is detrimental to health and may be a factor in the rapid rise in modern chronic health disorders.

There is a strong relationship between physical inactivity and insulin resistance (99; 161; 183). This is supported by observations that insulin sensitivity falls off within days when physically active humans become sedentary, with the decreased physical activity decreasing insulin-mediated glucose uptake. For example, the area under the insulin curve during an oral glucose tolerance test increased 73, 30, or 93% when endurance-trained individuals did not

exercise for 7-10, 14, or 10 days, respectively (8; 111; 129). Measured by submaximal hyperinsulinemic, euglycemic clamp techniques, glucose disposal rate decreased 23% after 10 days of no exercise in physically trained subjects (151), and the insulin concentration required for 50% of maximal glucose uptake increased 23% after 5 days of decreased physical activity in endurance-trained subjects (187). Thus, it is clear that insulin sensitivity declines within days of decreasing physical activity in humans. However, little is known about the cellular basis for the effect.

Skeletal muscle accounts for 75-95% of insulin-stimulated glucose disposal in humans (15; 58). Seider *et al*. (258) have shown that insulin resistance develops in the mouse soleus muscle after one day of hindlimb immobilization. Other studies have shown that following swim-training, insulin-stimulated glucose uptake into the isolated rat epitrochlearis muscle decreases to sedentary levels 40-90 hours following the last swimming bout (125; 143; 233). Taken together, the above reports suggest that skeletal muscle could be the source of the physical inactivity-induced decline in whole body, insulin-stimulated glucose disposal in humans.

To gain a better understanding of the mechanisms by which decreased physical activity decreases insulin-stimulated glucose uptake, I wanted to employ an animal model mimicking what happens when previously active subjects stop exercising. The use of voluntary running wheels more closely approximates the manner in which humans have historically engaged in physical activity in that rats both eat and engage in voluntary physical activity on an intermittent basis during

their waking nocturnal hours (243). This allows study of the animals during a time when the animals are normally sleeping, not physically active, and not eating (191; 243). In addition, I chose to study rats in a postprandial state, rather than in a fasted state, as the postprandial state, in my opinion, represents the more common condition in modern humans. Locking the running wheels so that the animals cannot run permits study of what occurs with decreased physical activity (284). One purpose of this study was to determine the time course of decline in glucose uptake into the epitrochlearis muscle with a return to regular sedentary cage activity following 21 days of voluntary wheel running. Based on these results, I next hypothesized that a reduction in measures of insulin receptor signaling would first occur at either 29 or 53 hours after locking of the running wheels. A major finding of this study is that the insulin receptor β-subunit (IRβ) protein level and two essential components of insulin receptor activation, insulin binding and tyrosine phosphorylation, decrease to sedentary levels in the rat epitrochlearis muscle between 29 and 53 hours after cessation of voluntary running activity following 3 weeks of voluntary wheel running.

METHODS

Materials

2-[1,2-^{3}H(N)]deoxyglucose and D-[1-^{14}C]mannitol were from American Radiolabeled Chemicals (St. Louis, Missouri). [^{125}I]insulin was from New England Nuclear (Boston, Massachusetts). IRβ polyclonal, phosphotyrosine

monoclonal, protein tyrosine phosphatase-1B (PTP1B) monoclonal, protein kinase C-theta (PKCθ) monoclonal, and Src homology phosphatase-2 (SHP2) monoclonal antibodies were from BD Biosciences (San Jose, California). IRβ, Akt, and Akt Ser^{473} phosphorylation specific polyclonal antibodies and protein A agarose were from Upstate Biotechnology (Waltham, Massachusetts). Glucose transporter-4 (GLUT4) polyclonal antibody was from Biogenesis (Kingston, New Hampshire). Horseradish peroxidase (HRP)-linked anti-mouse and anti-rabbit secondary antibodies and HRP-linked protein A were from Amersham (Piscataway, New Jersey). Vectastain ABC kit was from Vector Laboratories (Burlingame, California).

Animal protocol

The animal protocol was approved by the Institutional Animal Care and Use Committee at the University of Missouri-Columbia. Fischer 344 X Brown Norway F1 hybrid rats (Harlan, Indianapolis, Indiana) were obtained at age 21-23 days and allowed to acclimatize one week. The animals were housed in approved temperature-controlled animal quarters with a 0400-1600 light:1600-0400 dark cycle that was maintained throughout the experimental period. After one week (day 0), the rats were randomly assigned to one of four groups: wheel lock 5 (WL5), wheel lock 29 (WL29), or wheel lock 53 (WL53): 21 days of voluntary wheel access followed by 5, 29, or 53 hours of wheel lock that prevents access to voluntary running, respectively; or SED5: regular sedentary cage activity group without running wheel access for the entire 21 days (See Fig. 1 in

Chapter 2, p. 39). At this time, the animals were separated into individual cages of the same dimensions; cages for animals in the running groups (WL5, WL29, and WL53) were equipped with a voluntary running wheel outfitted with a Sigma Sport BC 800 bicycle computer (Cherry Creek Cyclery, Foster Falls, Virginia) for measuring running activity. After 21 days, the wheels were locked for all running groups at 0400. SED5 and WL5 were sacrificed at 0900. The WL29 group remained in their cages with locked wheels before being sacrificed the following day (on day 22) at 0900 (after 29 hours of wheel lock), and WL53 remained in their cages with locked wheels until day 23 when they were sacrificed at 0900 (after 53 hours of wheel lock). The animals had *ad libitum* access to food at all times until the day of sacrifice, when food was removed at 0400. At the time of sacrifice, the animals were anesthetized with 60 mg pentobarbital/kg body mass. Epitrochlearis muscles were carefully dissected out, rinsed in pre-oxygenated Krebs-Henseleit buffer (KHB: 116 mM NaCl, 4.6 mM KCl, 1.16 mM KH_2PO_4, 25.3 mM $NaHCO_3$, 2.5 mM $CaCl_2$, 1.16 mM $MgSO_4$, pH 7.4)/40 mM mannitol, and used for experiments as described below. The animals were exsanguinated by removal of the heart.

2-Deoxyglucose uptake

2-Deoxyglucose uptake was performed essentially as described (121) with minor modifications. Briefly, muscles were pre-incubated in KHB/0.1% BSA/38 mM mannitol/2 mM sodium acetate for 30 minutes. The muscles were then transferred to the same solution either without insulin (basal) or with 60 μU/ml

(submaximal, 0.4 nM) or 2 mU/ml (maximal, 12.8 nM) insulin for 10 minutes. In all cases, the left epitrochlearis muscle was incubated without insulin and the contralateral right muscle was incubated with either submaximal or maximal insulin. The muscles were rinsed by incubation in KHB/0.1% BSA/40 mM mannitol with or without insulin for 10 minutes. The muscles were then incubated in KHB/0.1% BSA/38 mM mannitol (0.2 µCi/ml)/2 mM [^{3}H]2-deoxyglucose (1.5 µCi/ml) for 20 minutes after which they were blotted dry over ice on filter paper pre-wet with incubation medium, rapidly cut cross-wise into two pieces (~1/3 and 2/3 of the muscle size), placed in aluminum foil, and frozen in liquid nitrogen. During all incubation steps, the muscles were kept in stoppered vials under a constant stream of 95% O_2/5% CO_2 in a 37º C shaking water bath at 60 rpm. For determination of 2-deoxyglucose uptake, measurement of radiolabel in the muscle was performed as described by Hansen *et al*., using mannitol to determine the extracellular space (104). Briefly, the approximate one-third section of the muscle was weighed, boiled in 1 ml of water for 10 minutes, cooled on ice for 10 minutes, and centrifuged to remove the non-soluble material. Aliquots of the supernatant were counted in duplicate on a scintillation counter with pre-programmed windows for dual scintillation counting of ^{3}H and ^{14}C. As basal 2-deoxyglucose uptake did not differ within groups when the contralateral muscle was used for either submaximal or maximal 2-deoxyglucose uptake (data not shown), the results are combined for presentation of the data. Extracellular space was calculated from [^{14}C]mannitol, which does not cross the sarcolemma (51) and did not differ among groups (data not shown).

Insulin binding

Insulin binding experiments were performed essentially as described (21; 169). Epitrochlearis muscles were pre-incubated in KHB/0.1% BSA/40 mM mannitol. After 15 minutes, the muscles were transferred to KHB/0.1% BSA/40 mM mannitol containing [^{125}I]insulin (0.12 µCi/ml). The right epitrochlearis muscles were exposed to 0.4 nM insulin and the contralateral left muscles were incubated with 7.5 µM insulin. During these steps, the muscles were kept in stoppered vials under a constant stream of 95% O_2/5% CO_2 in a shaking water bath at 60 rpm at 37º C. The muscles were then washed 8 times for 5 minutes each in 5 ml of ice-cold KHB/0.1% BSA/40 mM mannitol, dissolved in 1 N NaOH, and neutralized with 2 N HCl. Aliquots were counted in duplicate on a gamma counter. Non-specific binding was determined from samples incubated with 7.5 µM insulin and subtracted from the contralateral muscle to obtain values for specific insulin binding. Non-specific binding did not differ between groups (data not shown). An aliquot of the dissolved muscle was used for determining protein concentration using the Bradford method (26).

Immunoblots and immunoprecipitations

Immunoanalysis was performed on the remaining 2/3 of the epitrochlearis muscles from animals where the right muscle was incubated with submaximal insulin. The left epitrochlearis muscles, which were incubated without insulin, were homogenized in 15 ml/g homogenization buffer (50 mM HEPES, pH

7.4, 4 mM EGTA, 10 mM EDTA·Na_4, 15 mM $Na_4P_2O_7$, 100 mM β-glycerophosphate, 25 mM NaF, 1% Igepal CA630, 5 mM activated Na_3VO_4, and 50 µg/ml each of leupeptin, pepstatin, and aprotinin), rotated end-over-end at 4º C for 1 hour, centrifuged at 16,000 *g* at 4º C for 20 minutes, and the supernatant was frozen in aliquots at -80º C following a Bradford assay for protein determination (26). These samples were used for immunoblot analysis and citrate synthase activity as described below. The right epitrochlearis muscles (incubated with submaximal insulin) were treated in the same manner, except that they were homogenized in immunoprecipitation buffer (50 mM Tris-HCl, pH 8.2, 150 mM NaCl, 1 mM EDTA·Na_4, 1 mM EGTA, 1% Triton X-100, 0.25% deoxycholic acid, 0.25% lauryl sulfobetaine, 0.25% caprylyl sulfobetaine, 0.5% 3-(1-pyridino)-1-propanesulfonate, 2.5 mM activated Na_3VO_4, 2.5 mM phenylmethanesulfonyl fluoride, and 25 µg/ml each of leupeptin, pepstatin, and aprotinin); these samples were used for immunoprecipitation experiments as described below.

For immunoblot analysis, homogenate protein from the left muscles was subjected to sodium dodecyl sulfate-polyacrylamide gel electrophoresis and transferred to a nitrocellulose membrane. The membranes were stained with Ponceau-S to verify equal loading and blocked for one hour. Following an overnight incubation with primary antibodies at 4º C, the membranes were washed, incubated with secondary antibody for one hour, washed again, treated with an enhanced chemiluminescent reagent, and exposed to film for visualization of the protein. Protein bands were quantified using a laser

densitometer (Molecular Dynamics, Piscataway, New Jersey). Optimal blocking conditions, primary antibody dilutions and conditions, washing protocol and reagent, and secondary antibody concentration and conditions were determined separately for each protein assayed. All gels were loaded with an equal amount of a loading control which was used for normalization of data between blots. The loading control for PTP1B was SW13 cell extract; the loading control for all other antibodies was homogenate of an insulin-stimulated epitrochlearis muscle from a non-experimental rat. Immunoblots for Akt and Akt Ser^{473} phosphorylation were performed on muscles stimulated with submaximal insulin and homogenized in immunoprecipitation buffer.

For immunoprecipitation analysis, 500 µg of homogenate protein from muscles incubated with submaximal insulin was rotated end-over-end overnight at 4º C with 5 µg of polyclonal anti-IRβ antibody. A 50% protein A agarose bead slurry (100 µl) was added and the samples were rotated end-over-end at 4º C for 2 hours, after which the beads were washed and boiled in 60 µl of sample buffer. Samples were loaded on a gel and subjected to immunoblot analysis for phosphotyrosine or IRβ using monoclonal antibodies as described above. The membranes were then stripped using Re-Blot Plus Mild (Chemicon) according to the manufacturer's instructions and re-probed for IRβ, PTP1B, SHP2, or PKCθ as indicated in the figure legends. Quantification of each blot with IRβ immunoprecipitate is expressed relative to the amount of IRβ detected in the same lane on the blot and normalized to the loading control. As a negative control, an equivalent amount of submaximal insulin-stimulated muscle was also

subjected to the immunoprecipitation protocol using 5 µg of rabbit immunoglobulin G in place of anti-IRβ antibody.

Citrate synthase activity

Muscle homogenate (50 and 100 µg) from samples incubated without insulin was used for determination of citrate synthase activity (262). Briefly, samples were diluted into a final volume of 400 µl of 100 mM KH_2PO_4/100 mM K_2HPO_4, pH 7.4/50 µM EGTA/50 µM EDTA·Na_4 and kept on ice. Duplicate samples of 100 µl and 200 µl each were mixed into a final volume of 900 µl of 100 mM Tris, pH 8.0/0.167 mM acetyl coenzyme A/0.111 mM 5,5'-dithiobis-(2-nitrobenzoic acid) and placed in a 30º C water bath for 5 minutes. Oxaloacetic acid (100 µl at 5 mM) was immediately added and the reaction was measured in a spectrophotometer at 412 nM for 3 minutes.

Glycogen concentration

The approximately 2/3 sections of the left epitrochlearis muscles incubated without insulin (from animals where the right muscle was incubated with maximal insulin) were used for determination of glycogen concentration using the anthrone method (107). Briefly, frozen muscle samples were dissolved in 5 M KOH, and glycogen was precipitated with ethanol. The glycogen precipitate was then hydrolyzed by boiling in 5 N HCl for one hour, neutralized with 5 N NaOH, and an aliquot of sample was boiled in 95% H_2SO_4/0.1%

anthrone for 15 minutes. The concentration of glucosyl units was then determined against glucose standards in a spectrophotometer at 620 nM.

Statistics

Groups were compared using analysis of variance (ANOVA), and the Student Neuman-Keuls post-hoc test was used to determine which groups were different. Total running distance, running distance during the third week and on day 21, initial and final body mass, total food intake, and food intake on the night before sacrifice (see Chapter 5) were each considered and eliminated as possible covariates for 2-deoxyglucose uptake. Experiments involving PTP1B, SHP2, and PKCθ were also analyzed using ANOVA with a contrast statement (200) to compare the mean of WL5 and WL29 to the mean of WL53 and SED5. Since an analysis of residuals showed some extreme values, the results were verified using the nonparametric Wilcoxon Rank Sum test. A one-sided alternative was used for both the contrasts and the Rank Sum test. Significance for all tests was defined at $p < 0.05$. All data are presented ± the standard error of the mean (SEM). Statistics were performed using either SigmaStat (Systat Software, Inc., Point Richmond, California) or SAS (SAS Institute Inc., Cary, North Carolina).

RESULTS

2-Deoxyglucose uptake

2-Deoxyglucose is a glucose analog whose uptake into isolated skeletal muscle preparations has been shown to accurately estimate glucose uptake (104). 2-Deoxyglucose uptake into the isolated epitrochlearis muscle *in vitro* was measured either without insulin (basal) or in the presence of a submaximally (60 μU/ml) or maximally (2 mU/ml) stimulating insulin concentration. Basal 2-deoxyglucose uptake did not differ among the four treatment groups, indicating that the post-exercise increase in basal 2-deoxyglucose uptake had dissipated (235). Maximal insulin-stimulated 2-deoxyglucose uptake was also not different among the groups (Fig. 8). Submaximal insulin-stimulated 2-deoxyglucose uptake (μmol 2-deoxyglucose/ml intracellular space/20 min) in WL53 (0.740 ± 0.093) was significantly lower relative to WL5 (1.166 ± 0.090); WL29 (1.027 ± 0.139) was intermediate between, but not different from, WL5 and WL53. SED5

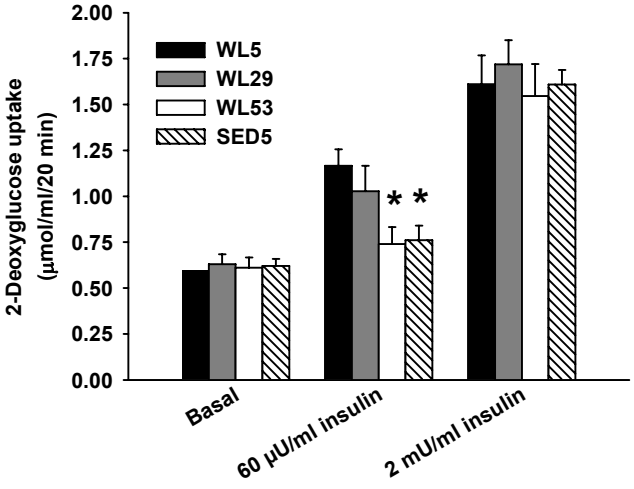

Figure 8. Effect of reduced physical activity on 2-deoxyglucose uptake into isolated epitrochlearis muscle under basal (no added insulin), submaximal insulin (60 μU/ml), and maximal insulin-stimulated (2mU/ml) conditions.
Groups had wheels locked for 5 (WL5), 29 (WL29), or 53 (WL53) hours after three weeks of voluntary wheel running or were sedentary (SED5) without running wheels. Bars are mean ± SEM. *, significantly different from groups not containing an asterisk within the same insulin concentration (ANOVA, $p < 0.05$). n = 15-16 in each group for basal and 7-8 in each group for both insulin concentrations.

(0.761 ± 0.079) was also lower than WL5 and not different from WL53 (See Fig. 1 in Chapter 2 for group descriptions on p. 39). Thus, submaximal 2-deoxyglucose uptake declined from WL5 values to SED5 values after 53 hours of wheel lock. For subsequent immunoanalyses, only muscle from animals used for the submaximal insulin concentrations was assayed as this was the only insulin treatment producing significant differences.

Insulin binding, insulin receptor protein level, and insulin receptor tyrosine phosphorylation

A change in submaximal response with no change in maximal response has been interpreted to suggest that there are alterations at the receptor level (94; 140). This interpretation is based on data showing that in skeletal muscle and adipose tissue, only 10-20% of the receptors need to be bound by insulin to invoke the maximal response (155; 169). Thus, modest changes in receptor affinity or number do not affect the maximum response to insulin. However, increased receptor affinity, insulin receptor content, or insulin receptor activation enhances the likelihood of hormone-receptor interaction; resulting in the same physiological concentration of insulin eliciting a greater submaximal response (94; 140). Thus, an increased submaximal insulin-stimulated 2-deoxyglucose transport with no accompanying increase in the maximal insulin response indicates alterations in insulin signaling at or before the receptor. As the results for 2-deoxyglucose uptake demonstrated this pattern, the next studies were directed toward the insulin receptor.

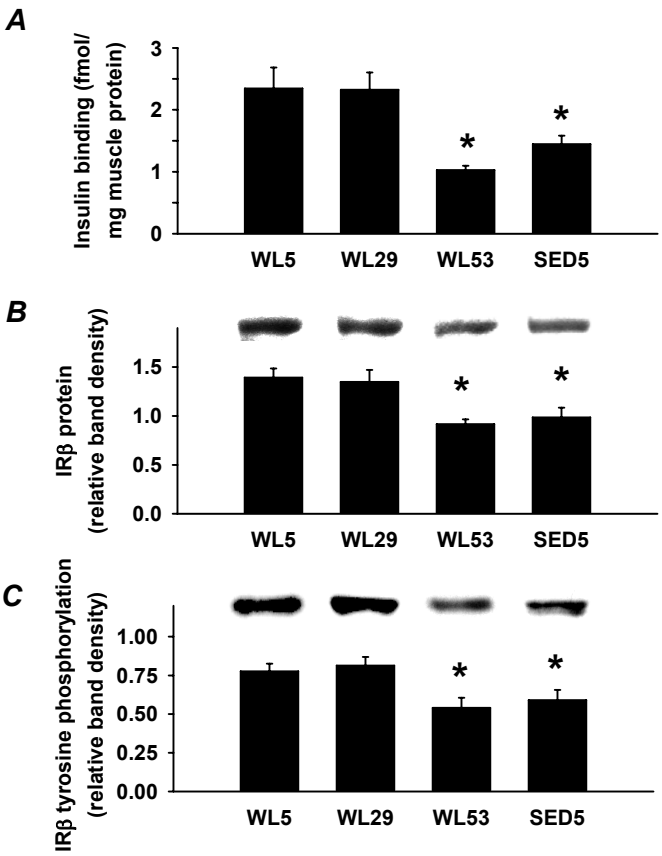

Figure 9. Effect of decreased physical activity on descriptive indices of the insulin receptor and its activation in epitrochlearis muscle.

A: Submaximal insulin binding to the epitrochlearis muscle. *B*: IRβ protein levels relative to loading control (see Methods) with a representative immunoblot (above graph). *C*: Tyrosine phosphorylation of IRβ in response to 40 minutes of submaximal insulin stimulation with a representative immunoblot (above graph). IRβ immunoprecipitates were subjected to immunoblotting for phosphotyrosine, then stripped and re-probed for IRβ (see Methods). Data were normalized to a loading control (see Methods) and are expressed relative to the normalized band intensity for IRβ protein present in the same lane. Bars are mean ± SEM. *, signficantly different (ANOVA, $p < 0.05$) from groups without an asterisk. n = 6-8 in each group.

Specific insulin binding (fmol/mg total protein) at submaximal insulin in the epitrochlearis muscle was lower in WL53 (1.027 ± 0.069) compared to both WL5 and WL29 (2.346 ± 0.336 and 2.324 ± 0.279, respectively; Fig. 9A). WL53 and SED5 (1.446 ± 0.137) were not significantly different. IRβ protein level in WL53 was decreased by 34% and 32% compared to WL5 and WL29, respectively, and was 29% and 27% lower in SED5 than in WL5 and WL29, respectively (Fig. 9B). Relative to the amount of IRβ on the same blot, submaximal insulin-stimulated IRβ tyrosine phosphorylation was decreased by 30% and 27% in WL53 compared to WL5 and WL29, respectively, and was 24% and 27% lower in SED than in WL5 and WL29, respectively (Fig. 9C). Thus, three descriptive indices of the insulin receptor (insulin binding, IRβ protein, and IRβ tyrosine

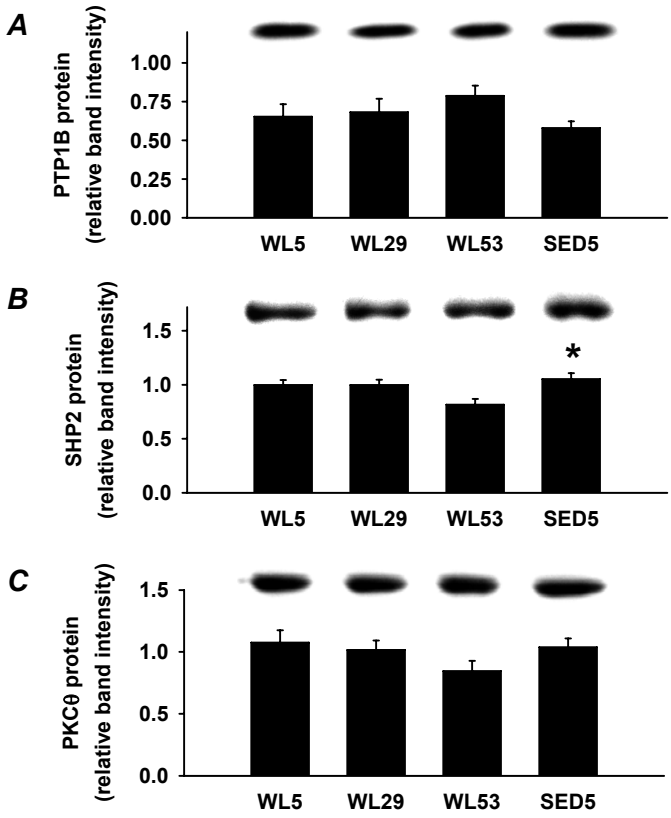

Figure 10. Effect of decreased physical activity on negative regulators of insulin receptor activation in epitrochlearis muscle.

PTP1B (*A*), SHP2 (*B*), and PKCθ (*C*) protein levels normalized to a loading control (see Methods) with representative immunoblots (above graphs). Bars are mean ± SEM. *, significantly different from WL53 (ANOVA, $p < 0.05$). n = 6-8 in each group.

phosphorylation) showed identical treatment patterns, being unchanged from WL5 to WL29, and decreasing in WL53 to SED5 levels.

PTP1B, SHP2, and PKCθ

To obtain information on potential factors producing the change in IRβ tyrosine phosphorylation, levels of three proteins (PTP1B, SHP2, and PKCθ) that can negatively regulate IRβ tyrosine phosphorylation were measured in homogenates and in IRβ immunoprecipitates (74; 213; 239; 268; 316). The pre-hoc hypothesis was that the level of each of these proteins and their association with IRβ upon submaximal insulin stimulation would show an inverse pattern of change compared to the pattern of change in IRβ tyrosine phosphorylation

observed in the earlier portion of the present study, i.e. in comparison to Fig. 9C where WL53 and SED5 were lower than WL5 and WL29 for IRβ tyrosine phosphorylation, WL53 and SED5 would exhibit higher levels of PTP1B, SHP2, and PKCθ than WL5 and WL29. Total protein levels of PTP1B and PKCθ did not differ between groups (Figs. 10A and 10C), while SHP2 protein level was 23% lower in WL53 than SED5 (Fig. 10B). The amount of PTP1B, SHP2, or PKCθ associated with IRβ, expressed per unit of IRβ on the same blot, also was not different between groups ($p = 0.07$ for PTP1B; Fig. 11). Because it had been hypothesized *a priori* that, relative to both WL5 and WL29, both WL53 and SED5 would each have a greater level of PTP1B, SHP2, and PKCθ, and that the association of PTP1B, SHP2, and PKCθ with IRβ would be higher, I further tested this specific hypothesis using ANOVA with a contrast statement (200). Using this analysis, it was found that the mean of SED5 and WL53 had a significantly higher IRβ-associated PTP1B than the mean of WL5 and WL29 (Fig. 11B, inset); PTP1B, SHP2, and PKCθ total protein levels (data not shown) and IRβ-associated SHP2 and PKCθ were not significantly different (Figs. 11C and 11D, insets). These results were confirmed using the Wilcoxon Rank Sum test.

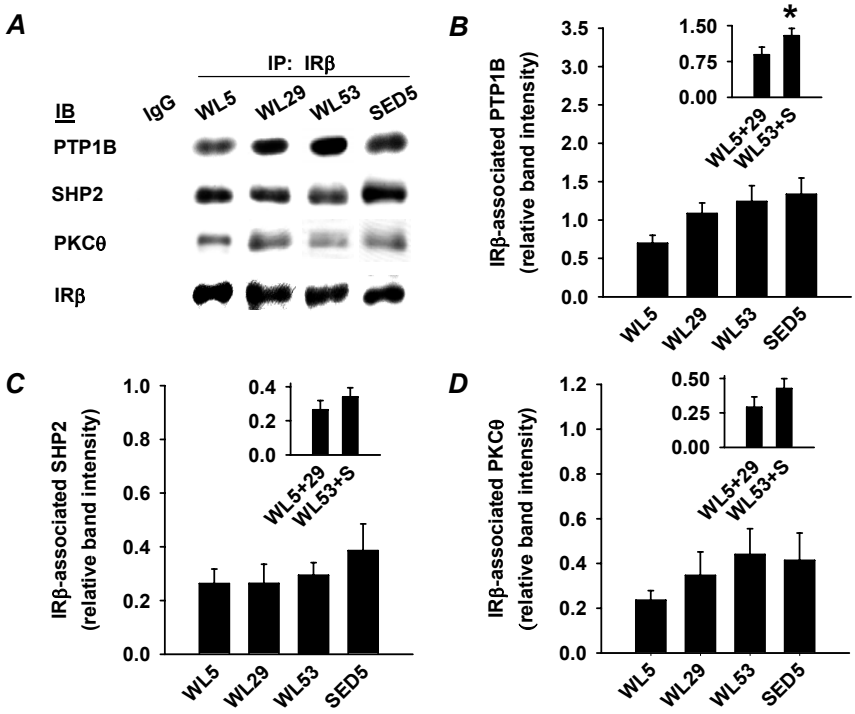

Figure 11. Effect of reduced physical activity on the interaction of PTP1B, SHP2, and PKCθ with IRβ.

IRβ immunoprecipitates were subjected to immunoblotting for IRβ, then stripped and re-probed for PTP1B, SHP2, or PKCθ (see Methods). Data in each panel were normalized to a loading control (see Methods) on the same blot and are expressed relative to the normalized band intensity for IRβ present in the same lane. IgG in the first lane of panel *A* was immunoprecipitated with rabbit immunoglobulin G and is a negative control with no detectable signal. Bars for the main graphs represent the means for each group ± SEM. The bars in the insets illustrate the means ± SEM for the linear combination of the individual group means for WL5 and WL29 (WL5+29) and for WL53 and SED (WL53+S). See Results for more detail. IP, immunoprecipitation; IB, immunoblot; *, significantly different (ANOVA with contrast statement, $p < 0.05$). n = 6-8 in each group.

Akt, citrate synthase activity, glycogen concentration, and GLUT4

Akt total protein content did not differ between groups (data not shown). Akt Ser^{473} phosphorylation per unit of Akt on the same blot was 32% and 40% lower in WL53 and SED5, respectively, than in WL5 (Fig. 12A), providing confirmation that signaling downstream of the insulin receptor is also decreased

after 53 hours of wheel lock. Citrate synthase activity (nmol/mg protein/min) in the epitrochlearis was lower in SED5 compared to all other groups (169 ± 8 in WL5, 167 ± 11 in WL29, 160 ± 6 in WL53, and 134 ± 5 in SED; Fig. 12B), indicating that oxidative capacity (123) of the epitrochlearis muscle did not decline after 53 hours of wheel lock. As other studies have shown a relationship between 2-deoxyglucose uptake and glycogen concentration (114; 126; 137) or GLUT4 protein level (113; 125; 143; 233), these were also measured in the present study. Consistent with other studies using voluntary wheel running (121; 241), epitrochlearis muscle glycogen levels in the present study were not significantly different between groups (Fig. 12C), suggesting that glycogen is not playing a regulatory role in the diminished submaximal insulin-stimulated 2-deoxyglucose uptake in the wheel lock period. GLUT4 protein level in WL53 decreased 29% and 21% relative to WL5 and WL29, respectively (Fig. 12D). GLUT4 was also less in SED5 by 31% and 24% relative to WL5 and WL29, respectively.

DISCUSSION

In rats prohibited from voluntary running after 21 days of access to voluntary running wheels, submaximal insulin-stimulated 2-deoxyglucose uptake in the 53-hour wheel lock group (WL53) exhibited a significant decline to values similar to those in the sedentary group (SED5; Fig. 8). A novel observation of the current study is that insulin binding, IRβ protein level, and insulin-mediated IRβ tyrosine phosphorylation remained at 5-hour wheel lock (WL5) values for 29

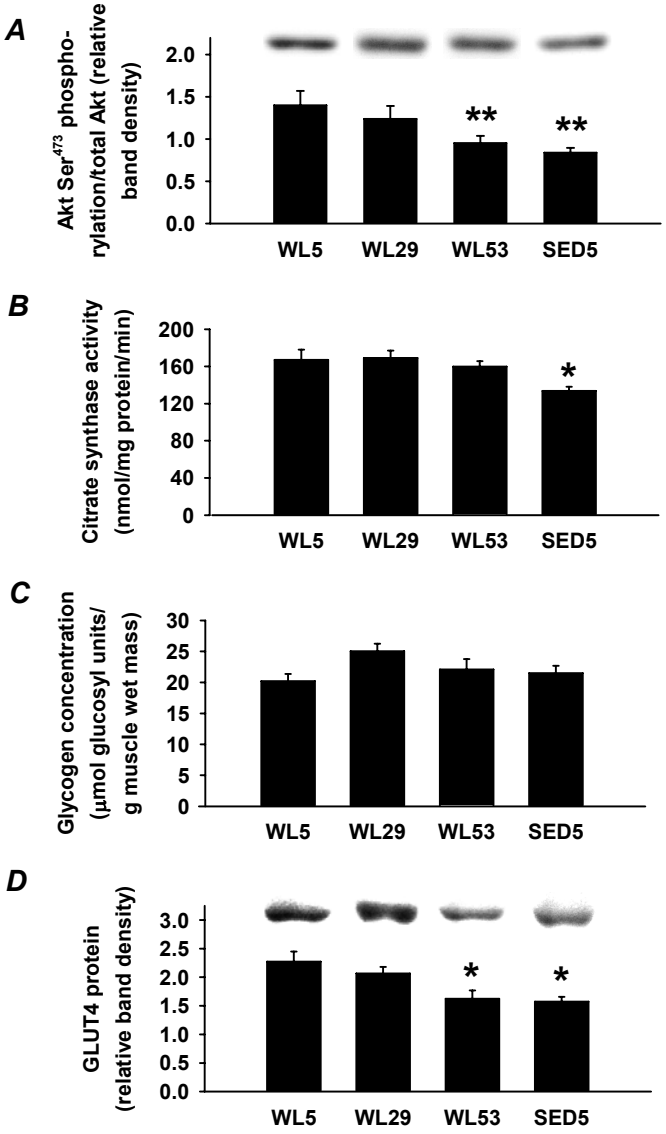

Figure 12. Biochemical adaptations to decreased physical activity in the epitrochlearis muscle.

A: Akt Ser^{473} phosphorylation relative to the total amount of Akt in the same lane and normalized to a loading control (see Methods) with a representative immunoblot (above graph). *B*: Citrate synthase activity. *C*: Glycogen concentration. *D*: GLUT4 protein levels normalized to a loading control (see Methods) with a representative immunoblot (above graph). Bars are mean ± SEM. *, signficantly different (ANOVA, $p < 0.05$) from groups without an asterisk. **, significantly different (ANOVA $p < 0.05$) from WL5. n = 6-8 in each group.

hours of wheel lock (WL29), but declined to SED5 values after 53 hours of wheel lock (Fig. 9). Moreover, GLUT4 protein levels followed this same pattern, declining to SED5 values between 29 and 53 hours of wheel lock (Fig. 12D). These observations are important as they identify by association some of the potential factors that may be involved in diminished submaximal insulin-mediated glucose uptake into the epitrochlearis muscle upon decreased physical activity. Furthermore, the observations demonstrate that these reductions coordinately

	WL29	WL53	SED5
60 μU/ml insulin-stimulated 2-DOG uptake	↔	↓	↓
Insulin binding	↔	↓	↓
IRβ protein level	↔	↓	↓
IRβ tyrosine phosphorylation	↔	↓	↓
Akt Ser^{473} phosphorylation	↔	↓	↓
GLUT4 protein level	↔	↓	↓

Table 1. Directional changes in groups having wheels locked for 29 (WL29) or 53 (WL53) hours and in sedentary (SED5) group relative to 5 hours of wheel lock.

Arrows indicate the relative direction of significant changes (ANOVA, $p < 0.05$) for each of the measured variables. The table demonstrates the similar pattern of change observed in the listed variables.

transpired between 29 and 53 hours after the running wheels were locked (Table 1).

The decrease in IRβ tyrosine phosphorylation per unit of IRβ at 53 hours of wheel lock suggests that, in addition to the decrease in IRβ protein level, there are also concurrent adaptations which diminish IRβ phosphorylation. An important step regulating signal transduction through the insulin receptor is the action of protein tyrosine phosphatases, which dephosphorylate tyrosine residues on the receptor, rendering it inactive (44). To further investigate potential changes in the regulation of IRβ tyrosine phosphorylation, I examined two protein tyrosine phosphatases, PTP1B and SHP2 (25; 74; 239; 257; 316). In addition, I examined PKCθ, which decreases insulin-stimulated tyrosine phosphorylation by inducing serine phosphorylation of IRβ, although it is unclear whether this is a direct or indirect effect (268); transgenic mice that lack PKCθ

are protected from insulin resistance induced by a high fat diet (148). PTP1B, SHP2, and PKCθ protein levels did not differ among WL5, WL29, and WL53, while WL53 was higher than SED5 for SHP2 protein level (Fig. 10). Due to a scarcity of tissue, I was unable to determine the possibility that there is altered localization of PKCθ to the sarcolemma, which could affect its activity and association with the insulin receptor (4; 133). PTP1B, SHP2, and PKCθ associated with IRβ also did not differ between groups (Fig. 11). When ANOVA was used with a contrast statement, the mean of WL53 and SED5 was found to be significantly greater than the mean of WL5 and WL29 for IRβ-associated PTP1B, but not for IRβ-associated SHP2 or PKCθ (Fig. 11, insets). This provides some support for the hypothesis that IRβ-associated PTP1B would be higher in WL53 and SED5 than in WL5 and WL29. Based on evidence showing that PTP1B negatively regulates IRβ tyrosine phosphorylation and skeletal muscle glucose uptake (44; 74; 154; 316), this suggests that PTP1B might play a role in the downregulation of submaximal insulin-stimulated tyrosine phosphorylation between 29 and 53 hours of wheel lock, but further experiments are needed to test this hypothesis.

Insulin stimulates glucose uptake into skeletal muscle by inducing translocation of GLUT4 to the cell membrane (300). Others have shown an association between decreases in epitrochlearis muscle GLUT4 protein level and insulin-stimulated glucose uptake 40-90 hours following the cessation of swim- or treadmill-training (125; 143; 233). In the current study, GLUT4 protein level declined to SED values between 29 and 53 hours of wheel lock, confirming the

previous studies and extending them to include cessation of voluntary wheel running. It is noteworthy that GLUT4 protein level exhibited the same time pattern of decrease as insulin binding, IRβ protein level, and IRβ tyrosine phosphorylation (Table 1), as it raises the intriguing possibility that a single regulatory event could be responsible for the synchronization.

A potential translational significance of the current study to human physiology is that many studies have shown that decreased physical activity produces lower insulin sensitivity in healthy human subjects in as little as 5 days following the cessation of habitual exercise (see Introduction). Despite the clear relationships between physical inactivity and insulin resistance and between insulin resistance and chronic disease (22), there have been few studies examining the initial cellular changes by which a reduction of voluntary physical activity to sedentary levels decreases insulin-stimulated glucose uptake. A unique aspect of the present study is the emphasis on cessation of voluntary running activity in freely fed rats, and the results demonstrate that submaximal 2-deoxyglucose uptake into the epitrochlearis muscle declines to sedentary levels between 5 and 53 hours after cessation of voluntary wheel running (Fig. 8). Moreover, this decline is accompanied by a concomitant decrease in insulin binding, IRβ protein level, submaximal insulin-stimulated IRβ tyrosine phosphorylation, Akt Ser^{473} phosphorylation, and GLUT4 protein level (Table 1). Others have reported the decline in GLUT4 protein following cessation of swim- or treadmill-training (125; 143; 233), but this is the first study to demonstrate a rapid reduction in IRβ protein and essential components of insulin receptor

activation upon the cessation of voluntary wheel running, although my interpretations must be tempered by not knowing whether there is a difference in these variables in the non-insulin-stimulated condition.

In conclusion, decreased physical activity precipitated a rapid and synchronous decline in submaximal insulin-stimulated glucose uptake, descriptive indices of the insulin receptor and its activation, and GLUT4 protein. This suggests that in rats accustomed to daily voluntary wheel running, multiple adaptations regulating insulin-mediated glucose uptake into the epitrochlearis muscle take place between 29 and 53 hours of decreased physical activity, and it raises the possibility that a single regulatory event could be responsible for the coordinated decrease.

Chapter 5: Lower Muscle Mass in Rats without Running Wheels: Growth and Food Intake Comparisons.

INTRODUCTION

Rats undergoing different forms of physical activity such as voluntary wheel running, swim training, or treadmill training, have different responses for food intake and growth. These differential responses are further complicated by gender-dependent responses. Moreover, there are a wide variety of responses reported by different laboratories, and growth and food intake may also be dependent upon the specific rat strain [reviewed in (202)]. In humans, individuals that are more physically active on a regular basis normally consume more calories per body mass than less active individuals (19).

In preliminary experiments, I observed that rats with regular sedentary cage activity ate less and had a lower body mass at the end of the 21-day experimental period relative to rats with access to running wheels (data not shown). As differences in growth and/or food intake could potentially affect other variables being measured, such as glucose uptake into muscle (Chapter 4) or adiposity (Chapter 6), this study was performed to determine the growth rate and food intake of Fischer 344 X Brown Norway F1 hybrid rats with voluntary running

wheels relative to regular sedentary cage activity. In addition, the effect of reducing physical activity by locking the wheels was examined.

Previous reports have shown that some specific skeletal muscles, such as the soleus and extensor digitorum longus, demonstrate hypertrophy in response to voluntary wheel running (29; 242; 243), whereas this hypertrophic effect is not observed in studies involving swim or treadmill training. I therefore considered it possible that the accelerated growth in rats with running wheels that was observed in preliminary experiments might be due to an accelerated growth of skeletal muscle. As rats on running wheels pull with the forelimbs as well as the hindlimbs, it was possible that skeletal muscles from different anatomical locations, i.e. the hindlimb, forelimb, shoulder, and back, might have a hypertrophic response to the wheel training stimulus. This study investigated this possibility.

METHODS

Animal protocol

The animal protocol was approved by the Institutional Animal Care and Use Committee at the University of Missouri-Columbia. Male Fischer 344 x Brown Norway F1 hybrid rats (Harlan) were obtained at age 21-23 days and allowed to acclimatize for one week. The animals were housed in approved temperature-controlled animal quarters (21°C) with a 0400-1600 light : 1600-0400 dark cycle that was maintained throughout the experimental period. After

one week (day 0), the rats were randomly assigned to one of six experimental groups: wheel lock 5 (WL5), wheel lock 10 (WL10), wheel lock 29 (WL29), or wheel lock 53 (WL53), which consisted of 21 days of voluntary wheel access followed by 5, 10, 29, or 53 hours of wheel lock that prevents access to voluntary running, respectively; or SED5 or SED10, which were sedentary groups without running wheel access for the entire 21 days, then sacrificed at either the same time point as WL5 or WL10, respectively (See Fig. 1 in Chapter 2, p. 39). At this time (on day 0), the animals were separated into individual cages of the same dimensions; cages for animals in the running groups (WL5, WL10, WL29, and WL53) were equipped with a voluntary running wheel outfitted with a Sigma Sport BC 800 bicycle computer (Cherry Creek Cyclery, Foster Falls, Virginia) for measuring running activity. All animals were provided with 200 g of standard rodent chow (Formulab 5008, Purina Mills, St. Louis, Missouri) at the beginning of each week (days 0, 7, and 14) when cages were changed, and running activity (for groups with wheel access), body mass, and food intake were measured daily between 0400-0500 hours. On day 21 (after 21 days of running activity), the wheels were locked for all running groups at 0400 hours. SED5 and WL5 were sacrificed at 0900 hours, and SED 10 and WL10 were sacrificed at 1400 hours. The WL29 group remained in their cages with locked wheels before being sacrificed the following day (on day 22) at 0900 hours (after 29 hours of wheel lock), and WL53 remained in their cages with locked wheels until day 23 when they were sacrificed at 0900 hours (after 53 hours of wheel lock). All animals had *ad libitum* access to food at all times until the day of sacrifice, when food was

removed at 0400 hours. At the time of sacrifice, the animals were anesthetized with an intraperitoneal injection of 60 mg pentobarbital/kg body mass. The animals were exsanguinated by removal of the heart. The soleus, gastrocnemius/plantaris complex, and quadriceps muscles were harvested from 10 animals each from the WL5 and SED5 groups from the same rats as those used in the experiments in Chapter 4. In addition, soleus, triceps, epitrochlearis, acromiotrapezius, and latissimus dorsi muscles were obtained from 7-10 animals each from the WL5 and SED5 groups used for experiments with epididymal fat described in Chapters 6 and 7. Due to time considerations during surgery, it was not possible to also remove any abdominal or chest muscles nor was it possible to obtain any facial muscles that would likely not be recruited during voluntary wheel running.

Statistics

Comparisons in Table 2 were made using analysis of variance (ANOVA), with initial body mass being used as a co-variate for body mass on day 21. The Student-Neuman-Keuls *post-hoc* test was used to determine group differences. For comparisons of growth and food intake, all groups with wheel access (WL5, WL10, WL29, and WL53) were combined into one group for the 21 days of unrestricted wheel access (RUN) and those without wheel access (SED5 and SED10) were combined into one group (SED); comparisons between the two groups were made using Student's t-test, as were comparisons between SED5

and WL5 for muscle mass. Correlations were determined using Pearson's product-moment correlation coefficient.

To compare growth and food intake before and after wheel lock, two comparisons were made. *Comparison 1 (before and after wheel lock for WL29 and WL53 groups)*: To determine if wheel lock altered growth and food intake in WL29 and WL53, a linear regression equation was fitted for each animal's data for days 4-21 (days 1-3 were not used as animals in each group exhibited considerable variability during this time (data not shown), presumably due to acclimatization to running wheels, new cages, and/or isolation); the regression equation was used to predict what the value for each animal would be on days 22 and 23 if the wheels had not been locked (i.e. if the animals had continued access to running wheels). The differences between the predicted values and the observed values for the same animal were compared using Student's t-test. *Comparison 2 (between SED and the combined WL29 and WL53 groups after wheel lock)*: To determine if growth and food intake after wheel lock in WL29 and WL53 differed from SED, linear regression equations (using days 4-21) were determined for each animal in SED; these equations were used to predict growth and food intake values for each animal in SED for days 22 and 23 had they not been sacrificed on day 21. For comparison of the predicted values from SED and the observed values from the combined WL29 and WL53, multiple statistical approaches were employed dependent on the normality of the measured parameter. *Food intake* values were compared using Student's t-test. For *growth* and *feed efficiency*, an analysis of residuals demonstrated some extreme

values such that the data did not exhibit a Gaussian distribution; therefore, these variables were compared using the non-parametric Mann-Whitney rank-sum test. For both comparison 1 and comparison 2, WL29 and WL53 were combined into one group for the comparisons on day 22.

Significance for all tests was set at $p < 0.05$. All data are presented as mean ± standard error of the mean (SEM). Microsoft *Excel* (Redmond, Washington) was used for regression and prediction of growth and food intake data for days 22 and 23; all other statistics were performed using SigmaStat software (Systat Software, Inc., Point Richmond, California).

RESULTS

Running activity

There was no difference among wheel lock groups undergoing voluntary running in their total 21-day running distance, in total 21-day time run, or in the distance or time run on the last night of running (Table 2). The average daily running distance for all groups is presented in Fig. 13A. There was a significant negative correlation between the initial body mass (on day 0) and the total distance run ($r = -0.332$, $p = 0.002$; Fig. 13C).

Group	BM day 0 (g)	BM day 21 (g)	BM on day of sacrifice (g)	Absolute increase in BM from day 0 to day 21 (g)	Fold-increase in BM from day 0 to day 21
WL5	75.9±1.9	211.0±2.7	211.0±2.7	135.1±1.6	2.81±0.05
WL10	74.1±2.6	206.8±5.9	206.8±5.9	132.7±4.9	2.81±0.09
WL29	70.6±1.6	205.2±3.3	208.3±3.3	134.6±2.4	2.92±0.05
WL53	70.3±1.3	208.5±2.5	215.7±2.6	138.3±1.8	2.98±0.04
SED5	75.3±2.3	187.2±3.4***	187.2±3.4***	111.9±1.8***	2.51±0.04**
SED10	76.6±3.2	192.3±3.0*	192.3±3.0*	115.7±2.3***	2.54±0.08*

Group	Total running distance (km)	Running distance on last night (km)	Total running time from day 0 to day 21 (h)	Running time on last night (h)	Total food intake from day 0 to day 21 (g)	Food intake (g) per body mass (g) on day before sacrifice (X 1000)
WL5	98.46±5.28	5.87±0.46	41.5±1.9	2.1±0.1	373±5	104±1[a]
WL10	98.61±5.36	4.60±0.80	41.5±2.1	1.7±0.3	361±9	102±1[a,b]
WL29	98.68±5.78	5.53±0.49	41.6±2.1	2.0±0.2	364±5	96±1
WL53	102.79±4.46	6.36±0.52	43.3±1.7	2.3±0.2	370±4	100±1[b]
SED5					313±4***	89±1***
SED10					315±4***	87±1***

Table 2. Comparison of body mass (BM), growth, running activity, and food intake variables across all groups.

Data for all groups were compared using ANOVA, with the Student-Neuman-Keuls *post-hoc* test. For body mass on day 21, initial body mass (body mass on day 0) was used as a co-variate. Values are means ± SEM. *, **, and ***, significantly different ($p < 0.05$, 0.005, and 0.001, respectively) vs. WL5, WL10, WL29, and WL53. Wheel lock groups not sharing a letter for relative food intake on the last night are significantly different ($p<0.05$). n = 26 each for WL5, WL29, WL53, and SED5. n = 10 each for WL10 and SED10.

Growth rate

SEDENTARY RATS GREW MORE SLOWLY THAN RUNNERS BEGINNING ON DAY 4.

There was no difference in the initial body mass between RUN and SED (75.6 ± 1.8 and 72.5 ± 0.9 g, respectively; Fig. 14A, left panel). On days 1-3, SED had a greater absolute body mass than RUN (Fig. 14A, left panel). This was due to

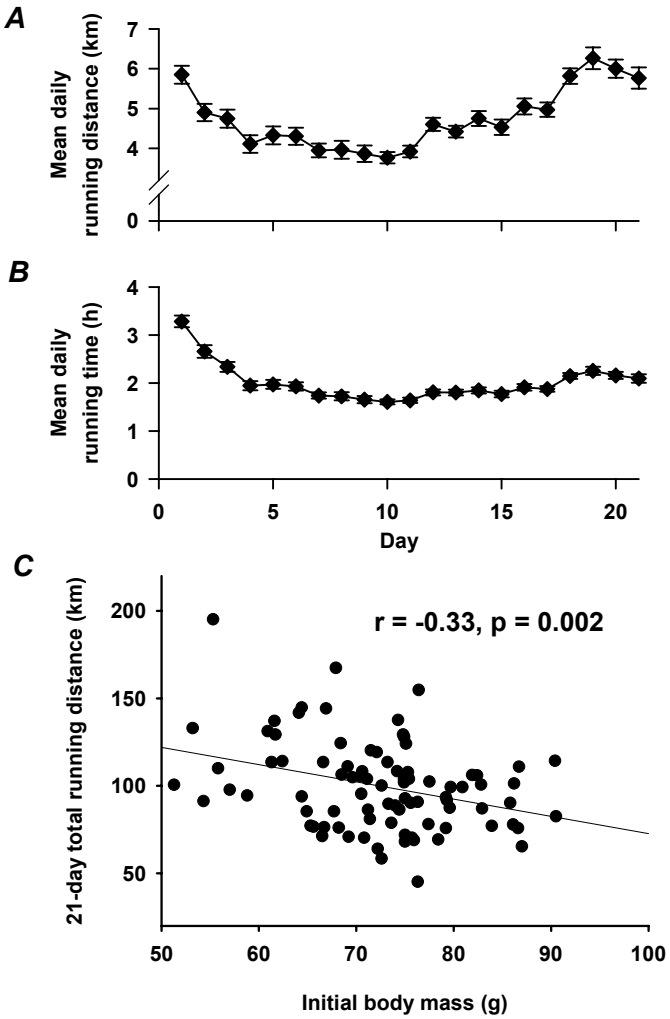

Figure 13. Running activity and relationship to initial body mass.

The mean daily running distance (*A*) and time (*B*) of the combined running groups and the negative correlation of total 21-day running distance to initial body mass (*C*) are shown. Data points for (*A*) and (*B*) represent the mean ± SEM for each day's running activity. n = 88.

greater absolute and relative growth rates on day 1 in SED relative to RUN, but growth rates were not different on days 2 or 3 (Figs. 14B and 14C, left panels). However, beginning on day 4 both the absolute and relative growth rates were less in SED than in RUN (Figs. 14B and 14C, left panels); this was reflected in a significantly lower body mass in SED than RUN beginning on day 12 and remaining through day 21 (Fig. 14A, left panel), such that SED weighed 9.4% less ($p < 0.001$) on day 21 than did RUN. Over the 21-day experimental period, SED animals gained an average of 113.0 ± 8.8 g and RUN animals gained an average of 135.6 ± 10.7 g ($p < 0.001$ between groups). This represented a fold-increase in body mass of 2.52 ± 0.04 in SED and 2.89 ± 0.03 in RUN ($p < 0.001$ between groups). There was not a significant correlation between total running distance

and fold-increase in body mass ($r = 0.15$, $p = 0.16$; Fig. 15). Body mass and growth data for individual groups are presented in Table 2.

GROWTH RATE DECREASED ON THE FIRST DAY OF NO VOLUNTARY RUNNING. *Comparison 1 (before and after wheel lock comparison for WL29 and WL53 groups; see Methods):* Upon the cessation of voluntary wheel running, the absolute increase in body mass on days 22 and 23 was 56% and 43% less, respectively, than their predicted growth values (Fig. 14B, middle panel). Relative increase in body mass for wheel lock groups on days 22 and 23 was 47% and 26% less, respectively, than their predicted values (Fig. 14C, middle panel).

SEDENTARY RATS GREW FASTER THAN RUNNERS WHEN VOLUNTARY RUNNING CEASED. *Comparison 2 (between SED and the combined WL29 and WL53 groups after wheel lock; see Methods):* The predicted absolute increase in body mass for SED on days 22 and 23 was 73% and 33% greater, respectively, than the observed values for the wheel lock groups after running ceased (Fig. 14B, right panel). The predicted relative change in body mass for SED on day 22 was 65% greater than the observed value for the wheel lock groups, but on day 23, the predicted and observed values were not significantly different (Fig. 14C, right panel).

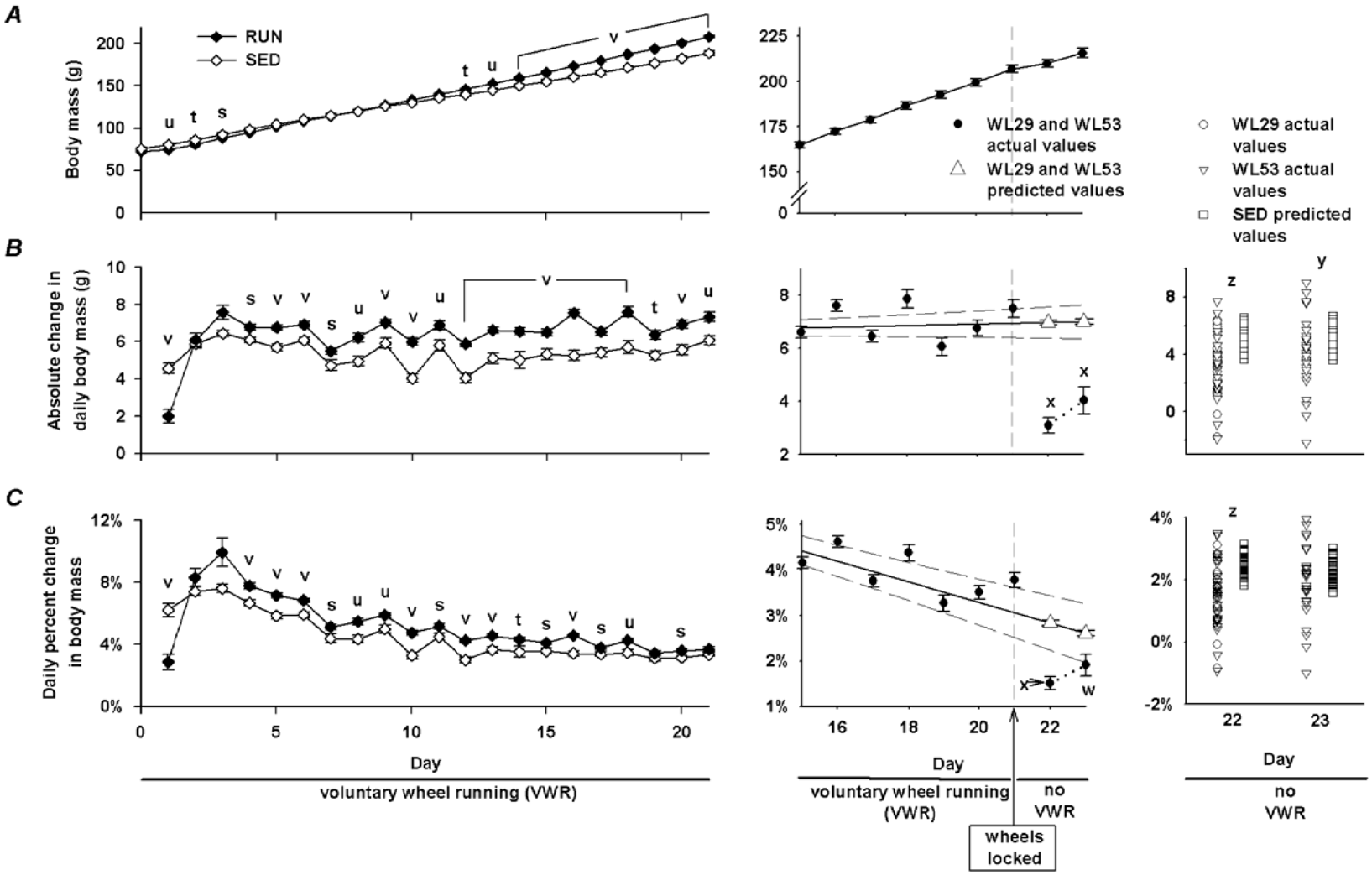

Figure 14. Growth characteristics. Legend on next page.

Figure 14. Growth characteristics. (previous page)

(*A*) Growth curve, (*B*) absolute growth rate, and (*C*) relative growth rate. Absolute growth rate (*B*) is daily growth expressed as the absolute change from the previous day's mass. Relative growth rate (*C*) is the daily growth rate expressed as percent change relative to the previous day's mass. *Left panels*: *Comparison of combined groups with unrestricted voluntary running wheel access (RUN; solid diamond) and groups with regular sedentary cage activity (SED; open diamond) during 21 days of voluntary wheel running.* Data points represent the mean ± SEM. s, t, u, and v, significant difference ($p < 0.05$, 0.01, 0.005, and 0.001, respectively, between SED and RUN; Student's t-test). n = 88 for RUN and 36 for SED. *Middle panels*: *Growth characteristics for 7 days prior and 2 days after running wheels were locked.* Voluntary running wheels were locked beginning on day 21 (indicated by arrow; see Methods) so that the rats could no longer run. The legend for data points in the lower portion of *A* is for the middle panels of *A*, *B*, and *C*. *Middle panel for (A):* The solid line connects actual values of the combined WL29 and WL53 groups for days 15-23. No predicted values are displayed in this panel. *Middle panels for (B) and (C):* (*Comparison 1*, see Methods): Expected values for days 22 and 23 for WL29 and WL53 were predicted from linear regression equations for each animal based on values from days 4-21 (only data starting on day 15 are shown for clarity of the figure). The open triangles represent the predicted values on days 22 and 23, and the solid circles represent the actual values from days 15- 23. The solid line represents the regression line, and the dashed lines represent the 95% confidence intervals. The dotted line in the lower right-hand corner connects the observed values for days 22 and 23. The differences between the predicted and observed values for each animal were compared using Student's t-test. Data points represent the mean ± SEM. w and x, significant difference ($p < 0.05$ and 0.001, respectively) between observed and predicted values. n = 52 for day 22, and n = 26 for day 23. *Right panels*: (*Comparison 2*, see Methods): *Scatter plots of observed values for WL29 (open circle in columns 1 and 3) and WL53 (open inverted triangle in columns 1 and 3) and predicted values for SED (open square in columns 2 and 4) for absolute and relative growth rates on days 22 and 23.* The legend for data points is located above right panel *B*. Data points represent the individual values for each animal. Values for SED were predicted for each animal using linear regression analysis and were compared to observed values for WL29 and WL53 using the Mann-Whitney rank-sum test. y and z, significantly different ($p < 0.005$ and 0.001, respectively). n = 26 each for WL29 and WL53 (total of 52 on day 22) and 36 for SED. For both *Comparison 1* and *Comparison 2*, WL29 and WL53 were combined for analysis of day 22; only WL53 was used for analysis of day 23.

Food intake

FOOD INTAKE WAS LOWER IN SEDENTARY RATS THAN IN RUNNERS BEGINNING ON DAY 5. Absolute food intake was greater in the combined sedentary groups (SED) than the combined running groups (RUN) on day 1, but was lower in SED than RUN beginning on day 5 and extending through day 21 (Fig. 16A, left panel). Relative food intake was greater in SED than RUN on day 1, but was lower in SED than RUN on all other days except for day 4 (Fig. 16B, left panel), such that relative

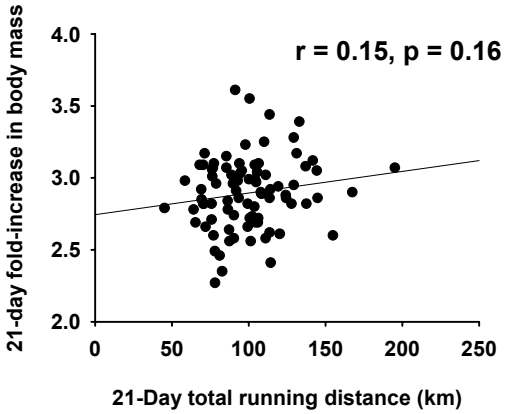

Figure 15. Relationship between 21-day total running distance and fold-increase in body mass.

n = 88.

daily food intake was an average of 10.8% ($p < 0.001$) lower in SED than RUN from days 4-21. Feed efficiency, defined as the absolute increase in body mass (g) per total amount of food ingested (g), was higher in SED than in RUN (0.360 ± 0.003 and 0.352 ± 0.002, respectively, Fig. 16C, left panel). Food intake data for individual groups are presented in Table 2.

ABSOLUTE FOOD INTAKE AND FEED EFFICIENCY DECREASED IN RUNNERS WHEN VOLUNTARY RUNNING CEASED. *Comparison 1 (before and after wheel lock comparison for WL29 and WL53 groups; see Methods):* Absolute food intake for wheel lock groups on days 22 and 23 after running wheels were locked was 11% and 10% lower, respectively, than their predicted values (Fig. 16A, right panel). Relative food intake for wheel lock groups on day 22 was 3.4% lower than their predicted values, but was not different from their predicted values on day 23 (Fig. 16B, right panel). Feed efficiency for wheel lock groups on days 22 and 23 were 48% and 33% lower, respectively, than their predicted values (Fig. 16C, middle panel).

SEDENTARY RATS CONTINUED TO EAT LESS THAN RUNNERS WHEN VOLUNTARY RUNNING CEASED. *Comparison 2 (between SED and the combined WL29 and WL53 groups after wheel lock; see Methods):* The predicted absolute food intake for SED on days 22 and 23 was 17% and 20% lower, respectively, than the observed values for the wheel lock groups (Fig. 16A, right panel). The predicted relative food intake for SED on days 22 and 23 was 17% and 23% lower, respectively, than the observed values for the wheel lock groups (Fig. 16B, right panel). The predicted feed efficiency for SED on days 22 and 23 was 109% and

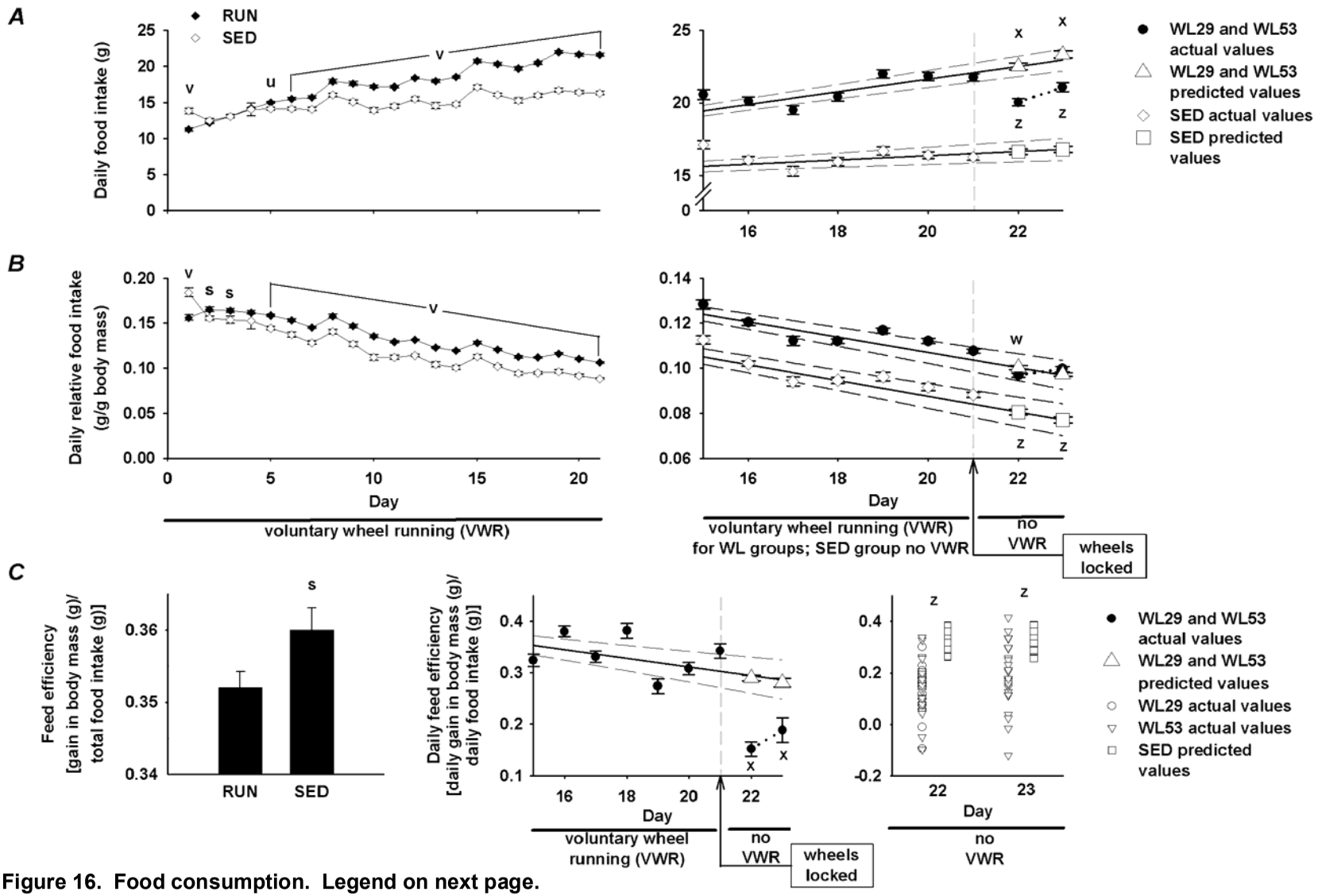

Figure 16. Food consumption. Legend on next page.

Figure 16. Food consumption. (previous page)
Absolute food intake (*A*), relative food intake (*B*), and feed efficiency (*C*). *Leftmost panels*: *Comparison of combined groups (WL5, WL10, WL29, and WL53) with unrestricted voluntary running wheel access (RUN, solid diamond) and sedentary groups (SED, open diamond).* The group legend for the left panels of (*A*) and (*B*) is located at the top of (*A*). Feed efficiency in the left panel of (*C*) is the gain in body mass from days 0 to 21 relative to the total food intake for the same period. Data points and bars represent the mean ± SEM. s, u, and v; significant difference ($p < 0.05$, 0.005, and 0.001, respectively; Student's t-test) between SED and RUN. n = 88 for RUN and 36 for SED. *Right panels for (A) and (B): Food intake before and after running wheels were locked.* Voluntary running wheels were locked beginning on day 21 (indicated by the arrow; see Methods) so that the rats could not run. Predicted values for days 22 and 23 for WL29 and WL53 (open triangle) and for SED (open square) were predicted from linear regression equations for each animal based on actual values from days 4-21 for WL29 and WL53 (solid circle) and SED (open diamond). Only data starting on day 15 are shown for clarity of the figure. The solid lines represent the regression lines, and the dashed lines represent the 95% confidence intervals. The dotted line connects the observed values for days 22 and 23. (*Comparison 1*, see Methods): The differences between the predicted and observed values for each animal in WL29 and WL53 on days 22 and 23 were compared using Student's t-test. w and x, significant difference ($p < 0.005$ and $p < 0.001$, respectively) between predicted and actual values for WL29 and WL53. (*Comparison 2*, see Methods): The differences between predicted values for SED and the observed WL29 and WL53 values were compared using Student's t-test. z, significant difference ($p < 0.001$) between predicted values for SED and actual values for WL29 and WL53. Data points represent the mean ± SEM. n = 52 for both the actual and predicted values for the combined WL29 and WL53 on day 22, n = 26 for WL53 on day 23, and n = 36 for SED for both the actual and predicted values. *Middle panel for (C): Same presentation as for right panels of (A) and (B), except that SED values are not plotted and only Comparison 1* is made. *Right panel for (C): Scatter plots of observed feed efficiency values for WL29 (open circle in columns 1 and 3) and WL53 (open inverted triangle in columns 1 and 3) and predicted values for SED (open square in columns 2 and 4) during no voluntary wheel running (VWR) on days 22 and 23.* Data points represent the individual values for each animal. (*Comparison 2*, see Methods): Values for SED were predicted for each animal using linear regression analysis and were compared to observed values for WL29 and WL53 with the Mann-Whitney rank-sum test (see Methods). z, significant difference ($p < 0.001$) between predicted values for SED and actual values for WL29 and WL53. n = 26 each for WL29 and WL53 (total of 52 on day 22) and 36 for SED. For both *Comparison 1* and *Comparison 2*, WL29 and WL53 were combined for analysis of day 22; only WL53 was used for analysis of day 23.

66% greater, respectively, than the observed values in the wheel lock groups (Fig. 16C, right panel).

Skeletal and left ventricular muscle mass

SEDENTARY RATS HAD SMALLER SKELETAL MUSCLE MASS THAN RUNNERS. The absolute wet mass of each muscle that was dissected out was significantly lower in SED5 than in WL5 (Fig. 17A). Muscle wet mass relative to body mass was not different for 6 of the 7 muscles (Fig. 17B). Left ventricular mass was 16% lower ($p < 0.001$) in SED5 than in WL5 (0.395 ± 0.017 and 0.472 ± 0.014 g, respectively; data not shown). This relationship remained true when left ventricular mass was expressed relative to body mass (2.063 ± 0.023 and 2.203 ± 0.030 [(g/g body mass) x 1000], respectively, ($p < 0.005$; data not shown).

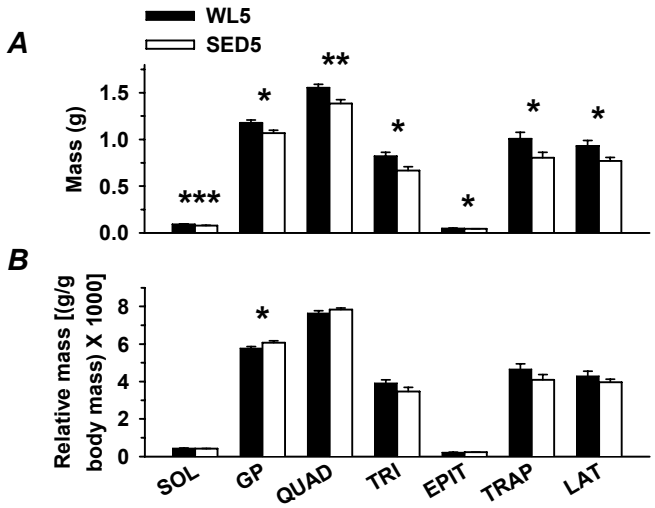

Figure 17. Skeletal muscle mass increases with voluntary wheel running.

Absolute (*A*) and relative (*B*) wet masses for the soleus (SOL), gastrocnemius/plantaris complex (GP), quadriceps (QUAD), triceps (TRI), epitrochlearis (EPIT), acromiotrapezius (TRAP), and latissimus dorsi (LAT) muscles. Muscles were removed from the left side only; the values shown demonstrate only the unilateral masses. Bars represent the means ± SEM. *, **, and ***, significant difference ($p < 0.05$, 0.01, and 0.001, respectively; Student's t-test) between WL5 and SED5 for a given muscle. n = 20 for SOL; 10 for GP, QUAD, TRI, and EPIT; and 7 for TRAP and LAT.

DISCUSSION

Growth rate and food intake

Rapidly growing male rats with regular sedentary cage activity grew at a slower rate than those with access to voluntary running wheels, so that they gained 22.6 g less body mass than the runners when body mass approximately tripled over 21 days (Fig. 14A, left panel). This phenomenon has been observed in some (308), but not all (50; 121; 139; 317), studies using voluntary running wheels with younger male rats; however, the present study used rats that were ~1-2 weeks younger at beginning of the experiment, and I speculate that it may be necessary to expose the rats to running wheels at an earlier age to elicit the acceleration in growth observed herein (Fig. 14B and 14C). One probable contributing factor to the difference in body mass between rats with regular sedentary cage activity and those with running wheel access could be the lower food intake observed in rats with regular sedentary cage activity (Fig. 16A, left

panel). Although a lower food intake might be expected of the animals with regular sedentary cage activity because of their lower body mass, their food intake per body mass was also lower (Fig. 16B, left panel); this is consistent with some (308; 317), but not all (50; 139) studies; the reason for the discrepancy is unclear. Despite the lower food intake and body mass in the group with regular sedentary cage activity, there was a higher feed efficiency in this group relative to the one with wheel access (Fig. 16C, left panel); this is most likely a result of additional calories expended on the running wheel by the group that had wheel access.

Intriguingly, in the current study the accelerated rise in body mass in young male rats with voluntary running was attenuated with one day of decreased physical activity, whereas it took four days to accelerate growth rate at the initiation of voluntary wheel running (Fig. 14B, left and middle panels); this attenuation in growth rate occurred, at least in part, as a result of a lower feed efficiency (Fig. 16C, middle panel) that is consistent with the observations of Lambert *et al*. (165), who showed that feed efficiency in rats during the first and second week of reduced physical activity after 8 weeks of voluntary wheel training decreased 35% and 22%, respectively . It is paradoxical that feed efficiency and growth rate would demonstrate such a drastic reduction during a time in which relative food intake did not change and the animals most likely are expending less energy because they are no longer running. Preliminary data indicate that altered muscle mass is not responsible for the attenuated growth rate (data not shown). The attenuated growth rate also occurred during the

same time frame in which epididymal fat mass increased 25% and omental fat mass increased 48% (see Figs. 18A and 18B in Chapter 6), indicating that although whole-body growth rate was attenuated, these fat pad masses were increasing. Future investigations, including measurement of water intake, intestinal contents, and whole body composition analysis, are needed to further define what factors may contribute to the acceleration in growth with voluntary wheel running and the subsequent attenuation in growth rate when physical activity is reduced.

Although food intake was consistently lower with regular sedentary cage activity relative to rats with running wheels, on day 23, when the animals had not run for 2 days, relative food intake in rats that had their wheels locked for 53 hours was not different than what was predicted if they would have had continued unrestricted access to the running wheel (Fig. 16B, middle panel). Thus, despite a reduction in physical activity, relative food intake on the second day of no voluntary running did not decrease, suggesting a possible lingering increase in voluntary food intake upon the cessation of voluntary running. It is possible that this protracted maintenance of elevated food consumption might contribute to the decreased insulin sensitivity in the epitrochlearis muscle (see Fig. 8 in Chapter 1, p. 73).

Skeletal muscle mass

In addition to lower food intake, another potential contributing factor to the lower body mass in rapidly growing male rats with regular sedentary cage activity

than those with running wheel access is an anabolic response in the skeletal muscle in response to voluntary wheel running. To determine whether differences in skeletal muscle mass contributed to the difference in body mass between rats with and without wheel access, the masses of 7 different muscles [6 predominantly type II and one predominately type I muscle (62; 199)] were measured. A lower skeletal muscle mass in animals with regular sedentary cage activity accounts, at least partly, for the lower growth rate (Fig. 17A). The difference in the combined masses of the 7 muscles was responsible for 8.3% of the lower body mass in sedentary as compared to voluntary running groups. Given that the combined masses of these 7 muscles compose <25% of the muscle mass of the hindlimb, forelimb, back, and trunk (62; 197), it is possible that skeletal muscle mass could account for about one-third of the difference in body mass. Rodnick *et al*. (242; 243) have reported that 6 weeks of voluntary running is associated with larger soleus (predominantly type I), but not plantaris (predominantly type II), muscle mass in male rats with initial body masses of 180 grams; thus, their time points did not encapsulate the period of body weight increase from 70 to 200 grams in male rats as reported herein. The present report extends these findings to rapidly growing rats and demonstrates for the first time that type II muscles undergo increased growth in pubertal male rats in response to voluntary wheel running. Hypertrophy of the predominately type II extensor digitorum longus muscle in adult and old female rats who had 5 or 23 months of voluntary wheel running beginning at 4 months of age has also been reported (29).

Clinical relevance

The presumption is that the lower muscle mass in animals with regular sedentary cage activity is a result of not having access to running wheels during what is a period of rapid growth. Human studies support a proposed concept that physical inactivity during whole body growth results in lower skeletal muscle mass. Physically inactive, 10-year-old children consumed 196 fewer kcal per day, had 3.5% more of their body as fat, had a lower fat-free mass, and exhibited similar body mass index as compared to more physically active children (59). Wells (302) cites reports that children in more current times are more physically inactive with less fat-free mass as compared to the reference child (84). Wells (302) suggests further investigation to test the possibility that children are building up lower levels of fat-free mass during childhood due to declining physical activity levels; an idea supported by the current data. Taken together, a concept is offered that physical inactivity in childhood contributes to lesser growth of skeletal muscle mass.

The observation that there is a lower skeletal muscle mass with regular sedentary cage activity compared to voluntary wheel running in rapidly growing rats may have potential important implications for human health. One potential implication is the possibility that decreased physical activity during childhood and/or adolescent growth might contribute to suboptimal muscular development. Another implication of the lower muscle mass in rats without wheel access is that skeletal muscle accounts for 75-95% of insulin-mediated glucose disposal in

humans (15), so a smaller mass of skeletal muscle would result in less tissue for insulin-mediated glucose disposal. The lower mass of the predominately type I soleus muscle in rats without running wheel access may also have an important health implication as a lower percentage of type I fibers in humans is associated with lower measures of insulin sensitivity (119; 160; 175) and greater adiposity (119; 160; 175; 277; 292).

Summary

In summary, food intake was lower and growth rate was reduced in rats with regular sedentary cage activity relative to voluntary runners, an effect that is at least partially accounted for by less muscle mass. When wheels were locked for voluntary runners, growth rate was diminished despite preservation of relative food intake at pre-wheel lock levels, resulting in a lower feed efficiency. The persistence of relative food intake in runners when physical activity is reduced is associated with decreased submaximal insulin-stimulated glucose uptake into the epitrochlearis muscle (Chapter 4) and increased epididymal adipocyte size (Chapter 6).

Chapter 6: Sustained Rise in Triacylglycerol Synthesis Precedes increased Epididymal Fat Mass when Rats Cease Voluntary Wheel Running

INTRODUCTION

Obesity is a burgeoning problem in the United States and throughout the world (82; 225), with the most disturbing increase occurring among children and adolescents (207; 285). It is generally agreed that the rampant rise in obesity is due to a change in lifestyle factors interacting with a genetic predisposition to accumulate body fat (22; 179; 260; 280; 301). Although several lifestyle factors have been suggested to contribute to the development of obesity, decreasing levels of physical activity are likely a major underlying cause (131; 253; 275; 301). One of the complications frequently associated with obesity is insulin resistance (63; 290); this relationship is particularly true for abdominal obesity (63; 88; 91; 228). There exist strong associations between low physical activity and obesity, between low physical activity and insulin resistance, and between obesity and insulin resistance (22; 248). Despite the strength of these triadic associations, relatively few studies have investigated their integration.

One approach to study the effects of reduced physical activity is to observe changes that occur when physically active animals return to their regular

sedentary cage activity. Some (54; 68; 165), but not all (6), studies have reported indices of fat content increasing 4-14 days after ending physical training in rats. For example, there is a 41% increase in epididymal fat mass (68), a 53% increase in parametrial adipocyte volume (54), and a 23% increase in epididymal adipocyte diameter (165) 14, 4, and 7 days, respectively, following the cessation of exercise training. None of these three studies reported indices of fat content earlier than 4 days following the last bout of exercise. In Chapter 4, I reported that rats that have had access to voluntary running wheels for 21 days exhibit a decline in submaximal insulin-stimulated 2-deoxyglucose transport into the epitrochlearis muscle after their wheels have been locked for 53 hours. Because of the strong inverse association between insulin sensitivity and abdominal fat (63; 88; 91; 228), one purpose of the current study was to test the hypothesis that an increase in the mass and cellularity of epididymal adipose tissue would occur 53 hours after reducing physical activity, coincident with the previously reported loss of enhanced insulin sensitivity in the epitrochlearis muscle.

METHODS

Materials

Dulbecco's phosphate-buffered saline (PBS) was from Gibco (Grand Island, NY, USA). Nylon mesh was from Sefar America (Kansas City, MO, USA). 2-[1,2-^{3}H(N)]deoxyglucose and [carboxyl-^{14}C]trioleoylglycerol were from American Radiolabeled Chemicals (St. Louis, Missouri). [9,10-^{3}H]palmitic acid

was from Sigma (St. Louis, Missouri). Mouse anti-CCAAT/enhancer binding protein-α (C/EBPα) monoclonal and rabbit anti-peroxisome proliferator-γ (PPARγ) polyclonal antibodies were from Affinity Bioreagents (Golden, Colorado).

Animal protocol

The animal protocol was approved by the Institutional Animal Care and Use Committee at the University of Missouri-Columbia. Male Fischer 344 x Brown Norway F1 hybrid rats (Harlan, Indianapolis, Indiana) were obtained at age 21-23 days and allowed to acclimatize for one week. The animals were housed in approved temperature-controlled animal quarters (21°C) with a 0400-1600 light : 1600-0400 dark cycle that was maintained throughout the experimental period. After one week (day 0), the rats were randomly assigned to one of six experimental groups: wheel lock 5 (WL5), wheel lock 10 (WL10), wheel lock 29 (WL29), or wheel lock 53 (WL53), which consisted of 21 days of voluntary wheel access followed by 5, 10, 29, or 53 hours of wheel lock that prevents access to voluntary running, respectively; or SED5 or SED10, which were sedentary groups without running wheel access for the entire 21 days, then sacrificed at either the same time point as WL5 or WL10, respectively (see Chapter 2, Fig. 1, p. 39). At this time (on day 0), the animals were separated into individual cages of the same dimensions; cages for animals in the running groups (WL5, WL10, WL29, and WL53) were equipped with a voluntary running wheel outfitted with a Sigma Sport BC 800 bicycle computer (Cherry Creek

Cyclery, Foster Falls, Virginia) for measuring running activity. All animals were provided with 200 g of standard rodent chow (Formulab 5008, Purina Mills, St. Louis, Missouri) at the beginning of each week (days 0, 7, and 14) when cages were changed, and running activity (for groups with wheel access), body mass, and food intake were measured daily between 0400-0500 hours; these variables were reported in Chapter 5. On day 21 (after 21 days of running activity), the wheels were locked for all running groups at 0400 hours. SED5 and WL5 were sacrificed at 0900 hours, and SED 10 and WL10 were sacrificed at 1400 hours. The WL29 group remained in their cages with locked wheels before being sacrificed the following day (on day 22) at 0900 hours (after 29 hours of wheel lock), and WL53 remained in their cages with locked wheels until day 23 when they were sacrificed at 0900 hours (after 53 hours of wheel lock). All animals had *ad libitum* access to food at all times until the day of sacrifice, when food was removed at 0400 hours. At the time of sacrifice, the animals were anesthetized with an intraperitoneal injection of 60 mg pentobarbital/kg body mass. The animals were exsanguinated by removal of the heart. Sixty-four animals (16 each from WL5, WL29, WL53, and SED5) were used in the study reported in Chapter 4; epididymal adipose tissue from these animals was weighed and used for cellularity experiments or for determination of 2-deoxyglucose uptake as described below. A second set of rats was used exclusively for the current report (10 each from WL5, WL10, WL29, WL53, SED5, and SED10); epididymal and omental adipose tissue from these animals were weighed, quickly frozen in liquid N_2, and stored at -80º C until homogenized as described below and used for

immunoblot analysis or measurement of triacylglycerol synthesis. Plasma was collected via cardiac puncture.

Adipocyte isolation

Adipocytes from epididymal fat pads were isolated by a modification of the Rodbell method (240). Briefly, epididymal fat pads were rinsed in 37º C PBS, minced finely with a scalpel, and incubated at 4 ml/g tissue in Krebs-Ringer-HEPES buffer (KRHB; 130 mM NaCl, 4.7 mM KCl, 1.2 mM KH_2PO_4, 10 mM HEPES, 1 mM $CaCl_2$, 1.2 mM $MgSO_4$, 0.25 mg/ml free fatty acid-free BSA, pH 7.4) containing 2 mg/ml type II-S collagenase and 2 mM sodium pyruvate at 37º C with shaking at 60 rpm for 1 hour. Disrupted cells were centrifuged through 250-µm nylon mesh at 100 *g* for 1 minute and washed twice with 37º KRHB. Packed cells were used in experiments as described below.

Adipocyte size and number

Preparation of epididymal adipose tissue for determination of cell size and number was performed essentially as described (38). Three 60-80 mg epididymal adipose tissue fragments per animal were trimmed from the fat pad, washed twice in 0.9% NaCl, twice in 50 mM 2,4,6-trimethylpyridine/0.9% NaCl, and fixed in 0.12 M osmium tetroxide/50 mM 2,4,6-trimethylpyridine/0.9% NaCl for 8 days at room temperature. Samples were then stored at 4º C for 10-14 days, after which they were washed with 0.9% NaCl and then left in 0.9% NaCl at room temperature for 24 hours. They were subsequently washed with 8 M

urea/0.9% NaCl and then left in this solution at room temperature for 72 hours. Samples were then rinsed through 250-μm nylon mesh with 0.9% NaCl/0.1% Triton X-100 and collected on 20-μm nylon mesh. The cells were then washed from the mesh into beakers containing Isoton II (Beckman-Coulter, Fullerton, California):glycerol (90:10, v:v). Cell size was determined on a Coulter Multisizer II pre-calibrated with 43 μm-diameter latex beads. Background readings were subtracted from each sample prior to analysis. Cell number was calculated from cell volume as described (66), and is calculated as the total amount in both the left and right epididymal fat pads.

Cell volume was also determined in isolated adipocytes. Triplicate aliquots of 60 μl packed isolated adipocytes were fixed in 0.12 M osmium tetroxide/50 mM 2,4,6-trimethylpyridine/0.9% NaCl at room temperature for 1 day, stored at 4º C for 10-14 days, rinsed with 0.9% NaCl/0.1% Triton X-100 onto 20-μm nylon mesh, washed into Isoton II/10% glycerol, and counted on a Coulter counter as described above. Mean cell volume from isolated adipocytes was used to determine the density of the packed cells for calculations of cellular lipid content and 2-deoxyglucose uptake.

Cellular lipid content

For determination of lipid content, 60 μl of packed isolated epididymal adipocytes were added to 2.75 ml of Dole's solution (isopropanol:heptane:1 N H_2SO_4, 80:20:5, v:v:v):heptane:H_2O (27:18:10, v:v:v), vortexed, and allowed to sit for 60 minutes. Samples were then re-vortexed and centrifuged at 450 *g* for 5

minutes. Two milliliters of the upper phase were added to a pre-weighed glass scintillation vial and allowed to dry uncovered in a ventilated hood for 2 days. Vials were then weighed again to determine the amount of lipid.

2-Deoxyglucose uptake

A packed cell volume of 60 µl was added to 290 µl of KRHB containing either no additions, 0.4 nM insulin, 12.8 nM insulin, or 70 µM cytochalasin B and incubated at 37º C for 45 minutes. At this time, 10 µl of [^{3}H]2-deoxyglucose was added to a final concentration of 200 µM (1.5 µCi/ml) and incubated at 37º C for 3 minutes; the reaction was stopped by adding 300 µl of ice-cold cytochalasin B in KRHB to a final concentration of 250 µM. The cells were separated from the medium by centrifugation through dinonyl phthalate oil at 1,000 *g* for 10 seconds. The infranatant layer containing the media was removed by aspiration with a gel-loading tip, and the cells were washed three times with KRHB prior to scintillation counting. Values from the samples containing cytochalasin B, representing non-specific 2-deoxyglucose uptake, were subtracted from each of the other values from the same animal to yield carrier-mediated 2-deoxyglucose uptake. Non-specific 2-deoxyglucose uptake was <10% of basal uptake in all samples and did not differ among groups (14% coefficient of variation; data not shown).

Triacylglycerol synthesis

Approximately 500 mg of frozen epididymal adipose tissue was homogenized in 1.5 volumes of homogenization buffer (50 mM Tris-HCl, 225 mM

sucrose, 1 mM EDTA·Na_4, pH 7.4, 1 mM benzamidine, 1 µg/ml pepstatin, 1 µg/ml leupeptin, 1 µg/ml aprotinin, 1 mM activated Na_3VO_4). The protein concentration of the samples was determined with 5 µl of homogenate using the CB-X protein assay kit (Genotech, St. Louis, Missouri) according to the manufacturer's instructions, except that only ½ of the recommended volume of each solution was used. Aliquots of samples were further diluted in homogenization buffer to a concentration of 2 µg protein/µl. The incorporation of palmitic acid into triacylglycerol was used as a measure of triacylglycerol synthesis (90). Briefly, triacylglycerol synthesis assay buffer [final composition 42 mM K_2HPO_4, 7 mM cysteine, 2 mM $MgCl_2$, 42 mM NaF, 1 mg/ml free fatty acid-free BSA, 15 mM glycerol-3-phosphate, 0.8 mM coenzyme A, 12 mM ATP, 50 µM [^{3}H]palmitic acid (1 µCi/ml), pH 7.4] was added to 20 µl of the 2 µg/µl homogenate protein (40 µg total homogenate protein) to a final volume of 200 µL. Samples were vortexed and incubated at 37º C for 45 minutes. The reaction was stopped by adding 1.5 ml of isopropanol:heptane:H_2O (80:20:2, v:v:v). After 10 minutes, 1 ml of heptane, 500 µl of H_2O, and 10 µl of 100 µg/ml [^{14}C]trioleoylglycerol (100 pCi/µl) were added. Samples were vortexed, centrifuged at 450 *g* for 2 minutes, and washed 3 times with 2 ml of 1 N NaOH:ethanol:H_2O (5:50:45, v:v:v). Six hundred microliters of the upper heptane layer were evaporated in a rotary vacuum (SpeedVac, Savant, Irvine, CA, USA); the residue was re-constituted in chloroform, separated using high-performance thin layer chromatography with hexane:ether:glacial acetic acid (80:20:2, v:v:v) as solvent, sprayed with 0.01% primulin in acetone:H_2O (80:20, v:v), and visualized under ultraviolet light. A

tripalmitoylglycerol standard was applied with the samples to the chromatography plates, and the appropriate band was scraped and subjected to dual label scintillation counting. Recovery of [^{14}C]trioleoylglycerol was used to correct for any differences in recovery between samples. Triplicate tubes containing no sample were run in parallel to determine background, and the mean was subtracted from the values of the samples. The assay was linear with respect to time and the amount of protein, and the concentrations of all substrates and co-factors were within the saturation range.

Immunoblots

Homogenate protein from epididymal fat pads was subjected to immunoblotting as described in Chapter 4; blots were probed for either PPARγ or C/EBPα. The epididymal fat homogenate of three non-experimental animals was combined together and used as a loading control, which was loaded in triplicate on each blot. All results are expressed as arbitrary densitometric units relative to the loading control.

Plasma assays

Plasma glucose, glycerol, triacylglycerol (Sigma, St. Louis, Missouri), free fatty acids (Wako Chemicals, Richmond, Virginia), and insulin (Linco Research, St. Charles, Missouri) were measured using commercially available kits according to the manufacturer's instructions.

Statistics

Comparisons between WL5, WL29, WL53, and SED5 were made using analysis of variance (ANOVA). For comparisons between WL5, WL10, SED5, and SED10, a 2-way ANOVA was used: activity (WL or SED) X time of sacrifice (5 or 10 hours into the light cycle). Significance for all tests was set at $p < 0.05$, and the Student-Neuman-Keuls *post-hoc* test was used to determine group differences. Correlations were determined using Pearson's product-moment correlation coefficient. All data are presented as mean ± standard error of the mean (SEM). Statistics were performed using SigmaStat software (Systat Software, Inc., Point Richmond, California).

RESULTS

Adipose mass and cellularity

Epididymal fat pad mass was significantly higher in WL53 (1.311 ± 0.032 g) relative to all other groups (1.047 ± 0.030 g for WL5, 1.160 ± 0.039 g for WL29, and 1.054 ± 0.041 g for SED5; Fig. 18A). The relative mass of the epididymal fat pad [(g/g body mass) x 1000] was significantly greater in all other groups (5.548 ± 0.133 for WL29, 6.069 ± 0.111 for WL53, and 5.595 ± 0.140 for SED5) compared to WL5 (4.945 ± 0.088), and it was also significantly greater in WL53 relative to WL29 and SED5 (Fig. 18B). There was a significant negative correlation between total distance run and the relative epididymal fat mass in WL5 and WL10 ($r = -0.42$, $p = 0.01$; Fig. 18C). Omental fat pad mass was

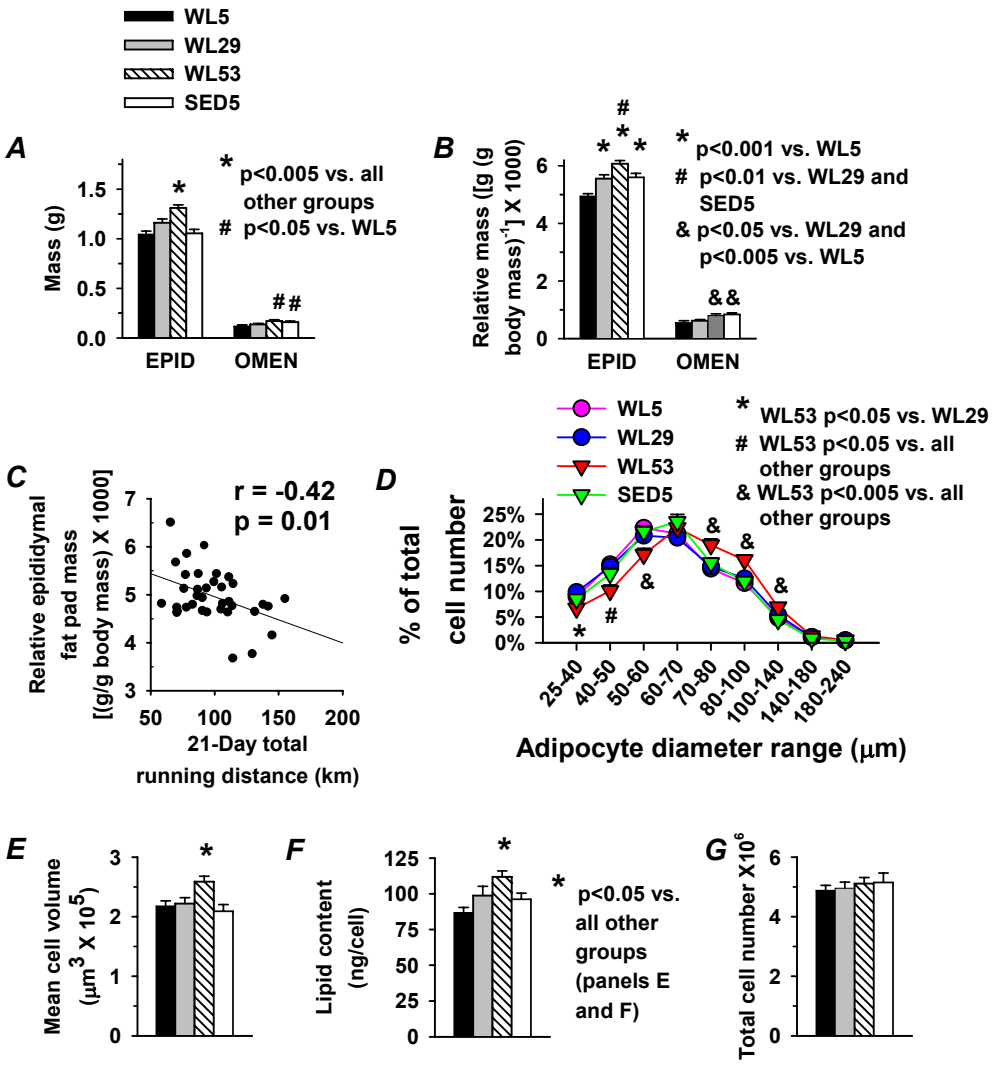

Figure 18. Adipose mass and cellularity.

Epididymal (EPID) and omental (OMEN) (*A*) absolute and (*B*) relative fat mass; (*C*) negative relationship between total 21-day running distance and epididymal fat mass in WL5; (*D*) relative epididymal adipocyte distribution based on cell diameter; (*E*) mean epididymal adipocyte cell volume; (*F*) epididymal fat cellular lipid content; and (*G*) epididymal fat pad total cell number for both left and right pads. Bars represent the means ± SEM. Legends for significance are shown separately with each graph; E and F share a significance legend to the right of F. ANOVA with Student-Neuman-Keuls *post-hoc* test was used for all comparisons. n = 26 for epididymal fat mass, 10 for omental fat, 26 for figure (*C*), and 13-16 for cellularity measurements.

greater in WL53 (0.172 ± 0.012 g) and SED5 (0.160 ± 0.010 g) than in WL5 (0.116 ± 0.016 g; Fig. 18A); WL29 (0.136 ± 0.009 g) was intermediate between, but not different from, WL5 and WL53. Relative omental fat mass [(g/g body mass) x 1000] was significantly higher in WL53 (0.800 ± 0.055) and SED (0.836 ± 0.054) than in WL5 (0.544 ± 0.072) or WL29 (0.616 ± 0.039; Fig. 18B).

The percentage of epididymal adipocytes with a diameter between 25-60 μm was lower in WL53 than in the other groups, while the percent of cells with a diameter between 70-140 μm was greater in WL53 than in all other groups (Fig. 18D). The mean epididymal adipocyte volume ($\mu m^3 \times 10^5$) was significantly higher in WL53 (2.58 ± 0.94) than all other groups (2.09 ± 1.11 for SED5, 2.18 ± 0.83 for WL5, and 2.22 ± 0.99 for WL29; Fig. 18E). Mean epididymal adipocyte diameter (μm) was also significantly higher ($p < 0.005$) in WL53 (70.6 ± 0.9) than all other groups (65.7 ± 0.7 for WL5, 65.9 ± 1.0 for WL29, and 65.7 ± 1.0 for SED; data not shown). The amount of lipid (ng) per cell was greater in WL53 (111.8 ± 4.2) than in all other groups (86.6 ± 3.8 for WL5, 98.7 ± 5.5 for WL29, and 96.2 ± 4.2 for SED5; Fig. 18F). Total epididymal adipocyte number ($\times 10^6$) was not significantly different between groups (4.88 ± 0.17 for WL5, 4.95 ± 0.20 for WL29, 5.11 ± 0.21 for WL53, and 5.14 ± 0.32 for SED5; Fig. 18G).

Plasma analytes

Plasma insulin (pM) was higher in WL53 (220 ± 2) than in WL5 (209 ± 4). Plasma insulin for WL29 (215 ± 3) and SED5 (212 ± 3) were intermediate between, but not different from, WL5 or WL53 (Fig. 19). Plasma triacylglycerol (μM) was greater in WL53 (205 ± 26) relative to all other groups (139 ± 14 for WL5, 145 ± 20 for WL29, and 120 ± 10 for SED5). Thus, there are associations for increased plasma insulin, increased epididymal and omental fat masses (162), and decreased epitrochlearis muscle insulin sensitivity (163) during the 48

hours of reduced physical activity between WL5 and WL53. Plasma glucose, free fatty acids, and glycerol were not different between groups.

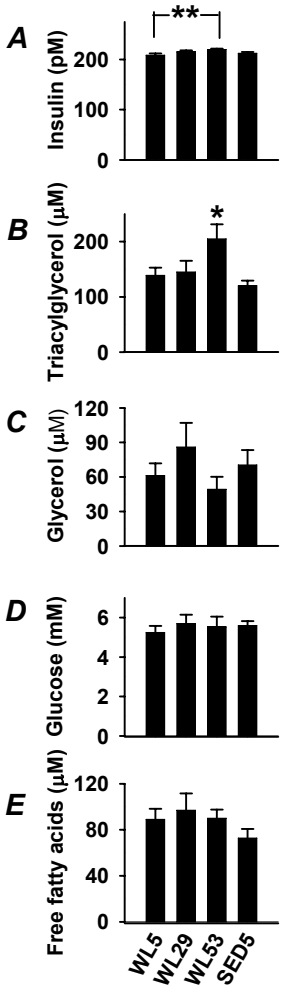

Figure 19. Effect of reduced physical activity on various plasma analytes.

(*A*) Plasma insulin, (*B*) triacylglycerol, (*C*) glycerol, (*D*) glucose, and (*E*) free fatty acids. *, p< 0.05 vs. all other groups; **, p < 0.05 vs. WL5. Bars represent the mean ± SEM. n = 10/group.

2-Deoxyglucose uptake

There were no significant differences between groups for 2-deoxyglucose uptake into isolated epididymal adipocytes with either no insulin or at 0.4 nM or 12.8 nM insulin (Fig. 20).

Triacylglycerol synthesis

Triacylglycerol synthesis was estimated by measuring the incorporation of palmitic acid into triacylglycerol (pmol/mg homogenate protein/min).

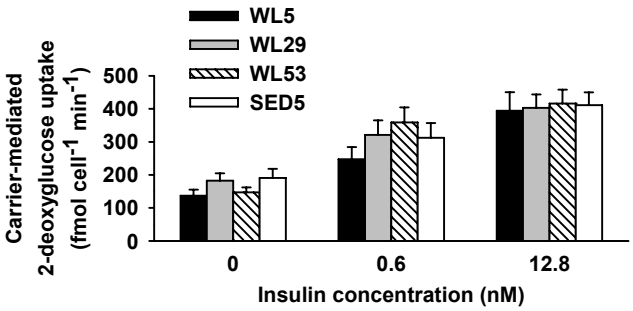

Figure 20. 2-Deoxyglucose uptake into isolated epididymal adipocytes.

2-Deoxyglucose uptake values in the presence of 70 µm cytochalasin B for each animal were subtracted from the other values measured in the absence of cytochalasin B (see Methods). Values within a given insulin concentration were compared using ANOVA with the Student-Neuman Keuls *post-hoc* test. n = 12-16/group.

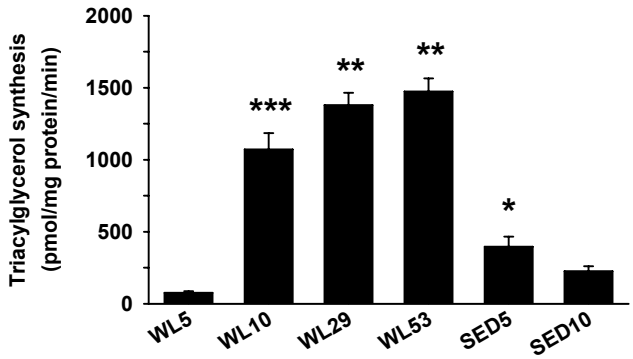

Figure 21. Effect of reduced physical activity on triacylglycerol synthesis in epididymal fat.

The capacity for triacylglycerol synthesis was measured in epididymal fat homogenates and is expressed as pmol of palmitic acid incorporated into triacylglycerol per mg of homogenate protein per minute. Comparisons between WL5, WL29, WL53, and SED5 were performed using ANOVA; comparisons between WL5, WL10, SED5, and SED10 were performed using a 2-way ANOVA (see Methods). The Student-Neuman-Keuls *post-hoc* test was used as follow-up for both comparisons. *, $p < 0.005$ vs. WL5. **, $p < 0.001$ vs. SED5 and WL5. ***, $p < 0.001$ vs. SED10 and WL5. n = 10 in each group.

Triacylglycerol synthesis was greater in SED5 (395 ± 71) than in WL5 (76 ± 12; Fig. 21). Triacylglycerol synthesis was lower in WL5 and SED 5 than in both WL29 (1379 ± 86) and WL53 (1475 ± 91). Since triacylglycerol synthesis in WL5 was markedly suppressed relative to SED5, it was also measured in WL10 and SED10. WL5 and SED10 (226 ± 35) were less than WL10 (1072 ± 112); SED10 did not differ significantly from SED5.

Immunoblots

PPARγ protein levels did not differ among groups (Fig. 22A). C/EBPα protein levels were 30%, 20%, and 41% higher in SED5 than in WL5, WL29, and WL53, respectively (Fig. 22B).

DISCUSSION

An important finding of the current study is that epididymal fat mass increases 25% in just 48 hours, from 5 to 53 hours after cessation of 21 days of

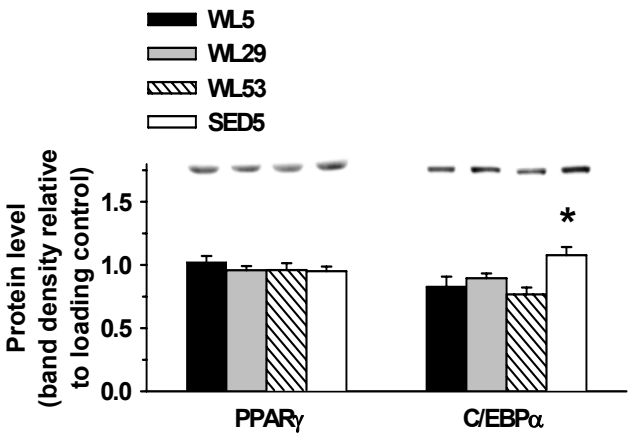

Figure 22. The effect of voluntary wheel running on PPARγand C/EBPα protein levels in epididymal fat.

Protein levels are relative to loading control (see Methods). A representative immunoblot for each protein is located above the graph. *, significantly different from all other groups ($p < 0.05$, ANOVA with Student-Neuman-Keuls *post-hoc* test). n= 10 in each group.

voluntary running. The increase in epididymal adipose tissue led to a new hypothesis that, relative to 5 hours of no voluntary running, triacylglycerol synthesis would be enhanced between 29 and 53 hours after cessation of 21 days of voluntary running. The dramatic increase in triacylglycerol synthesis between the 5 and 10 hours of no voluntary running was unexpected, as well as the magnitude of the increased triacylglycerol synthesis, a 3.5 to 4.7-fold overshoot at 10, 29, and 53 hours of no voluntary running relative to the groups with regular sedentary cage activity. Another potentially important finding in the present study is the higher epididymal fat protein level of C/EBPα with regular sedentary cage activity relative to 21 days of voluntary wheel running.

Epididymal adipose tissue mass and cellularity

The epididymal and omental fat pads increased in mass by 25% and 48%, respectively, following 53 hours of no voluntary running compared to 5 hours of no voluntary running (Fig. 18A). During this same period, mean epididymal adipocyte volume increased 19% with no change in cell number (Figs. 18E and 18G), suggesting that there is an increase in the amount of cellular lipid. This

implication was further supported by the finding that the amount of lipid per epididymal adipocyte increased 29% between 5 and 53 hours of no voluntary running (Fig. 18F). Thus, increases in epididymal pad mass, adipocyte volume, and lipid per adipocyte occurred concurrently between 29 and 53 hours of no voluntary running, a coincident time frame during which there is decreased submaximal insulin-stimulated glucose uptake into the epitrochlearis muscle relative to 5 hours of no voluntary running (see Chapter 4). Although the similar time course is currently only associative, it is tempting to speculate that there might be changes in adipose-derived factors that could provide a causal link to induce the decreased insulin sensitivity in skeletal muscle. Further experiments are needed to test this possibility.

Triacylglycerol levels in adipose tissue are the result of a balance between storage and lipolysis; increased storage could be affected by multiple factors, such as increases in substrate (plasma glucose, free fatty acids, and triacylglycerol) supply and uptake (increased adipocyte insulin sensitivity and lipoprotein lipase activity), enhanced *de novo* synthesis of fatty acids in adipocytes, and augmented incorporation of fatty acids or other substrates into triacylglycerol in adipocytes (reviewed in Chapter 1). Adipose tissue triacylglycerol stores could also be increased by enhanced re-incorporation rate of lipolysis-derived fatty acids into triacylglycerol (87; 180). Of the possible mechanisms regulating triacylglycerol storage in adipose tissue when daily exercise stops, previous studies have reported that plasma triacylglycerol (6; 197), glucose uptake (54), lipoprotein lipase activity (6; 165), the capacity for fatty

acid synthesis [as measured by fatty acid synthase activity (284)], and glycerolipid synthesis (12) are elevated 72 hours, 1-9 days, 84 hours-7 days, 12 days, and 24 hours, respectively, following the last exercise bout in exercise-trained animals relative to sedentary controls. Exercise training in rats enhances epinephrine-induced lipolysis (13), but basal lipolysis is unchanged (144) relative to sedentary controls up to 48 hours after the last exercise bout, thus decreased lipolysis is not suggested as a likely contributor to the increased epididymal fat upon cessation of voluntary exercise. In addition to these potential metabolic mechanisms, the transcription factors PPARγ and C/EBPα are important positive regulators of adipocyte differentiation and lipogenic metabolism (80; 97; 261). Of these prospective mechanisms, I considered that plasma triacylglycerol, glucose uptake, triacylglycerol synthesis, PPARγ and C/EBPα protein levels, and food intake might be associated with the increased epididymal fat mass observed with the cessation of voluntary wheel running, although there are likely other mechanisms that could be involved.

Plasma triacylglycerol

Plasma triacylglycerol increased 47% after 53 hours relative to 5 hours of reduced physical activity (Fig. 19) and may contribute to the increased mass of the epididymal and omental fat pads that occurred during this same time frame.

2-Deoxyglucose uptake into isolated epididymal adipocytes

As insulin-stimulated glucose uptake into adipocytes has previously been shown to increase in response to exercise training for 1-9 days following the last training bout (54), and that exercise training-induced increases in glucose uptake negatively correlate with adipocyte size (52; 167), I tested the possibility that enhanced glucose uptake could contribute to the increase in indices of epididymal adipose cellularity following cessation of voluntary wheel running. In contrast to the previous studies (52; 54; 167), I observed no changes in insulin-stimulated 2-deoxyglucose uptake into isolated epididymal adipocytes up to 53 hours after cessation of voluntary running (Fig. 20). The reason for this is unclear, but may be related to the type of physical activity or the smaller increase in adipocyte size upon cessation of exercise training in the current study as compared to literature reports (54).

Epididymal fat triacylglycerol synthesis

A new hypothesis was generated that an increase in the capacity to synthesize triacylglycerol could contribute to the increased epididymal adipose mass. This hypothesis was based on findings showing that glycerolipid synthesis, including synthesis of diacylglycerol and triacylglycerol, in epididymal fat increased 59% 24 hours after the last exercise bout following 12 weeks of treadmill training in rats relative to untrained controls (12). My findings A) extend this earlier report (12) by filling in some of the time points within the first 24 hours

of ending voluntary running and B) suggest the existence of a daily cycle of triacylglycerol synthesis with daily running, both of which are discussed next.

TIME POINTS WITHIN THE FIRST 24 HOURS OF NO VOLUNTARY RUNNING. At 5 hours of regular sedentary cage activity after 21 days of voluntary running, triacylglycerol synthesis was 4.2-fold greater in the group with regular sedentary cage activity than in the 5-hour wheel lock group. However, only 5 hours later, at the 10th hour of no voluntary running, triacylglycerol synthesis rose to be 14-fold higher than after the 5th hour of no voluntary running, so that regular sedentary cage activity values were now only 21% of the triacylglycerol synthesis rates in 10-hour wheel lock rats (Fig. 21). Thus, a dramatic rise and overshoot in the activity of the triacylglycerol synthetic pathway occurs between the 5th and 10th hour of no voluntary running, which remains elevated above regular sedentary cage activity values to at least the 53rd hour of no voluntary running. The 3.5- to 4.7-fold overshoot in triacylglycerol synthesis in epididymal fat between the 10th and 53rd hour of no voluntary running could contribute to the concomitant increases in its mass and cell size.

DAILY CYCLE OF TRIACYLGLYCEROL SYNTHESIS WITH DAILY RUNNING. Since my observations were made in the first 12 hours of no voluntary running (the light cycle), these observations imply what was likely occurring during each light cycle of the third week of voluntary wheel running. Triacylglycerol synthesis would have been ~19% of the value of regular sedentary cage activity at the 5th hour of the light cycle, and then would have been ~370% of the value of regular sedentary cage activity at the 10th hour of the light cycle, demonstrating a cycling

of epididymal triacylglycerol synthesis in reoccurrence with daily running. The triacylglycerol synthesis cycling conjecture is supported by the findings of Park *et al*. (215), who demonstrated that the activity of the mitochondrial form of glycerol-3-phosphate acyltransferase in rat epididymal fat is suppressed ~50% following a single 30-minute treadmill run. Glycerol-3-phosphate acyltransferase catalyzes the initial step of triacylglycerol synthesis (49). Thus, an observation emerges that epididymal triacylglycerol synthesis cycles when daily physical activity is employed, being suppressed, likely during and to at least 5 hours post-physical activity in the animals in the current report. Triacylglycerol synthesis then overshoots (relative to regular sedentary cage activity) until the dark cycle begins and voluntary running resumes. The data from Park *et al*. (215) showing that mitochondrial glycerol-3-phosphate activity is suppressed immediately after 30 minutes of exercise suggests that triacylglycerol synthesis could be suppressed early in the dark cycle when nightly running first begins. However, if running does not occur, such as took place in the groups that had their wheels locked so that they could not run, then triacylglycerol synthesis is at least 3.5-fold greater than sedentary for 10-53 hours post-voluntary running. I speculate that the overshoot in triacylglycerol synthesis continues until the next bout of physical activity or until enlargement of the adipocyte provides negative feedback on triacylglycerol synthesis. Collectively, an important concept materializes: Daily physical activity is associated with cycling of triacylglycerol synthesis in the epididymal fat pad of rats, but the cycling vanishes when physical activity ceases and triacylglycerol synthesis stalls at its apparent zenith. The prolonged

maintenance of high triacylglycerol synthesis is associated with increased deposition of lipid in epididymal fat.

PPARγ and C/EBPα protein levels

PPARγ and C/EBPα are important regulators of adipocyte differentiation and lipid metabolism (80; 97; 261), and PPARγ activators lead to increased deposition of fat (306). It was therefore of interest to determine if PPARγ or C/EBPα protein levels in epididymal fat were associated with the increased fat mass upon cessation of voluntary wheel running. To my knowledge, PPARγ and C/EBPα expression in adipose tissue have not before been reported in a paradigm of physical activity or inactivity. PPARγ protein levels did not differ between groups, and C/EBPα protein levels did not change upon cessation of voluntary running (Fig. 22). However, C/EBPα protein levels were 30% greater with regular sedentary cage activity than in the 5-hour wheel-lock group. Although epididymal adipocyte number did not change in the present study (Fig. 18G), the increased C/EBPα protein levels in the sedentary group might suggest that if a longer period of running were employed, there could be an increase in epididymal adipocyte number with regular sedentary cage activity compared to access to running wheels. This concept is supported by data from Craig *et al*. (53), who showed that male rats with regular sedentary cage activity had 108% more epididymal adipocytes than rats who had voluntary wheel access from 6-12 months of age, although the runners were subjected to an ~8% food restriction for approximately the last 2 months. In addition, I have observed that 87-week-

old female rats with regular sedentary cage activity have 123% more fat cells in the ovarian fat pad than do age-matched rats that have had access to running wheels beginning at 4 weeks of age (see Appendix B, Fig. 37C, p. 204). It is also noteworthy that C/EBPα mRNA in human adipose tissue has been shown to higher in obese than in lean humans (158).

Food intake

Another possible cause of the increased epididymal and omental fat mass when voluntary running ceases is the maintenance of both absolute and relative food intake above predicted sedentary values (see Chapter 5, Figs. 16A and 16B, right panels). This is further supported by the finding that on day 23, relative food intake in rats that had their wheels locked for 53 hours was not different than what was predicted if they would have had continued unrestricted access to the running wheel (Fig. 16B, middle panel). Also of note is that the increase in fat mass and cell size occurred during a time in which growth rate was attenuated (Fig. 14B).

Clinical significance

There are several findings of the current study that, if applicable to humans, might carry important implications for human health. One of these implications is the importance of regular physical activity to prevent increases in abdominal fat (120), especially given the strong evidence that regular physical activity protects against obesity (275; 286). This may be particularly true for

already overweight or obese individuals who are trying to reduce body fat. It has been suggested that a consistent element of successful weight loss programs is regular exercise (254; 286). Indeed, it is difficult for overweight or obese individuals to reduce body weight and prevent future weight re-gain. The current results may provide one possible mechanism by which difficulty in weight loss with irregular daily exercise might occur, i.e., with regular exercise there is a cyclic suppression of triacylglycerol synthesis in adipose tissue; however, if exercise frequency is irregular, an elevation above baseline of triacylglycerol synthesis occurs that might tend to offset any progress in body fat reduction. Additionally, it has been suggested that pharmacological inhibition of components of triacylglycerol synthesis may be a treatment for obesity (43; 46; 271; 281). The findings of the current study, in conjunction with those of Park *et al*. (215), would suggest that daily physical activity/exercise may be an effective non-pharmacological intervention to suppress triacylglycerol synthesis in adipose tissue. The enlarged fat cells with decreased physical activity may also bear some clinical importance, as it is believed that it is adipocyte enlargement *per se* that may be responsible for the relationship between obesity and disease (28; 108). Another implication is the further development and elucidation of a model of physical inactivity and its concomitant health implications, with multiple changes occurring within 53 hours of no voluntary running [decline in insulin sensitivity in the epitrochlearis muscle (Chapter 4), increase in epididymal and omental adipose tissue mass and epididymal adipocyte size, and overshoot in triacylglycerol synthesis in epididymal fat]. The rapid increase in fat mass and

cell size observed upon cessation of voluntary running is analogous to the decreased physical activity and resulting increase in adiposity occurring in modern humans. As obesity is slow in developing, the mechanisms responsible may only have small differences between physically active and inactive humans, making it difficult to detect the underlying pathophysiology. However, with the locking of running wheels in highly physically active rats, as undertaken in the current study, a more rapid and pronounced increase in epididymal fat allows for future mechanistic studies. The potential implications have tremendous relevance to human health, as "A shortage of credible information exists on . . . physical activity patterns that have the potential to reverse the national obesity epidemic and reduce the risk of . . . chronic diseases" (226).

Conclusion

In summary, there is a rapid increase and overshoot in triacylglycerol synthesis between 5 and 10 hours of no voluntary running that is sustained at 29 and 53 hours of no voluntary running. It is likely that the sustained overshoot could contribute to an increase in epididymal fat mass and adipocyte size between 29 and 53 hours of no voluntary running, although other mechanisms, such as increased fatty acid synthesis (7; 68; 284; 297), and lipoprotein lipase activity (6; 165) may also be involved. Further research is needed to investigate mechanisms responsible for the increase and overshoot in triacylglycerol synthesis and other possible mechanisms contributing to increased body fat with reduced physical activity.

Chapter 7: Increased Glycerol-3-Phosphate Acyltransferase Protein Level and Enzyme Activity in Rat Epididymal Fat upon Cessation of Wheel Running

INTRODUCTION

The escalating pandemic of obesity has occurred concurrently with a precipitous decline in the total amount of daily physical activity (30; 39; 71; 182; 285; 286). In chapters 4, 5, and 6, I simulated the decline in physical activity in humans using a rat model where male rats that were physically active on voluntary running wheels for 21 days had their running wheels locked for 5-53 hours. During this time frame (between 5 and 53 hours of reduced physical activity), epididymal fat mass increased 25% as a result of an increase in cell size (see Chapter 6, Fig. 18A). Palmitic acid incorporation into triacylglycerol (a measurement of triacylglycerol synthesis) in epididymal fat homogenates was suppressed 80% in rats that had access to voluntary running wheels when sacrificed 5 hours after the reduction in physical activity as compared to 7-week-old rats with regular sedentary cage activity. In contrast, when sacrificed after 10 hours of reduced physical activity, triacylglycerol synthesis was 3.7-fold greater than rats with continual regular sedentary cage activity and 14-fold greater than

the rats sacrificed after 5 hours of reduced physical activity (Fig. 21). However, it is unknown whether these same phenomena might be observed after shorter term physical activity (such as after a single bout of exercise in untrained animals or after 24 hours of running wheel access) as after the 21 days of voluntary wheel running. One purpose of the current study was to test this possibility. Determination of whether the effect is from a single bout or repeated daily bouts of physical activity will be helpful guidance for future experiments to explain the underlying mechanisms.

The incorporation of fatty acid into triacylglycerol is accomplished by 5 successive steps catalyzed by the following enzymes: 1. Acyl coenzyme A synthetase, 2. Acyl coenzyme A:glycerol-*sn*-3-phosphate acyltransferase (GPAT), 3. 1-Acylglycerol-*sn*-3-phosphate acyltransferase, 4. Phosphatidate phosphatase, and 5. 1,2-Diacylglycerol:acyl coenzyme A acyltransferase (DGAT). Of these steps, GPAT catalyzes the initial and committed step in the synthesis of glycerolipids, including diacylglycerol, triacylglycerol, and membrane phospholipids, and it has been suggested that GPAT may be rate-limiting for these processes (49). DGAT, which converts diacylglycerol to triacylglycerol by addition of an acyl coenzyme A, catalyzes the terminal and only dedicated step exclusive to triacylglycerol synthesis. There is evidence that both GPAT and DGAT are regulated both transcriptionally and post-translationally (49). A second purpose of the current study was to test the possibility that changes in GPAT or DGAT activity might be associated with the physical inactivity-induced

dysregulation of triacylglycerol synthesis and, if so, to determine what mechanisms might contribute to changes in enzyme activity.

METHODS

Materials

[9,10-^{3}H]palmitic acid was from Sigma (St. Louis, Missouri). L-[2-^{3}H(N)]glycerol-3-phosphate and [pal-9,10-^{3}H]palmitoyl coenzyme A were from American Radiolabeled Chemicals (St. Louis, Missouri). Mitochondrial GPAT antiserum was the generous gift of Dr. Rosalind Coleman (University of North Carolina, Chapel Hill, North Carolina). Sterol regulatory element binding protein-1 (SREBP-1) polyclonal antibody and cyclic AMP enhancer binding protein (CBP) and casein kinase II-α monoclonal antibodies were from Santa Cruz Biotechnology (Santa Cruz, California). Nuclear factor Y-β polyclonal antibody was the kind gift of Dr. Roberto Mantovani (University of Milan, Milan, Italy). Sp1 monoclonal antibody was from BD Biosciences (San Jose, California). Adenosine 5'-monophosphate-activated protein kinase-α (AMPK-α), AMPK-α Thr^{172} phosphorylation-specific, and acetyl coenzyme A carboxylase Ser^{79} phosphorylation-specific polyclonal antibodies were from Cell Signaling (Beverly, Massachusetts). For real-time polymerase chain reaction (PCR), the primers were from Integrated DNA Technologies (Coralville, Iowa), and the probe was from Applied Biosystems (Foster City, California)

21 days of voluntary running

Details of the experimental design were described in Chapter 6. Briefly, 21- to 23-day-old Fischer-Brown Norway F1 generation male rats (Harlan) were allowed to acclimatize for one week, after which they were randomly divided into 6 groups. Four groups were given access to voluntary running wheels for 21 days, after which the running wheels were locked for 5 (WL5), 10 (WL10), 29 (WL29), or 53 (WL53) hours. Two other groups (SED5 and SED10) had only regular sedentary cage activity with no access to voluntary running wheels and were sacrificed at the same time as WL5 and WL10, respectively. The animals were anesthetized with 60 mg pentobarbital/kg body mass, and epididymal fat pads were removed free of the spermatic vessels and used in experiments as described below. Animals used for 21 days of voluntary running are the same as those previously used for measurement of triacylglycerol synthesis in Chapter 6. There were 10 animals per group.

One-day (acute) physical activity

Initially, rats of the same age as at the end of 21 days of voluntary wheel running (~7 weeks) were used. The animals arrived at 21-23 days of age and were housed 5-6 animals per cage for 28 days. At the start of the light cycle, two groups were placed in individual cages containing voluntary running wheels, while two other groups were placed in individual cages without voluntary running wheels so that they only had regular sedentary cage activity; after 24 hours, the

wheels were locked and food was removed from all groups. One group of runners and one group with regular sedentary cage activity were sacrificed 5 hours after the wheels were locked, and the other two groups were sacrificed 10 hours after the wheels were locked. During the 24 hours of wheel access, the rats averaged 1.50 ± 0.11 km (n = 9/group), which is only about 25% of the running activity observed on either the first or last night of running as previously reported when 28- to 30-day old rats were given access to voluntary running wheels for 21 days [see Chapter 5, Fig. 13 (p. 92) and Table 2 (p. 91)]. As it was desired to more closely approximate the activity observed on the last night after 21 days of voluntary running wheel access, I employed two additional approaches.

It was observed that 28- to 30-day-old rats that are given access to running wheels run 5-6 km during the first 24 hours, which is similar to the distance observed during the last night after 21 days of wheel access (see Chapter 5, Fig. 13, p. 92). I therefore allowed 21- to 23-day-old rats to acclimatize one week, then they were separated into four groups as described above for the 7-week-old animals. In agreement with my previous observation, the 4-week-old rats averaged 5.05 ± 0.65 km during 24 hours of voluntary running wheel access. Animals were sacrificed and epididymal fat pads harvested as described above for 21 days of voluntary running. There were 8 animals per group with running wheel access and 6 animals per group with regular sedentary cage activity.

Because of the possibility of an age effect between the 4-week- and 7-week-old rats, we employed a second method to approximate the last night of activity following 21 days of running wheel access. Five-week-old rats were allowed to acclimatize for one week, after which they were familiarized with running on a motorized treadmill (Quinton Instruments, Seattle, Washington) at the start of the light cycle for 7 days. The familiarization protocol consisted of 10 minutes on the treadmill at 15 km/hr, gradually adjusting the incline to 6% on the fifth day. On the eighth day, at ~7 weeks of age, the rats were assigned to an experimental group. This subjective assignment was made based on my observations during the one-week treadmill familiarization protocol. When an individual rat was observed to be unwilling to run on any given day, a mark was made on its tail. The rats with the most marks on the tail at the end of the treadmill familiarization period were assigned to one of the regular sedentary cage activity groups, and the remainder was assigned to the treadmill group. Within each group, the animals were then randomly assigned to be sacrificed either immediately (0 hours), 5 hours, or 10 hours after the last bout of treadmill activity. There were no within-group differences (i.e., assigned to be sacrificed at 0, 5, or 10 hours) for the number of tail marks (Kruskal-Wallis analysis of variance on ranks; data not shown). At the start of the light cycle, access to food was removed, and all animals were transported to the treadmill room. Animals assigned to the acute treadmill activity group ran 12 X 10-minute bouts on the treadmill at 21 km/hr on a 6% incline. There were 5-minute rest periods between bouts, during which time the animals were returned to their cages and given

access to water. Rats with regular sedentary cage activity remained in their cages for the duration. Sacrifices of the 0-hour groups were completed within 40 minutes following completion of the last activity interval, and the other animals were returned to their housing quarters until sacrificed either 5 or 10 hours later. The animals were sacrificed and epididymal fat pads harvested as described above for 21 days of voluntary running. There were 6-7 animals per group.

Enzyme activity

Triacylglycerol synthesis was measured as the incorporation of radiolabeled palmitic acid into triacylglycerol as described in Chapter 6.

GPAT activity was measured as the incorporation of radiolabeled palmitoyl coenzyme A into lysophosphatidic acid (255). Forty microliters of a 2 µg protein/µl concentration of epididymal fat homogenate was incubated at 30° C for 15 minutes in a final volume of 400 µl of 75 mM Tris-HCl, 4 mM $MgCl_2$, 2 mg/ml free fatty acid-free BSA, 8 mM NaF, pH 7.4, 50 µM palmitoyl coenzyme A, 300 µM [^{3}H]glycerol-3-phosphate (5 µCi/ml), with or without 2 mM N-ethylmaleimide. The reaction was terminated by the addition of 3 ml of chloroform:methanol (1:2, v:v) and 600 µl of 10% trichloroacetic acid. After 10 minutes, 500 µl of chloroform and 500 µl of 10% trichloroacetic acid were added to each tube. Samples were then vortexed, centrifuged at 450 *g* for 2 minutes, the upper phase aspirated, washed 4 times with 2 ml of 10% trichloroacetic acid, 1 ml of the lower chloroform layer evaporated in a rotary vacuum, re-constituted in chloroform/5% glacial acetic acid, and separated using thin layer chromatography by developing

to 8 cm in chloroform:methanol:H_2O (65:25:4, v:v:v) and then to 16 cm in hexane:ethyl ether:glacial acetic acid (80:20:2, v:v:v). A lysophosphatidic acid standard was run jointly, and the appropriate band was scraped and subjected to scintillation counting. Total GPAT activity was determined in the absence of N-ethylmaleimide. Mitochondrial GPAT activity, which is resistant to inhibition by N-ethylmaleimide (17), was determined in the presence of 2 mM N-ethylmaleimide and subtracted from the total activity to yield the microsomal GPAT activity.

DGAT activity was measured as the incorporation of radiolabeled glycerol-3-phosphate into triacylglycerol (48). Twenty microliters of a 2 µg protein/µl epididymal fat homogenate (40 µg homogenate protein) was incubated at 37° C in a final volume of 200 µl of 175 mM Tris-HCl, 8 mM $MgCl_2$, 1 mg/ml free fatty acid-free BSA, pH 8.0, 200 µM dioleoylglycerol, and 30 mM [^{3}H]palmitoyl coenzyme A (1 µCi/ml) for 30 minutes. The reaction was terminated and samples processed as described for triacylglycerol synthesis (see Chapter 6).

Immunoblots

Immunoblots were performed according to standard procedures as described in Chapter 4. Blots for AMPK-α Thr^{172} phosphorylation were stripped by incubation in 62.5 mM Tris-HCl, pH 6.8/2% SDS/100 mM β-mercaptoethanol at 50° C with light rocking for 30 minutes and subsequently blocked and re-probed for AMPK-α. All blots were corrected for a loading control as described in Chapter 6.

Real-time PCR

Isolation of mRNA from ~50 mg epididymal adipose tissue was accomplished using the RNeasy Lipid Tissue Mini Kit (Qiagen, Valencia, California), and 700 ng of mRNA was subjected to cDNA synthesis using Superscript III (Invitrogen, Carlsbad, California). Real-time PCR for mitochondrial GPAT was performed on 25 ng of cDNA as described (219); the sequence for the forward primer was 5'-CAGTCCCGGAGTCTGAGTACCT-3', the sequence for the reverse primer was 5'-TCCTCTCCGTCCTGGTGAGA-3', and the probe sequence was AGAAGCTGCACAGGTAC. Statistical analysis was performed using the mean cycle threshold for each group with 18S mRNA as a normalization control, and data are presented as the fold-difference relative to WL5.

Statistics

For 21 days of voluntary running, comparisons between WL5, WL29, WL53, and SED5 were made using ANOVA, and comparisons between WL5, WL10, SED5, and SED10 were made using 2-way ANOVA: activity (WL or SED) X time of sacrifice (5 or 10 hours after running wheels were locked). For 28- to 30-day-old animals with 24 hours of running wheel access, comparisons were made using 2-way ANOVA: activity (access to a running wheel or regular sedentary cage activity) X time of sacrifice (5 or 10 hours after running wheels were locked). For 7-week-old animals undergoing acute treadmill activity,

comparisons were made using 2-way ANOVA: activity (treadmill activity or regular sedentary cage activity) X time of sacrifice (0, 5, or 10 hours following the last activity bout on the treadmill). Where ANOVA analysis yielded a p-value < 0.05, the Student-Neuman-Keuls *post-hoc* method was used to determine between-group differences, with significance set at $p<0.05$. All statistics were analyzed using SigmaStat (Systat Software, Inc., Point Richmond, California).

RESULTS

Triacylglycerol synthesis following one-day (acute) physical activity

I previously reported that triacylglycerol synthesis was 3-4-times greater at 10, 29, and 53 hrs after cessation of 21 days of voluntary wheel running as compared to time-matched rats with regular sedentary cage activity (see Chapter 6, Fig. 21, p. 118). The question posed was whether this response would occur after the first day of voluntary running or a single bout of treadmill exercise.

24 HOURS OF VOLUNTARY RUNNING WHEEL ACCESS. Triacylglycerol synthesis in the epididymal fat homogenates from 7-week-old rats given access to running wheels for 24 hours was not different from rats that had regular sedentary cage activity, likely due to their running only 1.5 km during the 24 hours of wheel access (data not shown). In order to increase the duration of increased physical activity for acute exercise, I used two additional methods to determine whether

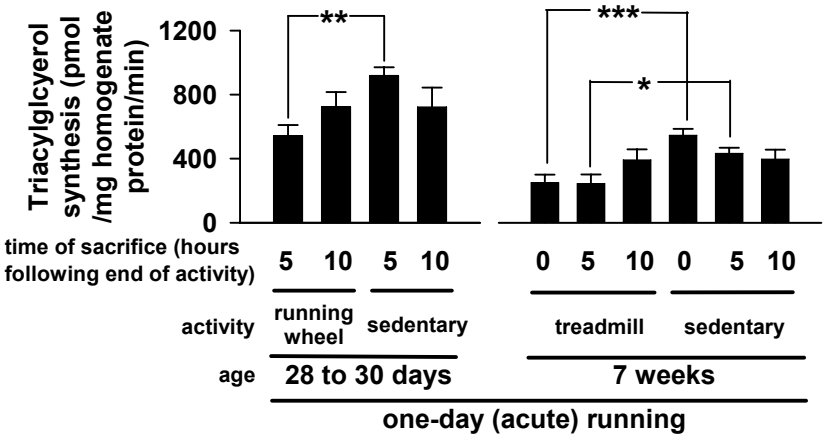

Figure 23. Triacylglycerol synthesis in epididymal fat homogenates following one-day (acute) physical activity.

Acute physical activity was either 24 hours of access to a voluntary running wheel (left panel) or 2 hours of intermittent treadmill activity (right panel). Triacylglycerol synthesis was measured as the incorporation of palmitic acid into triacylglycerol. Time of sacrifice indicates the hours following locking of voluntary running wheels for running wheel groups (left panel) and time since the end of the last bout of treadmill activity for treadmill groups (right panel). Sedentary groups had only regular sedentary cage activity. Groups connected by lines are significantly different: *, $p<0.05$; **, $p<0.01$; ***, $p<0.001$.

triacylglycerol synthesis is altered with one day of physical activity: one using younger (28- to 30-day-old) rats with 24 hours of running wheel access to match the type of activity, and the other using age-matched (7-week-old) rats with 120 minutes of intermittent treadmill activity (see Methods). When 28- to 30-day-old rats with 24 hours of running wheel access (during which time they ran ~5 km) were sacrificed 5 hours after running wheels were locked, triacylglycerol synthesis (544 ± 67 pmol/mg homogenate protein/min) was suppressed 41% when compared to age-matched rats with regular sedentary cage activity (918 ± 52; Fig. 23, left panel). By 10 hours after the running wheels were locked, triacylglycerol synthesis values were not different between animals with 24 hours of running wheel access (724 ± 91) and those with regular sedentary cage activity (722 ± 122).

TREADMILL ACTIVITY. Seven-week-old rats that engaged in 120 total minutes of intermittent activity on a motorized treadmill and that were sacrificed at either 0 or 5 hours after the last treadmill activity bout had a suppressed triacylglycerol synthesis (249 ± 50 and 243 ± 58 pmol/mg homogenate protein/min, respectively) compared to those that had regular sedentary cage activity that were sacrificed at the same time [545 ± 41 (0 hrs) and 432 ±35 (5 hrs); Fig. 23, right panel]. By 10 hours after the last treadmill activity bout, triacylglycerol synthesis values between animals that underwent treadmill activity (392 ± 66) were not different than those with regular sedentary cage activity (397 ± 58).

GPAT and DGAT enzyme activities upon cessation of 21 days of voluntary running

Mitochondrial GPAT activity (pmol/mg homogenate protein/min) was significantly greater in WL53 (117 ± 12) and WL29 (107 ± 10) than in WL5 (34 ± 5) or SED5 (74 ± 6), and it was significantly greater in SED5 than in WL5. Mitochondrial GPAT activity was significantly higher in WL10 (99 ± 8) than in WL5 or SED10 (67 ± 8; Fig. 24A). Neither the total GPAT activity nor that of the microsomal isoform differed among groups. DGAT activity was not significantly different among groups (Fig. 24B).

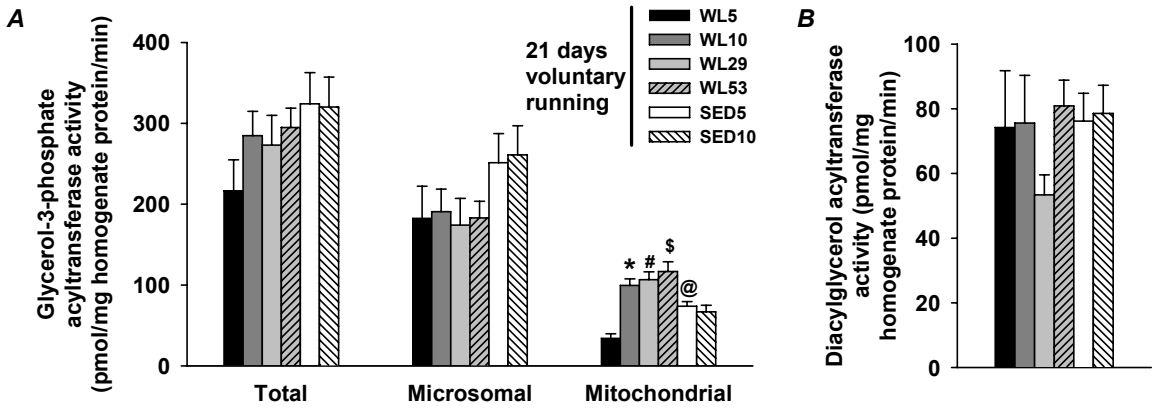

Figure 24. GPAT (*A*) and DGAT (*B*) activities in epididymal fat homogenates upon cessation of 21 days of voluntary wheel running.

Enzyme activities were measured as described in the Methods. *, p<0.005 vs. WL5 and SED10; #, p<0.05 vs. SED5 and p<0.001 vs. WL5; $, p<0.005 vs. WL5 and SED5; @, p<0.005 vs. WL5. Bars represent the mean ± SEM. See Methods for group descriptions and statistics.

Mitochondrial GPAT protein level

21 DAYS OF VOLUNTARY RUNNING. Mitochondrial GPAT protein level was significantly lower in SED5 than in WL5, WL29, or WL53, and it was lower in SED10 than in WL10 (Fig. 25A).

ONE-DAY (ACUTE) PHYSICAL ACTIVITY. Mitochondrial GPAT protein level was not different between one-day runners (either 24 hours of wheel access or treadmill activity) and regular sedentary cage activity groups (Fig. 25B).

Mitochondrial GPAT mRNA upon cessation of 21 days of voluntary running

Using real-time PCR techniques, I measured mitochondrial GPAT mRNA. However, 18S, which was used as a normalization control, tended to decrease in WL29 and WL53 (p=0.12; Fig. 26A). Exclusion of these two groups from the analysis (comparison of WL5, WL10, SED5, and SED10 only) yielded more

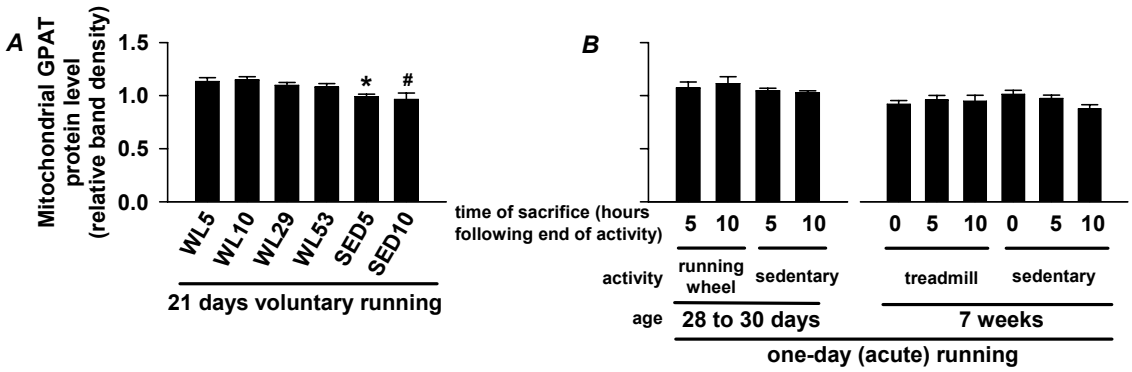

Figure 25. Mitochondrial GPAT protein level in epididymal fat (*A*) upon cessation of 21 days of voluntary wheel running and (*B*) following one-day (acute) physical activity.

Levels are relative to a loading control, which consisted of epididymal fat homogenate protein from a non-experimental animal that was loaded in triplicate on each blot. Time of sacrifice for one-day (acute) physical activity (panel *B*) indicates the hours following locking of voluntary running wheels for running wheel groups (left panel) and time since the end of the last bout of treadmill activity for treadmill groups (right panel). Sedentary groups had only regular sedentary cage activity. *, $p<0.05$ vs. all other 21-day voluntary running groups; #, $p<0.005$ vs. WL10. Bars represent the mean ± SEM. See Methods for group descriptions and statistics.

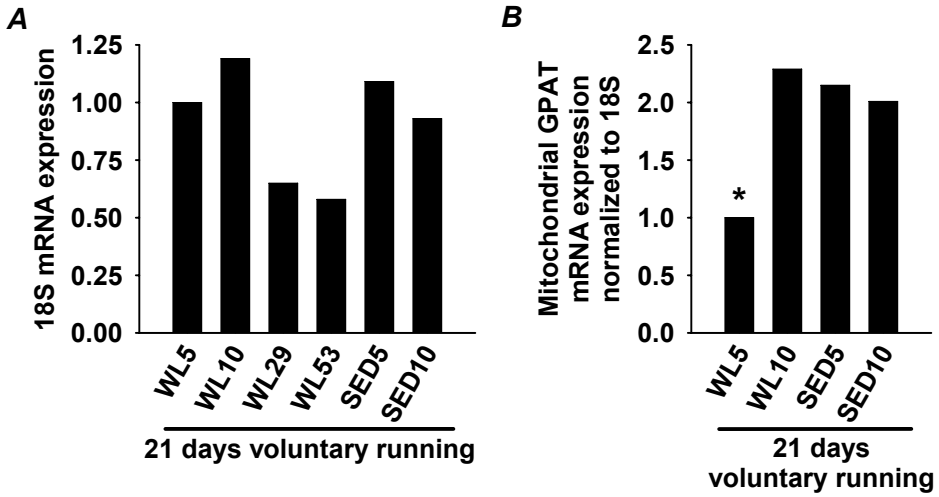

Figure 26. 18S (*A*) and mitochondrial GPAT (*B*) mRNA expression upon cessation of 21 days of voluntary wheel running.

The data bars represent the fold-difference relative to WL5 as calculated from the mean cycle threshold values for each group. Statistics were calculated on the cycle threshold as described in the Methods. As 18S mRNA had a tendency to change ($p=0.12$) in WL29 and WL53, these groups were omitted from the analysis of mitochondrial GPAT mRNA for panel *B* (see Results for further discussion). *, $p<0.05$ vs. all other groups. See Methods for group descriptions.

acceptable results ($p=0.84$). Therefore, analysis of mitochondrial GPAT mRNA was only performed on WL5, WL10, SED5, and SED10; the mean cycle threshold for mitochondrial GPAT mRNA normalized to 18S mRNA was significantly lower in WL10, SED5, and SED10 (14.4 ± 0.3, 14.5 ± 0.3, and 14.6 ±

0.3, respectively) than the cycle threshold for WL5 (15.6 ± 0.2). This indicates that mitochondrial GPAT mRNA was 2.3-, 2.2-, and 2.0-fold higher in WL10, SED5, and SED10, respectively, than in WL5 (Fig. 26B). These experiments are being repeated with glyceraldehyde phosphate dehydrogenase as a normalization control.

SREBP-1, nuclear factor Y-β, CBP, and Sp1 protein levels

21 DAYS OF VOLUNTARY RUNNING. No significant protein differences were found for the protein levels of truncated (Fig. 27A), full-length (Fig. 27C), and total SREBP-1 (Fig. 27D), or the ratio of truncated SREBP-1 to total SREBP-1 (Fig. 27E). CBP protein levels were significantly higher in SED5 than in WL29 (Fig. 27F) and approached significance when compared to WL5 and WL53 ($p=0.09$ and 0.053, respectively). Protein levels of nuclear factor Y-β and Sp1 were not different among groups (Fig. 27G and 27H).

ONE-DAY (ACUTE) PHYSICAL ACTIVITY. Truncated SREBP-1 protein levels were not different between one-day runners and regular sedentary cage activity groups (Fig. 27B).

AMPK Thr^{172} phosphorylation

21 DAYS OF VOLUNTARY RUNNING. Protein levels for AMPK-α (Fig. 28A), AMPK-α Thr^{172} phosphorylation (Fig. 28C), and acetyl coenzyme A carboxylase Ser^{79} phosphorylation (Fig. 28G) were not different among groups.

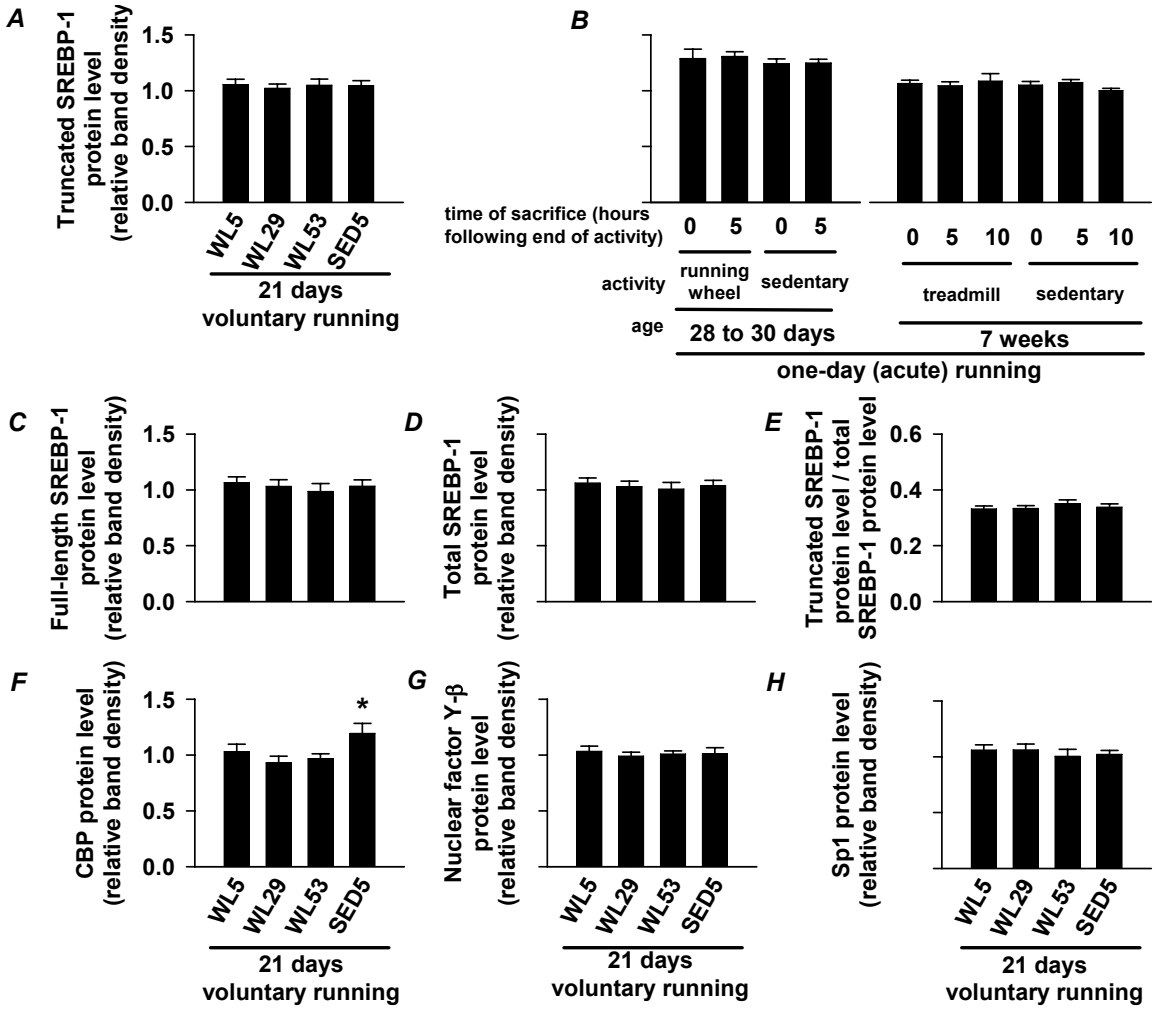

Figure 27. Protein levels of SREBP-1 (*A-E*), CBP (F), nuclear factor Y-β (*G*), and Sp1 (*H*) upon cessation of 21 days of voluntary wheel running.

Panels *A* and *C-H* are protein levels upon cessation of 21 days of voluntary wheel running, and panel *B* represents protein levels following one-day (acute) physical activity. Truncated SREBP-1 protein levels (panels *A* and *B*) represent the band at 68 kD, full-length SREBP-1 protein levels (panel *C*) represent the band present at 125 kD, and total SREBP-1 protein levels (panel *D*) is the total densitometric units of both bands. Levels of all proteins are expressed relative to a loading control, which consisted of epididymal fat homogenate protein from a non-experimental animal that was loaded in triplicate on each blot. *, p=0.09 vs. WL5, p<0.05 vs. WL29, and p=0.053 vs. WL53. Bars represent the mean ± SEM. See Methods for group descriptions and statistics.

<u>ONE-DAY (ACUTE) PHYSICAL ACTIVITY.</u> *AMPK-α Thr^{172} phosphorylation*:

AMPK-α Thr^{172} phosphorylation was significantly higher in 7-week-old rats at 0 hours following one bout of treadmill running relative both to regular sedentary cage activity and to 5 and 10 hours following one bout of treadmill running (Fig.

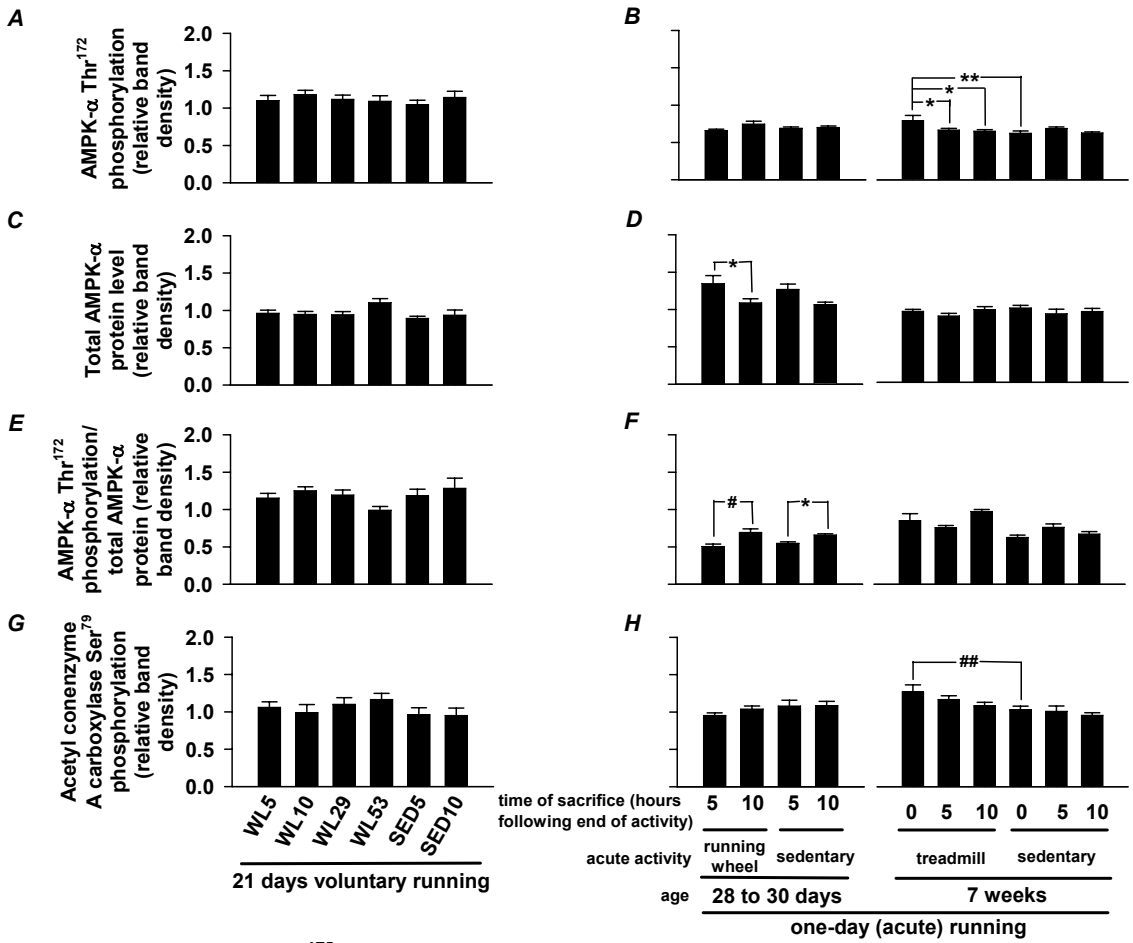

Figure 28. AMPK-α Thr^{172} phosphorylation (*A*, *B*), total AMPK-α protein levels (*C*, *D*), ratio of AMPK-α Thr^{172} phosphorylation to total AMPK-α protein (*E*, *F*), and acetyl coenzyme A carboxylase Ser^{79} phosphorylation (*G*, *H*).

Leftmost panels (*A, C, E, and G*) are upon cessation of 21 days of voluntary wheel running, and panels *B*, *D*, *F*, and *H* are following one-day (acute) physical activity as indicated at the bottom of the figure. Time of sacrifice for one-day (acute) physical activity indicates the hours following locking of voluntary running wheels for running wheel groups (left panel) and time since the end of the last bout of treadmill activity for treadmill groups (right panel). Sedentary groups had only regular sedentary cage activity. Levels are expressed relative to a loading control, which consisted of epididymal fat homogenate protein from a non-experimental animal that was loaded in triplicate on each blot. Groups connected by lines are significantly different: *, p<0.05; **, p<0.005; #, p<0.001; ##, p=0.01. A 2-way ANOVA indicated a significant effect of time of sacrifice (5 or 10 hours after running wheels were locked) for total AMPK protein level (not indicated; p<0.01; panel *D*) and ratio of AMPK-α Thr^{172} phosphorylation to total AMPK protein (not indicated; p<0.001; panel *F*), while an interaction effect between time of sacrifice (0, 5, or 10 hours) and activity (treadmill or sedentary) approached significance (p=0.06) for the ratio of AMPK-α Thr^{172} phosphorylation to total AMPK protein. Bars represent the mean ± SEM. See Methods for group descriptions and statistics.

28B, right panel). AMPK-α Thr^{172} phosphorylation was not different for 28- to 30-day old rats between those with or without 24 hours of running wheel access (Fig. 28B, left panel). ***Total AMPK-α protein levels*:** Total AMPK-α protein levels at 0, 5, and 10 hours after a single bout of treadmill running in 7-week-old

rats were not different from respective time-matched regular sedentary cage activity animals (Fig. 28D, right panel). In contrast, in 28- to 30-day-old animals with 24 hours of running wheel access, there was an effect of time of sacrifice (as determined by 2-way ANOVA) that was independent of the activity level of the animals (either with running wheels or regular sedentary cage activity), such that there was a significantly lower level ($p = 0.006$) of AMPK-α protein between groups sacrificed at 10 hours compared to 5 hours following the start of the light cycle (Fig. 28D, left panel); this significant difference between the 5- and 10-hour groups was retained in the groups that had running wheel access ($p = 0.02$), but not in those with regular sedentary cage activity ($p = 0.08$). The reason for the lower level of total AMPK-α protein at the 10-hour time point is unclear, but as it occurs independently of activity level, it could possibly be related to the initial stress of being housed in isolated cages. ***Relative AMPK-α Thr^{172} phosphorylation*:** As AMPK-α Thr^{172} phosphorylation did not change with 24 hours of running wheel access, the decrease in total AMPK-α at the 10-hour time point resulted in a significantly greater degree of Thr^{172} phosphorylation per level of total AMPK-α in the running wheel groups sacrificed at 10 hours relative to 5 hours (Fig. 28F, left panel). The degree of AMPK-α Thr^{172} phosphorylation per level of total AMPK-α was not significantly different in the acute treadmill activity groups ($p = 0.06$ interaction effect; Fig. 28F, right panel). ***Acetyl coenzyme A carboxylase Ser^{79} phosphorylation*:** Acetyl coenzyme A carboxylase Ser^{79} phosphorylation was not different between groups in the 28- to 30-day-old animals with one day of voluntary wheel running (Fig. 28H, left panel). Acetyl

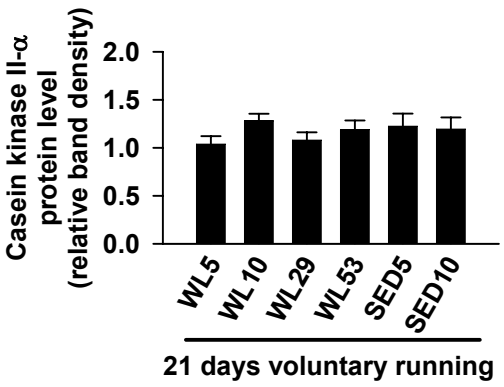

Figure 29. Casein kinase II-α protein levels upon cessation of 21 days of voluntary wheel running.

Protein level is relative to a loading control, which consisted of epididymal fat homogenate protein from a non-experimental animal that was loaded in triplicate on each blot. Bars represent the mean ± SEM. See Methods for group descriptions and statistics.

coenzyme A carboxylase Ser[79] phosphorylation was significantly higher at 0 hours in the one-day treadmill running group relative to the regular sedentary cage activity group sacrificed at the same time (Fig. 28H, right panel).

Casein kinase II-α

Protein levels for casein kinase II-α were not different between 21-day voluntary running groups (Fig. 29).

DISCUSSION

The key findings of the current study are that 1) triacylglycerol synthesis in epididymal fat did not increase at 10 hours following one day of increased physical activity relative to regular sedentary cage activity, 2) mitochondrial GPAT activity in epididymal fat was suppressed at 5 hours, but was elevated (actually overshooting regular sedentary cage activity values) at 10, 29, and 53 hours following 21 days of voluntary running wheel access, and 3) increased mitochondrial GPAT protein expression in epididymal fat was associated with the overshoot in mitochondrial GPAT activity at 10, 29, and 53 hours of reduced

physical activity. In addition, increased AMPK-α Thr^{172} phosphorylation in epididymal fat immediately following treadmill activity precedes the suppression of mitochondrial GPAT activity at 5 hours of reduced physical activity, supporting the previous findings of Park *et al*. (215).

More than a single day of physical activity is needed to produce the physical inactivity-induced overshoot in triacylglycerol synthesis.

One-day (acute) physical activity, either in the form of 24 hours of voluntary running wheel access or of a 2-hour duration of intermittent treadmill running, resulted in suppression of triacylglycerol synthesis in epididymal fat up to 5 hours, but was not different from regular sedentary cage activity at 10 hours following locking of the running wheels or the end of the last treadmill activity bout (Fig. 23). It was shown in Chapter 6 (Fig. 21, 118) that triacylglycerol synthesis in epididymal fat is also suppressed at 5 hours following 21 days of voluntary running wheel access, but that after 10 hours of reduced physical activity, triacylglycerol synthesis remarkably overshoots regular sedentary cage activity values by over 3-fold. Taken together, it is evident that more than a single day of enhanced physical training is required to produce the physical inactivity-induced overshoot in triacylglycerol synthesis, but that one bout of activity is sufficient to suppress triacylglycerol synthesis in epididymal fat. A potential interpretation is that the “suppression effect” on triacylglycerol synthesis observed at 0-5 hours post-physical activity involves suppression of enzyme

activity by a post-transcriptional mechanism since it occurs in rats naïve to increased physical activity. In contrast, the “overshoot effect” at 10, 29, and 53 hours following 21 days of voluntary wheel running, which did not occur in rats naïve to enhanced physical activity, supports the conjecture that changes occur in gene expression of either enzymes involved in triacylglycerol synthesis or of kinases or other proteins that could modulate enzyme activity.

Mitochondrial GPAT activity and protein increase, but its mRNA does not change.

To begin to understand which enzymes involved in triacylglycerol synthesis might be involved in the observed “suppression” and “overshoot” effects; I measured the activities of GPAT and DGAT. It was found that mitochondrial GPAT activity was associated with both the immediate suppressive effect at 5 hours of reduced physical activity and the later overshoot effect on triacylglycerol synthesis at 10 hours of reduced physical activity (Fig. 24A). No change in the activity of the microsomal form of GPAT occurred, indicating the effect was specific to the mitochondrial GPAT isoform. Both a suppressive and an overshoot effect for rat mitochondrial GPAT activity have also been reported in a paradigm of fasting-refeeding, with mitochondrial GPAT activity being suppressed ~30% following a 48-hour fast, then increasing ~110% after 24 hours of refeeding so that the activity upon refeeding was ~50% greater than control values; these changes in mitochondrial GPAT activity were accompanied by changes in the protein level (171), providing evidence that mitochondrial GPAT

activity can be changed by regulating protein levels. There is also evidence that mitochondrial GPAT may be regulated by phosphorylation (49; 195; 210; 211). Therefore, my next experiments were directed toward understanding how my observed suppression and overshoot of mitochondrial GPAT activity might be regulated.

Using immunoblotting techniques, I determined whether the overshoot in mitochondrial GPAT activity with reduced physical activity above that of regular sedentary cage activity could be due to changes in the protein level of the enzyme. An increased epididymal fat mitochondrial GPAT protein level accompanied the increased mitochondrial GPAT activity at 10, 29, and 53 hours (Fig. 25A). Overexpression of mitochondrial GPAT in either CHO or HEK293 cells results in preferential incorporation of fatty acids into triacylglycerol relative to phospholipids (134), indicating that the higher mitochondrial GPAT protein level at 10, 29, and 53 hours of reduced physical activity after cessation from 21 days of voluntary running may be contributing to the higher triacylglycerol synthesis observed at these time points and that it may also play some role in the increased epididymal fat mass that that was observed after 53 hours of reduced physical activity (see Chapter 6, Fig. 21, 118). Interestingly, the increased mitochondrial GPAT protein level was not accompanied by an increase in its mRNA (Fig. 26). Indeed, 5 hours after 21 days of voluntary running, mRNA level was suppressed 54% relative to regular sedentary cage activity, but at 10 hours, mitochondrial GPAT mRNA had risen 130% so that it was not different than the sedentary animals. Lewin *et al*. (171) have shown that, relative to other organs

in rat adipose tissue in the sedentary state, there is a high level of mitochondrial GPAT mRNA expression, but a low level of protein. Thus, the small increase in mitochondrial GPAT protein in the present study following 21 days of voluntary running might be due to enhanced translation efficiency of mitochondrial GPAT, a lower mitochondrial GPAT protein degradation, or increases in mitochondrial GPAT mRNA earlier during the 21 days of voluntary wheel running that is not maintained after 21 days due to the adaptive increases in mitochondrial GPAT protein.

To determine whether changes in transcription factors might be responsible for the 54% suppression in mitochondrial GPAT mRNA after 5 hours of reduced physical activity following 21 days of voluntary wheel running, I hypothesized that there would be a decrease in the protein level of truncated SREBP-1 protein that would be associated with the transitory suppression of mitochondrial GPAT mRNA. SREBP-1 is known to increase the expression of multiple lipogenic genes (124), including mitochondrial GPAT (72; 78), which has 3 consensus SREBP-1 binding sites in the murine promoter (138) that are conserved in the rat promoter (Accession# AY693775). Full-length SREBP-1 is located in the endoplasmic reticulum. In response to cellular signals such as sterol depletion, the N-terminus of SREBP-1 is cleaved and translocates to the nucleus, where it can bind to the promoter and activate transcription (229). The antibody used to detect SREBP-1 in immunoblots was raised against the N-terminal region and recognizes both the full-length and truncated forms of SREBP-1. There was no difference in the amount of truncated SREBP-1 either

after 21 days of voluntary wheel running (Fig. 27A) or after acute increases in physical activity in untrained rats (Fig. 27B). CBP (18; 41; 77; 209; 274), nuclear factor Y-β (18; 147; 279), and Sp1 (18; 42; 147) are known to associate with truncated SREBP-1 and affect its transcriptional activity and nuclear stability. Therefore, we also measured the levels of these proteins. There were no changes in the protein levels of either nuclear factor Y-β (Fig. 27G) or Sp1 (Fig. 27H). However, there was a greater CBP protein level in SED5 relative to the other groups (Fig. 27F) so that it was not positively associated with the decrease in mitochondrial GPAT mRNA in WL5 or the increase in mitochondrial GPAT activity at 10, 29, or 53 hours after the running wheels were locked. However, the possibility remains that there might be a decreased transcriptional activation of the mitochondrial GPAT promoter by SREBP-1 by either altered phosphorylation (156; 245; 269) or association with nuclear factor Y-β, CBP, or Sp1, or possibly by changes in phosphorylation or other post-transcriptional modifications of CBP (57; 93; 288), nuclear factor Y-β (315), or Sp1 (173), although this is merely speculative.

It is intriguing that the protein level of CBP should be elevated with regular sedentary cage activity, demonstrating the same pattern of response as the adipogenic transcription factor CCAAT/enhancer binding protein (C/EBP)-α (see Chapter 6, Fig. 22, p. 119). C/EBP-α has been shown to be upregulated by C/EBP-β (178), overexpression of constitutively active CBP in 3T3-L1 preadipocytes induces expression of C/EBP-β (318), and CBP is a co-activator for both C/EBP-α and C/EBP-β (55), as well as for peroxisome proliferator-

activated receptors (146). Thus, it is possible that the higher level of C/EBP-α with regular sedentary cage activity that was previously observed is an indirect consequence of higher CBP expression, although the physiological relevance is currently unclear and more testing is needed. Transgenic mice heterozygous for CBP have increased fat mass as a consequence of increased adipocyte size but not adipocyte number (307).

Post-transcriptional regulation of mitochondrial GPAT activity

The increase observed in mitochondrial GPAT protein level was modest (9-19%) compared to the overshoot in enzyme activity (45-58%) for 10, 29, and 53 hours of reduced physical activity compared to regular sedentary cage activity groups, indicating that, in addition to a higher level of mitochondrial GPAT protein, there may also be post-transcriptional mechanisms involved in the overshoot effect. This is consistent with a previous report showing that, relative to other organs, rat adipose tissue has a relatively low level of mitochondrial GPAT protein, but a high level of activity, indicating a high degree of acute regulation in adipose tissue (171). Mitochondrial GPAT activity has been shown to be decreased in response to phosphorylation by AMPK (49; 195) and increased in response to phosphorylation by casein kinase II (210; 211). Park *et al.* (215) have previously shown that immediately following an acute 30-minute bout of treadmill activity, a decrease in mitochondrial GPAT activity is accompanied by an increase in activity of the α2 isoform of AMPK. In the current study, AMPK-α Thr^{172} phosphorylation, which closely correlates with AMPK

activity (56; 110; 265), was increased immediately following 120 minutes of intermittent treadmill activity, but had returned to the same level as regular sedentary cage activity 5 hours later (Fig. 28B). That AMPK activity had increased is supported by the finding that phosphorylation of acetyl coenzyme A carboxylase Ser^{79}, a primary target of AMPK (194), was also increased immediately following treadmill activity, but had decreased to sedentary levels 5 hours later (Fig. 28H, right panel). In contrast, triacylglycerol synthesis was suppressed both immediately following and 5 hours after acute treadmill activity and did not increase to regular sedentary cage activity levels until 10 hours following the treadmill activity (Fig. 23B); these results are similar to those of mitochondrial GPAT activity following 21 days of voluntary wheel running (Fig. 24A). These findings may indicate that the negative effect of increased AMPK activity on mitochondrial GPAT activity might be extended beyond the time that AMPK activity decreases back to control values. That there is no change in AMPK-α Thr^{172} phosphorylation at 10, 29, or 53 hours of reduced physical activity following 21 days of voluntary wheel running (Fig. 28A) does not suggest that a decrease in AMPK activity contributes to the elevated overshoot in mitochondrial GPAT activity after 21 days of voluntary wheel running compared to regular sedentary cage activity. Of note is that transgenic mice that are null for the AMPK-α-2 subunit have increased adiposity due to enlarged fat cells (289), emphasizing the potential importance of the post-physical activity increase in AMPK-α Thr^{172} phosphorylation in preventing accumulation of fat.

Casein kinase II, which positively regulates mitochondrial GPAT by direct phosphorylation (210; 211) is composed of an αβαβ tetramer (177). I measured the protein levels of the α catalytic subunit, and found no differences among groups after 21 days of voluntary wheel running (Fig. 29). It remains to be determined whether a change in casein kinase II activity is associated with either the suppression of mitochondrial GPAT activity at 5 hours or the overshoot of mitochondrial GPAT activity at 10, 29, or 53 hours following 21 days of voluntary wheel running compared to regular sedentary cage activity.

Summary and conclusions

In summary, mitochondrial GPAT activity is suppressed in the epididymal fat of rats with 5 hours of reduced physical activity following 21 days of voluntary wheel running relative to regular sedentary cage activity, but after 10 hours of reduced physical activity it overshoots to above regular sedentary cage activity values. An elevated level of AMPK-α Thr^{172} phosphorylation is associated with the lower mitochondrial GPAT activity in the epididymal fat at 5 hours of reduced physical activity compared to sedentary rats, while a small increase in mitochondrial GPAT protein level is associated with the overshoot in enzyme activity at 10, 29, and 53 hours of reduced physical activity compared to regular sedentary cage activity. The increased mitochondrial GPAT protein level at 29 and 53 hours following reduced physical activity, coupled with a failure to increase AMPK-α Thr^{172} phosphorylation due to no voluntary running, might

contribute to the physical inactivity-induced increase in epididymal fat mass and cell size.

Chapter 8: Discussion

The daily amount of physical activity in humans has been declining (22; 30; 71; 182). While this is largely due to increased mechanization and modernization of tasks that formerly required physical activity, modern-day society is also largely sedentary during leisure time by performing tasks such as watching television (30; 182). Decreased physical activity is strongly associated with insulin resistance (99; 161; 183; 222) and intraabdominal obesity (31; 214; 251), two trademark characteristics of type II diabetes (1; 16; 34; 63; 88; 91; 141; 214; 228; 287; 294; 298) and thus may explain the epidemic increase in the incidence of type II diabetes (216).

In this paper, I have simulated the decrease in physical activity using a rat model wherein rats are allowed access to voluntary running wheels, on which they are spontaneously active during their waking hours (243), just as humans have been throughout history until the last several decades. The wheels are then locked, and the animals reduce their activity from 5-6 km/night to regular cage activity, perhaps similar in the reduction that humans have recently experienced, and more akin to common reductions in physical activity that might occur such as when a recent college graduate, who is used to extensive walking on campus, is confined to a desk job. With the rat model used in the present studies, in just two days after the reduction in physical activity, there are multiple changes occurring that, if they also occur in humans, could provide a more direct

link for the relationship between a sedentary lifestyle and its devastating effects on human health.

For example, during the two days of reduced physical activity, there is a decrease in submaximal insulin-stimulated 2-deoxyglucose uptake into isolated epitrochlearis muscle (Chapter 4). This occurs concurrently with a decrease in insulin receptor β-subunit protein level and an impairment in insulin receptor function as measured by insulin-induced tyrosine phosphorylation of the receptor. There is also a decrease in Akt Ser^{473} phosphorylation, an important component of insulin signaling, and a decrease in the protein level of glucose transporter-4, which translocates to the cell surface in response to insulin stimulation to increase glucose uptake. Other potentially important findings in muscle include the increased muscle mass with voluntary wheel running (Chapter 5), which may improve whole body glucose uptake by providing increased tissue for glucose uptake, and the increase in mass of the soleus muscle, a predominately type I muscle that is associated with lower incidence of obesity and type II diabetes (119; 160; 175).

Also occurring during the two days of reduced physical activity is an increase in the mass of both the epididymal and omental fat masses. Follow-up experiments in the epididymal fat pad revealed that the increase in mass was the result of larger cells (Chapter 6). Further testing demonstrated that the increased epididymal adipocyte size was associated with an overshoot in the increase in the synthesis of triacylglycerol above that of regular sedentary cage activity. The overshoot in triacylglycerol synthesis is consistent with Booth and Chakravarthy's

corollary to Neel's thrifty gene hypothesis (196), which is that with regular physical activity, such as would have occurred during evolution and continued until recent times, there would be physical activity-rest cycles, and that during the rest cycle, there would be mechanisms to ensure efficient replenishment of energy stores that were expended during the activity (40).

To further examine the cause of the overshoot in triacylglycerol synthesis, the activity of glycerol-3-phosphate acyltransferase (GPAT), which is potentially the rate-limiting step of triacylglycerol synthesis (49), was examined. It was found that, similar to triacylglycerol synthesis, the activity of the mitochondrial isoform of GPAT also had an overshoot at two days of reduced physical activity (Chapter 7). Subsequent experiments showed that an increase in mitochondrial GPAT protein increased with voluntary wheel running, and likely contributes to the overshoot. The mechanism responsible for the increased mitochondrial GPAT protein is unclear, as the mitochondrial GPAT mRNA level is suppressed immediately post-activity, and does not increase above that of sedentary rats.

Together, the studies presented herein provide a novel and important contribution that is relevant to the fields of skeletal muscle and adipose tissue metabolism, biochemistry, and exercise physiology. They provide a seminal foundation of mechanistic insights on how reduced physical activity elicits physiological changes that are commonly associated with common modern chronic diseases, such as insulin resistance and increased intraabdominal fat mass and adipocyte size. Although there is a preponderance of epidemiological evidence that regular physical activity is crucial for optimal health maintenance

[reviewed in (22; 23; 71; 286)], the studies presented herein begin to provide a more biological basis for emphasizing the critical importance of regular activity, and they highlight the potential dangers of physical inactivity by illustrating the detrimental effects of a sedentary lifestyle. Coupled with potential future human studies, these studies could help to form a mechanistic foundation upon which recommendations for physical activity patterns can be made. Recommendations for prescribing physical activity that can initiate a reversal of the epidemics of obesity and type II diabetes are urgently needed (226). Future work in both animals and humans to follow up on these studies is needed to more clearly understand the cellular and molecular basis of how physical inactivity increases the risk of modern chronic disease.

Chapter 9: References

1. **Abbasi F, Brown BW, Jr., Lamendola C, McLaughlin T and Reaven GM**. Relationship between obesity, insulin resistance, and coronary heart disease risk. *J Am Coll Cardiol* 40: 937-943, 2002.

2. **Abella A, Garcia-Vicente S, Viguerie N, Ros-Baro A, Camps M, Palacin M, Zorzano A and Marti L**. Adipocytes release a soluble form of VAP-1/SSAO by a metalloprotease-dependent process and in a regulated manner. *Diabetologia* 47: 429-438, 2004.

3. **Almeras N, Lemieux S, Bouchard C and Tremblay A**. Fat gain in female swimmers. *Physiol Behav* 61: 811-817, 1997.

4. **Altman A and Villalba M**. Protein kinase C-theta (PKCtheta): it's all about location, location, location. *Immunol Rev* 192: 53-63, 2003.

5. **Anantharaman-Barr HG and Decombaz J**. The effect of wheel running and the estrous cycle on energy expenditure in female rats. *Physiol Behav* 46: 259-263, 1989.

6. **Applegate EA and Stern JS**. Exercise termination effects on food intake, plasma insulin, and adipose lipoprotein lipase activity in the Osborne-Mendel rat. *Metabolism* 36: 709-714, 1987.

7. **Applegate EA, Upton DE and Stern JS**. Exercise and detraining: effect on food intake, adiposity and lipogenesis in Osborne-Mendel rats made obese by a high fat diet. *J Nutr* 114: 447-459, 1984.

8. **Arciero PJ, Smith DL and Calles-Escandon J**. Effects of short-term inactivity on glucose tolerance, energy expenditure, and blood flow in trained subjects. *J Appl Physiol* 84: 1365-73, 1998.

9. **Argiles JM, Lopez-Soriano J, Almendro V, Busquets S and Lopez-Soriano FJ**. Cross-talk between skeletal muscle and adipose tissue: a link with obesity? *Med Res Rev* 25: 49-65, 2005.

10. **Armstrong RB, Saubert CW, Sembrowich WL, Shepherd RE and Gollnick PD**. Glycogen depletion in rat skeletal muscle fibers at different intensities and durations of exercise. *Pflugers Arch* 352: 243-256, 1974.

11. **Askew EW, Dohm GL, Doub WH, Jr., Husotn RL and Van Natta PA**. Lipogenesis and glyceride synthesis in the rat: response to diet and exercise. *J Nutr* 105: 190-199, 1975.

12. **Askew EW, Huston RL and Dohm GL**. Effect of physical training on esterification of glycerol-3-phosphate by homogenates of liver, skeletal muscle, heart, and adipose tissue of rats. *Metabolism* 22: 473-480, 1973.

13. **Askew EW, Huston RL, Plopper CG and Hecker AL**. Adipose tissue cellularity and lipolysis. Response to exercise and cortisol treatment. *J Clin Invest* 56: 521-529, 1975.

14. **Bagby GJ, Johnson JL, Bennett BW and Shepherd RE**. Muscle lipoprotein lipase activity in voluntarily exercising rats. *J Appl Physiol* 60: 1623-1627, 1986.

15. **Baron AD, Brechtel G, Wallace P and Edelman SV**. Rates and tissue sites of non-insulin- and insulin-mediated glucose uptake in humans. *Am J Physiol* 255: E769-E774, 1988.

16. **Bell PM**. Clinical significance of insulin resistance. *Diabet Med* 13: 504-509, 1996.

17. **Bell RM and Coleman RA**.In: The Enzymes, edited by Boyer PD. New York: Academic Press, 1983, p. 87-112.

18. **Bennett MK and Osborne TF**. Nutrient regulation of gene expression by the sterol regulatory element binding proteins: increased recruitment of gene-specific coregulatory factors and selective hyperacetylation of histone H3 in vivo. *Proc Natl Acad Sci U S A* 97: 6340-6344, 2000.

19. **Blundell JE, Stubbs RJ, Hughes DA, Whybrow S and King NA**. Cross talk between physical activity and appetite control: does physical activity stimulate appetite? *Proc Nutr Soc* 62: 651-661, 2003.

20. **Bogardus C, Thuillez P, Ravussin E, Vasquez B, Narimiga M and Azhar S**. Effect of muscle glycogen depletion on in vivo insulin action in man. *J Clin Invest* 72: 1605-1610, 1983.

21. **Bonen A, Clune PA and Tan MH**. Chronic exercise increases insulin binding in muscles but not liver. *Am J Physiol* 251: E196-E203, 1986.

22. **Booth FW, Chakravarthy MV, Gordon SE and Spangenburg EE**. Waging war on physical inactivity: using modern molecular ammunition against an ancient enemy. *J Appl Physiol* 93: 3-30, 2002.

23. **Booth FW, Gordon SE, Carlson CJ and Hamilton MT**. Waging war on modern chronic diseases: primary prevention through exercise biology. *J Appl Physiol* 88: 774-787, 2000.

24. **Booth MA, Booth MJ and Taylor AW**. Rat fat cell size and number with exercise training, detraining and weight loss. *Fed Proc* 33: 1959-1963, 1974.

25. **Boute N, Boubekeur S, Lacasa D and Issad T**. Dynamics of the interaction between the insulin receptor and protein tyrosine-phosphatase 1B in living cells. *EMBO Rep* 4: 313-319, 2003.

26. **Bradford MM**. A rapid and sensitive method for the quantitation of microgram quantities of protein utilizing the principle of protein-dye binding. *Anal Biochem* 72: 248-254, 1976.

27. **Bransome ED, Jr.** The design of double label radioisotope experiments. *Methods Enzymol* 40: 293-302, 1975.

28. **Bray GA**. Medical consequences of obesity. *J Clin Endocrinol Metab* 89: 2583-2589, 2004.

29. **Brown M, Ross TP and Holloszy JO**. Effects of ageing and exercise on soleus and extensor digitorum longus muscles of female rats. *Mech Ageing Dev* 63: 69-77, 1992.

30. **Brownson RC, Boehmer TK and Luke DA**. DECLINING RATES OF PHYSICAL ACTIVITY IN THE UNITED STATES: What Are the Contributors? *Annu Rev Public Health* 26: 421-443, 2005.

31. **Buemann B and Tremblay A**. Effects of exercise training on abdominal obesity and related metabolic complications. *Sports Med* 21: 191-212, 1996.

32. **Bukowiecki L, Lupien J, Follea N, Paradis A, Richard D and LeBlanc J**. Mechanism of enhanced lipolysis in adipose tissue of exercise-trained rats. *Am J Physiol* 239: E422-E429, 1980.

33. **Burstein R, Polychronakos C, Toews CJ, MacDougall JD, Guyda HJ and Posner BI**. Acute reversal of the enhanced insulin action in trained athletes. Association with insulin receptor changes. *Diabetes* 34: 756-60, 1985.

34. **Caprio S**. Insulin resistance in childhood obesity. *J Pediatr Endocrinol Metab* 15 Suppl 1: 487-492, 2002.

35. **Cartee GD, Briggs-Tung C and Kietzke EW**. Persistent effects of exercise on skeletal muscle glucose transport across the life-span of rats. *J Appl Physiol* 75: 972-978, 1993.

36. **Cartee GD, Douen AG, Ramlal T, Klip A and Holloszy JO**. Stimulation of glucose transport in skeletal muscle by hypoxia. *J Appl Physiol* 70: 1593-1600, 1991.

37. **Cartee GD, Young DA, Sleeper MD, Zierath J, Wallberg-Henriksson H and Holloszy JO**. Prolonged increase in insulin-stimulated glucose transport in muscle after exercise. *Am J Physiol* 256: E494-E499, 1989.

38. **Cartwright AL**. Determination of adipose tissue cellularity. In: Biology of the Adipocyte: Research Approaches, edited by Hausman GJ and Martin R. New York: Von Nostrand Reinhold Company, 1987.

39. **Chakravarthy MV and Booth FW**. Eating, exercise, and "thrifty" genotypes: connecting the dots toward an evolutionary understanding of modern chronic diseases. *J Appl Physiol* 96: 3-10, 2004.

40. **Chakravarthy MV and Booth FW**. Eating, exercise, and "thrifty" genotypes: connecting the dots toward an evolutionary understanding of modern chronic diseases. *J Appl Physiol* 96: 3-10, 2004.

41. **Chakravarty K, Leahy P, Becard D, Hakimi P, Foretz M, Ferre P, Foufelle F and Hanson RW**. Sterol regulatory element-binding protein-1c mimics the negative effect of insulin on phosphoenolpyruvate carboxykinase (GTP) gene transcription. *J Biol Chem* 276: 34816-34823, 2001.

42. **Chakravarty K, Wu SY, Chiang CM, Samols D and Hanson RW**. SREBP-1c and Sp1 interact to regulate transcription of the gene for phosphoenolpyruvate carboxykinase (GTP) in the liver. *J Biol Chem* 279: 15385-15395, 2004.

43. **Chen HC and Farese RV, Jr.** Inhibition of triglyceride synthesis as a treatment strategy for obesity: lessons from DGAT1-deficient mice. *Arterioscler Thromb Vasc Biol* 25: 482-486, 2005.

44. **Cheng A, Dube N, Gu F and Tremblay ML**. Coordinated action of protein tyrosine phosphatases in insulin signal transduction. *Eur J Biochem* 269: 1050-1059, 2002.

45. **Chibalin AV, Yu M, Ryder JW, Song XM, Galuska D, Krook A, Wallberg-Henriksson H and Zierath JR**. Exercise-induced changes in expression and activity of proteins involved in insulin signal transduction in skeletal muscle: differential effects on insulin-receptor substrates 1 and 2. *Proc Natl Acad Sci U S A* 97: 38-43, 2000.

46. **Cianflone K**. Acylation stimulating protein and triacylglycerol synthesis: potential drug targets? *Curr Pharm Des* 9: 1397-1410, 2003.

47. **Clevenger CM, Parker JP, Tanaka H, Seals DR and DeSouza CA**. Decline in insulin action with age in endurance-trained humans. *J Appl Physiol* 93: 2105-2111, 2002.

48. **Coleman R and Bell RM**. Triacylglycerol synthesis in isolated fat cells. Studies on the microsomal diacylglycerol acyltransferase activity using ethanol-dispersed diacylglycerols. *J Biol Chem* 251: 4537-4543, 1976.

49. **Coleman RA and Lee DP**. Enzymes of triacylglycerol synthesis and their regulation. *Prog Lipid Res* 43: 134-176, 2004.

50. **Collier G, Leshner AI and Squibb RL**. Dietary self-selection in active and non-active rats. *Physiol Behav* 4: 79-82, 1969.

51. **Constable SH, Favier RJ, Cartee GD, Young DA and Holloszy JO**. Muscle glucose transport: interactions of in vitro contractions, insulin, and exercise. *J Appl Physiol* 64: 2329-2332, 1988.

52. **Craig BW and Foley PJ**. Effects of cell size and exercise on glucose uptake and metabolism in adipocytes of female rats. *J Appl Physiol* 57: 1120-5, 1984.

53. **Craig BW, Garthwaite SM and Holloszy JO**. Adipocyte insulin resistance: effects of aging, obesity, exercise, and food restriction. *J Appl Physiol* 62: 95-100, 1987.

54. **Craig BW, Thompson K and Holloszy JO**. Effects of stopping training on size and response to insulin of fat cells in female rats. *J Appl Physiol* 54: 571-5, 1983.

55. **Darlington GJ, Ross SE and MacDougald OA**. The role of C/EBP genes in adipocyte differentiation. *J Biol Chem* 273: 30057-30060, 1998.

56. **Davies SP, Helps NR, Cohen PT and Hardie DG**. 5'-AMP inhibits dephosphorylation, as well as promoting phosphorylation, of the AMP-activated protein kinase. Studies using bacterially expressed human protein phosphatase-2C alpha and native bovine protein phosphatase-2AC. *FEBS Lett* 377: 421-425, 1995.

57. **De Cesare D. and Sassone-Corsi P**. Transcriptional regulation by cyclic AMP-responsive factors. *Prog Nucleic Acid Res Mol Biol* 64: 343-369, 2000.

58. **DeFronzo RA, Jacot E, Jequier E, Maeder E, Wahren J and Felber JP**. The effect of insulin on the disposal of intravenous glucose. Results from indirect calorimetry and hepatic and femoral venous catheterization. *Diabetes* 30: 1000-1007, 1981.

59. **Deheeger M, Rolland-Cachera MF and Fontvieille AM**. Physical activity and body composition in 10 year old French children: linkages with nutritional intake? *Int J Obes Relat Metab Disord* 21: 372-379, 1997.

60. **Dela F, Mikines KJ, von LM, Secher NH and Galbo H**. Effect of training on insulin-mediated glucose uptake in human muscle. *Am J Physiol* 263: E1134-E1143, 1992.

61. **Dela F, Ploug T, Handberg A, Petersen LN, Larsen JJ, Mikines KJ and Galbo H**. Physical training increases muscle GLUT4 protein and mRNA in patients with NIDDM. *Diabetes* 43: 862-865, 1994.

62. **Delp MD and Duan C**. Composition and size of type I, IIA, IID/X, and IIB fibers and citrate synthase activity of rat muscle. *J Appl Physiol* 80: 261-270, 1996.

63. **Despres JP**. Abdominal obesity as important component of insulin-resistance syndrome. *Nutrition* 9: 452-459, 1993.

64. **Despres JP, Bouchard C, Savard R, Tremblay A, Marcotte M and Theriault G**. Effects of exercise-training and detraining on fat cell lipolysis in men and women. *Eur J Appl Physiol Occup Physiol* 53: 25-30, 1984.

65. **Devlin JT, Hirshman M, Horton ED and Horton ES**. Enhanced peripheral and splanchnic insulin sensitivity in NIDDM men after single bout of exercise. *Diabetes* 36: 434-439, 1987.

66. **Di Girolamo M, Mendlinger S and Fertig JW**. A simple method to determine fat cell size and number in four mammalian species. *Am J Physiol* 221: 850-858, 1971.

67. **Ding ST, McNeel RL, Smith EO and Mersmann HJ**. Modulation of porcine adipocyte beta-adrenergic receptors by a beta-adrenergic agonist. *J Anim Sci* 78: 919-926, 2000.

68. **Dohm GL, Barakat HA, Tapscott EB and Beecher GR**. Changes in body fat and lipogenic enzyme activities in rats after termination of exercise training. *Proc Soc Exp Biol Med* 155: 157-159, 1977.

69. **Dudley GA, Abraham WM and Terjung RL**. Influence of exercise intensity and duration on biochemical adaptations in skeletal muscle. *J Appl Physiol* 53: 844-850, 1982.

70. **Dvorak RV, DeNino WF, Ades PA and Poehlman ET**. Phenotypic characteristics associated with insulin resistance in metabolically obese but normal-weight young women. *Diabetes* 48: 2210-2214, 1999.

71. **Eaton SB and Eaton SB**. An evolutionary perspective on human physical activity: implications for health. *Comp Biochem Physiol A Mol Integr Physiol* 136: 153-159, 2003.

72. **Edwards PA, Tabor D, Kast HR and Venkateswaran A**. Regulation of gene expression by SREBP and SCAP. *Biochim Biophys Acta* 1529: 103-113, 2000.

73. **Ehrhart-Bornstein M, Lamounier-Zepter V, Schraven A, Langenbach J, Willenberg HS, Barthel A, Hauner H, McCann SM, Scherbaum WA and Bornstein SR**. Human adipocytes secrete mineralocorticoid-releasing factors. *Proc Natl Acad Sci U S A* 100: 14211-14216, 2003.

74. **Elchebly M, Payette P, Michaliszyn E, Cromlish W, Collins S, Loy AL, Normandin D, Cheng A, Himms-Hagen J, Chan CC, Ramachandran C, Gresser MJ, Tremblay ML and Kennedy BP**. Increased insulin sensitivity and obesity resistance in mice lacking the protein tyrosine phosphatase-1B gene. *Science* 283: 1544-1548, 1999.

75. **Enevoldsen LH, Stallknecht B, Fluckey JD and Galbo H**. Effect of exercise training on in vivo lipolysis in intra-abdominal adipose tissue in rats. *Am J Physiol Endocrinol Metab* 279: E585-E592, 2000.

76. **Enevoldsen LH, Stallknecht B, Langfort J, Petersen LN, Holm C, Ploug T and Galbo H**. The effect of exercise training on hormone-sensitive lipase in rat intra-abdominal adipose tissue and muscle. *J Physiol* 536: 871-877, 2001.

77. **Ericsson J and Edwards PA**. CBP is required for sterol-regulated and sterol regulatory element-binding protein-regulated transcription. *J Biol Chem* 273: 17865-17870, 1998.

78. **Ericsson J, Jackson SM, Kim JB, Spiegelman BM and Edwards PA**. Identification of glycerol-3-phosphate acyltransferase as an adipocyte determination and differentiation factor 1- and sterol regulatory element-binding protein-responsive gene. *J Biol Chem* 272: 7298-7305, 1997.

79. **Etgen GJ, Jr., Brozinick JT, Jr., Kang HY and Ivy JL**. Effects of exercise training on skeletal muscle glucose uptake and transport. *Am J Physiol* 264: C727-C733, 1993.

80. **Ferre P**. The biology of peroxisome proliferator-activated receptors: relationship with lipid metabolism and insulin sensitivity. *Diabetes* 53 Suppl 1: S43-S50, 2004.

81. **Flegal KM, Carroll MD, Kuczmarski RJ and Johnson CL**. Overweight and obesity in the United States: prevalence and trends, 1960-1994. *Int J Obes Relat Metab Disord* 22: 39-47, 1998.

82. **Flegal KM, Carroll MD, Ogden CL and Johnson CL**. Prevalence and trends in obesity among US adults, 1999-2000. *JAMA* 288: 1723-1727, 2002.

83. **Fleshner M, Moraska A, Nguyen KT, Mazzeo RM and Roth DA**. Voluntary execise potentiates whereas forced exercise suppresses anti-KLH responses. *Soc Neurosci Abstr* 23: 314, 1997.

84. **Fomon SJ, Haschke F, Ziegler EE and Nelson SE**. Body composition of reference children from birth to age 10 years. *Am J Clin Nutr* 35: 1169-1175, 1982.

85. **Ford ES, Giles WH and Dietz WH**. Prevalence of the metabolic syndrome among US adults: findings from the third National Health and Nutrition Examination Survey. *JAMA* 287: 356-359, 2002.

86. **Fradette J, Wolfe D, Goins WF, Huang S, Flanigan RM and Glorioso JC**. HSV vector-mediated transduction and GDNF secretion from adipose cells. *Gene Ther* 12: 48-58, 2005.

87. **Franckhauser S, Munoz S, Pujol A, Casellas A, Riu E, Otaegui P, Su B and Bosch F**. Increased fatty acid re-esterification by PEPCK overexpression in adipose tissue leads to obesity without insulin resistance. *Diabetes* 51: 624-630, 2002.

88. **Frayn KN**. Visceral fat and insulin resistance--causative or correlative? *Br J Nutr* 83 Suppl 1: S71-S77, 2000.

89. **Gajendran N, Frey JR, Lefkovits I, Kuhn L, Fountoulakis M, Krapfenbauer K and Brenner HR**. Proteomic analysis of secreted muscle components: search for factors involved in neuromuscular synapse formation. *Proteomics* 2: 1601-1615, 2002.

90. **Galton DJ**. Lipogenesis in human adipose tissue. *J Lipid Res* 9: 19-26, 1968.

91. **Gan SK, Kriketos AD, Poynten AM, Furler SM, Thompson CH, Kraegen EW, Campbell LV and Chisholm DJ**. Insulin action, regional fat, and myocyte lipid: altered relationships with increased adiposity. *Obes Res* 11: 1295-1305, 2003.

92. **Giada F, Vigna GB, Vitale E, Baldo-Enzi G, Bertaglia M, Crecca R and Fellin R**. Effect of age on the response of blood lipids, body composition, and aerobic power to physical conditioning and deconditioning. *Metabolism* 44: 161-165, 1995.

93. **Giandomenico V, Simonsson M, Gronroos E and Ericsson J**. Coactivator-dependent acetylation stabilizes members of the SREBP family of transcription factors. *Mol Cell Biol* 23: 2587-2599, 2003.

94. **Goodman HM**. Endocrinology concepts for medical students. *Adv Physiol Educ* 25: 213-224, 2001.

95. **Goodyear LJ, Hirshman MF, Valyou PM and Horton ES**. Glucose transporter number, function, and subcellular distribution in rat skeletal muscle after exercise training. *Diabetes* 41: 1091-1099, 1992.

96. **Goodyear LJ and Kahn BB**. Exercise, glucose transport, and insulin sensitivity. *Annu Rev Med* 49: 235-261, 1998.

97. **Gregoire FM**. Adipocyte differentiation: from fibroblast to endocrine cell. *Exp Biol Med (Maywood)* 226: 997-1002, 2001.

98. **Gulve EA, Rodnick KJ, Henriksen EJ and Holloszy JO**. Effects of wheel running on glucose transporter (GLUT4) concentration in skeletal muscle of young adult and old rats. *Mech Ageing Dev* 67: 187-200, 1993.

99. **Gustat J, Srinivasan SR, Elkasabany A and Berenson GS**. Relation of self-rated measures of physical activity to multiple risk factors of insulin resistance syndrome in young adults: the Bogalusa Heart Study. *J Clin Epidemiol* 55: 997-1006, 2002.

100. **Gutin B and Owens S**. Role of exercise intervention in improving body fat distribution and risk profile in children. *Am J Human Biol* 11: 237-247, 1999.

101. **Hamilton MT, Etienne J, McClure WC, Pavey BS and Holloway AK**. Role of local contractile activity and muscle fiber type on LPL regulation during exercise. *Am J Physiol* 275: E1016-E1022, 1998.

102. **Han DH, Hansen PA, Host HH and Holloszy JO**. Insulin resistance of muscle glucose transport in rats fed a high-fat diet: a reevaluation. *Diabetes* 46: 1761-1767, 1997.

103. **Hansen P, Gulve E, Gao J, Schluter J, Mueckler M and Holloszy J**. Kinetics of 2-deoxyglucose transport in skeletal muscle: effects of insulin and contractions. *Am J Physiol* 268: C30-C35, 1995.

104. **Hansen PA, Gulve EA and Holloszy JO**. Suitability of 2-deoxyglucose for in vitro measurement of glucose transport activity in skeletal muscle. *J Appl Physiol* 76: 979-985, 1994.

105. **Hardman AE, Lawrence JE and Herd SL**. Postprandial lipemia in endurance-trained people during a short interruption to training. *J Appl Physiol* 84: 1895-1901, 1998.

106. **Harte AL, McTernan PG, McTernan CL, Smith SA, Barnett AH and Kumar S**. Rosiglitazone inhibits the insulin-mediated increase in PAI-1 secretion in human abdominal subcutaneous adipocytes. *Diabetes Obes Metab* 5: 302-310, 2003.

107. **Hassid WZ and Abraham S**. Chemical procedures for analysis of polysaccharides. *Methods Enzymol* 3: 34-50, 1957.

108. **Hausman DB, DiGirolamo M, Bartness TJ, Hausman GJ and Martin RJ**. The biology of white adipocyte proliferation. *Obes Rev* 2: 239-254, 2001.

109. **Hawley JA**. Exercise as a therapeutic intervention for the prevention and treatment of insulin resistance. *Diabetes Metab Res Rev* 20: 383-393, 2004.

110. **Hawley SA, Davison M, Woods A, Davies SP, Beri RK, Carling D and Hardie DG**. Characterization of the AMP-activated protein kinase kinase from rat liver and identification of threonine 172 as the major site at which it phosphorylates AMP-activated protein kinase. *J Biol Chem* 271: 27879-27887, 1996.

111. **Heath GW, Gavin JR3, Hinderliter JM, Hagberg JM, Bloomfield SA and Holloszy JO**. Effects of exercise and lack of exercise on glucose tolerance and insulin sensitivity. *J Appl Physiol* 55: 512-7, 1983.

112. **Hebert JA and Lopez A**. Metabolic effects of exercise. II. Residual metabolic effects of exercise in rats. *Proc Soc Exp Biol Med* 148: 646-649, 1975.

113. **Henriksen EJ, Bourey RE, Rodnick KJ, Koranyi L, Permutt MA and Holloszy JO**. Glucose transporter protein content and glucose transport capacity in rat skeletal muscles. *Am J Physiol* 259: 593-8, 1990.

114. **Henriksen EJ and Halseth AE**. Early alterations in soleus GLUT-4, glucose transport, and glycogen in voluntary running rats. *J Appl Physiol* 76: 1862-7, 1994.

115. **Henriksen EJ and Holloszy JO**. Effect of diffusion distance on measurement of rat skeletal muscle glucose transport in vitro. *Acta Physiol Scand* 143: 381-386, 1991.

116. **Herd SL, Hardman AE, Boobis LH and Cairns CJ**. The effect of 13 weeks of running training followed by 9 d of detraining on postprandial lipaemia. *Br J Nutr* 80: 57-66, 1998.

117. **Hespel P and Richter EA**. Glucose uptake and transport in contracting, perfused rat muscle with different pre-contraction glycogen concentrations. *J Physiol* 427: 347-359, 1990.

118. **Hickey MS, Carey JO, Azevedo JL, Houmard JA, Pories WJ, Israel RG and Dohm GL**. Skeletal muscle fiber composition is related to adiposity and in vitro glucose transport rate in humans. *Am J Physiol* 268: 453-7, 1995.

119. **Hickey MS, Carey JO, Azevedo JL, Houmard JA, Pories WJ, Israel RG and Dohm GL**. Skeletal muscle fiber composition is related to adiposity and in vitro glucose transport rate in humans. *Am J Physiol* 268: E453-E457, 1995.

120. **Hill JO, Wyatt HR, Reed GW and Peters JC**. Obesity and the environment: where do we go from here? *Science* 299: 853-855, 2003.

121. **Hokama JY, Streeper RS and Henriksen EJ**. Voluntary exercise training enhances glucose transport in muscle stimulated by insulin-like growth factor I. *J Appl Physiol* 82: 508-512, 1997.

122. **Holloszy JO and Booth FW**. Biochemical adaptations to endurance exercise in muscle. *Annu Rev Physiol* 38: 273-291, 1976.

123. **Holloszy JO, Oscai LB, Don IJ and Mole PA**. Mitochondrial citric acid cycle and related enzymes: adaptive response to exercise. *Biochem Biophys Res Commun* 40: 1368-1373, 1970.

124. **Horton JD**. Sterol regulatory element-binding proteins: transcriptional activators of lipid synthesis. *Biochem Soc Trans* 30: 1091-1095, 2002.

125. **Host HH, Hansen PA, Nolte LA, Chen MM and Holloszy JO**. Rapid reversal of adaptive increases in muscle GLUT-4 and glucose transport capacity after training cessation. *J Appl Physiol* 84: 798-802, 1998.

126. **Host HH, Hansen PA, Nolte LA, Chen MM and Holloszy JO**. Glycogen supercompensation masks the effect of a traininginduced increase in GLUT-4 on muscle glucose transport. *J Appl Physiol* 85: 133-8, 1998.

127. **Houmard JA, Egan PC, Neufer PD, Friedman JE, Wheeler WS, Israel RG and Dohm GL**. Elevated skeletal muscle glucose transporter levels in exercise-trained middle-aged men. *Am J Physiol* 261: 437-43, 1991.

128. **Houmard JA, Shaw CD, Hickey MS and Tanner CJ**. Effect of short-term exercise training on insulin-stimulated PI 3- kinase activity in human skeletal muscle. *Am J Physiol* 277: 1055-60, 1999.

129. **Houmard JA, Shinebarger MH, Dolan PL, Leggett-Frazier N, Bruner RK, McCammon MR, Israel RG and Dohm GL**. Exercise training increases GLUT-4 protein concentration in previously sedentary middle-aged men. *Am J Physiol* 264: 896-901, 1993.

130. **Houmard JA, Tyndall GL, Midyette JB, Hickey MS, Dolan PL, Gavigan KE, Weidner ML and Dohm GL**. Effect of reduced training and training cessation on insulin action and muscle GLUT-4. *J Appl Physiol* 81: 1162-1168, 1996.

131. **Hu FB**. Sedentary lifestyle and risk of obesity and type 2 diabetes. *Lipids* 38: 103-108, 2003.

132. **Hughes VA, Fiatarone MA, Fielding RA, Kahn BB, Ferrara CM, Shepherd P, Fisher EC, Wolfe RR, Elahi D and Evans WJ**. Exercise increases muscle GLUT-4 levels and insulin action in subjects with impaired glucose tolerance. *Am J Physiol* 264: E855-E862, 1993.

133. **Idris I, Gray S and Donnelly R**. Insulin action in skeletal muscle: isozyme-specific effects of protein kinase C. *Ann N Y Acad Sci* 967: 176-182, 2002.

134. **Igal RA, Wang S, Gonzalez-Baro M and Coleman RA**. Mitochondrial glycerol phosphate acyltransferase directs the incorporation of exogenous fatty acids into triacylglycerol. *J Biol Chem* 276: 42205-42212, 2001.

135. **Izawa T, Komabayashi T, Mochizuki T, Suda K and Tsuboi M**. Enhanced coupling of adenylate cyclase to lipolysis in permeabilized adipocytes from trained rats. *J Appl Physiol* 71: 23-29, 1991.

136. **Janke J, Engeli S, Gorzelniak K, Luft FC and Sharma AM**. Mature adipocytes inhibit in vitro differentiation of human preadipocytes via angiotensin type 1 receptors. *Diabetes* 51: 1699-1707, 2002.

137. **Jensen J, Aslesen R, Ivy JL and Brors O**. Role of glycogen concentration and epinephrine on glucose uptake in rat epitrochlearis muscle. *Am J Physiol* 272: E649-E655, 1997.

138. **Jerkins AA, Liu WR, Lee S and Sul HS**. Characterization of the murine mitochondrial glycerol-3-phosphate acyltransferase promoter. *J Biol Chem* 270: 1416-1421, 1995.

139. **Johnson PB, Kochan R and Graves D**. Voluntary exercise, food intake pattern, and early growth in young male albino rats. *Med Sci Sports* 9: 54, 1977.

140. **Kahn CR**. Insulin resistance, insulin insensitivity, and insulin unresponsiveness: a necessary distinction. *Metabolism* 27: 1893-1902, 1978.

141. **Karelis AD, St-Pierre DH, Conus F, Rabasa-Lhoret R and Poehlman ET**. Metabolic and body composition factors in subgroups of obesity: what do we know? *J Clin Endocrinol Metab* 89: 2569-2575, 2004.

142. **Katz LD, Glickman MG, Rapoport S, Ferrannini E and DeFronzo RA**. Splanchnic and peripheral disposal of oral glucose in man. *Diabetes* 32: 675-679, 1983.

143. **Kawanaka K, Tabata I, Katsuta S and Higuchi M**. Changes in insulin-stimulated glucose transport and GLUT-4 protein in rat skeletal muscle after training. *J Appl Physiol* 83: 2043-2047, 1997.

144. **Kawanami H, Nomura S, Sakurai T, Sakurai T, Yamagishi H, Komabayashi T and Izawa T**. Possible role of nitric oxide on adipocyte lipolysis in exercise-trained rats. *Jpn J Physiol* 52: 343-352, 2002.

145. **Kershaw EE and Flier JS**. Adipose tissue as an endocrine organ. *J Clin Endocrinol Metab* 89: 2548-2556, 2004.

146. **Kersten S, Desvergne B and Wahli W**. Roles of PPARs in health and disease. *Nature* 405: 421-424, 2000.

147. **Kim JH, Lee JN and Paik YK**. Cholesterol biosynthesis from lanosterol. A concerted role for Sp1 and NF-Y-binding sites for sterol-mediated regulation of rat 7-dehydrocholesterol reductase gene expression. *J Biol Chem* 276: 18153-18160, 2001.

148. **Kim JK, Fillmore JJ, Sunshine MJ, Albrecht B, Higashimori T, Kim DW, Liu ZX, Soos TJ, Cline GW, O'Brien WR, Littman DR and Shulman GI**. PKC-theta knockout mice are protected from fat-induced insulin resistance. *J Clin Invest* 114: 823-827, 2004.

149. **Kim JY, Nolte LA, Hansen PA, Han DH, Ferguson K, Thompson PA and Holloszy JO**. High-fat diet-induced muscle insulin resistance: relationship to visceral fat mass. *Am J Physiol Regul Integr Comp Physiol* 279: R2057-R2065, 2000.

150. **Kim JY, Nolte LA, Hansen PA, Han DH, Kawanaka K and Holloszy JO**. Insulin resistance of muscle glucose transport in male and female rats fed a high-sucrose diet. *Am J Physiol* 276: R665-R672, 1999.

151. **King DS, Dalsky GP, Clutter WE, Young DA, Staten MA, Cryer PE and Holloszy JO**. Effects of exercise and lack of exercise on insulin sensitivity and responsiveness. *J Appl Physiol* 64: 1942-6, 1988.

152. **Kirwan JP, del Aguila LF, Hernandez JM, Williamson DL, O'Gorman DJ, Lewis R and Krishnan RK**. Regular exercise enhances insulin

activation of IRS-1-associated PI3- kinase in human skeletal muscle. *J Appl Physiol* 88: 797-803, 2000.

153. **Kirwan JP and Jing M**. Modulation of insulin signaling in human skeletal muscle in response to exercise. *Exerc Sport Sci Rev* 30: 85-90, 2002.

154. **Klaman LD, Boss O, Peroni OD, Kim JK, Martino JL, Zabolotny JM, Moghal N, Lubkin M, Kim YB, Sharpe AH, Stricker-Krongrad A, Shulman GI, Neel BG and Kahn BB**. Increased energy expenditure, decreased adiposity, and tissue-specific insulin sensitivity in protein-tyrosine phosphatase 1B-deficient mice. *Mol Cell Biol* 20: 5479-5489, 2000.

155. **Kono T and Barham FW**. The relationship between the insulin-binding capacity of fat cells and the cellular response to insulin. Studies with intact and trypsin-treated fat cells. *J Biol Chem* 246: 6210-6216, 1971.

156. **Kotzka J, Muller-Wieland D, Koponen A, Njamen D, Kremer L, Roth G, Munck M, Knebel B and Krone W**. ADD1/SREBP-1c mediates insulin-induced gene expression linked to the MAP kinase pathway. *Biochem Biophys Res Commun* 249: 375-379, 1998.

157. **Kratchmarova I, Kalume DE, Blagoev B, Scherer PE, Podtelejnikov AV, Molina H, Bickel PE, Andersen JS, Fernandez MM, Bunkenborg J, Roepstorff P, Kristiansen K, Lodish HF, Mann M and Pandey A**. A proteomic approach for identification of secreted proteins during the differentiation of 3T3-L1 preadipocytes to adipocytes. *Mol Cell Proteomics* 1: 213-222, 2002.

158. **Krempler F, Breban D, Oberkofler H, Esterbauer H, Hell E, Paulweber B and Patsch W**. Leptin, peroxisome proliferator-activated receptor-gamma, and CCAAT/enhancer binding protein-alpha mRNA expression in adipose tissue of humans and their relation to cardiovascular risk factors. *Arterioscler Thromb Vasc Biol* 20: 443-449, 2000.

159. **Krichevsky MI, Zaveler SA and Bulkeley J**. Computer-aided single of dual isotope channels ratio quench correction in liquid scintillation counting. *Anal Biochem* 22: 442-464, 1968.

160. **Kriketos AD, Pan DA, Lillioja S, Cooney GJ, Baur LA, Milner MR, Sutton JR, Jenkins AB, Bogardus C and Storlien LH**. Interrelationships between muscle morphology, insulin action, and adiposity. *Am J Physiol* 270: 1332-9, 1996.

161. **Kriska AM, LaPorte RE, Pettitt DJ, Charles MA, Nelson RG, Kuller LH, Bennett PH and Knowler WC**. The association of physical activity with obesity, fat distribution and glucose intolerance in Pima Indians. *Diabetologia* 36: 863-869, 1993.

162. **Kump DS and Booth FW**. Sustained rise in triacylglycerol synthesis and increased epididymal fat mass when rats cease voluntary wheel running. *J Physiol* In press DOI:10.113/jphysiol.2005.084625, 2005.

163. **Kump DS and Booth FW**. Alterations in insulin receptor signaling in the rat epitrochlearis muscle upon cessation of voluntary exercise. *J Physiol* 562: 829-838, 2005.

164. **Kump DS and Booth FW**. Increased glycerol-3-phosphate acyltransferase protein level and enzyme activity in rat epididymal fat upon cessation of wheel running. *Manuscript in preparation* 2005.

165. **Lambert EV, Wooding G, Lambert MI, Koeslag JH and Noakes TD**. Enhanced adipose tissue lipoprotein lipase activity in detrained rats: independent of changes in food intake. *J Appl Physiol* 77: 2564-2571, 1994.

166. **Larkin LM, Reynolds TH, Supiano MA, Kahn BB and Halter JB**. Effect of aging and obesity on insulin responsiveness and glut-4 glucose transporter content in skeletal muscle of Fischer 344 x Brown Norway rats. *J Gerontol A Biol Sci Med Sci* 56: B486-B492, 2001.

167. **Lawrence JC, Jr., Colvin J, Cartee GD and Holloszy JO**. Effects of aging and exercise on insulin action in rat adipocytes are correlated with changes in fat cell volume. *J Gerontol* 44: B88-B92, 1989.

168. **Lazar MA**. How obesity causes diabetes: not a tall tale. *Science* 307: 373-375, 2005.

169. **Le Marchand-Brustel Y and Freychet P**. Studies of insulin insensitivity in soleus muscles of obese mice. *Metabolism* 27: 1982-1993, 1978.

170. **LeMura LM, von Duvillard SP, Andreacci J, Klebez JM, Chelland SA and Russo J**. Lipid and lipoprotein profiles, cardiovascular fitness, body composition, and diet during and after resistance, aerobic and combination training in young women. *Eur J Appl Physiol* 82: 451-458, 2000.

171. **Lewin TM, Granger DA, Kim JH and Coleman RA**. Regulation of mitochondrial sn-glycerol-3-phosphate acyltransferase activity: response to feeding status is unique in various rat tissues and is discordant with protein expression. *Arch Biochem Biophys* 396: 119-127, 2001.

172. **Li A, Li H, Jin G and Xiu R**. A proteomic study on cell cycle progression of endothelium exposed to tumor conditioned medium and the possible role of cyclin D1/E. *Clin Hemorheol Microcirc* 29: 383-390, 2003.

173. **Li L, He S, Sun JM and Davie JR**. Gene regulation by Sp1 and Sp3. *Biochem Cell Biol* 82: 460-471, 2004.

174. **Lichtenstein P, Holm NV, Verkasalo PK, Iliadou A, Kaprio J, Koskenvuo M, Pukkala E, Skytthe A and Hemminki K**. Environmental and heritable factors in the causation of cancer--analyses of cohorts of twins from Sweden, Denmark, and Finland. *N Engl J Med* 343: 78-85, 2000.

175. **Lillioja S, Young AA, Culter CL, Ivy JL, Abbott WG, Zawadzki JK, Yki-Jarvinen H, Christin L, Secomb TW and Bogardus C**. Skeletal muscle capillary density and fiber type are possible determinants of in vivo insulin resistance in man. *J Clin Invest* 80: 415-424, 1987.

176. **Lim JW and Bodnar A**. Proteome analysis of conditioned medium from mouse embryonic fibroblast feeder layers which support the growth of human embryonic stem cells. *Proteomics* 2: 1187-1203, 2002.

177. **Litchfield DW**. Protein kinase CK2: structure, regulation and role in cellular decisions of life and death. *Biochem J* 369: 1-15, 2003.

178. **MacDougald OA and Lane MD**. Transcriptional regulation of gene expression during adipocyte differentiation. *Annu Rev Biochem* 64: 345-373, 1995.

179. **Maffeis C**. Aetiology of overweight and obesity in children and adolescents. *Eur J Pediatr* 159 Suppl 1: S35-S44, 2000.

180. **Magnuson MA, She P and Shiota M**. Gene-altered mice and metabolic flux control. *J Biol Chem* 278: 32485-32488, 2003.

181. **Marko-Varga G and Fehniger TE**. Proteomics and disease--the challenges for technology and discovery. *J Proteome Res* 3: 167-178, 2004.

182. **Marshall SJ, Biddle SJ, Gorely T, Cameron N and Murdey I**. Relationships between media use, body fatness and physical activity in children and youth: a meta-analysis. *Int J Obes Relat Metab Disord* 28: 1238-1246, 2004.

183. **Mayer-Davis EJ, D'Agostino R, Jr., Karter AJ, Haffner SM, Rewers MJ, Saad M and Bergman RN**. Intensity and amount of physical activity in relation to insulin sensitivity: the Insulin Resistance Atherosclerosis Study. *JAMA* 279: 669-674, 1998.

184. **McCoy M, Proietto J and Hargreves M**. Effect of detraining on GLUT-4 protein in human skeletal muscle. *J Appl Physiol* 77: 1532-1536, 1994.

185. **Mikines KJ, Sonne B, Farrell PA, Tronier B and Galbo H**. Effect of physical exercise on sensitivity and responsiveness to insulin in humans. *Am J Physiol* 254: E248-E259, 1988.

186. **Mikines KJ, Sonne B, Farrell PA, Tronier B and Galbo H**. Effect of training on the dose-response relationship for insulin action in men. *J Appl Physiol* 66: 695-703, 1989.

187. **Mikines KJ, Sonne B, Tronier B and Galbo H**. Effects of acute exercise and detraining on insulin action in trained men. *J Appl Physiol* 66: 704-11, 1989.

188. **Mokdad AH, Bowman BA, Ford ES, Vinicor F, Marks JS and Koplan JP**. The continuing epidemics of obesity and diabetes in the United States. *JAMA* 286: 1195-1200, 2001.

189. **Moller DE and Kaufman KD**. Metabolic syndrome: a clinical and molecular perspective. *Annu Rev Med* 56: 45-62, 2005.

190. **Mondon CE, Dolkas CB and Reaven GM**. Site of enhanced insulin sensitivity in exercise-trained rats at rest. *Am J Physiol* 239: E169-E177, 1980.

191. **Moraska A and Fleshner M**. Voluntary physical activity prevents stress-induced behavioral depression and anti-KLH antibody suppression. *Am J Physiol Regul Integr Comp Physiol* 281: R484-R489, 2001.

192. **Mujika I and Padilla S**. Detraining: loss of training-induced physiological and performance adaptations. Part I: short term insufficient training stimulus. *Sports Med* 30: 79-87, 2000.

193. **Mujika I and Padilla S**. Detraining: loss of training-induced physiological and performance adaptations. Part II: Long term insufficient training stimulus. *Sports Med* 30: 145-154, 2000.

194. **Munday MR**. Regulation of mammalian acetyl-CoA carboxylase. *Biochem Soc Trans* 30: 1059-1064, 2002.

195. **Muoio DM, Seefeld K, Witters LA and Coleman RA**. AMP-activated kinase reciprocally regulates triacylglycerol synthesis and fatty acid oxidation in liver and muscle: evidence that sn-glycerol-3-phosphate acyltransferase is a novel target. *Biochem J* 338 (Pt 3): 783-791, 1999.

196. **Neel J**. Diabetes mellitus a "thrifty" genotype rendered detrimental by "progress"? *Am J Human Genet* 14: 352-353, 1962.

197. **Nesher R, Karl IE, Kaiser KE and Kipnis DM**. Epitrochlearis muscle. I. Mechanical performance, energetics, and fiber composition. *Am J Physiol* 239: E454-E460, 1980.

198. **Nesher R, Karl IE and Kipnis DM**. Epitrochlearis muscle. II. Metabolic effects of contraction and catecholamines. *Am J Physiol* 239: E461-E467, 1980.

199. **Nesher R, Karl IE and Kipnis DM**. Dissociation of effects of insulin and contraction on glucose transport in rat epitrochlearis muscle. *Am J Physiol* 249: C226-C232, 1985.

200. **Neter J, Wasserman W, Kutner MH and Nachtscheim CJ**. *Applied Linear Statistical Models*. Boston: Richard D. Irwin, Inc., 1996.

201. **Neufer PD, Shinebarger MH and Dohm GL**. Effect of training and detraining on skeletal muscle glucose transporter (GLUT4) content in rats. *Can J Physiol Pharmacol* 70: 1286-1290, 1992.

202. **Nikoletseas MM**. Food intake in the exercising rat: a brief review. *Neurosci Biobehav Rev* 4: 265-267, 1980.

203. **Nishizawa H, Matsuda M, Yamada Y, Kawai K, Suzuki E, Makishima M, Kitamura T and Shimomura I**. Musclin, a novel skeletal muscle-derived secretory factor. *J Biol Chem* 279: 19391-19395, 2004.

204. **Nolte LA, Hansen PA, Chen MM, Schluter JM, Gulve EA and Holloszy JO**. Short-term exposure to tumor necrosis factor-alpha does not affect insulin-stimulated glucose uptake in skeletal muscle. *Diabetes* 47: 721-726, 1998.

205. **Numa S**. Regulation of fatty-acid synthesis in higher animals. *Ergeb Physiol* 69: 54-96, 1974.

206. **Nystrom FH and Quon MJ**. Insulin signalling: metabolic pathways and mechanisms for specificity. *Cell Signal* 11: 563-574, 1999.

207. **Ogden CL, Flegal KM, Carroll MD and Johnson CL**. Prevalence and trends in overweight among US children and adolescents, 1999-2000. *JAMA* 288: 1728-1732, 2002.

208. **Olefsky JM and Kolterman OG**. Mechanisms of insulin resistance in obesity and noninsulin-dependent (type II) diabetes. *Am J Med* 70: 151-168, 1981.

209. **Oliner JD, Andresen JM, Hansen SK, Zhou S and Tjian R**. SREBP transcriptional activity is mediated through an interaction with the CREB-binding protein. *Genes Dev* 10: 2903-2911, 1996.

210. **Onorato TM, Chakroborty S and Haldar D**. Phosphorylation of rat liver mitochondrial glycerol-3-phosphate acyltransferase by casein kinase 2. *J Biol Chem* In press [Epub ahead of print], 2005.

211. **Onorato TM and Haldar D**. Casein kinase II stimulates rat liver mitochondrial glycerophosphate acyltransferase activity. *Biochem Biophys Res Commun* 296: 1091-1096, 2002.

212. **Oshida Y, Yamanouchi K, Hayamizu S, Nagasawa J, Ohsawa I and Sato Y**. Effects of training and training cessation on insulin action. *Int J Sports Med* 12: 484-486, 1991.

213. **Ouwens DM, van der Zon GC and Maassen JA**. Modulation of insulin-stimulated glycogen synthesis by Src Homology Phosphatase 2. *Mol Cell Endocrinol* 175: 131-140, 2001.

214. **Ouyang P, Sung J, Kelemen MD, Hees PS, DeRegis JR, Turner KL, Bacher AC and Stewart KJ**. Relationships of insulin sensitivity with fatness and fitness and in older men and women. *J Womens Health (Larchmt)* 13: 177-185, 2004.

215. **Park H, Kaushik VK, Constant S, Prentki M, Przybytkowski E, Ruderman NB and Saha AK**. Coordinate regulation of malonyl-CoA decarboxylase, sn-glycerol-3-phosphate acyltransferase, and acetyl-CoA carboxylase by AMP-activated protein kinase in rat tissues in response to exercise. *J Biol Chem* 277: 32571-32577, 2002.

216. **Pate RR, Pratt M, Blair SN, Haskell WL, Macera CA, Bouchard C, Buchner D, Ettinger W, Heath GW, King AC and .** Physical activity and public health. A recommendation from the Centers for Disease Control and Prevention and the American College of Sports Medicine. *JAMA* 273: 402-407, 1995.

217. **Pattison JS, Folk LC, Madsen RW and Booth FW**. Selected Contribution: Identification of differentially expressed genes between young and old rat soleus muscle during recovery from immobilization-induced atrophy. *J Appl Physiol* 95: 2171-2179, 2003.

218. **Pattison JS, Folk LC, Madsen RW, Childs TE and Booth FW**. Transcriptional profiling identifies extensive downregulation of extracellular matrix gene expression in sarcopenic rat soleus muscle. *Physiol Genomics* 15: 34-43, 2003.

219. **Pattison JS, Folk LC, Madsen RW, Childs TE, Spangenburg EE and Booth FW**. Expression profiling identifies dysregulation of myosin heavy chains IIb and IIx during limb immobilization in the soleus muscles of old rats. *J Physiol* 553: 357-368, 2003.

220. **Pattison JS, Folk LC, Madsen RW, Childs TE, Spangenburg EE and Booth FW**. Expression profiling identifies dysregulation of myosin heavy chains IIb and IIx during limb immobilization in the soleus muscles of old rats. *J Physiol* 553: 357-368, 2003.

221. **Pedersen BK, Steensberg A, Fischer C, Keller C, Keller P, Plomgaard P, Wolsk-Petersen E and Febbraio M**. The metabolic role of IL-6 produced during exercise: is IL-6 an exercise factor? *Proc Nutr Soc* 63: 263-267, 2004.

222. **Pereira MA, Kriska AM, Joswiak ML, Dowse GK, Collins VR, Zimmet PZ, Gareeboo H, Chitson P, Hemraj F, Purran A and .** Physical inactivity and glucose intolerance in the multiethnic island of Mauritius. *Med Sci Sports Exerc* 27: 1626-1634, 1995.

223. **Perseghin G, Price TB, Petersen KF, Roden M, Cline GW, Gerow K, Rothman DL and Shulman GI**. Increased glucose transport-phosphorylation and muscle glycogen synthesis after exercise training in insulin-resistant subjects. *N Engl J Med* 335: 1357-1362, 1996.

224. **Petibois C, Cassaigne A, Gin H and Deleris G**. Lipid profile disorders induced by long-term cessation of physical activity in previously highly endurance-trained subjects. *J Clin Endocrinol Metab* 89: 3377-3384, 2004.

225. **Popkin BM**. The nutrition transition and its health implications in lower-income countries. *Public Health Nutr* 1: 5-21, 1998.

226. **Prentice RL, Willett WC, Greenwald P, Alberts D, Bernstein L, Boyd NF, Byers T, Clinton SK, Fraser G, Freedman L, Hunter D, Kipnis V, Kolonel LN, Kristal BS, Kristal A, Lampe JW, McTiernan A, Milner J, Patterson RE, Potter JD, Riboli E, Schatzkin A, Yates A and Yetley E**. Nutrition and physical activity and chronic disease prevention: research strategies and recommendations. *J Natl Cancer Inst* 96: 1276-1287, 2004.

227. **Rabilloud T, Strub JM, Luche S, van DA and Lunardi J**. A comparison between Sypro Ruby and ruthenium II tris (bathophenanthroline disulfonate) as fluorescent stains for protein detection in gels. *Proteomics* 1: 699-704, 2001.

228. **Rattarasarn C, Leelawattana R, Soonthornpun S, Setasuban W and Thamprasit A**. Gender differences of regional abdominal fat distribution and their relationships with insulin sensitivity in healthy and glucose-intolerant thais. *J Clin Endocrinol Metab* 89: 6266-6270, 2004.

229. **Rawson RB**. The SREBP pathway--insights from Insigs and insects. *Nat Rev Mol Cell Biol* 4: 631-640, 2003.

230. **Reaven G**. Metabolic syndrome: pathophysiology and implications for management of cardiovascular disease. *Circulation* 106: 286-288, 2002.

231. **Ren JM, Marshall BA, Gulve EA, Gao J, Johnson DW, Holloszy JO and Mueckler M**. Evidence from transgenic mice that glucose transport is rate-limiting for glycogen deposition and glycolysis in skeletal muscle. *J Biol Chem* 268: 16113-5, 1993.

232. **Ren JM, Semenkovich CF, Gulve EA, Gao J and Holloszy JO**. Exercise induces rapid increases in GLUT4 expression, glucose transport capacity, and insulin-stimulated glycogen storage in muscle. *J Biol Chem* 269: 14396-401, 1994.

233. **Reynolds TH, Brozinick JT, Jr., Larkin LM and Cushman SW**. Transient enhancement of GLUT-4 levels in rat epitrochlearis muscle after exercise training. *J Appl Physiol* 88: 2240-2245, 2000.

234. **Reynolds TH, Brozinick JT, Jr., Rogers MA and Cushman SW**. Effects of exercise training on glucose transport and cell surface GLUT-4 in isolated rat epitrochlearis muscle. *Am J Physiol* 272: E320-E325, 1997.

235. **Richter EA**. Glucose utilization. In: Handbook of Physiology, Section 12, Exercise: Regulation and integration of multiple systems, edited by Rowell LB and Shepherd LT. New York: Oxford Univ. Press, 1996, p. 870-911.

236. **Richter EA, Garetto LP, Goodman MN and Ruderman NB**. Enhanced muscle glucose metabolism after exercise: modulation by local factors. *Am J Physiol* 246: E476-E482, 1984.

237. **Richter EA, Mikines KJ, Galbo H and Kiens B**. Effect of exercise on insulin action in human skeletal muscle. *J Appl Physiol* 66: 876-85, 1989.

238. **Roberts CK and Barnard RJ**. Effects of exercise and diet on chronic disease. *J Appl Physiol* 98: 3-30, 2005.

239. **Rocchi S, Tartare-Deckert S, Sawka-Verhelle D, Gamha A and van OE**. Interaction of SH2-containing protein tyrosine phosphatase 2 with the insulin receptor and the insulin-like growth factor-I receptor: studies of the domains involved using the yeast two-hybrid system. *Endocrinology* 137: 4944-4952, 1996.

240. **Rodbell M**. Metabolism of isolated fat cells. *J Biol Chem* 239: 375-380, 2005.

241. **Rodnick KJ, Henriksen EJ, James DE and Holloszy JO**. Exercise training, glucose transporters, and glucose transport in rat skeletal muscles. *Am J Physiol* 262: 9-14, 1992.

242. **Rodnick KJ, Holloszy JO, Mondon CE and James DE**. Effects of exercise training on insulin-regulatable glucose-transporter protein levels in rat skeletal muscle. *Diabetes* 39: 1425-9, 1990.

243. **Rodnick KJ, Reaven GM, Haskell WL, Sims CR and Mondon CE**. Variations in running activity and enzymatic adaptations in voluntary running rats. *J Appl Physiol* 66: 1250-1257, 1989.

244. **Rogers MA, King DS, Hagberg JM, Ehsani AA and Holloszy JO**. Effect of 10 days of physical inactivity on glucose tolerance in master athletes. *J Appl Physiol* 68: 1833-7, 1990.

245. **Roth G, Kotzka J, Kremer L, Lehr S, Lohaus C, Meyer HE, Krone W and Muller-Wieland D**. MAP kinases Erk1/2 phosphorylate sterol regulatory element-binding protein (SREBP)-1a at serine 117 in vitro. *J Biol Chem* 275: 33302-33307, 2000.

246. **Rous S**. The origin of hydrogen in fatty acid synthesis. *Adv Lipid Res* 9: 73-118, 1971.

247. **Ruan H, Zarnowski MJ, Cushman SW and Lodish HF**. Standard isolation of primary adipose cells from mouse epididymal fat pads induces inflammatory mediators and down-regulates adipocyte genes. *J Biol Chem* 278: 47585-47593, 2003.

248. **Ryan DH**. Diet and exercise in the prevention of diabetes. *Int J Clin Pract Suppl* 28-35, 2003.

249. **Saltiel AR and Pessin JE**. Insulin signaling pathways in time and space. *Trends Cell Biol* 12: 65-71, 2002.

250. **Saltin B**. Physiological adaptation to physical conditioning. Old problems revisited. *Acta Med Scand Suppl* 711: 11-24, 1986.

251. **Samaras K and Campbell LV**. The non-genetic determinants of central adiposity. *Int J Obes Relat Metab Disord* 21: 839-845, 1997.

252. **Santos RF, Mondon CE, Reaven GM and Azhar S**. Effects of exercise training on the relationship between insulin binding and insulin-stimulated tyrosine kinase activity in rat skeletal muscle. *Metabolism* 38: 376-386, 1989.

253. **Saris WH**. Fit, fat and fat free: the metabolic aspects of weight control. *Int J Obes Relat Metab Disord* 22 Suppl 2: S15-S21, 1998.

254. **Saris WH, Blair SN, van Baak MA, Eaton SB, Davies PS, Di PL, Fogelholm M, Rissanen A, Schoeller D, Swinburn B, Tremblay A, Westerterp KR and Wyatt H**. How much physical activity is enough to prevent unhealthy weight gain? Outcome of the IASO 1st Stock Conference and consensus statement. *Obes Rev* 4: 101-114, 2003.

255. **Schlossman DM and Bell RM**. Triacylglycerol synthesis in isolated fat cells. Evidence that the sn-glycerol-3-phosphate and dihydroxyacetone phosphate acyltransferase activities are dual catalytic functions of a single microsomal enzyme. *J Biol Chem* 251: 5738-5744, 1976.

256. **Seals DR, Hagberg JM, Allen WK, Hurley BF, Dalsky GP, Ehsani AA and Holloszy JO**. Glucose tolerance in young and older athletes and sedentary men. *J Appl Physiol* 56: 1521-1525, 1984.

257. **Seely BL, Staubs PA, Reichart DR, Berhanu P, Milarski KL, Saltiel AR, Kusari J and Olefsky JM**. Protein tyrosine phosphatase 1B interacts with the activated insulin receptor. *Diabetes* 45: 1379-1385, 1996.

258. **Seider MJ, Nicholson WF and Booth FW**. Insulin resistance for glucose metabolism in disused soleus muscle of mice. *Am J Physiol* 242: 12-8, 1982.

259. **Shepherd RE, Noble EG, Klug GA and Gollnick PD**. Lipolysis and cAMP accumulation in adipocytes in response to physical training. *J Appl Physiol* 50: 143-148, 1981.

260. **Shuldiner AR and Munir KM**. Genetics of obesity: more complicated than initially thought. *Lipids* 38: 97-101, 2003.

261. **Smith SA**. Peroxisome proliferator-activated receptors and the regulation of mammalian lipid metabolism. *Biochem Soc Trans* 30: 1086-1090, 2002.

262. **Srere PA**. Citrate synthase. *Methods Enzymol* 13: 3-5, 1969.

263. **Steensberg A**. The role of IL-6 in exercise-induced immune changes and metabolism. *Exerc Immunol Rev* 9: 40-47, 2003.

264. **Stein CJ and Colditz GA**. The epidemic of obesity. *J Clin Endocrinol Metab* 89: 2522-2525, 2004.

265. **Stein SC, Woods A, Jones NA, Davison MD and Carling D**. The regulation of AMP-activated protein kinase by phosphorylation. *Biochem J* 345 Pt 3: 437-443, 2000.

266. **Stern JS and Johnson PR**. Spontaneous activity and adipose cellularity in the genetically obese Zucker rat (fafa). *Metabolism* 26: 371-380, 1977.

267. **Stone NJ**. Focus on lifestyle change and the metabolic syndrome. *Endocrinol Metab Clin North Am* 33: 493-4vi, 2004.

268. **Strack V, Hennige AM, Krutzfeldt J, Bossenmaier B, Klein HH, Kellerer M, Lammers R and Haring HU**. Serine residues 994 and 1023/25 are important for insulin receptor kinase inhibition by protein kinase C isoforms beta2 and theta. *Diabetologia* 43: 443-449, 2000.

269. **Streicher R, Kotzka J, Muller-Wieland D, Siemeister G, Munck M, Avci H and Krone W**. SREBP-1 mediates activation of the low density lipoprotein receptor promoter by insulin and insulin-like growth factor-I. *J Biol Chem* 271: 7128-7133, 1996.

270. **Stubbs CO and Lee AJ**. The obesity epidemic: both energy intake and physical activity contribute. *Med J Aust* 181: 489-491, 2004.

271. **Subauste A and Burant CF**. DGAT: novel therapeutic target for obesity and type 2 diabetes mellitus. *Curr Drug Targets Immune Endocr Metabol Disord* 3: 263-270, 2003.

272. **Suda K, Izawa T, Komabayashi T, Tsuboi M and Era S**. Effect of insulin on adipocyte lipolysis in exercise-trained rats. *J Appl Physiol* 74: 2935-2939, 1993.

273. **Sullivan TE and Armstrong RB**. Rat locomotory muscle fiber activity during trotting and galloping. *J Appl Physiol* 44: 358-363, 1978.

274. **Sundqvist A and Ericsson J**. Transcription-dependent degradation controls the stability of the SREBP family of transcription factors. *Proc Natl Acad Sci U S A* 100: 13833-13838, 2003.

275. **Swinburn BA, Caterson I, Seidell JC and James WP**. Diet, nutrition and the prevention of excess weight gain and obesity. *Public Health Nutr* 7: 123-146, 2004.

276. **Tan MH and Bonen A**. Effect of exercise training on insulin binding and glucose metabolism in mouse soleus muscle. *Can J Physiol Pharmacol* 65: 2231-2234, 1987.

277. **Tanner CJ, Barakat HA, Dohm GL, Pories WJ, MacDonald KG, Cunningham PR, Swanson MS and Houmard JA**. Muscle fiber type is associated with obesity and weight loss. *Am J Physiol Endocrinol Metab* 282: E1191-E1196, 2002.

278. **Tanner CJ, Koves TR, Cortright RL, Pories WJ, Kim YB, Kahn BB, Dohm GL and Houmard JA**. Effect of short-term exercise training on insulin-stimulated PI 3-kinase activity in middle-aged men. *Am J Physiol Endocrinol Metab* 282: E147-E153, 2002.

279. **Teran-Garcia M, Rufo C, Nakamura MT, Osborne TF and Clarke SD**. NF-Y involvement in the polyunsaturated fat inhibition of fatty acid synthase gene transcription. *Biochem Biophys Res Commun* 290: 1295-1299, 2002.

280. **Thibault L, Woods SC and Westerterp-Plantenga MS**. The utility of animal models of human energy homeostasis. *Br J Nutr* 92 Suppl 1: S41-S45, 2004.

281. **Thuresson ER**. Inhibition of glycerol-3-phosphate acyltransferase as a potential treatment for insulin resistance and type 2 diabetes. *Curr Opin Investig Drugs* 5: 411-418, 2004.

282. **Tian Q, Stepaniants SB, Mao M, Weng L, Feetham MC, Doyle MJ, Yi EC, Dai H, Thorsson V, Eng J, Goodlett D, Berger JP, Gunter B, Linseley PS, Stoughton RB, Aebersold R, Collins SJ, Hanlon WA and Hood LE**. Integrated genomic and proteomic analyses of gene expression in Mammalian cells. *Mol Cell Proteomics* 3: 960-969, 2004.

283. **Toode K, Viru A and Eller A**. Lipolytic actions of hormones on adipocytes in exercise-trained organisms. *Jpn J Physiol* 43: 253-258, 1993.

284. **Tsai AC, Bach J and Borer KT**. Somatic, endocrine, and serum lipid changes during detraining in adult hamsters. *Am J Clin Nutr* 34: 373-376, 1981.

285. **U.S.Department of Health and Human Services**. *The Surgeon General's call to action to prevent and decrease overweight and obesity.* Rockville, MD: U.S. Department of Health and Human Services, Public Health Service, Office of the Surgeon General, 2001.

286. **U.S.Department of Health and Human Services**. *Physical activity and health: a report of the Surgeon General.* Rockville, MD: U.S. Department of Health and Human Services, Public Health Service, Office of the Surgeon General, 1996.

287. **Utzschneider KM, Carr DB, Hull RL, Kodama K, Shofer JB, Retzlaff BM, Knopp RH and Kahn SE**. Impact of intra-abdominal fat and age on insulin sensitivity and beta-cell function. *Diabetes* 53: 2867-2872, 2004.

288. **van der Heide LP and Smidt MP**. Regulation of FoxO activity by CBP/p300-mediated acetylation. *Trends Biochem Sci* 30: 81-86, 2005.

289. **Villena JA, Viollet B, Andreelli F, Kahn A, Vaulont S and Sul HS**. Induced adiposity and adipocyte hypertrophy in mice lacking the AMP-activated protein kinase-alpha2 subunit. *Diabetes* 53: 2242-2249, 2004.

290. **Vollenweider P**. Insulin resistant states and insulin signaling. *Clin Chem Lab Med* 41: 1107-1119, 2003.

291. **Vukovich MD, Arciero PJ, Kohrt WM, Racette SB, Hansen PA and Holloszy JO**. Changes in insulin action and GLUT-4 with 6 days of inactivity in endurance runners. *J Appl Physiol* 80: 240-244, 1996.

292. **Wade AJ, Marbut MM and Round JM**. Muscle fibre type and aetiology of obesity. *Lancet* 335: 805-808, 1990.

293. **Wadley GD, Tunstall RJ, Sanigorski A, Collier GR, Hargreaves M and Cameron-Smith D**. Differential effects of exercise on insulin-signaling gene expression in human skeletal muscle. *J Appl Physiol* 90: 436-40, 2001.

294. **Wagenknecht LE, Langefeld CD, Scherzinger AL, Norris JM, Haffner SM, Saad MF and Bergman RN**. Insulin sensitivity, insulin secretion, and abdominal fat: the Insulin Resistance Atherosclerosis Study (IRAS) Family Study. *Diabetes* 52: 2490-2496, 2003.

295. **Wallace TM and Matthews DR**. The assessment of insulin resistance in man. *Diabet Med* 19: 527-534, 2002.

296. **Wang YT, Huang ZJ and Chang HM**. Proteomic analysis of human leukemic U937 cells incubated with conditioned medium of mononuclear cells stimulated by proteins from dietary mushroom of Agrocybe aegerita. *J Proteome Res* 3: 890-896, 2004.

297. **Wardzala LJ, Crettaz M, Horton ED, Jeanrenaud B and Horton ES**. Physical training of lean and genetically obese Zucker rats: effect on fat cell metabolism. *Am J Physiol* 243: E418-E426, 1982.

298. **Warram JH, Martin BC, Krolewski AS, Soeldner JS and Kahn CR**. Slow glucose removal rate and hyperinsulinemia precede the development of type II diabetes in the offspring of diabetic parents. *Ann Intern Med* 113: 909-915, 1990.

299. **Watanabe Y, Shibata K, Kikkawa F, Kajiyama H, Ino K, Hattori A, Tsujimoto M and Mizutani S**. Adipocyte-derived leucine aminopeptidase suppresses angiogenesis in human endometrial carcinoma via renin-angiotensin system. *Clin Cancer Res* 9: 6497-6503, 2003.

300. **Watson RT and Pessin JE**. Intracellular organization of insulin signaling and GLUT4 translocation. *Recent Prog Horm Res* 56: 175-93, 2001.

301. **Webber J**. Energy balance in obesity. *Proc Nutr Soc* 62: 539-543, 2003.

302. **Wells JC**. Body composition in childhood: effects of normal growth and disease. *Proc Nutr Soc* 62: 521-528, 2003.

303. **Whitehead JP, Clark SF, Urso B and James DE**. Signalling through the insulin receptor. *Curr Opin Cell Biol* 12: 222-228, 2000.

304. **Wojtaszewski JF, Hansen BF, Kiens B and Richter EA**. Insulin signaling in human skeletal muscle: time course and effect of exercise. *Diabetes* 46: 1775-81, 1997.

305. **Wu G, Olivecrona G and Olivecrona T**. Extracellular degradation of lipoprotein lipase in rat adipose tissue. *BMC Cell Biol* 6: 4, 2005.

306. **Yamauchi T, Kamon J, Waki H, Murakami K, Motojima K, Komeda K, Ide T, Kubota N, Terauchi Y, Tobe K, Miki H, Tsuchida A, Akanuma Y, Nagai R, Kimura S and Kadowaki T**. The mechanisms by which both heterozygous peroxisome proliferator-activated receptor gamma (PPARgamma) deficiency and PPARgamma agonist improve insulin resistance. *J Biol Chem* 276: 41245-41254, 2001.

307. **Yamauchi T, Oike Y, Kamon J, Waki H, Komeda K, Tsuchida A, Date Y, Li MX, Miki H, Akanuma Y, Nagai R, Kimura S, Saheki T, Nakazato M, Naitoh T, Yamamura K and Kadowaki T**. Increased insulin sensitivity despite lipodystrophy in Crebbp heterozygous mice. *Nat Genet* 30: 221-226, 2002.

308. **Yano H, Yano L, Kinoshita S and Tsuji E**. Effect of voluntary exercise on maximal oxygen uptake in young female Fischer 344 rats. *Jpn J Physiol* 47: 139-141, 1997.

309. **Yeaman SJ**. Hormone-sensitive lipase--new roles for an old enzyme. *Biochem J* 379: 11-22, 2004.

310. **Young DA, Uhl JJ, Cartee GD and Holloszy JO**. Activation of glucose transport in muscle by prolonged exposure to insulin. Effects of glucose and insulin concentrations. *J Biol Chem* 261: 16049-16053, 1986.

311. **Young DA, Wallberg-Henriksson H, Sleeper MD and Holloszy JO**. Reversal of the exercise-induced increase in muscle permeability to glucose. *Am J Physiol* 253: E331-E335, 1987.

312. **Young JC, Enslin J and Kuca B**. Exercise intensity and glucose tolerance in trained and nontrained subjects. *J Appl Physiol* 67: 39-43, 1989.

313. **Youngren JF, Keen S, Kulp JL, Tanner CJ, Houmard JA and Goldfine ID**. Enhanced muscle insulin receptor autophosphorylation with short-term aerobic exercise training. *Am J Physiol Endocrinol Metab* 280: 528-33, 2001.

314. **Yu M, Blomstrand E, Chibalin AV, Wallberg-Henriksson H, Zierath JR and Krook A**. Exercise-associated differences in an array of proteins involved in signal transduction and glucose transport. *J Appl Physiol* 90: 29-34, 2001.

315. **Yun J, Chae HD, Choi TS, Kim EH, Bang YJ, Chung J, Choi KS, Mantovani R and Shin DY**. Cdk2-dependent phosphorylation of the NF-Y transcription factor and its involvement in the p53-p21 signaling pathway. *J Biol Chem* 278: 36966-36972, 2003.

316. **Zabolotny JM, Haj FG, Kim YB, Kim HJ, Shulman GI, Kim JK, Neel BG and Kahn BB**. Transgenic overexpression of protein-tyrosine phosphatase 1B in muscle causes insulin resistance, but overexpression with leukocyte antigen-related phosphatase does not additively impair insulin action. *J Biol Chem* 279: 24844-24851, 2004.

317. **Zachwieja JJ, Hendry SL, Smith SR and Harris RB**. Voluntary wheel running decreases adipose tissue mass and expression of leptin mRNA in Osborne-Mendel rats. *Diabetes* 46: 1159-1166, 1997.

318. **Zhang JW, Klemm DJ, Vinson C and Lane MD**. Role of CREB in transcriptional regulation of CCAAT/enhancer-binding protein beta gene during adipogenesis. *J Biol Chem* 279: 4471-4478, 2004.

319. **Zierath JR**. Invited review: Exercise training-induced changes in insulin signaling in skeletal muscle. *J Appl Physiol* 93: 773-781, 2002.

Appendix A: Preliminary Data: 2-D Gel Proteomic Analysis of Proteins Secreted by Adipose Tissue and Skeletal Muscle and the Effect of Reduced Physical Activity

INTRODUCTION

Adipose tissue is known to secrete a number of proteins with various endocrine, paracrine, and autocrine effects (145), including effects on muscle insulin sensitivity and adipose tissue triacylglycerol synthesis and lipid storage. Thus, it is possible that there are changes in adipose tissue secretions that could help to explain the decreased epitrochlearis muscle insulin sensitivity (Chapter 4), increased adipocyte size, and the overshoot in triacylglycerol synthetic activity (Chapter 6) observed after two days of reduced physical activity. Conditioning media by incubation with primary adipocytes or adipose tissue fragments has previously been used to measure secretions of specific adipose-derived proteins (2; 73; 86; 106; 136; 299; 305). Two-dimensional (2-D) gels, which allow the separation of a complex mixture of proteins that can be identified based on their isoelectric point and molecular mass (181), have been used to identify proteins secreted during adipocyte differentiation (157), and from conditioned media from other tissue types (89; 172; 176; 282; 296). Thus, it seemed feasible that fragments of adipose tissue could be incubated, and then the conditioned media

analyzed by 2-D gel electrophoresis to determine the secreted proteins. This study was conducted to examine this possibility.

More recently, it has also been shown that skeletal muscle may act as an endocrine organ (9; 203; 221; 263). Using incubation techniques similar to that used for 2-deoxyglucose uptake, it seemed possible that proteins secreted by skeletal muscle could also be examined using the 2-D gel approach.

The success of this technique would accomplish two things: 1) it would allow most secreted proteins to be identified, including novel and heretofore unknown proteins, and 2) it would allow comparison to see if there are any proteins that are differentially secreted with reduced physical activity.

METHODS

Conditioning media with adipose tissue fragments

Because the adipocyte isolation procedure *per se* may induce secretion of specific proteins such as tumor necrosis factor-α (247), it was decided to condition media using explanted adipose tissue fragments. Following humane animal sacrifice as described in Chapter 4, 250 mg of adipose tissue were minced into 1-3 mm fragments and washed in Krebs-HEPES-Ringer buffer (KRHB; 130 mM NaCl, 4.7 mM KCl, 1.2 mM KH_2PO_4, 1 mM $CaCl_2$, 1.2 mM $MgSO_4$, pH 7.4)/5 mM glucose 5 X 5 minutes. The fragments were then incubated in 2 ml of KRHB/5 mM glucose at 37º C for the indicated length of time

in the figures in a shaking water bath at 30 rpm. The conditioned media was then sterile-filtered and frozen at -80º C.

Conditioning media with epitrochlearis or split soleus muscle

Epitrochlearis and split soleus muscles were dissected out, weighed, and washed 4 X 10 minutes in 5 ml of Krebs-Henseleit Buffer (KHB; 0.116 M NaCl, 4.6 mM KCl, 1.16 mM KH_2PO_4, 25.3 mM $NaHCO_3$, 2.5 mM $CaCl_2$, 1.16 mM $MgSO_4$, pH 7.4)/5 mM glucose/35 mM mannitol at 37º C under constant gas phase of 95% O_2/5% CO_2 in a shaking water bath at 30 rpm. Muscles were then incubated for the times indicated in the figures in 50 ml/g muscle KHB/5 mM glucose/35 mM mannitol at 37º C under constant gas phase of 95% O_2/5% CO_2 in a shaking water bath at 30 rpm, at which time the conditioned media was sterile-filtered and stored at -80º C. Protein concentrations of all conditioned media samples were tested using the Bradford assay.

Lactate dehydrogenase (LDH) activity

Adipose tissue-conditioned media (25 µl) was assayed for Type H LDH activity by adding it to 900 µl HEPES-buffered saline (HBS; 140 mM NaCl, 20 mM Na-HEPES, 2.5 mM $MgSO_4$, 1 mM $CaCl_2$, 5 mM KCl, pH 7.4)/20 mM pyruvate/30 µM NADH in a cuvette, vortexing, then reading the absorbance at 340 nm over 4 minutes in a spectrophotometer. Muscle-conditioned media (25 µl) was assayed for Type M LDH activity by adding it to 900 µl HBS/20 mM

lactate/50 μM NAD^+ in a cuvette, vortexing, then reading the absorbance at 340 nm over 4 minutes.

RESULTS AND DISCUSSION

Appearance of LDH activity in the incubation media was used as a measure of viability of the samples (67). LDH-M activity in the muscle-conditioned media rose gradually from 1-6 hours, then sharply increased at 8 and 12 hours (Fig. 30A), indicating that under these conditions, the muscle may start to lose its viability between 6 and 8 hours of incubation. LDH-H activity in the adipose tissue-conditioned media remained relatively steady over 24 hours, indicating that the tissue is maintaining its viability (Fig. 30B).

The linearity of protein release into the media was linear from 2-24 hours for epididymal fat fragments

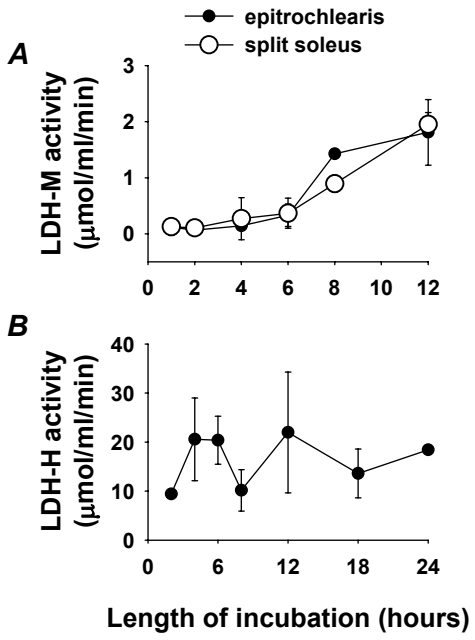

Figure 30. LDH activity over time in media conditioned by (*A*) skeletal muscle or (*B*) epididymal adipose tissue fragments.

n = 2; error bars represent the standard deviation.

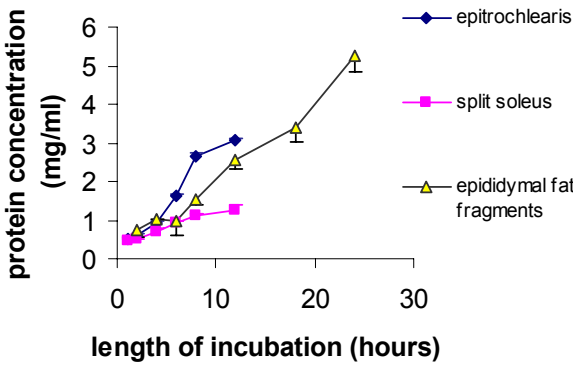

Figure 31. Protein concentration over time in media conditioned by (*A*) skeletal muscle or (*B*) epididymal adipose tissue fragments.

n = 2; error bars represent the standard deviation.

(Fig. 31), 1-12 hours for epitrochlearis muscle, and 1-8 hours in split soleus muscle.

When protein concentrations were compared between experimental groups (see Chapter 4 for description), there were no differences between groups for media conditioned by epididymal fat fragments or epitrochlearis muscle. In contrast, split soleus muscle-conditioned media had a higher protein concentration in SED5 (0.927 ± 0.073 mg/ml) relative to WL29 (0.635 ± 0.091) and WL53 (0.657 ± 0.063), but was not significantly different from WL5 (0.769 ± 0.069; p=0.14), indicating that there might be an activity-dependent response in proteins secreted by the soleus muscle (Fig. 32). Further work is needed to verify this, and 2-D gels could potentially be used to determine any differentially secreted proteins. One soleus muscle-conditioned media has been subjected to 2-D gel electrophoresis by the University of Missouri Proteomics Core, confirming that 2-D gel proteomics can successfully be conducted on these samples (Fig. 33).

Although exciting, there are several weaknesses to this approach. First is the potential for plasma proteins to still be present in the sample, although the washing steps are designed to minimize this possibility (data not shown). Another potential problem is that the muscles are

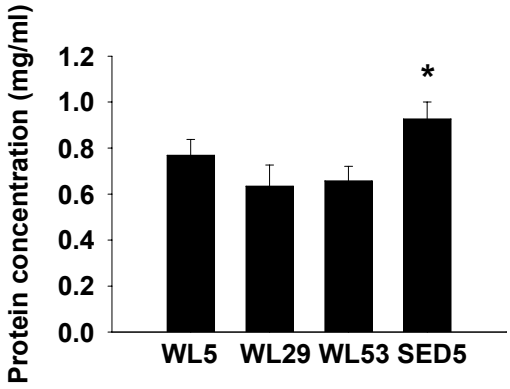

Figure 32. Protein concentration in media conditioned by split soleus.

*, p<0.05 vs. WL29 and WL53, p=0.14 vs. WL5. n=10 per group

not at resting length, although this problem could be solved by measuring the resting length then fixing the muscle at this length. For the soleus, there is also the potential that splitting the muscle could induce release of proteins. Another problem lies in identifying whether the secreted proteins circulate in the plasma, or if they are restricted locally to their source tissue. This raises challenges in determining the function of any given secreted protein.

However, these initial experiments raise the distinct possibility that proteomic examination of muscle- and fat-secreted proteins can be accomplished. This approach might have future utility in determining how changes in physical activity affect the secretion of proteins by muscle and fat.

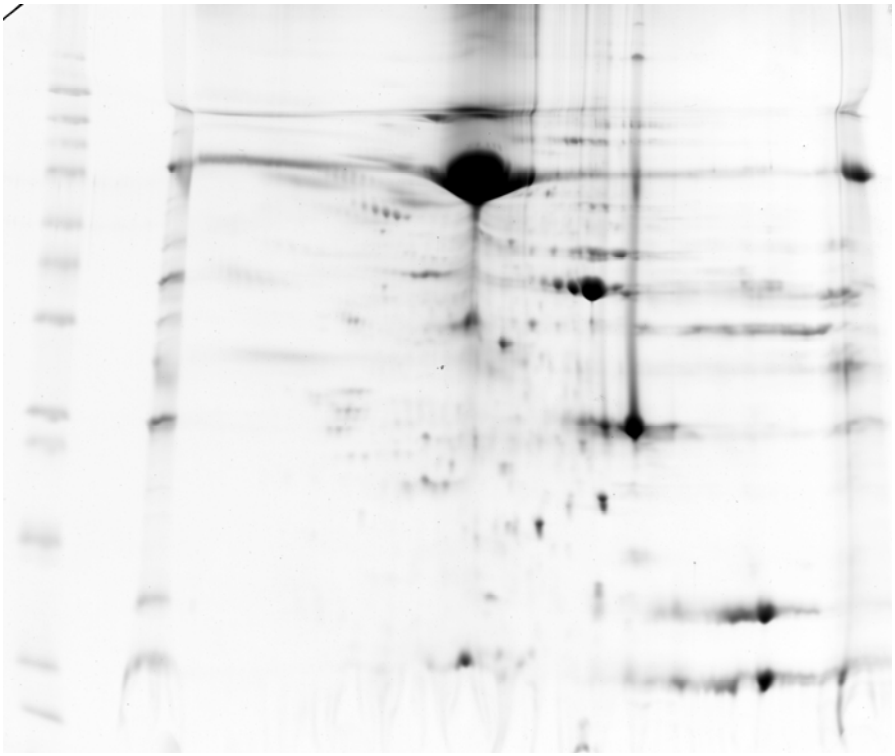

Figure 33. 2-D gel of soleus-conditioned media.
Each spot represents a protein. The large spot near the upper middle portion of the gel is BSA, which had been added (0.1%) to the media for this particular preliminary sample.

APPENDIX B: PRELIMINARY DATA: THE EFFECT OF 83 WEEKS OF VOLUNTARY WHEEL RUNNING ON ADIPOSE CELLULARITY IN FEMALE RATS

METHODS

Chapters 4, 5, 6, and 7 deal with reduced activity in male rats following a period of access to voluntary running wheels. As it was my subjective observation that male rats ran better when females were present in the same room, 6 female Fischer 344 X Brown Norway F1 hybrid rats (Harlan, Indianapolis, Indiana) were present in the room throughout the experimental period, for a total of 83 weeks. This presented the opportunity to study female rats with prolonged exposure to a voluntary running wheel. As with the males,

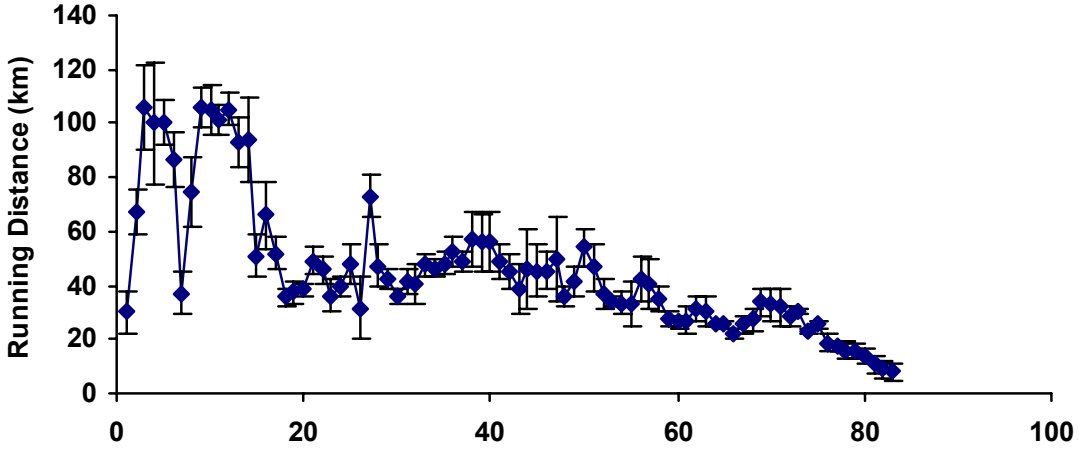

Figure 34. Weekly running distance for 83 weeks for female rats with voluntary running wheels.

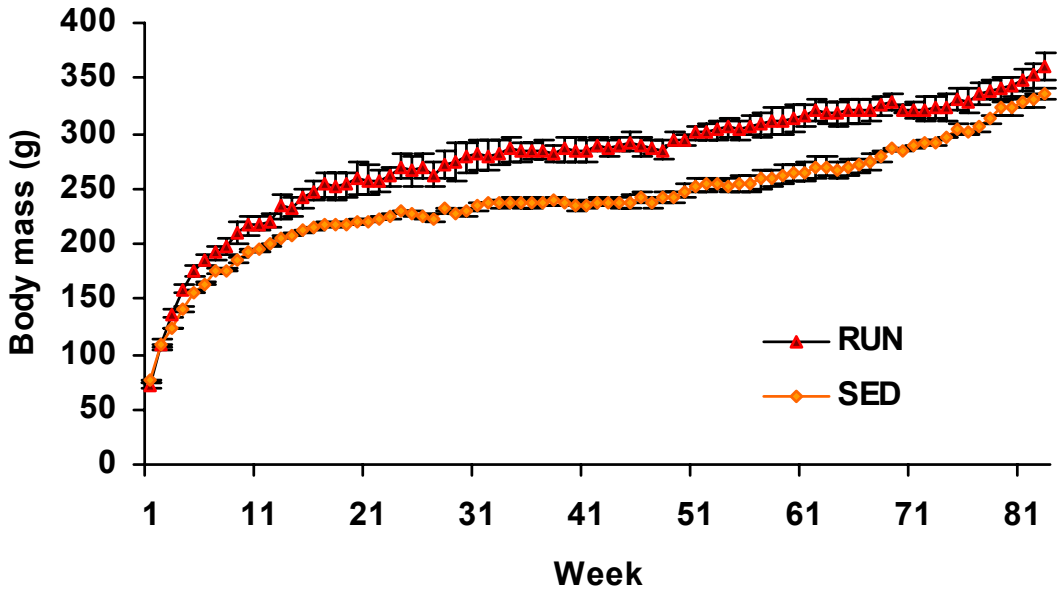

Figure 35. Growth curve of female rats with and without running wheels,

the females arrived at 21-23 days of age and were allowed to acclimatize one week prior to randomly being assigned to a cage either with or without a running wheel. Animals were provided with 200 g of standard rodent chow on the first day of each week when the cages were changed; running activity, body mass, and food intake were measured on the first day of each week between 0400-0500 hours. On the day before sacrifice, wheels were locked at 0400 to eliminate any effect of the last activity bout. On the day of sacrifice, food was removed from the animals at 0400 hours. A portion of epididymal fat was used for cell size determinations as described in Chapter 6 or frozen at -80º C until homogenized. Groups were compared using Student's t-test, with significance set at $p < 0.05$.

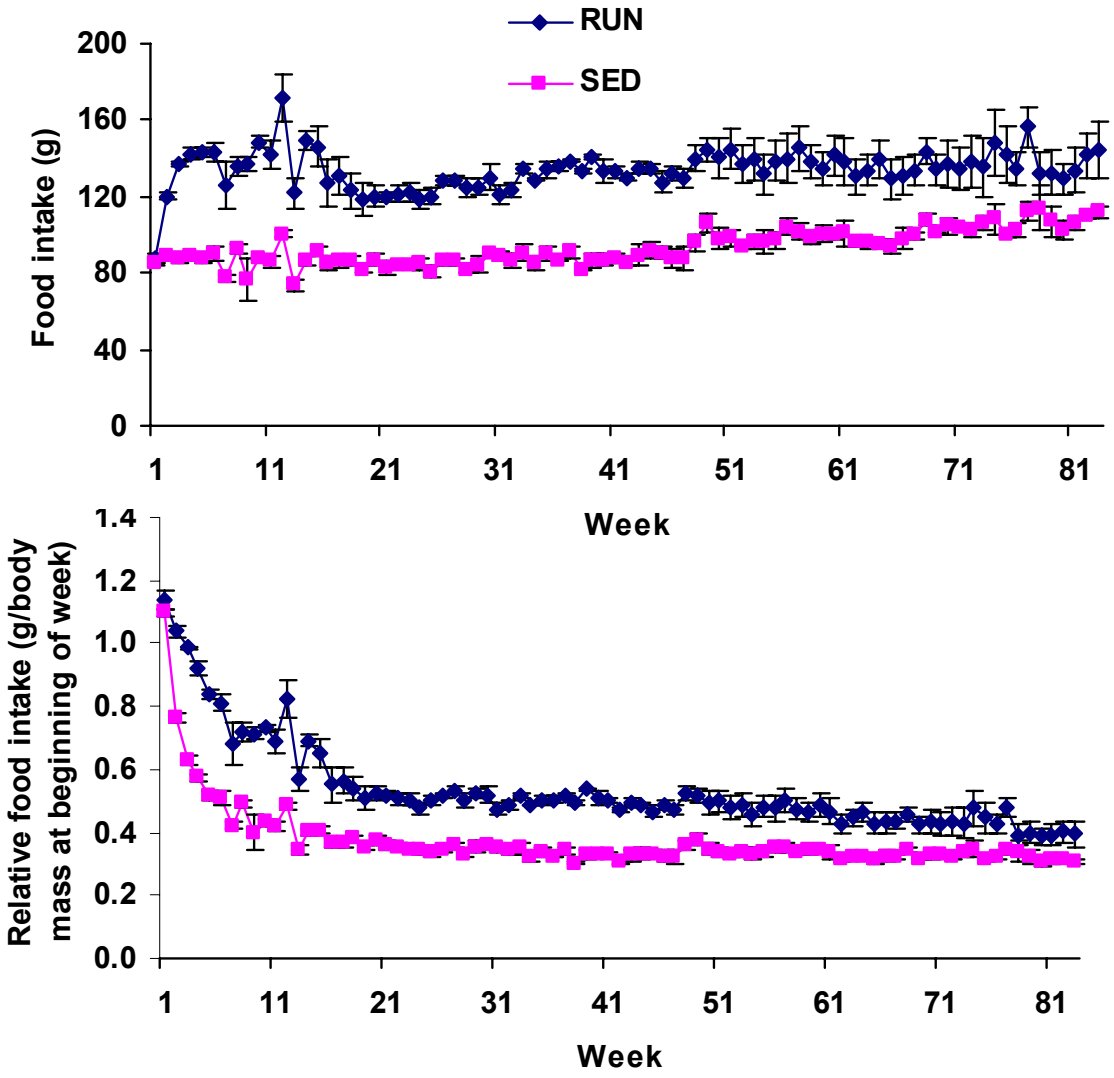

Figure 36. Absolute (A) and relative (B) food consumption in female rats with or without running wheels.

RESULTS

Running distance over the 83 weeks is shown in Fig. 34. Initial body mass (g) was not different between 83-week runners (72.0 ± 2.8) and sedentary animals (75.6 ± 0.9). Final body mass (g) was lower in sedentary animals (332 ± 8) than in 83-week runners (368 ± 10; $p < 0.05$). Growth rate was accelerated in the 83-week runners, but plateaued to essentially the same slope as sedentary runners at ~52 weeks (Fig. 35), approximately the same time as running activity began to decline more dramatically (Fig. 34). Both absolute (Fig. 36A) and relative food intakes (Fig. 36B) were consistently lower in sedentary, but had begun to approach that of the runners over the last ~10 weeks of the experiment.

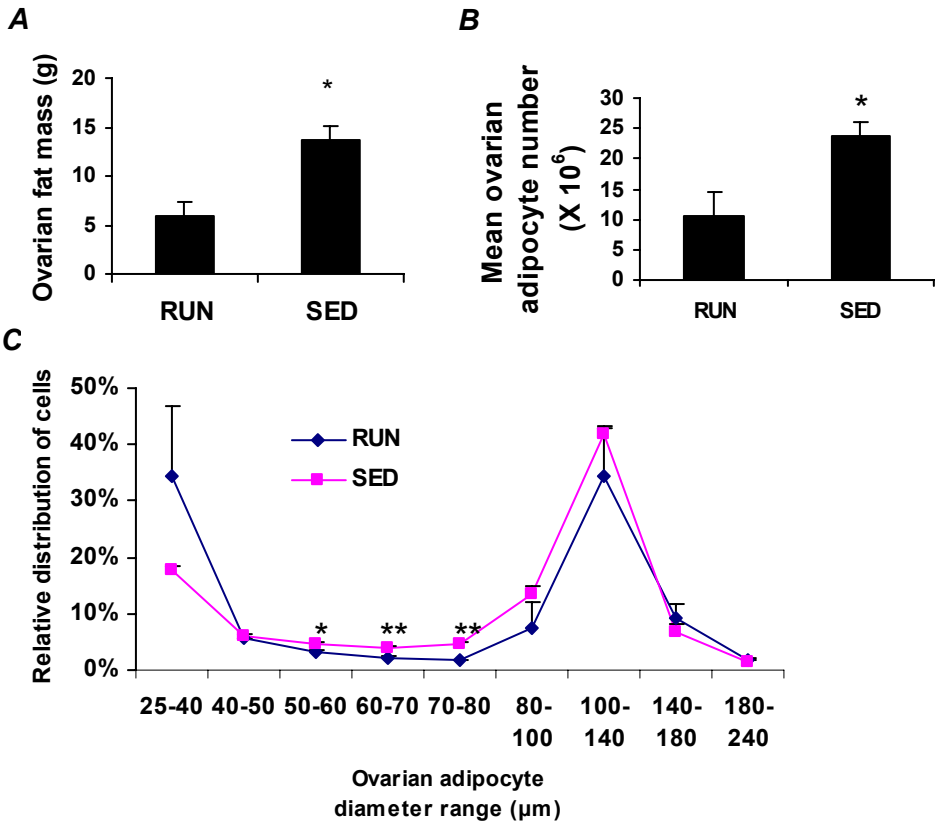

Figure 37. Ovarian fat mass and cellularity in female rats with or without 83 weeks of running wheel access. *A*) ovarian fat mass, *B*) adipocyte number, and *C*) distribution of cells by diameter range. *, $p<0.05$; **, $p<0.005$. n = 3/group

Soleus mass was less ($p<0.05$; data not shown) in sedentary animals than in runners both in absolute terms (g; 0.162 ± 0.012 for runners and 0.096 ± 0.009 for sedentary) and relative terms ([(g/g body mass) X 10,000]; 4.41 ± 0.41 for runners and 2.90 ± 0.30 for sedentary). Ovarian fat pad mass (g) was significantly greater (Fig. 37A) in sedentary (13.64 ± 1.46) than in runners (5.97 ± 1.31). Relative ovarian fat pad mass [(g/g body mass) X 1,000] was significantly greater ($p < 0.05$; data not shown) in sedentary animals (41.3 ± 5.0) than in runners (16.3 ± 3.7). The greater ovarian fat mass in the sedentary animals was associated with a greater percentage of cells with a diameter of 50-80 μm (Fig. 37C) and a greater total number of ovarian adipocytes (Fig. 37B).

CONCLUSIONS

The most striking difference between the 83-week runners and those that were sedentary was the 128% greater ovarian fat pad mass and 122% greater number of ovarian fat cells in the sedentary group. In conjunction with the findings of Craig *et al*. (53), this provides evidence that prolonged access to a voluntary running wheel has either an inhibitory effect on adipocyte differentiation or that it promotes a loss of adipocytes. One possible mechanism may be the modestly higher protein level of CCAAT/enhancer binding protein-α (C/EBP-α) in 7-week-old sedentary male rats that was described in Chapter 6. C/EBP-α is a transcription factor that is essential for differentiation of pre-adipocytes into adipocytes (97). It is interesting to speculate that, over a prolonged period of time, the slightly (30%) higher C/EBP-α protein level in the epididymal fat of

sedentary rats, in conjunction with other mechanisms, drives the differentiation of new fat cells. Although inconclusive, these findings warrant further investigation.

Appendix C: Detailed Protocols

2-DOG TRANSPORT IN ISOLATED SKELETAL MUSCLE

Protocol

Prepare one day ahead

1. Make any needed solutions.
2. Label 20-ml polypropylene scintillation vials (Fisher 03-337-23):
    a. Label 2 vials/animal with the animal number. Label one vial "L" and the other vial "R". Label these vials "rec".
    b. Label 2 vials/animal with the animal number. Label one vial "L" and the other vial "R". Label these vials "PI".
    c. Label 2 vials/animal with the animal number. Label one vial "L" and the other vial "R". Label these vials "R".
    d. Label 2 vials/animal with the animal number. Label one vial "L" and the other vial "R". Label these vials "inc".
3. Label 2 foils/animal with the animal number. One foil should be labeled "L" and the other should be labeled "R".
4. Dry down 45 µl [^{3}H]2-DOG (45 µCi) in the speed vac for 2 hr 24 min.
5. Have the following ready:
    a. 500-ml bottle (33-mm neck) labeled "KHB".
    b. 250-ml bottle labeled "KHB/0.1% BSA".
    c. 250-ml beaker labeled "dissection bx"

d. 100-ml beaker labeled “recovery”.

e. 15-ml conical tube labeled “pre-inc”.

f. 50-ml conical tube labeled “rinse”.

g. 15-ml conical tube labeled “rinse ins”.

h. 50-ml conical tube labeled “inc”.

i. 15-ml conical tube labeled “inc ins”.

j. 2 X 1.5-ml screw-cap microcentrifuge tube labeled “mus inc-1” and “mus inc-2” with the date of the experiment. Add 900 µl H_2O to each tube and place in radioactive area.

Day of experiment

6. Have the following items ready:

    a. Ice bucket with ice.

    b. Liquid N_2.

    c. Styrofoam container.

    d. Surgical diaper.

    e. Surgical tools.

    f. Medium-size weigh boat.

    g. 100-mm culture dishes.

    h. 10-cm Whatman paper.

7. Prepare Krebs-Henseleit Buffer (KHB: 0.116 M NaCl, 4.6 mM KCl, 1.16 mM KH_2PO_4, 25.3 mM $NaHCO_3$, 2.5 mM $CaCl_2$, 1.16 mM $MgSO_4$, pH 7.4):

    a. NOTE: This must always be made fresh on the day of the experiment. Ca^{2+} and Mg^{2+} form insoluble carbonates at alkaline

pH (i.e. at the pH of ungassed medium containing HCO_3^-). Thus the HCO_3^- is kept separate from the Ca^{2+} and Mg^{2+} before use.

b. To the 500-ml glass bottle (33-mm neck) labeled “KHB”, add 400 ml H_2O. Add 50 ml 10X Krebs-Henseleit Buffer Stock I. Gas with 95% O_2/5% CO_2 at 4 psi under paraffin on ice for 20 minutes to equilibrate the pH. Add 50 ml 10X Krebs-Henseleit Buffer Stock II and gas for 10 more minutes. Check pH using standard pH paper (Sigma P3536); the pH should be ~7.0-7.2. (NOTE: pH will change to 7.4 after solution warms to 37˚ C.) After solutions have been gassed, keep them on ice under paraffin as much as possible. Otherwise, CO_2 will exit the solution, pH will become alkaline, and insoluble carbonates will form.

8. While KHB is being gassed, place the following on ice to thaw:
   a. 100 U/ml insulin stock.
   b. 3 M sodium acetate.
   c. 1 M 2-deoxyglucose.
9. Prepare KHB/0.1% BSA:
   a. Add 150 ml of KHB to a 250-ml bottle.
   b. Weigh out 0.15 g of RIA-grade BSA (Sigma A-7888) and add to the bottle.
   c. Cap and bottle and set on ice.
   d. Allow BSA to dissolve into the solution (~15 minutes).
10. Make 1 U/ml insulin:

a. Label a 1.5-ml microcentrifuge tube “1 U”.
b. Add 990 µl KHB/0.1% BSA to a 1.5-ml microcentrifuge tube.
c. Add 10 µl 100 U/ml insulin stock.
d. Vortex.
e. Keep on ice.
f. If a submaximal concentration of insulin is to be used, prepare 10 mU/ml insulin:
    i. Label a 1.5-ml microcentrifuge tube “10 mU”.
    ii. Add 990 µl of KHB/0.1% BSA to a 1.5-ml microcentrifuge tube.
    iii. Add 10 µl of 1 U/ml insulin.
    iv. Vortex.
    v. Keep on ice.

11. Prepare dissection buffer (KHB, 40 mM mannitol):
    a. To the 250-ml beaker labeled “dissection bx”, add 200 ml of.
    b. Add 6.6 ml of 0.625 M mannitol Stock I.
    c. Add 6.6 ml of 0.625 M mannitol Stock II.
    d. Swirl to mix.
12. Prepare recovery solution (rec; KHB/0.1% BSA, 38 mM mannitol, 2 mM sodium acetate):
    a. To the 100-ml beaker labeled “recovery”, add 60 ml of KHB/0.1% BSA.
    b. Add 1.88 ml of 0.625 M mannitol Stock I (940 µl X 2).

c. Add 1.88 ml of 0.625 M mannitol Stock I (940 µl X 2).

d. Add 21.3 µl 3 M sodium acetate. (See NOTE at end of protocol.)

e. Swirl gently to mix.

f. Keep covered on ice.

13. Prepare insulin pre-incubation solution [PI; KHB/0.1% BSA, 38 mM mannitol, 2 mM sodium acetate, either 2 mU/ml (maximal) or 60 µU/ml (submaximal) insulin]:

    a. Transfer 15 ml of the recovery solution to the 15-ml conical tube labeled “pre-inc”.

    b. If a maximal concentration of insulin is to be used, add 30 µl of 1 U/ml insulin.

    c. If a submaximal concentration of insulin is to be used, add 90 µl of 10 mU/ml insulin.

    d. Cap and invert tube several times to mix.

    e. Cover and keep on ice.

14. Prepare rinse solution (R; KHB/0.1% BSA, 40 mM mannitol):

    a. Add 30 ml of KHB/0.1% BSA to the 50-ml conical tube labeled “rinse”.

    b. Add 992 µl of 0.625 M mannitol Stock I.

    c. Add 992 µl of 0.625 M mannitol Stock II.

    d. Swirl gently to mix.

    e. Cover and keep on ice.

15. Prepare rinse solution with insulin [KHB/0.1% BSA, 40 mM mannitol, either 2 mU/ml (maximal) or 60 µU/ml (submaximal) insulin]:
    a. Transfer 15 ml of rinse solution to the 15-ml conical tube labeled “rinse ins”.
    b. If a maximal concentration of insulin is to be used, add 30 µl of 1 U/ml insulin.
    c. If a submaximal concentration of insulin is to be used, add 90 µl of 10 mU/ml insulin.
    d. Cap and invert tube several times to mix.
    e. Cover and keep on ice.
16. Prepare incubation solution [inc; KHB/0.1% BSA, 38 mM mannitol (0.2 µCi/ml), 2 mM 2-deoxyglucose (1.5 µCi/ml)]:
    a. To the 50-ml conical tube labeled “inc”, add 30 ml of KHB/0.1% BSA.
    b. Add 942 µl 0.625 M mannitol Stock I.
    c. Add 942 µl 0.625 M mannitol Stock II.
    d. Add 60.1 µl 1 M 2-deoxyglucose.
    e. Cap and invert several times to mix.
    f. Add 50 µl to the tube containing the 45 µCi dried down [^{3}H]2-DOG.
    g. Using the pipette tip, scrape the bottom of the tube several times.
    h. Transfer back to the 50-ml conical tube.
    i. Repeat steps g and h.

j. Add 60 µl (6 µCi) [^{14}C]mannitol (American Radiolabeled Chemicals ARC-127).

k. Cap and invert several times to mix.

l. Add 900 µl H_2O to duplicate screw-cap microcentrifuge tubes.

m. Add 100 µl incubation solution to each tube.

n. Cap, vortex, and keep in refrigerator for scintillation counting.

o. Keep on ice.

17. Prepare incubation solution with insulin [KHB/0.1% BSA, 38 mM mannitol (0.2 µCi/ml), 2 mM 2-deoxyglucose (1.5 µCi/ml), either 2 mU/ml (maximal) or 60 µU/ml (submaximal) insulin]:

    a. Transfer 14 ml of incubation solution to the 15-ml conical tube labeled “inc ins”.

    b. If a maximal insulin concentration is to be used, add 28 µl 1 U/ml insulin.

    c. If a submaximal insulin concentration is to be used, add 84 µl 10 mU/ml insulin.

    d. Cap and invert to mix.

    e. Keep on ice.

18. Prepare incubation vials:

    a. To each of the scintillation vials labeled “rec”, add 2 ml of recovery solution.

    b. Plug with a rubber stopper (either #0 or #1 stoppers will work).

    c. To each of the scintillation vials labeled “PI”, add 2 ml of:

i. recovery solution for basal transport.
ii. pre-incubation solution for insulin-stimulated transport.
iii. Plug with a rubber stopper (either #0 or #1 stoppers will work).

d. To each of the scintillation vials labeled “R”, add 2 ml of:
i. rinse solution for basal transport.

e. rinse solution with insulin for insulin-stimulated transport.

f. Plug with a rubber stopper (either #0 or #1 stoppers will work).

g. To each of the scintillation vials labeled “inc”, add 2 ml of:
i. incubation solution for basal transport.
ii. incubation solution with insulin for insulin-stimulated transport.
iii. Plug with a rubber stopper (either #0 or #1 stoppers will work).

h. Leave the vials at room temperature.

19. Dissect appropriate muscle(s), rinse in dissection buffer, and place in recovery solution at 37˚ C in a shaking water bath under 95% O_2/5% CO_2 for 30 minutes. NOTE: The gas should be kept at a constant 2 psi throughout the experiment.

20. Gently remove muscle (hold by tendon with forceps) from recovery solution and place in pre-incubation solution at 37˚ C in a shaking water bath under 95% O_2/5% CO_2 for 10 minutes.

21. Gently remove muscle (hold by tendon with forceps) from pre-incubation solution and place in rinse solution at 37˚ C in a shaking water bath under 95% O_2/5% CO_2 for 10 minutes.
22. Gently remove muscle (hold by tendon with forceps) from rinse solution and place in incubation solution at 37˚ C in a shaking water bath under 95% O_2/5% CO_2 for 20 minutes.
23. During step 22, pre-wet filter paper in a culture dish with rinse solution. Leave on ice.
24. Gently remove muscle from incubation solution and place on filter paper in culture dish over ice. Cut off any non-muscle tissue. Place in the appropriately foil and flash freeze in liquid N_2.
25. Fill out radiation log: ~90% liquid, ~9% solid, ~1% other.
26. Fill out drug log.
27. Take animal cages to dirty room.
28. Dispose of animal carcasses appropriately.
29. Wash surgical tools.

NOTE: This procedure was optimized for a particular purpose. To better match existing assays and to decrease the likelihood of error, it is desirable to first incubate the muscle 30 minutes in a solution that contains 6 M glucose, but not acetate or insulin. Mannitol is adjusted to keep the total molarity constant at 40 mM. The muscle is then transferred to the same solution with or without insulin and incubated an additional 30 minutes. The subsequent washing and

incubation steps are the same. The procedure may also be used with split solei or other muscles appropriate for incubation techniques.

Processing of muscles for measurement of glucose transport

30. Have ready:
    a. Pre-heat heat block to 100˚ C.
    b. Sheet with loading order.
    c. Ice bucket with ice.
    d. Liquid N_2.
    e. One 2-ml screw-cap microcentrifuge tube (ISC BioExpress GeneMate C-3225-1S) per sample, labeled. Add 1 ml H_2O to each tube; cap and place on ice.
    f. 2 X 7-ml polypropylene scintillation vials (Fisher 03-337-20) per sample; 4 vials per day for the incubation medium. Label the tubes sequentially.
    g. Take the saved diluted incubation medium from the refrigerator.
31. Weigh muscles, record mass, and place into the appropriate tube containing water.
32. After all muscles have been weighed, place in the heat block and boil for 10 minutes.
33. Immediately place tubes in ice bath for 10 minutes.
34. Centrifuge at 16,000 *g* (13,000 rpm on Eppendorf C5415C) for 15 minutes.

35. Pipette 200 µl of supernatant in duplicate into the appropriate scintillation vials.
36. Pipette 100 µl of diluted incubation medium in duplicate into the appropriate scintillation vials.
37. Add 5.0 ml of BioSafe II scintillation cocktail (Research Products International 111195) to each vial; cap.
38. Count on scintillation counter.
39. Dispose of the samples in the appropriate container for unwanted radioactive material.
40. Fill out radiation log (using values from the stored radioactivity): 50% liquid, 20% solid, 30% scintillation.

Solutions

KREBS-HENSELEIT BUFFER STOCK I (10X)

1. In a 1-L beaker with a stir bar, add ~800 ml H_2O.
2. Add 67.79 g NaCl (EM Science SX0420-3).
3. Add 3.430 g KCl (Sigma P3911).
4. Add 1.578 g KH_2PO_4 (Sigma P0662).
5. Add 21.25 g $NaHCO_3$ (Sigma S7277).
6. Stir until dissolved.
7. Bring to pH to 7.4.
8. Bring final volume to 1 L in with H_2O in a graduated cylinder.
9. Filter through a 0.22-µm filter into an autoclaved glass bottle.

10. Store at 4˚ C.

KREBS-HENSELEIT BUFFER STOCK II (10X)

1. In a 1-L beaker with a stir bar, add ~800 ml H_2O.
2. Add 3.675 g $CaCl_2 \cdot 2H_2O$ (Sigma C3881).
3. Add 2.859 g $MgSO_4 \cdot 7H_2O$ (Sigma M9397).
4. Stir until dissolved.
5. Bring to pH to 7.4.
6. Bring final volume to 1 L in with H_2O in a graduated cylinder.
7. Filter through a 0.22-µm filter into an autoclaved glass bottle.
8. Store at 4˚ C.

1 M 2-DOG (10 ML)

1. Put ~7 ml H_20 in a 50-ml beaker with a small stir bar.
2. Add 1.642 g 2-deoxyglucose (Sigma D3179).
3. Spin at low speed on stir plate until completely dissolved.
4. Bring to final volume 10 ml in a 10-ml graduated cylinder.
5. Return to beaker.
6. Draw solution into a 10-ml syringe.
7. Attach a 0.22-µm filter to the syringe.
8. Filter into a sterile 15-ml conical tube.
9. Using repeat pipetter, aliquot into sterile 1.5-ml microcentrifuge tubes in 1.0-ml aliquots. Label tubes “1 M 2-DOG”.
10. Store tubes at -20° C.

100 U/ML INSULIN STOCK

1. NOTE: The calculations for this protocol are based on insulin with an activity of 27 U/mg. Adjust the volume of glacial acetic acid used depending on the activity of the lot.
2. If needed, make 1% glacial acetic acid solution.
    a. Add 10 ml H_2O to a 15-ml conical tube.
    b. Add 100 µl glacial acetic acid (Fisher A38).
    c. Cap and vortex.
3. Add 2.7 ml of 1% glacial acetic acid to a 10 mg stock vial of insulin (Sigma I5523).
4. Cap and then vortex for 1 minute.
5. Keep solution on ice.
6. Using a repeat pipetter, aliquot 25 µl into sterile 500-µl amber microcentrifuge tubes. Occasionally re-vortex the sample to ensure a homogeneous solution.
7. Store at -20° C.
8. NOTE: These are single-use aliquots only. Do not subject to re-freezing once it is thawed.

3 M SODIUM ACETATE

1. Aliquot purchased 3 M sodium acetate solution (Sigma 71196) in 400-µl aliquots into 500-µl microcentrifuge tubes.
2. Store both aliquotted and remaining solution at -20˚ C.

0.625 M MANNITOL STOCK

1. In a 400-ml beaker with a stir bar, add ~150 ml of 10X Krebs-Henseleit Buffer, Stock I.
2. Add 28.47 g of mannitol (Sigma M4125).
3. Stir at high speed until completely dissolved (may take quite a while and/or require some heating).
4. Bring to final volume 250 ml with H_2O in a graduated cylinder.
5. Filter through a 0.22-µm filter into an autoclaved 250-ml glass bottle.
6. Oxygenate with 95% O_2/5% CO_2 for 20 minutes.
7. Store at 4˚ C.

0.625 M MANNITOL STOCK II

1. In a 400-ml beaker with a stir bar, add ~150 ml of 10X Krebs-Henseleit Buffer, Stock II.
2. Add 28.47 g of mannitol (Sigma M4125).
3. Stir at high speed until completely dissolved (may take quite a while and/or require some heating).
4. Bring to final volume 250 ml with H_2O in a graduated cylinder.
5. Filter through a 0.22-µm filter into an autoclaved 250-ml glass bottle.
6. Oxygenate with 95% O_2/5% CO_2 for 20 minutes.
7. Store at 4˚ C.

INSULIN BINDING IN EPITROCHLEARIS MUSCLE

Protocol

I. Preparation:

a. Day ahead:

1. Label 20-ml scintillation vials for incubation.
2. Label 2 1.5-ml microcentrifuge tubes for insulin (1 U/ml and 10 mU/ml).
3. Label 1-L bottle (33-mm neck) KHB; add 800 ml H_2O to the bottle.
4. Label a 50-ml conical tube KHB-0.4 nM insulin.
5. Label a 50-ml conical tube KHB-7,500 nM insulin.
6. Label 12 X 75 mm tubes for counting the muscle.
7. Label 2-ml screw-cap microcentrifuge tubes; add 1 ml 1 M NaOH to each tube.
8. Label foils for ventricles and fat pads.

b. Have ready:

1. Rats weighed at lights on; wheels locked, and food removed.
2. Fill out rat census sheet.
3. Ice bucket with ice.
4. Large container with ice.
5. Diaper.

6. Carcass bag.
7. Surgical tools.
8. Blue weigh boats.
9. Sterile gauze.
10. Culture dish.
11. Scalpel blades.
12. Weigh boat for tissue.
13. 10-cm filter paper.
14. Liquid N_2.
15. Pentobarbital.

c. Turn on the water bath to 37° C.

d. Place the following on ice:

1. KHB stock buffers.
2. Insulin.
3. 3 M acetate.
4. [^{125}I] insulin (New England Nuclear NEX104).

e. Make KHB:

1. Add 100 ml KHB 10X Stock I to the 800 ml H_2O.
2. Bubble with 95% O_2/5% CO_2 for 20 minutes at 4 psi.
3. Add 100 ml KHB 10X Stock II to the 800 ml H_2O.
4. Bubble with 95% O_2/5% CO_2 for 10 minutes at 4 psi.
5. Check pH (~7).
6. Add 1.0 g BSA (final concentration = 0.1%; Sigma A7888)

7. Add 667 µl of 3 M sodium acetate (final concentration = 2 mM; Sigma 71196).
8. Add 6.9236 g mannitol (final concentration = 38 mM; Sigma M4125).
9. Allow to dissolve for 15 minutes, then swirl gently by hand to dissolve the remainder.

f. Make KHB-0.4 nM insulin (radioactive):
    1. Transfer 40 ml of the KHB to the labeled 50-ml conical tube.
    2. Add enough [^{125}I]insulin to make 0.12 µCi/ml. (Use decay chart to determine the amount.)
    3. Transfer 20 ml to the labeled 15-ml conical tube.
    4. Add 124.7 µl of 10 mU/ml insulin to the 50-ml conical tube (0.4 nM insulin).124.7
    5. Add 234 µl of 100 U/ml insulin to the 15-ml conical tube (7,500 nM insulin).

g. Add 5 ml of KHB to each of the rinsing vials.

h. Add 2 ml KHB-7,500 nM to the odd-numbered inc vials.

i. Add 2 ml KHB-0.4 nM to the even-numbered inc vials.

j. Add 5 ml of KHB to all of the remaining wash vials.

k. Use the remaining KHB for rinsing tissues.

II. Procedure:

a. Dissect out the epitrochlearis muscles.

b. Rinse in KHB.

c. Incubate in KHB 15 minutes at 37° C with shaking at 60 rpm.

d. Transfer to inc solution and incubate 4 hours at 37° C with shaking at 60 rpm.

e. Wash in ice-cold wash solution 8 times for 5 minutes each at 37° C with shaking at 60 rpm.

f. Blot the muscle on pre-wet filter paper (wet with unlabeled KHB), trim any extraneous tissue, and transfer to 1 ml of 1 M NaOH.

g. When all samples are complete, put all samples on a rocker at 4° C overnight.

III. Clean-up:

a. Put away drug.

b. Fill out drug log.

c. Put away frozen tissue samples.

d. Take running wheels, etc. from rat cages.

e. Take dirty cages.

f. Dispose of animal carcasses.

g. Fill out radiation log.

h. Wash surgical tools.

IV. First thing in the morning:

a. Vortex all samples.

b. Count 400 µl of the NaOH in duplicate on a gamma counter.

c. Count 400 µl of the KHB-0.4 nM insulin in quadruplicate to determine the specific activity.

d. Add 100 µl of 2 N HCl and vortex.

e. Freeze.

V. Protein determination:

a. Dilute 10 µl of the sample in 100 µl PBS (Gibco 14190-144).

b. Determine protein concentration using BSA as a standard (Bradford method).

c. For blanks and standard diluent, use a 2:1 mixture of 1 M NaOH and 2 N HCl and dilute it 1 part to 10 parts PBS.

Solutions

KREBS-HENSELEIT BUFFER STOCK I (10X)

11. In a 1-L beaker with a stir bar, add ~800 ml H_2O.
12. Add 67.79 g NaCl (EM Science SX0420-3).
13. Add 3.430 g KCl (Sigma P3911).
14. Add 1.578 g KH_2PO_4 (Sigma P0662).
15. Add 21.25 g $NaHCO_3$ (Sigma S7277).
16. Stir until dissolved.
17. Bring to pH to 7.4.
18. Bring final volume to 1 L in with H_2O in a graduated cylinder.
19. Filter through a 0.22-µm filter into an autoclaved glass bottle.
20. Store at 4˚ C.

KREBS-HENSELEIT BUFFER STOCK II (10X)

9. In a 1-L beaker with a stir bar, add ~800 ml H_2O.
10. Add 3.675 g $CaCl_2 \cdot 2H_2O$ (Sigma C3881).
11. Add 2.859 g $MgSO_4 \cdot 7H_2O$ (Sigma M9397).
12. Stir until dissolved.
13. Bring to pH to 7.4.
14. Bring final volume to 1 L in with H_2O in a graduated cylinder.
15. Filter through a 0.22-µm filter into an autoclaved glass bottle.
16. Store at 4˚ C.

100 U/ML INSULIN STOCK

9. NOTE: The calculations for this protocol are based on insulin with an activity of 27 U/mg. Adjust the volume of glacial acetic acid used depending on the activity of the lot.
10. If needed, make 1% glacial acetic acid solution.
    a. Add 10 ml H_2O to a 15-ml conical tube.
    b. Add 100 µl glacial acetic acid (Fisher A38).
    c. Cap and vortex.
11. Add 2.7 ml of 1% glacial acetic acid to a 10 mg stock vial of insulin (Sigma I5523).
12. Cap and then vortex for 1 minute.
13. Keep solution on ice.

14. Using a repeat pipetter, aliquot 25 µl into sterile 500-µl amber microcentrifuge tubes. Occasionally re-vortex the sample to ensure a homogeneous solution.
15. Store at -20° C.
16. NOTE: These are single-use aliquots only. Do not subject to re-freezing once it is thawed.

2 N HCL

1. Under the hood, add 41.3 ml of concentrated 5 N HCl (12.1 N; Fisher A144) to a glass bottle.
2. Add 58.7 ml H_2O.
3. Cap, mix thoroughly, and place in refrigerator until cool.
4. Store in a glass bottle under the hood.

1 M NAOH

1. Add ~80 ml H_2O to a glass beaker with a stir bar; place on stir plate under the hood.
2. Add 20.0 g NaOH (Fisher S318).
3. Stir until completely dissolved.
4. Bring to final volume 1 L in a graduated cylinder with H_2O.
5. Store in a glass bottle under the hood.

EPITROCHLEARIS HOMOGENIZATION PROTOCOL/BRADFORD ASSAY

Protocol

Have ready:

- 2 ice buckets with ice
- cooler for samples
- cooler for homogenized samples with a freezer box
- Pasteur pipettes
- liquid N_2
- marker
- plastic dish with dish-washing detergent in water
- 1 250-ml beaker
- labeled 1.5-ml microcentrifuge tubes (2/sample)
- labeled 500-µl microcentrifuge tubes (1/sample)
- 5 X 500-µl microcentrifuge tubes per sample, labeled with the sample number and “500”.
- 50-ml conical tube
- glass pestles
- homogenizer
- homogenization buffer stock (1% NP-40, keep on ice)
- Protease inhibitors (keep on ice)

- Bradford reagent
- Cuvettes for Bradford assay (3/sample + 3/standard + 1 blank)
- 10 mg/ml BSA (keep on ice)
- long forceps
- sharps container
- repeat pipetter

1. NOTE: Keep buffer and sample on ice at all times.
2. Make homogenization buffer:

	Final Volume				
	15 ml	25 ml	40 ml	50 ml	100 ml
Homogenization buffer stock (90% of final)	13.5 ml	22.5 ml	36 ml	45 ml	90 ml
Leupeptin (10 µg/µl)	75 µL	125 µL	200 µL	250 µL	500 µl
Pepstatin (1 µg/µl)	750 µL	1.25 ml	2.0 ml	2.5 ml	5 ml
Aprotinin (1.6 mg/ml; Sigma A6279)	60.5 µL	101 µL	161.6 µL	202 µL	404 µl
Na_3VO_4 (0.2 M)	75 µL	125 µL	200 µL	250 µL	500 µl
H_2O	540 µL	900 µL	1.44 ml	1.8 ml	3.6 ml

Final composition: 50 mM HEPES, pH 7.4, 4 mM EGTA, 10 mM EDTA, 15 mM $Na_4P_2O_7$, 100 mM β-glycerophosphate, 25 mM NaF, 5 mM activated Na_3VO_4, 1% Igepal CA630 and 50 µg/ml each of leupeptin, pepstatin, and aprotinin.

3. Homogenize in ice-cold homogenization buffer (15 ml/g wet weight less 300 µl).
4. Using a Pasteur pipette, transfer homogenate to a 1.5-ml microcentrifuge tube.

5. Add 300 µl Mueller buffer to the glass tube, homogenize briefly, and transfer remaining homogenate to the tube.
6. Place on rocker at 4˚ C for 1 hour.
7. Centrifuge at 16,000 *g* (13,000 rpm on the Heraeus) at 4˚ C for 20 minutes.
8. Aspirate the supernatant and transfer to a fresh 1.5-ml microcentrifuge tube.
9. Conduct a Bradford assay as described below.

Bradford assay

1. Turn on visible light on spectrophotometer.
2. Make BSA standards of 0.9, 0.75, 0.5, and 0.25 mg/ml.
    a. Use a 10 mg/ml stock solution of BSA. Make if needed:
        i. In a 15-ml conical tube, add 0.05 g BSA (Sigma A7888) to ~4.5 ml H_2O.
        ii. Vortex until completely dissolved.
        iii. Bring to final volume 5 ml in a 10-ml graduated cylinder.
        iv. Aliquot in 500-µl microcentrifuge tubes in 400-µl aliquots and store at -20° C.
    b. Make standard dilution buffer by diluting 500 µl homogenization buffer with 9.5 ml PBS in a 15-ml conical tube.
    c. Make standards according to the following table (vortex before pipetting each time); keep on ice:

Standard concentration (BSA, mg/ml)	Standard dilution buffer (1:20 homogenization buffer in PBS, µL; PBS from Gibco 14190-144)	BSA (µL, 10 mg/ml)
0.25	975	25
0.50	950	50
0.75	925	75
0.90	910	90

3. If needed, make Bradford reagent (1 part Bradford reagent concentrate (BioRad 500-0006), 4 parts H_2O, filtered through 0.45-µm filter).
    a. 200 ml:
        i. Place a stir bar in a 400-ml beaker.
        ii. Add 160 ml H_2O to the beaker. Begin stirring at moderate speed.
        iii. Add 40 ml Bradford reagent concentrate. Be careful drawing it up as it is slightly viscous.
        iv. Mix on stir plate at moderate speed for 10 minutes at room temperature.
        v. Filter through a 0.45-µm filter.
    b. Store at room temperature up to two weeks.
4. Using repeat pipetter, add 1.0 ml of Bradford reagent to appropriate cuvette.
5. Dilute sample:

a. On ice in a 500-µL microcentrifuge tube, dilute samples 1:20 with PBS.
    i. Add 190 µL of PBS to each tube.
    ii. Vortex the homogenate, then add 10 µL to each tube.
    iii. Vortex the diluted sample.

6. Pipette 10 µl of standard dilution buffer into the cuvette labeled as a blank.
7. Pipette 10 µL of BSA standard into the appropriate cuvettes. (Notes: 1. Vortex before pipetting. 2. Use a fresh tip each time.)
8. Pipette 10 µl of diluted sample into the appropriate cuvettes. (Notes: 1. Vortex before pipetting. 2. Use a fresh tip each time.)
9. Vortex blank and standard cuvettes.
10. Determine standard curve on spec.
    a. Open custom application BRDFRDDK.
    b. Ensure the settings are correct:
        i. Curve fit: Linear, non-zero intercept
        ii. Sampling device: auto smplr
        iii. Number of standards: 4
        iv. Read average time: 0.5 seconds
        v. Method name: BRDFRDDK
        vi. Units: mg/ml
        vii. Number of replicates: 3
        viii. Flag standards over: 10.0%
        ix. Standard concentrations: 0.25, 0.5, 0.75, and 0.9.

c. Place blank in auto sampler.

d. Click on blank at the bottom of the screen.

e. Remove blank.

f. Place 0.25 and 0.5 mg/ml standards in the auto sampler.

g. Click on Read 1.

h. Place 0.75 and 0.9 mg/ml standards in the auto sampler.

i. Click on Read 3.

j. Ensure that no standards are flagged for excessive CV. Re-do any standards that are flagged, re-making the standard if necessary before proceeding.

k. Click on DispStdCurve at the top of the screen.

l. Ensure that the r value is ≥0.99. If it is not, determine where the problem may lie and re-make standard(s) or make other adjustments as necessary before proceeding.

m. Click on Print at the top of the standard curve window.

n. While computer is printing the standard curve, remove the remaining standards from the spec.

o. Click on Exit at the top of the standard curve window.

p. Click on Print at the top of the top of the screen.

11. Determine sample concentrations on the spec.

a. While computer is printing the standard data, vortex the sample cuvettes.

b. Click on Samples at the top of the screen.

i. Ensure the settings are correct:

1. Dilution correction: [Yes]
2. Read average time: 0.5 seconds
3. Number of replicates: 3
4. Flag standards over: 10.0%
5. Sampling device: Auto smplr
6. Conc: mg/ml
7. Dilution factor: 20

c. Place first samples in the auto sampler.

d. Click on 1 under the Sample ID column.

e. Repeat until finished.

f. Re-do any samples flagged for excessive CV, re-making the diluted sample as needed.

g. Click on Print at the top of the screen.

h. Label the print-out with the sample numbers.

12. Click Quit at the top of the screen. Do not save any files.

13. Turn off the spec visible light.

Aliquot samples

1. Use an Excel spreadsheet to determine the volume of sample needed for 500 µg of protein.
2. Aliquot 500 µg of protein for each sample into 5 fresh 500-µl microcentrifuge tubes.

3. Store tubes in box submerged in liquid N_2.
4. Store at -80˚ C.

Solutions

HOMOGENIZATION BUFFER STOCK (~1.11X)

Final Volume	90 ml	180 ml	360 ml
H_2O	~30 ml	~60 ml	~120 ml
10.0% Igepal CA630	10.0 ml	20.0 ml	40.0 ml
1.0 M HEPES, pH 7.4	5.0 ml	10.0 ml	20.0 ml
100 mM EGTA	4 ml	8 ml	16 ml
500 mM EDTA·Na_4	2 ml	4 ml	8 ml
50 mM $Na_4P_2O_7$	30 ml	60 ml	120 ml
β-glycerophosphate (Sigma G6251)	2.16 g	4.32 g	8.64 g
NaF (Sigma S7920)	0.105 g	.210 g	.420 g

Adjust pH to 7.4. Bring final volume with H_2O. Filter through 0.22-µm filter into an autoclaved bottle and store at 4° C.

1.0 M HEPES, pH 7.4

1. Add ~30 ml H_2O to a 100-ml beaker with a spin bar.
2. Add 11.915 g HEPES (Sigma H4034).
3. Stir until completely dissolved.
4. Adjust pH to 7.4.
5. Bring to final volume 50 ml in a graduated cylinder using H_2O.

6. Sterile filter into a sterile 50-ml conical tube.
7. Store at 4˚ C.

50 mM $Na_4P_2O_7$

1. Add ~170 ml to a 250-ml beaker with a stir bar.
2. Add 4.461 g sodium pyrophosphate decahydrate ($Na_4P_2O_7 \cdot 10H_2O$, Sigma S6422).
3. Stir until completely dissolved.
4. Bring to final volume 200 ml with H_2O in a graduated cylinder.
5. Sterile filter into an autoclaved glass bottle.
6. Store at 4˚ C.

200 mM activated Na_3VO_4

1. Add ~450 ml H_2O to a 1-L beaker with a stir bar.
2. Add 18.39 g sodium orthovanadate (Sigma S6508).
3. Spin 1 hour at room temperature.
4. Adjust the pH to 10.0 using either concentrated NaOH or concentrated HCl. The starting pH of the Na_3VO_4 solution may vary with different lots of the chemical. At pH 10.0, the solution will be yellow.
5. Boil the solution in the microwave until it turns colorless (~10 min).
6. Cool to room temperature.
7. Readjust the pH to 10.0 and repeat steps 3-4 until the solution remains colorless and the pH stabilizes at 10.0.
8. Bring to final volume 500 ml using H_2O in a graduated cylinder.

9. Aliquot into sterile 1.5-ml microcentrifuge tubes in 1-ml aliquots.
10. Store at -20° C.

10% IGEPAL CA 630

1. Add 90 ml H_2O to an autoclaved 100-ml bottle with a stir bar.
2. Add 10 ml Igepal CA 630 (Sigma 56741).
3. Stir at moderately high speed on a stir plate until mixed.
4. Store at room temperature.

100 MM EGTA IN 1 M NAOH

1. If needed, make 100 ml of 1 M NaOH.
    a. Under a hood, add ~80 ml of H_2O to a 250-ml beaker with a stir bar.
    b. Add ~4 g sodium hydroxide (Fisher S318).
    c. Stir until completely dissolved.
    d. Bring to final volume 100 ml with H_2O in a graduated cylinder.
    e. Store in a glass bottle and room temperature.
2. Add ~40 ml of 1 M NaOH to a 100-ml beaker with a stir bar.
3. Add 1.902 g ethylene glycol-bis-N,N,N',N'-tetraacetic acid (Sigma E4378).
4. Stir until completely dissolved.
5. Bring to final volume of 50 ml with H_2O in a graduated cylinder.
6. Filter through a 0.22-μM filter into a sterile 50-ml conical tube.
7. Store at 4° C.

500 mM EDTA·Na_4

1. If needed, make 100 ml of 1 M NaOH.
    a. Under a hood, add ~80 ml of H_2O to a 250-ml beaker with a stir bar.
    b. Add ~4 g sodium hydroxide (Fisher S318).
    c. Stir until completely dissolved.
    d. Bring to final volume 100 ml with H_2O in a graduated cylinder.
    e. Store in a glass bottle and room temperature.
2. Put ~7.5 ml 1 M NaOH in a 15-ml conical tube.
3. Add 2.081 g ethylenediaminetetraacetic acid tetrasodium dihydrate (Sigma ED4SS).
4. Cap and vortex until completely dissolved.
5. Bring to final volume 10 ml with H_2O in a graduated cylinder.
6. Pour into a 25-ml beaker.
7. Filter through a 0.22-µm filter into a sterile 15-ml conical tube.
8. Store at 4° C.

1 mg/ml (1.46 mM) pepstatin

1. Add 10 ml dimethylsulfoxide (Sigma D8479) to a 10 mg stock vial of pepstatin A (Sigma P5318).
2. Vortex.
3. Aliquot into sterile 1.5-ml microcentrifuge tubes.
4. Store at -20° C.

10 MG/ML (21 MM) LEUPEPTIN

1. Add 5 ml of H_2O to a 50 mg stock vial of leupeptin hemisulfate (Sigma L2884).
2. Cap and vortex.
3. Aliquot into sterile 500-µL amber microcentrifuge tubes in 120-µL aliquots.
4. Store at -20° C.

Aprotinin solution may also be made instead of purchased from Sigma. Adjusts added volumes appropriately for the reduced concentration:

150 µM (1 MG/ML) APROTININ

1. Add 1.026 ml H_2O to a 1 mg stock vial of aprotinin (Sigma A4529).
2. Vortex.
3. Aliquot into sterile 500-µL amber microcentrifuge tubes in 120-µL aliquots.
4. Store at -20° C.

SDS-PAGE/IMMUNOBLOT

SDS-PAGE Protocol

1. Prepare:
    a. 2 plates/gel.
    b. 4 clamps/gel.
    c. Spacers.
    d. 1 comb/gel.
    e. 2 small Erlenmeyer flasks.
2. Wash plates thoroughly, dry, and clean with ethanol and Kimwipes.
3. Put plates together and clamp.
4. Microwave 1% agarose 40-60 seconds depending on quantity.
5. Apply agarose to sides of gel using transfer pipette; wait two minutes to polymerize.
6. Draw line 1.5 cm from bottom of spacer.
7. Prepare resolving gel (recipe is enough for 1 gel):
    a. Make solution for acrylamide resolving gel.
        i. In an Erlenmeyer flask, add the following:

1.

% gel	ml acrylamide solution (30% acrylamide/0.8% bisacrylamide)			
4	8	8	12	16
6	6	12	18	24
7.5	7.5	15	22.5	30
8	8	16	24	32
10	10	20	30	40
12	12	24	36	48
15	15	30	45	60
18	18	36	54	72

2. Resolving buffer:

    a. 1 gel: 7.5 ml

    b. 2 gels: 15 ml

    c. 3 gels: 22.5 ml

    d. 4 gels: 30 ml

3.

% gel	ml H_2O			
4	18	36	54	72
6	16	32	48	64
7.5	14.5	29	43.5	58
8	14	28	42	56
10	12	24	36	48
12	10	20	30	40
15	7	14	21	28
18	4	8	12	16

4. 20% SDS:
    a. 1 gel: 500 µl
    b. 2 gels: 1 ml
    c. 3 gels: 1.5 ml
    d. 4 gels: 2.0 ml
5. 10% ammonium persulfate:
    a. 1 gel: 100 µl
    b. 2 gels: 200 µl
    c. 3 gels: 300 µl
    d. 4 gels: 400 µl
6. 10 µl TEMED (Sigma T9281):
    a. 1 gel: 10 µl

b. 2 gels: 20 µl

c. 3 gels: 30 µl

d. 4 gels: 40 µl

ii. Mix gently.

b. Fill to just above line and overlay with ~0.5 cm 20% ethanol.

c. Let polymerize 1 hour.

8. While waiting for gel to polymerize, make transfer buffer and place in cooler overnight.

9. Prepare stacking gel:

a. With fifteen minutes remaining for polymerization of resolving gel, make solution for stacking gel.

i. In an Erlenmeyer flask, gently mix the following:

1. 30% acrylamide/0.8% bisacrylamide:

a. 1 gel: 1.3 ml

b. 2 gels: 2.6 ml

c. 3 gels: 3.9 ml

d. 4 gels: 5.2 ml

2. stacking buffer:

a. 1 gel: 2.5 ml

b. 2 gels: 5.0 ml

c. 3 gels: 7.5 ml

d. 4 gels: 10.0 ml

3. H_2O:

a. 1 gel: 5.6 ml

b. 2 gels: 11.2 ml

c. 3 gels: 16.8 ml

d. 4 gels: 22.4 ml

4. 20% SDS:

a. 1 gel: 500 µl

b. 2 gels: 1 ml

c. 3 gels: 1.5 ml

d. 4 gels: 2.0 ml

b. Prior to adding the TEMED and APS to the stacking solution (see below), pour off the ethanol solution from the resolving gel, rinse with H_2O, and blot off the remaining liquid using paper towel and/or Kimwipes.

c. Insert comb at a diagonal so that there is room at one end to use a transfer pipette.

d. Finish making the stacking solution: To the stacking buffer, add:

i. 10% ammonium persulfate:

1. 1 gel: 50 µl

2. 2 gels: 100 µl

3. 3 gels: 150 µl

4. 4 gels: 200 µl

ii. TEMED:

1. 1 gel: 10 µl

2. 2 gels: 20 µl
3. 3 gels: 30 µl
4. 4 gels: 40 µl

iii. Mix gently.

e. Using a transfer pipette, fill the remaining volume between the plates with the stacking buffer .

f. Insert the comb all the way and top off with stacking buffer.

g. Wait 1 hour to polymerize.

10. Gel must either be used immediately or stored at 4° C (max one week). For storage, wrap in paper towel soaked in H_2O, then make the wrap air-tight by wrapping it in Saran wrap.

11. Prepare samples:

a. Turn on heating block to 100° C.

b. Get samples from freezer to thaw on ice (it is helpful to move samples from -80° C to -20° C freezer the night before to shorten thaw time).

c. Remove stored gel from refrigerator.

d. Steps 11-14 can be completed while samples are thawing.

12. Preparation:

a. Electrophoresis cell and cords.

b. Power pack.

c. Ice bucket with ice.

13. Pour 1X electrophoresis buffer (need ~1100 ml for two gels, 1000 ml for one gel) in top and side wells of electrophoresis apparatus.
14. Prepare gel for electrophoresis:
    a. Remove bottom spacer and comb from gel.
    b. Insert gel carefully (at an angle) into wells on electrophoresis apparatus so that air bubbles will not get under the gel.
    c. Clamp gel to apparatus.
    d. Draw line at bottom of each well and label.
    e. Add additional 1X electrophoresis buffer to bottom wells if necessary.
    f. Wash out loading wells of the gel using a 200 µl pipette tip on the end of a 10 ml syringe.
    g. Hook up power pack and pre-run gel at 30 mA for 30 minutes.
15. Prepare samples:
    a. If needed: when samples are thawed, dilute with 4X sample buffer (25% of final volume) and H_2O according to desired protein concentration and content for loading.
    b. Poke hole in top of microcentrifuge tube using syringe needle.
       NOTE: Only poke holes in pop caps—screw-cap microcentrifuge tubes do not need to have the hole in the top.
    c. Boil samples 5 minutes.
    d. Centrifuge samples at 10,000 *g* (~13,000 rpm on Eppendorf 5415 C centrifuge) for 30 seconds.

16. While samples are boiling, take broad range (BR) and biotinylated (biot) molecular weight markers (MWM) from freezer.
    a. Place BR MWM in a rack.
    b. Poke hole in top of biot tube.
    c. Boil biot MWM 2 minutes and centrifuge at 10,000 *g* (~13,000 rpm on Eppendorf 5415 C centrifuge) for 30 seconds.
17. SDS-PAGE:
    a. Load the appropriate amount of protein for each sample (see chart) to the lanes of the gel according to the designed loading order, loading BR MWM at 10 µl/lane and biot MWM at 20 µl/lane or as otherwise determined. Take note of which lot the biot MWM came from for later comparison.
    b. Hook up power pack to gel.
    c. Run gel at 40 mA through the stacking gel (~30 min), then at 45 mA (~2 hours to run completely through the resolving gel).
    d. (Immunoblotting solutions can be made during this time or during the transfer.)
18. Materials to have ready for transfer:
    - Transfer cell with cords.
    - Transfer container.
    - Transfer cassette.
    - Thick sponge.
    - Thin sponge.

- 50 ml beaker.
- Large Pyrex dish (9” X 13”).
- 2 medium Pyrex dishes (or other medium-size dish that the plates can fit in).
- 2 pieces of 4.5”X6” Whatman filter paper per gel.
- 1 piece of 3.25”X5.625” nitrocellulose membrane (Osmonics, Inc. EP4HYA0010) per gel.
- Spin bar.
- Forceps.
- Membrane-sized dish.
- 1 extra sheet of filter paper for drying the membrane.
- Transfer buffer.
- 1000 ml beaker with milliQ H_2O.
- Dull #2 pencil.

19. Set up for transfer:
    a. When gel is close to running off, prepare transfer cell by placing in container and packing in ice.
    b. Pour ice-cold transfer buffer into cell, put spin bar in the bottom, and place both thick and thin sponges in the buffer.
    c. Pour small amount of transfer buffer in one of the medium-sized Pyrex dishes, place Whatman paper in the buffer (buffer should be enough to completely cover the filter paper).

d. Pour buffer in large Pyrex dish (9” X 13”) ~1/2 way up the sides and place black side of transfer cassette in buffer.
e. Pour a small amount of buffer into remaining medium-sized Pyrex dish.
f. Pour a small amount of buffer into the membrane-sized dish; place membrane gently on the surface of the buffer and allow it to equilibrate by capillary action.

20. Remove the thick sponge from the transfer cell, squeezing as it is removed from the transfer buffer. Place sponge over the black side of the transfer cassette.
21. Prepare gel for transfer:
    a. When gel runs off, turn off and completely disconnect the power pack.
    b. Using 50 ml beaker, drain top well into bottom wells.
    c. Remove gel plates.
    d. Remove one side spacer and pry plates apart.
    e. Gel will remain stuck to one plate.
    f. Using a spacer, make a corner cut underneath lane 1.
    g. Place glass down into the transfer buffer in the medium Pyrex dish.
    h. Allow to soak for 15 minutes.

Transfer

22. Assemble gel and membrane in cassette for transfer:

a. Remove one sheet of the Whatman paper from the transfer buffer and place it over the gel.
b. Applying slight pressure, remove the gel from the plate by having it stick to the paper.
c. Place the paper (with gel stuck to it) paper side down over the thick sponge.
d. Place membrane on top of gel, aligning the cut corners.
e. Place remaining sheet of filter paper over the top. Throughout this entire process, ensure there are no air bubbles!
f. Remove the thin sponge from the transfer cell, squeezing as it is removed from the transfer buffer.
g. Place it over the top sheet of filter paper.

23. Prepare the transfer cell for transfer:
    a. Secure the cassette and place in the transfer cell.
    b. Ensure the black side of the cassette is toward the black side of the cell (anode).
    c. Top off with transfer buffer.
    d. Place in cooler (4° C on spinner).
    e. Turn on spinner, and center the spin bar using a 2 ml pipette.
    f. Connect cell to power pack.
    g. Transfer proteins from gel to membrane using ~50 V for 1 gel and ~60 V for 2 gels for the appropriate length of time (see chart).
    h. Ensure that proper amperage is maintained.

24. While gel is transferring to the membrane, prepare antibody diluent and blocking buffer (see chart).
25. Visualization of transferred proteins:
    a. Disconnect cell from power pack and remove cassette.
    b. Remove the membrane from the cassette and place it in a small Pyrex dish.
    c. Label the membrane with a dull #2 pencil on the side the proteins were transferred to.
    d. Pour in a small amount of Ponceau solution (Sigma P7170) and agitate slightly for 1 minute.
    e. Pour solution back into container.
    f. Rinse Ponceau stain from the membrane 2X briefly in H_2O.
    g. Observe banding patterns to verify protein transfer, taking a picture (scan) if desired.
    h. Rinse the membrane with agitation in several changes of washing buffer (see chart) until Ponceau stain is no longer visible. Alternatively, the membrane can be rinsed in 0.1 M NaOH with slight agitation until the stain is no longer visible.
    i. If 0.1 M NaOH is used for de-staining, rinse blot in H_2O 1 X 30 seconds and 2 X 2 minutes.

Immunoblotting

1. While membrane is drying, prepare primary antibody in antibody diluent (see chart).
2. Incubate as described in the accompanying chart.
3. Drain antibody into saved tube. If this is the first time it has been saved, add 30 µl 10% sodium azide solution may be added to prevent bacterial growth. For antibody that is used repeatedly, the solution may also be spiked with 3 µl of antibody.
4. Rinse the blot according to the chart at slightly vigorous agitation.
5. During the last wash, prepare secondary antibody (see chart).
6. Place the blot in the secondary antibody solution and incubate with moderate agitation according to the chart.
7. Preparation:
    1. cassette
    2. film
    3. pipettes for reagents for chemiluminescence reaction
    4. two 4.5” X 6.5” Whatman
    5. conical tube for chemiluminescence reaction
    6. marking pen
    7. plastic bag for membrane
    8. timer set to 1 minute
8. Rinse and wash the blot according to the chart.

9. Autoradiographic detection:
    a. Following the wash, mix the chemiluminescent chemicals together in a conical tube (5 ml of each reagent per blot).
    b. Pour chemiluminescent solution into dish over blot and let sit for one minute (Perkin-Elmer substrate) or five minutes (Pierce SuperSignal substrate).
    c. Place membrane between sheets of Whatman paper and press together to remove extra solution.
    d. Place membrane inside of plastic bag (Kapak SealPak Pouches 403) in film cassette.
    e. Go to the dark room and expose film for the appropriate length of time (varies according to tissue, condition, and antibody: see chart).
    f. Membrane may either be stored in a sealed bag at 4° C or stripped and re-probed.

Stripping protocol

PROTOCOL #1

1. Immediately before use, dilute 10X mild antibody stripping solution (Chemicon 2502) to 1X by mixing 2 ml of the stripping solution and 18 ml of water per membrane to be stripped. (Can be made in the same container the stripping will take place in.)

2. Fill membrane-sized tray with 20 ml of 1X mild antibody stripping solution per membrane.
3. Using tweezers or forceps, submerge blot or blot strips (strips will require a lesser amount of solution) in stripping solution. Incubate with gentle mixing for 15 minutes at room temperature.
4. Wash membranes 2 X 5 minutes in the appropriate washing buffer (see chart).
5. Rinse blot in H_2O 1 X 30 seconds.
6. Return to immunoblotting protocol.

PROTOCOL #2

1. Submerge the membrane in stripping buffer (see recipe) and incubate at 50° C for 30 minutes with slight agitation. For more stringent conditions, the temperature may be increased up to 70º C.
2. Wash membrane 2 X 10 minutes in the appropriate washing buffer (see chart) on shaker at slightly vigorous speed at room temperature, using large volumes of buffer.
3. Return to the immunoblotting protocol.

VERIFICATION PROTOCOL FOR STRIPPING

1. Prior to immunoblotting, perform the chemiluminescence reaction on the membrane. There should be no evidence of protein on the film. This verifies the absence of secondary antibody.

2. Prior to immunoblotting, re-incubate the blot with secondary antibody including anti-biotin and perform the chemiluminescence reaction. Only molecular weight markers should be visible on the film. This verifies the absence of primary antibody.

Solutions

30% ACRYLAMIDE/0.8% BISACRYLAMIDE

1. Perform all steps, including weighing and mixing, under a hood.
2. Add ~ 325 ml of H_2O to a beaker with a stir bar.
3. Add 146.0 g of acrylamide (BioRad 161-0107).
4. Add 4.0 g of N,N'-methylene-bis acrylamide (United States Biochemical 19199).
5. Stir under paraffin until completely dissolved.
6. Bring to final volume of 500 ml with H_2O in a graduated cylinder.
7. Filter through a 0.45-µm filter into a glass bottle.
8. Store in the dark at 4º C.

RESOLVING (SEPARATING) BUFFER (1.5 M TRIS, PH 8.8)

1. Add ~350 ml H_2O to a beaker with a stir bar.
2. Add 90.75 g Tris base (Fisher BP152).
3. Stir until completely dissolved.
4. Adjust to pH 8.8 with HCl.
5. Bring to final volume of 500 ml with H_2O.

6. Filter through a 0.22-μm filter and store at 4° C.

STACKING BUFFER (0.5 M TRIS, PH 6.8)

1. Add ~200 ml H_2O to a beaker with a stir bar.
2. Add 15.0 g Tris base (Fisher BP152).
3. Stir until completely dissolved.
4. Adjust to pH 6.8 with HCl.
5. Bring to final volume of 250 ml with H_2O.
6. Filter through a 0.22-μm filter and store at 4° C.

20% SDS

1. Dissolve 100 g sodium dodecyl sulfate (Fisher BP166) in ~450 ml water with gentle stirring.
2. When completely dissolved, bring to final volume of 500 ml in a graduated cylinder.
3. Store at room temperature.

10% AMMONIUM PERSULFATE (APS)

1. Add ~100 mg ammonium persulfate (Sigma A3678) to a 1.5-ml microcentrifuge tube.
2. Add 1 ml water/100 mg APS.
3. Vortex until completely dissolved.
4. Make fresh weekly.

SAMPLE BUFFER (4X; 62.5 MM TRIS, PH 6.8, 20% GLYCEROL, 2% SDS, 5% B-MERCAPTOETHANOL, 0.05% BROMOPHENOL BLUE)

1. Add 3.747 ml H_2O to a 15-ml conical tube.
2. Add 1.0 ml stacking buffer.
3. Add 1.6 ml glycerol (Fisher G33).
4. Vortex until completely dissolved.
5. Add 800 µL 20% SDS.
6. Vortex until completely dissolved.
7. Add 400 µL 0.5% bromophenol blue.
8. Vortex thoroughly.
9. Store at room temperature.
10. Just before using, add 52.6 µL of β-mercaptoethanol (Sigma M7154)/ml of the final desired volume of 4X sample buffer. (Extra 4X buffer with β-mercaptoethanol may be stored for several months at -20º C.)

0.5% BROMOPHENOL BLUE

1. Add ~0.100 g bromophenol blue (Sigma B8026) to a 15-ml conical tube.
2. Add 10 ml H_2O/100 mg bromophenol blue.
3. Vortex until completely dissolved.
4. Store at room temperature.

5X ELECTROPHORESIS (RUNNING) BUFFER (1X: 25 MM TRIS, 192 MM GLYCINE, PH 8.3, 0.1% SDS)

1. Add 3.5 L H_2O to a bucket with a stir bar.

2. Add 60.4 g Tris base (Fisher BP152).
3. Add 288 g glycine (Fisher BP381).
4. Stir until completely dissolved.
5. Adjust pH to 8.3 if needed.
6. Add 100 ml 20% SDS.
7. Bring to final volume 4 L with H_2O in a graduated cylinder.
8. Store at 4º C.
9. Dilute to 1X prior to use.

10 X PBS-T (PBS=PHOSPHATE-BUFFERED SALINE; 1X: 120 MM NACL, 2.7 MM KCL, 10 MM NA2HPO4, PH 7.4, 0.1% TWEEN-20)

1. Add ~ 900 ml of H_2O to a beaker with a stir bar.
2. Add 70.128 g of NaCl (EM Science SX 0420-3).
3. Add 2.0131 g of KCl (Sigma P4504).
4. Add 26.807 g of $Na_2HPO_4 \cdot 7H_2O$ (sodium phosphate dibasic pentahydrate; EM Science SX 0715-1).
5. Stir until completely dissolved.
6. Adjust pH to 7.4.
7. Bring to final volume 1 L with H_2O in a graduated cylinder.
8. Filter through a 0.22-µM filter into an autoclaved glass bottle.
9. Add 10 ml Tween-20 (polyoxyethylene-sorbitan monolaurate; Sigma P5927).
10. Mix until completely dissolved.
11. Store at 4° C.

12. Make a 1X solution for washing when needed (see chart).

10 X TBS-T (TBS=TRIS-BUFFERED SALINE; 1X COMPOSITION: 20 MM TRIS, 137 MM NACL, PH 7.6, 0.1% TWEEN-20)

1. Add ~3.6 L H_2O to a beaker with a stir bar.
2. Add 96.8 g Tris base (Fisher BP152).
3. Add 320 g NaCl (EM Science SX 0420-3).
4. Stir until completely dissolved.
5. Adjust pH to 7.6.
6. Bring to final volume 4 L with H_2O in a graduated cylinder.
7. Filter through a 0.22-µm filter into an autoclaved glass bottle.
8. Add 10 ml Tween-20 (polyoxyethylene-sorbitan monolaurate; Sigma P5927).
9. Mix until completely dissolved.
10. Store at 4° C.
11. Make a 1X solution for washing when needed (see chart).

1% AGAROSE

1. Bring 100 ml of H_2O to boiling in an Erlenmeyer flask in a microwave.
2. Add 1 g of agarose (Gibco 15510-027) and stir on a heat block until completely dissolved.
3. Transfer to a glass bottle and store at room temperature.

TRANSFER BUFFER (STANDARD, FINAL WORKING COMPOSITION: 24.8 MM TRIS, 192 MM GLYCINE, 20% METHANOL)

1. If needed, make a 10X stock buffer:
    a. Add ~3 L of H_2O to a bucket with a stir bar.
    b. Add 120 g Tris base (Fisher BP152).
    c. Add 576 g glycine (Fisher BP381).
    d. Stir until completely dissolved.
    e. Bring to final volume 3.2 L with H_2O in a graduated cylinder.
    f. Store the 10X solution at room temperature.
2. To make the 1X working buffer:
    a. In a 4-L bucket with a stir bar, add:
        i. 400 ml of the 10X stock buffer.
        ii. 2.8 L H_2O.
        iii. 800 ml methanol (Fisher A454).
    b. Mix for ~10 minutes.
    c. Bring to final volume 4 L with H_2O.
    d. Cover and cool to 4º C overnight in the cooler before use.

TRANSFER BUFFER (BICARBONATE, FINAL WORKING COMPOSITION: 10 MM $NaHCO_3$, 3 MM Na_2CO_3, 20% METHANOL, 0.05%SDS)

1. In a 4-L bucket with a stir bar, add:
    a. ~3 ml of H_2O.
    b. 3.36 g $NaHCO_3$ (Sigma S7277).

c. 1.272 g Na_2CO_3 (Sigma S2127).

d. 800 ml methanol.

e. 10 ml 20% SDS.

2. Stir for 10-20 minutes.
3. Cover and cool to 4º C prior to use.

0.1 M NaOH

1. Put ~450 ml of H_2O in a 1-L beaker with a stir bar.
2. Add 2.0 g NaOH (Fisher S318).
3. Stir at moderately high speed until completely dissolved.
4. Bring to final volume of 500 ml with H_2O in a graduated cylinder.
5. Store in a glass bottle at room temperature.

10% SODIUM AZIDE

1. Use caution in handling sodium azide at all times.
2. Add 10 ml of H_2O to a 15-ml conical tube.
3. Add 1.0 g sodium azide (Fisher S227).
4. Vortex until completely dissolved.
5. Store at room temperature.

20% ETHANOL

1. Mix 50 ml 100% ethanol and 200 ml H_2O.
2. Store at room temperature.

5X STRIPPING BUFFER (1X: 62.5 MM TRIS-HCL, PH 6.8, 2% SDS, 100 MM B-MERCAPTOETHANOL)

1. Add ~800 ml H_2O to a glass beaker with a stir bar.
2. Add 49.25 g Tris-HCl (Chempure 423-395).
3. Stir until completely dissolved.
4. Adjust pH to 6.8.
5. Add 100 g SDS (Fisher BP166).
6. Bring to final volume 1 L with H_2O.
7. Filter through a 0.22-µm filter.
8. Store at room temperature.
9. Make 1 L of a 1X working buffer by diluting 100 ml of the 5X buffer into 900 ml of H_2O.
10. Immediately before use, add 7 µl β-mercaptoethanol (Sigma M7154)/ml 1X stripping buffer.

TBS-T/5% MILK

1. To a glass beaker with a stir bar, add:
    a. 10 ml 10X TBS-T/100 ml desired final volume.
    b. ~80 ml H_2O/100 ml desired final volume.
    c. 5 g non-fat dry milk (Carnation)/100 ml desired final volume.
2. Stir at moderately high speed 30 minutes.
3. Adjust pH to 7.6.
4. Bring to desired final volume with H_2O.

5. Spin down in 50-ml conical tubes 2,400 *g* for 3 minutes (Program #7 on Marathon 21000R) at room temperature.
6. Re-combine the solution from the different tubes.
7. Store no more than 48 hours at 4º C.

TBS-T/5% BSA

1. To a glass beaker with a stir bar, add:
    a. 10 ml 10X TBS-T/100 ml desired final volume.
    b. 90 ml H_2O/100 ml desired final volume.
    c. 5 g bovine serum albumin (Sigma A-7888)/100 ml desired final volume.
2. Stir at moderately high speed 30 minutes.
3. Adjust pH to 7.6.
4. Bring to desired final volume with H_2O.

TBS-T/1% BSA

1. To a glass beaker with a stir bar, add:
    d. 10 ml 10X TBS-T/100 ml desired final volume.
    e. 90 ml H_2O/100 ml desired final volume.
    f. 1 g bovine serum albumin (Sigma A-7888)/100 ml desired final volume.
2. Stir at moderately high speed 30 minutes.
3. Adjust pH to 7.6.
4. Bring to desired final volume with H_2O.

TBS-T/10% HORSE SERUM

1. Combine the following per 100 ml of the desired final volume:
    a. 10 ml horse serum (Gibco 16050-1226).
    b. 10 ml 10X TBS-T.
    c. 80 ml H_2O.
2. This solution needs to be made fresh daily.

PBS-T/5% BSA

1. To a glass beaker with a stir bar, add:
    g. 10 ml 10X PBS-T/100 ml desired final volume.
    h. 90 ml H_2O/100 ml desired final volume.
    i. 5 g bovine serum albumin (Sigma A-7888)/100 ml desired final volume.
2. Stir at moderately high speed 30 minutes.
3. Adjust pH to 7.4.
4. Bring to desired final volume with H_2O.

PBS-T/1% CASEIN/5% BSA

1. Pre-heat a water bath to 50º C.
2. Add ~60-70 ml/100 ml desired final volume to a glass beaker with a stir bar.
3. Add 10 ml of 10X PBS-T/100 ml desired final volume.
4. Place the beaker in the water bath for 15 minutes.
5. Add 0.75 g casein (Sigma C7078).

6. Stir for 15 minutes at a moderately high speed.
7. Return to the water bath for 15 minutes.
8. Stir for 15 minutes at a moderately high speed.
9. Return to the water bath for 15 minutes.
10. Stir for 15 minutes at a moderately high speed.
11. Adjust pH to 7.6.
12. Bring to desired final volume with H_2O.
13. Spin down in 50-ml conical tubes 2,400 *g* for 3 minutes (Program #7 on Marathon 21000R) at room temperature.
14. Re-combine the solution from the different tubes.
15. Store no more than 48 hours at 4º C.

SOURCES

Protein A (Amersham NA9120V)

Donkey anti-rabbit IgG (Amersham NA934V)

Sheep anti-mouse IgG (Amersham NA931V)

Vectastain ABC Elite kit (Vector Laboratories PK-6102; see note below on the proper way to make the enhancement solution for the immunoblot).

Horse anti-goat IgG (Vector Laboratories BA-9500)

Horseradish peroxidase-conjugated anti-biotin (Cell Signaling 7727, comes together with molecular mass standards)

How to prepare Vectastain for secondary detection on immunoblot

1. Add solution A at a 1:250 dilution to TBS-T/5% BSA. Vortex thoroughly.

2. Add solution B at a 1:250 dilution to TBS-T/5% BSA. Vortex thoroughly.
3. Vortex thoroughly every 10 minutes for the next 30 minutes prior to using for incubation of the membrane.

Protocols for different antibodies for use on immunoblots for epitrochlearis muscle

Antibody	**Akt rabbit polyclonal (Upstate 06-885)**	**Akt-phospho Ser-473 rabbit polyclonal (Upstate 12-458)**	**GLUT4 rabbit polyclonal (Biogenesis 4670-1704)**	**GLUT4 rabbit polycolonal (Chemicon AB1346)**
MW of target (kD)	60	60	43	43
% gel	10	10	12	12
Load amt (µg)	40	40	25	25
Transfer bx	Standard	Standard	Standard	Standard
Transfer time (hr)	2.5	2.5	2.5	2.5
Blocking bx	TBS-T/5% milk	TBS-T/5% milk	PBS-T/1% casein/5% BSA	TBS-T/5% milk
Blocking time (at room temp unless otherwise stated)	1 hour	1 hour	1 hour	1 hour
Rinse in washing buffer (all at room temp)	1 X briefly and 2 X 1 min in TBS-T	1 X briefly and 2 X 1 min in TBS-T	1 X briefly and 2 X 1 min in PBS-T	1 X briefly and 2 X 1 min in TBS-T
Primary antibody buffer and dilution	1:1,000 in TBS-T/5% BSA	1:500 in TBS-T/5% BSA	1:15,000 in TBS-T/5% BSA	1:800 in TBS-T/5% BSA
Primary antibody incubation	Overnight at 4° C	Overnight at 4° C	Overnight at 4° C	Overnight at 4° C
Rinse (all at room temp)	1 X briefly and 4 X 5 min in TBS-T	1 X briefly and 4 X 5 min in TBS-T	1 X briefly, 2 X 10 min, and 6 X 5 min in PBS-T	1 X briefly, 2 X 10 min, and 6 X 5 min in TBS-T
Secondary antibody (all use 1:4,000 anti-biotin unless otherwise indicated)	1:5,000 donkey α-rabbit in TBS-T/5% milk	1:5,000 donkey α-rabbit in TBS-T/5% milk	1:10,000 donkey α-rabbit in TBS-T/5% milk; 1:2,000 anti-biotin	1:5,000 donkey α-rabbit in TBS-T/5% milk
Secondary antibody incubation (all at room temp)	1 hour	1 hour	1 hour	1 hour
Rinse (all at room temp)	1 X briefly and 4 X 5 min in TBS-T	1 X briefly and 4 X 5 min in TBS-T	1 X briefly, 2 X 10 min, and 6 X 5 min in PBS-T	1 X briefly, 2 X 10 min, and 6 X 5 min in TBS-T
Rinse	1 X briefly and 1 X 5 min in H_2O	1 X briefly and 1 X 5 min in H_2O	1 X briefly and 1 X 5 min in H_2O	1 X briefly and 1 X 5 min in H_2O
Exposure time following ECL reaction (Perkin-Elmer ECL Substrate unless otherwise indicated)	30 sec-1min	2-5 min	15 seconds-2 minutes	15 seconds-2 minutes

Antibody	IRβ rabbit polyclonal (Upstate 06-492)	IRS-1 rabbit polyclonal (Upstate 06-248)	LAR goat polyclonal (Santa Cruz sc-1119)	LAR mouse monoclonal (BD Biosciences 610351)
MW of target (kD)	97	165	150	150
% gel	8	6	6	6
Load amt (µg)	30	30	50	50
Transfer bx	Standard	Standard	Standard	Standard
Transfer time (hr)	3	4	4	4
Blocking bx	TBS-T/5% milk	TBS-T/5% milk	TBS-T/5% milk	TBS-T/5% milk
Blocking time (at room temp unless otherwise stated)	1 hour	1 hour	1 hour	1 hour
Rinse in washing buffer (all at room temp)	1 X briefly and 2 X 1 min in TBS-T	1 X briefly and 2 X 1 min in TBS-T	1 X briefly and 2 X 1 min in TBS-T	1 X briefly and 2 X 1 min in TBS-T
Primary antibody buffer and dilution	1:1,000 in TBS-T/5% BSA	1:1,000 in TBS-T/5% BSA	1:250 in TBS-T/5% BSA	1:250 in TBS-T/5% BSA
Primary antibody incubation	Overnight at 4° C	Overnight at 4° C	Overnight at 4° C	Overnight at 4° C
Rinse (all at room temp)	1 X briefly and 6 X 5 min in TBS-T	1 X briefly, 2 X 10 min, and 4 X 5 min in TBS-T	1 X briefly, 2 X 10 min, and 6 X 5 min in TBS-T	1 X briefly and 2 X 5 min in TBS-T
Secondary antibody (all use 1:4,000 anti-biotin unless otherwise indicated)	1:5,000 Protein A (for IRβ IP) in TBS-T/5% milk or 1:5,000 donkey α-rabbit (for total homogenate)	1:5,000 donkey α-rabbit in TBS-T/5% milk	1:5,000 α-goat in TBS-T/5% milk	1:500 Vectastain α-mouse in TBS-T/5% milk for 30 min Wash vigorously 1 X briefly and 6 X 5 min in TBS-T
Secondary antibody incubation (all at room temp)	1 hour	1 hour	1 hour	1:100 of each Vectastain reagents A and B in TBS-T/5% milk for 30 min
Rinse (all at room temp)	1 X briefly and 6 X 5 min in TBS-T	1 X briefly, 2 X 10 min, and 4 X 5 min in TBS-T	1 X briefly, 2 X 10 min, and 6 X 5 min in TBS-T	Wash vigorously 1 X briefly and 6 X 5 min in TBS-T
Rinse	1 X briefly and 1 X 5 min in H_2O	1 X briefly and 1 X 5 min in H_2O	1 X briefly and 1 X 5 min in H_2O	1 X briefly and 1 X 5 min in H_2O
Exposure time following ECL reaction (Perkin-Elmer ECL Substrate unless otherwise indicated)	30 sec-1 min	1-2 min	Use Pierce SuperSignal, 2-10 minutes exposure	Use Pierce SuperSignal, 2-5 min exposure

Antibody	PKCθ mouse monoclonal (BD Biosciences 610090)	Phosphotyrosine mouse monoclonal (BD Biosciences 610000)	PTP1B mouse monoclonal (BD Biosciences 610139)	PTP1B mouse monoclonal (Oncogene PH01)
MW of target (kD)	79	Variable	48	48
% gel	10	Variable	10	10
Load amt (µg)	20	Variable	20	20
Transfer bx	Standard	Standard	Standard	Standard
Transfer time (hr)	2.5	Variable	2.5	2.5
Blocking bx	TBS-T/5% milk	TBS-T/10% horse serum (must be made fresh daily)	TBS-T/5% milk	TBS-T/5% milk
Blocking time (at room temp unless otherwise stated)	1 hour	1 hour	1 hour	1 hour
Rinse in washing buffer (all at room temp)	1 X briefly and 2 X 1 min in TBS-T	1 X briefly and 2 X 1 min in TBS-T	1 X briefly and 2 X 1 min in TBS-T	1 X briefly and 2 X 1 min in TBS-T
Primary antibody buffer and dilution	1:2,000 in TBS-T/5% BSA	1:1,000 in TBS-T/1% BSA	1:5,000 in TBS-T/5% BSA	1:5,000 in TBS-T/5% BSA
Primary antibody incubation	Overnight at 4° C	Overnight at 4° C	Overnight at 4° C	Overnight at 4° C
Rinse (all at room temp)	1 X briefly and 4 X 5 min in TBS-T	1 X briefly and 6 X 5 min in TBS-T	1 X briefly and 4 X 5 min in TBS-T	1 X briefly and 4 X 5 min in TBS-T
Secondary antibody (all use 1:4,000 anti-biotin unless otherwise indicated)	1:5,000 sheep anti-mouse in TBS-T/5% milk	1:5,000 sheep anti-mouse in TBS-T/10% horse serum	1:5,000 sheep anti-mouse in TBS-T/5% milk	1:5,000 sheep anti-mouse in TBS-T/5% milk
Secondary antibody incubation (all at room temp)		1 hour	1 hour	1 hour
Rinse (all at room temp)	1 hour	1 X briefly and 6 X 5 min in TBS-T	1 X briefly and 4 X 5 min in TBS-T	1 X briefly and 4 X 5 min in TBS-T
Rinse	1 X briefly and 4 X 5 min in TBS-T	1 X briefly and 1 X 5 min in H_2O	1 X briefly and 1 X 5 min in H_2O	1 X briefly and 1 X 5 min in H_2O
Exposure time following ECL reaction (Perkin-Elmer ECL Substrate unless otherwise indicated)	1 X briefly and 1 X 5 min in H_2O	varies	30 sec-1 min	30 sec-1 min

Antibody	**SHP-2 mouse monoclonal (BD Biosciences 610621)**			
MW of target (kD)	72			
% gel	10			
Load amt (µg)	20			
Transfer bx	Standard			
Transfer time (hr)	2.5			
Blocking bx	TBS-T/5% milk			
Blocking time (at room temp unless otherwise stated)	1 hour			
Rinse in washing buffer (all at room temp)	1 X briefly and 2 X 1 min in TBS-T			
Primary antibody buffer and dilution	1:5,000 in TBS-T/5% BSA			
Primary antibody incubation	Overnight at 4° C			
Rinse (all at room temp)	1 X briefly and 3 X 5 min in TBS-T			
Secondary antibody (all use 1:4,000 anti-biotin unless otherwise indicated)	1:5,000 sheep anti-mouse in TBS-T/5% milk			
Secondary antibody incubation (all at room temp)				
Rinse (all at room temp)	1 hour			
Rinse	1 X briefly and 3 X 5 min in TBS-T			
Exposure time following ECL reaction (Perkin-Elmer ECL Substrate unless otherwise indicated)	1 X briefly and 1 X 5 min in H_2O			

Protocols for different antibodies for use on immunoblots for epididymal fat

Antibody	**Acetyl CoA Carboxylase-phospho Ser-79 (Cell Signaling 3661)**	**AMPK rabbit polyclonal (Cell Signaling 2532)**	**AMPK-phospho Thr-172 rabbit polyclonal (Cell Signaling 2531)**	**Casein kinase II-α mouse monoclonal (Santa Cruz sc-12738)**
MW of target (kD)	265 (α), 280 (β)	61-63	61-63	49
% gel	4	8	8	12
Load amt (µg)	20	40	40	30
Transfer bx	Standard	Standard	Standard	Standard
Transfer time (hr)	8	2.5	2.5	3
Blocking bx	TBS-T/5% milk	TBS-T/5% milk	TBS-T/5% milk	TBS-T/5% milk
Blocking time (at room temp unless otherwise stated)	1 hour	1 hour	1 hour	1 hour
Rinse in washing buffer (all at room temp)	1 X briefly and 2 X 1 min in TBS-T	1 X briefly and 2 X 1 min in TBS-T	1 X briefly and 2 X 1 min in TBS-T	1 X briefly and 2 X 1 min in TBS-T
Primary antibody buffer and dilution	1:2,500 in TBS-T/5% BSA	1:500 in TBS-T/5% BSA	1:2,000 in TBS-T/5% BSA	1:500 in TBS-T/5% BSA
Primary antibody incubation	Overnight at 4º C	Overnight at 4° C	Overnight at 4° C	Overnight at 4º C
Rinse (all at room temp)	1 X briefly and 3 X 5 min in TBS-T	1 X briefly and 6 X 5 min in TBS-T	1 X briefly and 4 X 5 min in TBS-T	1 X briefly and 6 X 5 min in TBS-T
Secondary antibody (all use 1:4,000 anti-biotin unless otherwise indicated)	1:5,000 donkey α-rabbit in TBS-T/5% milk	1:5,000 donkey α-rabbit in TBS-T/5% milk	1:7,500 donkey α-rabbit in TBS-T/5% milk	1:5,000 sheep α-mouse in TBS-T/5% milk
Secondary antibody incubation (all at room temp)	1 hour	1 hour	1 hour	1 hour
Rinse (all at room temp)	1 X briefly and 3 X 5 min in TBS-T	1 X briefly and 6 X 5 min in TBS-T	1 X briefly and 4 X 5 min in TBS-T	1 X briefly and 6 X 5 min in TBS-T
Rinse	1 X briefly and 1 X 5 min in H_2O	1 X briefly and 1 X 5 min in H_2O	1 X briefly and 1 X 5 min in H_2O	1 X briefly and 1 X 5 min in H_2O
Exposure time following ECL reaction (Perkin-Elmer ECL Substrate unless otherwise indicated)	20 sec-1 min	2-5 min	1 min	2 min

Antibody	CBP mouse monoclonal (Santa Cruz sc-7300)	CBP mouse monoclonal (Chemicon MAB 1133)	C/EBPα mouse monoclonal (Affinity Bioreagents MA1-825)	mtGPAT rabbit polyclonal (from Dr. Rosalind Coleman, Unive. No. Carolina-Chapel Hill)
MW of target (kD)	265	265	45	85
% gel	4	4	12	8
Load amt (µg)	80	80	60	60
Transfer bx	Bicarbonate	Bicarbonate	Standard	Standard
Transfer time (hr)	24 @ 30 V	24 @ 30 V	2.5	4
Blocking bx	TBS-T/5% milk	TBS-T/5% milk	TBS-T/5% milk	PBS-T/5% milk
Blocking time (at room temp unless otherwise stated)	1 hour	1 hour	1 hour	1 hour
Rinse in washing buffer (all at room temp)	1 X briefly and 2 X 1 min in TBS-T	1 X briefly and 2 X 1 min in TBS-T	1 X briefly and 2 X 1 min in TBS-T	1 X briefly and 2 X 1 min in PBS-T
Primary antibody buffer and dilution	1:200 in TBS-T/t% BSA	1:500 in TBS-T/t% BSA	1:1,000 in TBS-T/5% BSA	1:2,000 in PBS-T/1% milk
Primary antibody incubation	Overnight at 4º C	Overnight at 4º C	Overnight at 4° C	Overnight at 4º C
Rinse (all at room temp)	1 X briefly and 3 X 5 min in TBS-T	1 X briefly and 6 X 5 min in TBS-T	1 X briefly and 4 X 5 min in TBS-T	1 X briefly and 6 X 5 min in PBS-T
Secondary antibody (all use 1:4,000 anti-biotin unless otherwise indicated)	1:2,000 sheep α-mouse in TBS-T/5% milk	1:2,000 sheep α-mouse in TBS-T/5% milk	1:7,500 sheep α-mouse in TBS-T/5% milk	1:12,000 donkey α-rabbit in PBS-T/1% milk
Secondary antibody incubation (all at room temp)	1 hour	1 hour	1 hour	1 hour
Rinse (all at room temp)	1 X briefly and 3 X 5 min in TBS-T	1 X briefly and 6 X 5 min in TBS-T	1 X briefly and 4 X 5 min in TBS-T	1 X briefly and 6 X 5 min in PBS-T
Rinse	1 X briefly and 1 X 5 min in H_2O	1 X briefly and 1 X 5 min in H_2O	1 X briefly and 1 X 5 min in H_2O	1 X briefly and 1 X 5 min in H_2O
Exposure time following ECL reaction (Perkin-Elmer ECL Substrate unless otherwise indicated)	10 min	10 min	30 sec-1 min	30 sec-1 min

Antibody	NF-Yβ (from Dr. Roberto Mantovani, University of Milan)	PPARγ rabbit polyclonal (Affinity Bioreagents PA3-820)	Sp1 mouse monoclonal (BD Biosciences 554129)	SREBP-1 rabbit polyclonal (Santa Cruz sc-8984)
MW of target (kD)	23	55	95,105	68, 125
% gel	18	10	6	7.5
Load amt (µg)	20	15	60	30
Transfer bx	Standard	Standard	Standard	Standard
Transfer time (hr)	4	2.5	3	4
Blocking bx	TBS-T/5% milk	TBS-T/5% milk	TBS-T/5% milk	TBS-T/5% milk
Blocking time (at room temp unless otherwise stated)	1 hour	1 hour	1 hour	1 hour
Rinse in washing buffer (all at room temp)	1 X briefly and 2 X 1 min in TBS-T	1 X briefly and 2 X 1 min in TBS-T	1 X briefly and 2 X 1 min in TBS-T	1 X briefly and 2 X 1 min in TBS-T
Primary antibody buffer and dilution	1:10,000 in TBS-T/5% BSA	1:6,000 in TBS-T/5% BSA	1:500 in TBS-T/5% BSA	1:500 in TBS-T/5% BSA
Primary antibody incubation	Overnight at 4º C	Overnight at 4° C	Overnight at 4º C	Overnight at 4º C
Rinse (all at room temp)	1 X briefly and 4 X 5 min in TBS-T	1 X briefly, 2 X 10 min, and 6 X 5 min in TBS-T	1 X briefly and 8 X 5 min in TBS-T	1 X briefly and 6 X 5 min in TBS-T
Secondary antibody (all use 1:4,000 anti-biotin unless otherwise indicated)	1:10,000 donkey α-rabbit in TBS-T/5% milk	1:7,500 donkey α-rabbit in TBS-T/5% milk	1:5,000 sheep α-mouse in TBS-T/5% milk	1:5,000 donkey α-rabbit in TBS-T/5% milk
Secondary antibody incubation (all at room temp)	1 hour	1 hour	1 hour	1 hour
Rinse (all at room temp)	1 X briefly and 4 X 5 min in TBS-T	1 X briefly, 2 X 10 min, and 6 X 5 min in TBS-T	1 X briefly and 8 X 5 min in TBS-T	1 X briefly and 6 X 5 min in TBS-T
Rinse	1 X briefly and 1 X 5 min in H_2O	1 X briefly and 1 X 5 min in H_2O	1 X briefly and 1 X 5 min in H_2O	1 X briefly and 1 X 5 min in H_2O
Exposure time following ECL reaction (Perkin-Elmer ECL Substrate unless otherwise indicated)	30 sec-1 min	30 sed-1 min	5 min	1-5 min

IMMUNOPRECIPITATION PROTOCOL FOR THE INSULIN RECEPTOR β-SUBUNIT

Notes

1. This protocol has been optimized for recovery of interacting proteins with IRβ in epitrochlearis muscle. Protocols for other proteins should be determined.
2. Epitrochlearis muscles should first be homogenized following the protocol for homogenization, using immunoprecipitation buffer instead of homogenization buffer.
3. Keep samples on ice or at 4º C throughout the protocol.

Protocol

1. Place samples and protease inhibitors on ice.
2. Label 2 1.5-ml microcentrifuge tubes/sample.
3. Determine volume of IP bx needed (= 45 µL/sample + 1.5 ml/sample + 4 ml for every 8 samples).
4. Add protease inhibitors to 2.5X IP buffer (IP bx); always keep the buffer on ice (final composition of IP bx at 1X = 50 mM Tris-HCl, pH 8.2, 150 mM NaCl, 1 mM EDTA·Na_4, 1 mM EGTA, 1% Triton X-100, 0.25% deoxycholic acid, 0.25% lauryl sulfobetaine, 0.25% caprylyl sulfobetaine, 0.5% 3-(1-pyridino)-1-propanesulfonate, 2.5 mM activated Na_3VO_4, 2.5 mM

phenylmethanesulfonyl fluoride, and 25 µg/ml each of leupeptin, pepstatin, and aprotinin):

a. NOTE: Add the following volumes per ml of the final desired volume of 2.5X IP bx.
b. 6.25 µL of 10 mg/ml leupeptin.
c. 62.5 µL of 1 mg/ml pepstatin.
d. 0.079 µL of aprotinin (1.6 mg/ml; Sigma A6279).
e. 31.25 µL of 200 mM activated Na_3VO_4.
f. 31.25 µL of 200 mM PMSF.
g. 18.67 µL of H_2O.

5. Determine how much muscle homogenate is needed for 500 µg of protein.
6. On ice, add 500 µg of homogenate protein to the appropriate 1.5-ml microcentrifuge tube.
7. Add H_2O to each sample to bring it to a volume of 135 µL.
8. Add 45 µL of 2.5X IP bx to each sample.
9. Add 5 µg of antibody (IRβ rabbit anti-mouse polyclonal; BD Biosciences 611277) to the sample. 5 µg of rabbit IgG (5 µL of 1 µg/µL) may be added as a negative control in place of primary antibody.
10. Vortex thoroughly.
11. Rotate end-over-end at 4˚ C overnight.
12. Prepare the beads (the following morning):
    a. Dilute 2.5X IP bx (with protease inhibitors as in Step #4) to a 1X buffer (IP bx: H_2O = 2:3, v:v).

b. Calculate the volume of beads that will be needed (= 100 µl of 50% bead slurry/sample).
c. Aliquot beads into 1.5-ml microcentrifuge tubes at no more than 800 µl of slurry/tube.
d. Centrifuge at 8,000 *g* (~10,500 rpm on Heraeus) for 30 seconds.
e. Remove the supernatant.
f. Wash the beads 3X with 500 µl of 1X IP bx, inverting the tube back and forth several times to wash and centrifuging at 8,000 *g* for 30 seconds between each wash. Use a gel-loading tip to completely aspirate the IP bx.
g. Re-suspend the beads with an equal volume of 1X IP bx using a wide-orifice pipette tip. Draw up and eject gently three times.

13. Add 100 µl of the washed 50% bead slurry to the sample.
14. Rotate end-over-end at 4˚ C for 2 hours. During this time, take 2X sample buffer from the freezer and put on ice to thaw.
15. Centrifuge the sample at 8,000 *g* for 30 seconds.
16. Aspirate the supernatant (supernatant may be saved as a control to determine the efficiency of precipitation).
17. Wash the beads 3X with 200 µl of 1X IP bx, inverting the tube back and forth several times to wash and centrifuging at 8,000 *g* for 30 seconds between each wash. Use a gel-loading tip to completely aspirate the IP bx.
18. Add 70 µl of 2X Laemmli sample buffer.

19. Vortex thoroughly.
20. Boil 5 minutes prior to loading on a gel.

Solutions

2.5X IP BX

1. NOTE: The buffer is prepared at 85% of the final volume. Addition of protease inhibitors in step #4 will bring the buffer to the appropriate volume at a 2.5X concentration.
2. Add ~275 ml H_2O to a glass beaker with a stir bar.
3. Add 11.59 g Tris-HCl (Chempure 423-398).
4. Add 12.89 g NaCl (EM Science SX0420-3).
5. Add 2.947 ml 500 mM EDTA·Na_4.
6. Add 14.735 ml 100 mM EGTA.
7. Add 73.5 ml of 20% Triton X-100.
8. Add 18.4 ml of 20% DOCA.
9. Add 18.4 ml of 20% lauryl sulfobetaine.
10. Add 18.4 ml of 20% caprylyl sulfobetaine.
11. Add 36.8 ml of 20% PPS.
12. Adjust pH to 8.2.
13. Bring to final volume of 500 ml with H_2O in a graduated cylinder.

20% DOCA

1. Pre-heat a water bath to 37 º C.

2. Add 40 ml of H_2O to a 50-ml conical tube.
3. Heat the H_2O to 37º C in the water bath.
4. Completely cover the tube with aluminum foil.
5. Add 8.0 g deoxycholic acid monohydrate (Sigma D5670) to the bottle.
6. Vortex thoroughly.
7. If solute does not dissolve, re-heat in the water bath and vortex again, repeating until it goes completely into solution.
8. Store at room temperature.

20% TRITON X-100

1. Add 64 ml of H_2O to a 50-ml conical tube.
2. Add 16 ml of Triton X-100 (Sigma T8787).
3. Vortex until completely dissolved.
4. Store at room temperature.

20% LAURYL SULFOBETAINE

1. Add 32 ml of H_2O to a 50-ml conical tube.
2. Add 8.0 g of lauryl sulfobetaine [3-(dodecyldimethylammonio) propanesulfonate inner salt; Sigma D4516].
3. Vortex until completely dissolved.
4. Store at room temperature.

20% CAPRYLYL SULFOBETAINE

1. Add 32 ml of H_2O to a 50-ml conical tube.

2. Add 8.0 g of caprylyl sulfobetaine (N-decyl-N,N-dimethyl-3-ammonio-1-propanesulfonate; Sigma D4266).
3. Vortex until completely dissolved.
4. Store at room temperature.

20% PPS

1. Add 32 ml of H_2O to a 50-ml conical tube.
2. Add 8.0 g of 3-(1-pyridino)-1-propanesulfonate (Sigma 82804).
3. Vortex until completely dissolved.
4. Store at room temperature.

500 mM EDTA·Na_4

1. If needed, make 100 ml of 1 M NaOH.
    a. Under a hood, add ~80 ml of H_2O to a 250-ml beaker with a stir bar.
    b. Add ~4 g sodium hydroxide (Fisher S318).
    c. Stir until completely dissolved.
    d. Bring to final volume 100 ml with H_2O in a graduated cylinder.
    e. Store in a glass bottle and room temperature.
2. Put ~7.5 ml 1 M NaOH in a 15-ml conical tube.
3. Add 2.081 g ethylenediaminetetraacetic acid tetrasodium dihydrate (Sigma ED4SS).
4. Cap and vortex until completely dissolved.
5. Bring to final volume 10 ml with H_2O in a graduated cylinder.
6. Pour into a 25-ml beaker.

7. Filter through a 0.22-µm filter into a sterile 15-ml conical tube.
8. Store at 4° C.

100 mM EGTA in 1 M NaOH

1. If needed, make 100 ml of 1 M NaOH.
    a. Under a hood, add ~80 ml of H_2O to a 250-ml beaker with a stir bar.
    b. Add ~4 g sodium hydroxide (Fisher S318).
    c. Stir until completely dissolved.
    d. Bring to final volume 100 ml with H_2O in a graduated cylinder.
    e. Store in a glass bottle and room temperature.
2. Add ~40 ml of 1 M NaOH to a 100-ml beaker with a stir bar.
3. Add 1.902 g ethylene glycol-bis-N,N,N',N'-tetraacetic acid (Sigma E4378).
4. Stir until completely dissolved.
5. Bring to final volume of 50 ml with H_2O in a graduated cylinder.
6. Filter through a 0.22-µM filter into a sterile 50-ml conical tube.
7. Store at 4° C.

200 mM activated Na_3VO_4

1. Add ~450 ml H_2O to a 1-L beaker with a stir bar.
2. Add 18.39 g sodium orthovanadate (Sigma S6508).
3. Spin 1 hour at room temperature.
4. Adjust the pH to 10.0 using either concentrated NaOH or concentrated HCl. The starting pH of the Na_3VO_4 solution may vary with different lots of the chemical. At pH 10.0, the solution will be yellow.

5. Boil the solution in the microwave until it turns colorless (~10 min).
6. Cool to room temperature.
7. Readjust the pH to 10.0 and repeat steps 3-4 until the solution remains colorless and the pH stabilizes at 10.0.
8. Bring to final volume 500 ml using H_2O in a graduated cylinder.
9. Aliquot into sterile 1.5-ml microcentrifuge tubes in 1-ml aliquots.
10. Store at -20° C.

200 mM PMSF IN ISOPROPANOL

1. Pre-heat a water bath to 37º C.
2. Add ~10 ml 100% isopropanol (Fisher A416) to a sterile 15-ml conical tube.
3. Bring to 37º C in the water bath.
4. Add 0.4181 g phenylmethylsulfonylfluoride (Sigma P7626).
5. Cap and vortex one minute.
6. Place in 37° C water bath 15 minutes.
7. Vortex.
8. Repeat steps 6-7 as needed until completely dissolved.
9. Bring to final volume 12 ml with 100% isopropanol in a graduated cylinder.
10. Return solution to the conical tube.
11. Store in 500-µl aliquots at -20º C.
12. NOTE: It may be necessary to re-heat to 37º prior to using.

1 MG/ML (1.46 MM) PEPSTATIN

1. Add 10 ml dimethylsulfoxide (Sigma D8479) to a 10 mg stock vial of pepstatin A (Sigma P5318).
2. Vortex.
3. Aliquot into sterile 1.5-ml microcentrifuge tubes.
4. Store at -20° C.

10 MG/ML (21 MM) LEUPEPTIN

1. Add 5 ml of H_2O to a 50 mg stock vial of leupeptin hemisulfate (Sigma L2884).
2. Cap and vortex.
3. Aliquot into sterile 500-µL amber microcentrifuge tubes in 120-µL aliquots.
4. Store at -20° C.

Aprotinin solution may also be made instead of purchased from Sigma. Adjust added volumes appropriately for the reduced concentration:

150 µM (1 MG/ML) APROTININ

5. Add 1.026 ml H_2O to a 1 mg stock vial of aprotinin (Sigma A4529).

1. Vortex.
2. Aliquot into sterile 500-µL amber microcentrifuge tubes in 120-µL aliquots.
3. Store at -20° C.

1 µG/µL RABBIT IGG

1. Add 10 ml of H_2O to a conical tube.

2. Add 0.010 g of rabbit immunoglobulin G (Sigma I5006).
3. Vortex until completely dissolved.
4. Store in 500-µL aliquots at -20º C.

2X SAMPLE BUFFER (1X: 62.5 MM TRIS, PH 6.8, 20% GLYCEROL, 2% SDS, 5% B-MERCAPTOETHANOL)

1. Make 4X sample buffer:
2. Add 3.5 ml H_2O to a 15-ml conical tube.
3. Add 1.0 ml stacking buffer.
4. Add 1.6 ml glycerol (Fisher G33).
5. Add 800 µL 20% SDS.
6. Add 0.4 ml 0.5% bromophenol blue.
7. Store at room temperature.
8. Add 52.6 µL of β-mercaptoethanol (Sigma M7154)/ml of 4X sample buffer.
9. Dilute the 4X buffer 1:1 (v:v) with H_2O.
10. Vortex.
11. Aliquot and store at -20º C.

STACKING BUFFER (0.5 M TRIS, PH 6.8)

1. Add ~200 ml H_2O to a beaker with a stir bar.
2. Add 15.0 g Tris base (Fisher BP152).
3. Stir until completely dissolved.
4. Adjust to pH 6.8 with HCl.
5. Bring to final volume of 250 ml with H_2O.

6. Filter through a 0.22-μm filter and store at 4° C.

20% SDS

1. Dissolve 100 g SDS (Fisher BP166) in ~450 ml water with gentle stirring.
2. When completely dissolved, bring to final volume of 500 ml in a graduated cylinder.
3. Store at room temperature.

0.5% BROMOPHENOL BLUE

1. Add ~0.100 g bromophenol blue (Sigma B8026) to a 15-ml conical tube.
2. Add 10 ml H_2O/100 mg bromophenol blue.
3. Vortex until completely dissolved.
4. Store at room temperature.

RuBPS GEL STAINING

Protocol

1. Protocol is from Rabilloud *et al*. (227).
2. Fix gel overnight in 30% ethanol/10% glacial acetic acid with gentle rocking at room temperature.
3. Rinse 4 X 30 min with moderate rocking in 20% ethanol.
4. Make RuBPS (200 nM ruthenium II bathophenanthroline disulfonate chelate, 1 μM ascorbic acid sodium salt, pH 7.0, 20% ethanol)
    a. Determine amount of RuBPS needed (~ ??? ml/gel).

b. Transfer the determined amount of 20% ethanol to a glass beaker with a stir bar.
c. Add 10 µL of 10^5X stock RuBPS/ml.
d. Stir until completely mixed.

5. Stain in RuBPS 3 hours with gentle rocking at room temperature.
6. Equilibrate in H_2O 3 X 10 min with gentle rocking at room temperature.
7. Scan at 488 nm on the Storm.

Solutions

30% ETHANOL/10% GLACIAL ACETIC ACID

1. Add 600 ml 100% ethanol to a 2-L glass bottle.
2. Add 1.2 L H_2O.
3. Add 200 ml glacial acetic acid (Fisher A38).
4. Mix thoroughly.

20% ETHANOL

1. Add 400 ml 100% ethanol to a 2-L glass bottle.
2. Add 1.6 L H_2O.
3. Mix thoroughly.

10^5X RUBPS STOCK

1. Pre-heat hot plate.
2. Pre-weigh the following:

a. 0.2 g potassium aquapentachlororuthenate ($K_2Cl_5Ru \cdot H_2O$; Alfa Aesar 41716).
b. 0.9 g bathophenanthrolinedisulfonic acid disodium salt trihydrate (Sigma 11890).

3. Add 20 ml of H_2O to a 150-ml glass beaker with a stir bar (a larger beaker is needed to prevent splattering and foaming over).
4. Bring the H_2O to a boil on the stir plate.
5. Start the stir bar spinning.
6. Add the pre-weighed chemicals from Step #2.
7. Turn off the heat.
8. Stir for 20 minutes, adding additional H_2O as needed if extensive evaporation occurs.
9. While stirring, make 500 mM ascorbic acid sodium salt:
    a. Add ~ 9 ml of H_2O to a 15-ml conical tube.
    b. Add 0.9905 g of ascorbic acid sodium salt (Sigma A4034).
    c. Vortex until completely dissolved.
    d. Bring to final volume of 10 ml with H_2O in a graduated cylinder.
10. To the ruthenate solution, add 5.2 ml of 500 mM ascorbic acid sodium salt. The remainder of the ascorbic acid may be discarded or stored in the dark at 4º C.
11. Stir for 20 minutes.
12. Transfer the solution to a 50-ml conical tube.
13. Allow the solution to cool to room temperature.

14. Adjust the pH to 7.0 with 0.1 N NaOH (it doesn't take much!).
15. Bring to a final volume of 26 ml with H_2O.
16. Store in the dark at 4º C. Solution is stable for at least 6 months.

CITRATE SYNTHASE ACTIVITY ASSAY

Protocol

1. Make any needed solutions.
2. Turn on the visible light on the spectrophotometer.
3. Pre-heat water bath to 30° C.
4. Place samples on ice to thaw.
5. Determine amount of DTNB needed and thaw at room temperature.
6. Label one 500-µl microcentrifuge tube/sample.
7. Label two cuvettes per sample.
8. Make 3 mM AcCoA in Tris buffer (recipe is enough for <20 samples; must be made fresh daily):
    a. Calculate how much to make and adjust following recipe.
    b. Add 1 ml of 100 mM Tris buffer to a 1.5-ml microcentrifuge tube.
    c. Add 0.0029 g acetyl coenzyme A (Sigma A2056).
    d. Vortex thoroughly.
    e. Keep at room temp.
9. Make 5 mM OAA in Tris buffer (recipe is enough for <20 samples; must be made fresh daily):

a. Calculate how much to make and adjust following recipe.
b. Add 2 ml of 100 mM Tris buffer to a 10-ml glass beaker with a stir bar.
c. Add 0.00260g of oxaloacetic acid (Sigma O4126).
d. Place on stir plate until completely dissolved.
e. Keep at room temp.

10. Check pH of 100 mM potassium phosphate buffer with pH paper. It should be 7.4.
11. Dilute 50 µg of epitrochlearis muscle homogenate into 100 mM potassium phosphate buffer, making a final volume of 400 µl. Keep on ice.
12. On the spectrophotometer:
    a. Click on “Kinetics/Time”.
    b. Make sure the method is set to A:\citrsynt
    c. For samples utilizing 100 µl of sample, enter a factor of 5.8824.
    d. For samples utilizing 200 µl of sample, enter a factor of 2.9412.
13. Prepare blank (may use the same blank repeatedly for up to 4 hours):
    a. To a 1.5-ml cuvette, add:
        i. 750 µl 100 mM Tris buffer.
        ii. 50 µl 3 mM AcCoA.
        iii. 100 µl 1 mM DTNB.
        iv. Vortex briefly.
        v. Load in the first well in the sampler for the spectrophotometer.

14. Prepare samples (100 µl aliquot, 5 at a time):
    a. To each of 5 1.5-ml cuvettes, add:
        i. 650 µl 100 mM Tris buffer.
        ii. 50 µl 3 mM AcCoA.
        iii. 100 µl 1 mM DTNB.
        iv. 100 µl sample.
    b. Vortex briefly.
    c. Place in 30° C water bath for 5 minutes. (During this time, make sure the correction factor on the spec program is entered at 58.8.)
    d. Using a repeat pipetter, add 100 µl of 5 mM OAA.
    e. Vortex briefly and wipe the sides of the cuvette clean with a Kimwipe.
    f. Place in sampler for spectrophotometer (the blank is always loaded in the first well).
    g. Check to see that the absorbance of the blank is ~0.
    h. Click on “Read Samples”. Samples will be read at 15-second intervals over the next 3 minutes. During this time, start to prepare the next samples. Print out the data when done, being sure to label the samples on the printout.
15. Prepare samples (200 µl aliquot, 5 at a time):
    a. To each of 5 1.5-ml cuvettes, add:
        i. 550 µl 100 mM Tris buffer.
        ii. 50 µl 3 mM AcCoA.

iii. 100 µl DTNB.

iv. 200 µl of the same sample used in the previous step.

b. Vortex briefly.

c. Place in 30° C water bath for 5 minutes. (During this time, make sure the correction factor on the spec program is entered at 29.4.)

d. Using a repeat pipetter, add 100 µl of 5 mM OAA.

e. Vortex briefly and wipe the sides of the cuvette clean with a Kimwipe.

f. Place in sampler for spectrophotometer (the blank is always loaded in the first well).

g. Click on "Read Samples". Samples will be read at 15-second intervals over the next 3 minutes. During this time, start to prepare the next samples. Print out the data when done, being sure to label the samples on the printout.

16. Repeat steps #9 and 10 as needed until all samples have been run.
17. Turn off spec light.

Solutions

2 M KOH

1. Add ~80 ml of H_2O to a beaker with a stir bar.
2. Add 11.22 g KOH (EM Science PX1480-1).
3. Stir until dissolved.
4. Bring to final volume 100 ml with H_2O.

5. Store at room temp.

100 mM Tris buffer, pH 8.0

1. Pre-heat a water bath to 30° C.
2. Add ~400 ml of H_2O to a beaker with a stir bar.
3. Add 4.02 g Tris-HCl (Chempure 423-398).
4. Add 2.97 g Tris base (Fisher BP152).
5. Stir until dissolved.
6. Place solution in a 30° water bath for 30 minutes.
7. Adjust pH to 8.0 with 2 M KOH if needed.
8. Bring to final volume 500 ml with H_2O.
9. Filter through a 0.22-µm filter into an autoclaved 500-ml glass bottle.
10. Store at 4º C.

1 mM DTNB

1. Add 30 ml of 100 mM Tris buffer to a beaker with a stir bar.
2. Add 0.0119 g of 5,5'-dithiobis-(2-nitrobenzoic acid) (Sigma D8130).
3. Stir until dissolved.
4. Aliquot 1.5 ml into 1.5-ml amber microcentrifuge tubes.
5. Store at -20° C.

100 mM potassium phosphate buffer

1. Add ~400 ml H_2O to a beaker with a stir bar.
2. Add 6.805 g of KH_2PO_4 (potassium phosphate dibasic, Fisher BP363).

3. Add 8.709 g of K_2HPO_4 (potassium phosphate monobasic, Sigma P0662).
4. Add 250 µl of 0.1 M EGTA.
5. Add 50 µl of 0.5 M EDTA·Na_4.
6. Stir until dissolved.
7. Adjust pH to 7.4 with 2 N KOH or HCl.
8. Bring to final volume 500 ml with H_2O.
9. Filter through a 0.22-µm filter into an autoclaved 500-ml glass bottle.
10. Store at 4º C.
11. Check pH with pH paper prior to each use.

GLYCOGEN ASSAY

NOTE: This assay is designed for glycogen determination in epitrochlearis muscle weighing 15-20 mg. Larger sample sizes can be dealt with by referring to the original protocol described by Hassid and Abraham (107).

Protocol

1. Turn on water bath to boiling temperature. NOTE: Keep lid on water bath at all times as much as possible.
2. While waiting for water bath to reach boiling, label the following:
    a. Three 13 X 100 mm glass culture tube (Fisher 14-961-27) per sample.
    b. One 13 X 100 mm glass culture tube for the bland and each standard (blk, 10, 20, 40, 60, 100, 200, 300, 400).

c. Two cuvettes for each sample and the standards and one cuvette for the blank.

3. Add 2 ml 30% KOH to each of the tubes labeled in 2a.
4. When the water bath reaches the boiling point, place the frozen muscle sample in the appropriately labeled tube containing 30% KOH. (If the muscle has not yet been weighed, weigh it immediately prior to adding to the tube.)
5. Place a marble on the tube.
6. Place in boiling water bath for 30 minutes (longer if needed for complete digestion of the muscle).
7. Remove from water bath.
8. Add 3 ml 95% ethanol.
9. Cap tube.
10. Vortex well.
11. Remove cap.
12. Add 1 ml saturated Na_2SO_4.
13. Cap tube.
14. Vortex well.
15. Remove cap.
16. Place a marble on the tube.
17. Place tube in boiling water bath and remove it as soon as it begins to boil. Because it will boil quickly, it is recommended that samples be spaced ~30 seconds apart.

18. Allow tube to sit at room temperature for 30 minutes.
19. While tube is sitting, add more water to the bath.
20. Centrifuge 5 minutes at 1,000 *g* (Program #16 on Marathon 21000R)
21. Discard supernatant.
22. Add 3 ml 80% ethanol.
23. Cap tube.
24. Vortex thoroughly until precipitate goes back into solution.
25. Centrifuge 5 minutes at 1,000 *g* (Program #16 on Marathon 21000R)
26. Remove caps.
27. Discard supernatant.
28. Place tubes in boiling water bath for 5 minutes to evaporate remaining solution.
29. Add 2 ml 5 N HCl to the tube.
30. Cap tube.
31. Vortex thoroughly until precipitate goes back into solution.
32. Remove cap.
33. Place a marble on the tube.
34. Place tube in boiling water bath for one hour.
35. Remove tube from water bath.
36. Allow to sit at room temperature for 30 minutes.
37. During this time, prepare the anthrone reagent:
    a. Under the hood, add 200 ml of 95% H_2SO_4 to a glass bottle.
    b. Add 0.4 g of anthrone (Fisher A836).

c. Cap the bottle and shake vigorously until anthrone is completely dissolved.

d. Put the bottle on ice.

38. Add 2 ml 5 N NaOH to the sample.

39. Add 2 ml H_2O to the sample.

40. Cap tube.

41. Vortex thoroughly.

42. Prepare standards and samples with anthrone reagent in the remaining tubes as follows:

a.

	Volume of H_2O (µL)	Volume of 1 mM glucose (µL)
Blank	1,000	0
10	990	10
20	980	20
40	960	40
60	940	60
100	900	100
200	800	200
300	700	300
400	600	400

b. Add 1 ml of each sample in triplicate to the appropriately labeled tubes, vortexing each sample just before adding.

c. Put tubes on ice.

d. Under the hood, add 2 ml anthrone reagent to each tube. Be careful to eject the reagent down the side of the tube. If it is pipetted directly onto the samples, they can boil over.

e. Cap tubes.

f. Vortex thoroughly.

g. Remove caps.

h. Place a marble on each tube.

43. Place tubes in boiling water bath for 20 minutes.

44. Turn on spectrophotometer.

45. Remove tubes from water bath and allow to sit at room temperature for 30 minutes.

46. Add more water to the bath; allow it maintain a boil in case samples need repeated.

47. Cap tubes.

48. Vortex thoroughly.

49. Add 800 µL of each standard (except for blank—only one is needed) and sample in duplicate to the appropriately labeled cuvettes.

50. Read the cuvettes in the spectrophotometer at 620 nm. (Use the Protein method on the spec and set method to Glycogen. This program will generate a standard curve and supply results in µM that can be used for subsequent calculations.)

51. For any triplicate samples that have >10% CV, repeat the steps starting at #42b.

52. Turn off the spectrophotometer and the water bath.

Solutions

95% ETHANOL

1. Combine 950 ml ethanol and 50 ml H_2O.
2. Shake until completely mixed.
3. Store at room temperature, preferably in a fireproof cabinet.

80% ETHANOL

1. Combine 800 ml ethanol and 200 ml H_2O.
2. Shake until completely mixed.
3. Store at room temperature, preferably in a fireproof cabinet.

95% H_2SO_4

1. Under a hood, add 50 ml of H_2O to a glass bottle.
2. Add 950 ml of concentrated sulfuric acid (EM Science SX-1244PC).
3. Shake until completely mixed.
4. Store under the hood.

30% KOH

1. Under the hood, add 150 g KOH (EM Science PX1480-1) to ~300 ml H_2O in a glass beaker with a stir bar.
2. Stir until completely dissolved.
3. Bring to final volume of 500 ml with H_2O.
4. Store at room temperature.

SATURATED Na_2SO_4

1. Add ~300 ml H_2O to a glass beaker with a stir bar.
2. Add ~60 g Na_2SO_4 (Sigma S9627).
3. Stir for 5-10 minutes.
4. If it completely dissolves, add ~10 g more Na_2SO_4.
5. Repeat steps 3-4 until Na_2SO_4 will no longer go into solution.

5 N HCL

1. Under the hood, add 413 ml of concentrated 5 N HCl (12.1 N; Fisher A144) to a glass bottle.
2. Add 587 ml H_2O.
3. Cap, mix thoroughly, and place in refrigerator until cool.
4. Store in a glass bottle under the hood.

5 N NAOH

1. Add ~800 ml H_2O to a glass beaker with a stir bar; place on stir plate under the hood.
2. Add 200 g NaOH (Fisher S318).
3. Stir until completely dissolved.
4. Bring to final volume 1 L in a graduated cylinder with H_2O.
5. Store in a glass bottle under the hood.

1 MM GLUCOSE STANDARD

1. If needed, make 1 M glucose:

a. Add ~45 ml H_2O to a glass beaker with a stir bar.

b. Add 9.01 g glucose (Sigma G7528).

c. Stir until completely dissolved.

d. Bring to final volume 50 ml in a graduated cylinder with H_2O.

e. Store in a 50-ml conical tube at 4º C.

2. Add 15 ml H_2O to a 15-ml conical tube.
3. Add 15 µL of 1 M glucose.
4. Vortex thoroughly.
5. Store at 4º C.

ISOLATION OF RAT PRIMARY ADIPOCYTES

PROTOCOL NOTE: This protocol works best for isolating fat samples ranging from ~0.5-2.0 g from rats <300 g. Adjustments should be made for larger samples (more washes, larger volumes for washing, higher collagenase concentration, longer incubation time, higher shaking speed). The larger adipocytes from the larger rats are more fragile due to their increased size, and the protocol would need amended and optimized to prevent cell lysis.

Protocol

1. Have ready:

a. 20-ml scintillation vials for incubation with collagenase.

b. 15-ml conical tubes lined with 250-µM nylon mesh (Sefar America 03-250/50).

c. Pasteur pipettes.

d. Transfer pipettes.

e. Empty 50-ml conical tube labeled “unwanted material”.

f. 10-ml serological pipettes.

g. 5-ml syringe with 22-gauge 1½-inch syringe needle.

h. 1 50-ml conical tube labeled “KRHB-collagenase”.

i. 1 500-ml glass bottle (45 mm neck) labeled “Krebs-Ringer-HEPES Buffer”.

j. 1 250-ml glass bottle labeled “KRHB/0.25% BSA”.

2. Thaw stock tubes for solutions:

   a. Take out stock tubes of 2 M sodium pyruvate. Allow to thaw at room temperature.

   b. Take out a bottle of type II collagenase (Sigma C1764).

3. Make KRHB (300 ml; final concentration = 130 mM NaCl, 4.7 mM KCl, 1.2 mM KH_2PO_4, 10 mM HEPES, 1 mM $CaCl_2$, 1.2 mM $MgSO_4$, pH 7.4).

   c. Pour 240 ml H_2O into bottle labeled “Krebs-Ringer-HEPES Buffer”.

   d. Add 30 ml of 10X KRHB Stock I.

   e. Add 30 ml of 10X KRHB Stock II.

   f. Place in 37˚ C water bath and warm solution to 37˚ C.

   g. Bring the pH of the solution to 7.4 with 6 N HCl while stirring constantly.

h. Cap solution and return to 37˚ C water bath.

i. NOTE: For assays other than 2-DOG transport, glucose should also be added to a final concentration of 6 mM to ensure cell viability, and the pyruvate should not be added to the collagenase solution in step 5.

4. Make KRHB/0.25% BSA (100 ml).

j. Transfer 100 ml of the KRHB to the bottle labeled “KRHB/0.25% BSA”.

k. Add 0.25 g FFA-free BSA (Sigma A7030).

l. Mix on stir plate until BSA is completely dissolved.

m. Return to 37˚ C water bath.

5. Make KRHB-collagenase (2 mg/ml).

n. Add 100 mg type II collagenase (Sigma C1764) to 50 ml KRHB/0.25% BSA in the labeled 50-ml conical tube.

o. Add 25 µl of 2 M sodium pyruvate. NOTE: Pyruvate is used when isolation is followed by the glucose transport assay. For other purposes, a 5-6 mM glucose concentration should be used instead.

p. Cap and invert several times to mix.

q. Place in 37° C water bath.

6. Isolation of primary adipocytes.

r. Sacrifice rat with 60 µg pentobarbital/g body mass (0.0012 ml/g of 50 mg/ml Nembutal).

s. Dissect out epididymal fat pad free of the internal spermatic vessels.

t. Rinse in KRHB.

u. Blot dry on sterile gauze.

v. Weigh the fat pad.

w. Holding the pad with forceps, mince it using a #10 scalpel blade into as small as pieces as possible.

x. Place minced fat in a 20-ml scintillation vial.

y. Add 4 ml KRHB-collagenase/g fat to scintillation vial for digestion of tissue.

z. Swirl by hand.

aa. Incubate at 37˚ C at 60 rpm for 60 minutes.

bb. Swirl by hand.

cc. Using 10-ml pipette, transfer to 15 ml conical tube lined with 250 µM nylon filter. Use the pipette tip to “push” additional cells through the mesh; cap.

dd. Spin at 100 g for 1 minute (Program #1 on the Fisher 21000R) at room temperature.

ee. Remove mesh filter; inspect it and make note of any excessive residue; dispose of filter.

ff. Using 5-ml syringe with a 1.5-inch 22-gauge needle, gently aspirate the infranatant, ensuring that any pelleted cells at the bottom of the

tube are removed; dispose of the infranatant in a 50-ml conical tube.

gg. Holding the tube at ~45˚ angle, add one transfer pipette (~2 ml) of KRHB/0.25% BSA to fat cake, letting the solution run down the side of the tube (do not squirt the media directly onto the fat cells!) (wash #1).

hh. Spin 30 seconds X 100 g (Program #2) at room temperature.

ii. Using 5-ml syringe with a 1.5-inch 22-gauge needle, gently aspirate infranatant and dispose in a 50-ml conical tube.

jj. Holding the tube at ~45˚ angle, add one transfer pipette (~2 ml) of KRHB/0.25% BSA to fat cake, letting the solution run down the side of the tube (wash #2).

kk. Spin 30 seconds X 100 g (Program #2) at room temperature.

ll. Using 5-ml syringe with a 1.5-inch 22-gauge needle, gently aspirate infranatant and dispose in a 50-ml conical tube.

mm. Holding the tube at ~45˚ angle, use a Pasteur pipette to gently remove any floating lipid from top of fat cake, being extra careful not to aspirate any cells.

nn. Spin 30 seconds X 100 g (Program #2) at room temperature.

oo. Using 5-ml syringe with a 1.5-inch 22-gauge needle, gently aspirate infranatant and dispose in a 50-ml conical tube.

pp. Holding the tube at ~45˚ angle, use a Pasteur pipette to gently remove any floating lipid from top of fat cake, being extra careful not to aspirate any cells.

qq. Spin 30 seconds X 100 g (Program #2) at room temperature.

rr. Using 5-ml syringe with a 1.5-inch 22-gauge needle, gently aspirate infranatant and dispose in a 50-ml conical tube.

7. The packed cells of the fat cake are now ready for assay.

Solutions

2 M SODIUM PYRUVATE

1. Put ~60 ml H_2O in a 150-ml beaker with a stir bar.
2. While stirring at a moderately high speed, add 22.0 g sodium pyruvate (pyruvic acid sodium salt; Sigma 15990).
3. Stir until completely dissolved.
4. Bring to final volume of 100 ml in a graduated cylinder.
5. Using a repeat pipetter, aliquot into sterile 500-µl microcentrifuge tubes in 400 µl aliquots.
6. Store at -20˚ C.

KREBS-RINGER-HEPES BUFFER STOCK I (10X)

1. To a 1-L beaker with a stir bar, add ~800 ml H_2O.
2. Add 75.97 g NaCl (EM Science SX0420-3).
3. Add 3.50 g KCl (Sigma P3911).

4. Add 1.63 g KH_2PO_4 (Sigma P0662).
5. Add 23.83 g HEPES (Sigma H4034).
6. Stir until completely dissolved.
7. Bring to final volume of 1 L with H_2O in a graduated cylinder.
8. Filter through a 022-µm filter into an autoclaved glass bottle.
9. Store at 4˚ C.

KREBS-RINGER-HEPES BUFFER STOCK II (10X)

1. To a 1-L beaker with a stir bar, add ~800 ml H_2O.
2. Add 1.47 g $CaCl_2 \cdot 2H_2O$ (Sigma C3881).
3. Add 2.96 g $MgSO_4 \cdot 7H_2O$ (Sigma M9397).
4. Stir until completely dissolved.
5. Bring to final volume of 1 L with H_2O in a graduated cylinder.
6. Filter through a 022-µm filter into an autoclaved glass bottle.
7. Store at 4˚ C.

OIL RED O STAINING OF PRIMARY ADIPCOYTES

Protocol

1. Isolate adipocytes.
2. Transfer fat cake to 35 mm culture dish using wide-orifice P1000.
3. Using transfer pipette, add neutral-buffered formalin; wait 15 minutes
4. Transfer to 15 ml conical tube using wide-orifice P1000.

5. Spin 30 seconds X 100 *g* (1000 rpm) at room temperature; aspirate infranatant using Pasteur pipette.
6. Using transfer pipette, add 60% isopropanol; invert tube over and back.
7. Spin 1 minute X 200 rpm (~50 *g*) at room temperature; aspirate infranatant and supernatant phases (fat cake may be in middle) using Pasteur pipette.
8. Transfer fat cake to 35 mm culture dish using wide-orifice P1000.
9. Using transfer pipette, add 0.35% oil red O in 60% isopropanol in excess; wait 20 minutes.
10. Transfer to 15 ml conical tube using wide-orifice P1000.
11. Spin 1 minute X 200 rpm (~50 *g*) at room temperature; aspirate infranatant and supernatant phases (fat cake may be in middle) using Pasteur pipette.
12. Using transfer pipette, add 60% isopropanol
13. Mix by drawing into a wide-orifice P1000 and ejecting 2-3 X, then transfer some to a 35 mm culture dish, transferring enough to cover the bottom; wait 5 minutes.
14. Add methyl green in excess; wait 15 minutes.
15. Drain off methyl green; rinse gently until clear using a transfer pipette and 60% isopropanol.
16. Add just enough 60% isopropanol to cover the bottom of the dish.
17. View under microscope.

Solutions

OIL RED O SOLUTION (0.35% IN 60% ISOPROPANOL)

1. Add 0.7 g of oil red O (Fisher BP112) to 200.0 ml of 100% isopropanol (Fisher A416).
2. Shake; leave overnight.
3. Filter through 0.22 µM filter.
4. Dilute 180 ml of oil red O solution with 120 ml of H_2O.
5. Leave overnight at 4° C.
6. Filter through 0.22 µM filter.
7. Let stand 30 minutes.
8. Filter through 0.22 µM filter.
9. Stable for 6-8 months.
10. Note: oil red O stains plastic ware! Use only glassware and rinse with 100% isopropanol immediately after use.
11. Source: Humason's Animal Tissue Techniques, 5th ed., pg. 248.

NEUTRAL BUFFERED FORMALIN

1. Carry out all steps under a hood.
2. Mix the following:
    a. 25 ml 37% formaldehyde (Fisher F79).
    b. 225 ml H_2O.
    c. 1.0 g $NaH_2PO_4 \cdot H_2O$ (sodium acid phosphate; Fisher BP330).

d. 1.625 g Na_2HPO_4 (anhydrous disodium phosphate; EM Science SX0715-1).

CELL VIABILITY ASSAY FOR PRIMARY ADIPOCYTES

1. Prepare ~500 µL of a cell suspension in PBS (Gibco 14190-144).
2. Add 500 µL of 0.4% Trypan Blue (Sigma T8154) to a 1.5-ml microcentrifuge tube.
3. Add 300 µL of PBS.
4. Add 200 µL of the cell suspension.
5. Vortex. (For primary adipocytes, DO NOT VORTEX as this will rupture the cells—simply mix by gently inverting several times.)
6. Allow the mixture to sit for 5-10 minutes (never more than 15). For primary adipocytes, 5 minutes is more than sufficient.
7. Vortex. (For primary adipocytes, DO NOT VORTEX as this will rupture the cells—simply mix by gently inverting several times.)
8. Count the cells on a hemacytometer. Only non-viable cells should be stained.

2-DEOXYGLUCOSE UPTAKE IN PRIMARY RAT ADIPOCYTES

NOTE: This protocol describes the process, but only describes solutions for no insulin, 0.4 nM insulin, and 12.8 nM insulin. For other insulin concentrations, it will be necessary to make changes.

Protocol

1. Dry down 18 µl [^{3}H]2-deoxyglucose (American Radiolabled Chemicals ART-103) in a colored 500-µl microcentrifuge tube 1 hr 54 min on speed vac with no temperature setting. Label the tube "radio-KRHB".
2. Have ready:
    - 250-ml graduated cylinder
    - 20-ml scintillation vials for incubation with collagenase, 1/sample.
    - 15-ml conical tube lined with 250-µM nylon mesh (Sefar America 03-250/50), 1/sample.
    - Pasteur pipettes, transfer pipettes, empty 50-ml conical tube labeled "unwanted material", 10-ml pipettes, 5-ml syringe with 22-gauge 1½-inch syringe needle.

- 6-ml scintillation vials (Fisher 03-337-41), 4/sample, labeled with the animal number and max, sub, cyto, or bas on both the cap and the side.
- 1.5-ml screw-cap microcentrifuge tubes (Fisher 05-669-26) containing 150 µl dinonyl phthalate (Sigma 80151), 4/sample, labeled with the animal number and max, sub, cyto, or bas on both the cap and the side.
- 4 15-ml conical tubes labeled “cyto b inc”, “max ins inc”, “submax ins inc”, and “bas inc”.
- Aluminum-foil wrapped 15-ml conical tube labeled “500 µM cyto B”.
- Label 2 1.5-ml screw-cap microcentrifuge tubes “fat inc” with the date. Add 950 µl of H_2O to each.
- 7-ml scintillation vials in counting racks, 1/sample plus 4 for the incubation medium, labeled sequentially (vials from Fisher 03-337-20).
- 1 50-ml conical tube labeled “KRHB-collagenase”.
- 1 500-ml glass bottle (45 mm neck) labeled “Krebs-Ringer-HEPES Buffer”. Add 320 ml of H_2O to the bottle.
- 1 250-ml glass bottle labeled “KRHB/0.25% BSA”.
- Time course sheet; loading order sheet.
- One box of gel-loading tips.

2. Thaw stock tubes for solutions:

a. Take out stock tubes of 100 U/ml insulin and 14 mM cytochalasin B. Place on ice to thaw.
b. Take out stock tubes of 0.2 M 2-deoxyglucose and 2 M sodium pyruvate. Allow to thaw at room temperature.
c. Take out a bottle of type II collagenase (Sigma C1764).

3. Make KRHB (130 mM NaCl, 4.7 mM KCl, 1.2 mM KH_2PO_4, 1 mM $CaCl_2$, 1.2 mM $MgSO_4$, pH 7.4).
    a. To the bottle labeled “Krebs-Ringer-HEPES Buffer” and containing 320 ml H_2O, add:
        i. Add 40 ml of KRHB Stock I.
        ii. Add 40 ml of KRHB Stock II.
    b. Place in 37˚ C water bath and warm solution to 37˚ C (30 minutes in a deep water bath).
    c. Bring the pH of the solution to 7.4 with HCl while stirring constantly.
    d. Cap solution and return to 37˚ C water bath.
4. Make KRHB/0.25% BSA (KRHB, 0.25% free-fatty acid-free BSA).
    a. Transfer 200 ml of the KRHB to the bottle labeled “KRHB/0.25% BSA”.
    b. Add 0.5 g FFA-free BSA (Sigma A7030).
    c. Mix on stir plate until BSA is completely dissolved.
    d. Return to 37˚ C water bath.
5. Make KRHB-collagenase (KRHB/0.25% BSA, 2 mg/ml type II collagenase).

a. Add 50 mg type II collagenase (Sigma C1764) to 25 ml KRHB/0.25% BSA in the labeled 50-ml conical tube.
b. Add 25 µl of 2 M sodium pyruvate.
c. Cap and invert twice to mix.
d. Place in 37° C water bath.

6. Make max insulin solution (1 U/ml).
    i. Add 990 µl KRHB/0.25% BSA to a 1.5-ml microcentrifuge tube. Label “1 U/ml”.
    ii. Add 10 µl of 100 mU/ml insulin stock.
    iii. Vortex.
    iv. Keep on ice.
7. Make 500 µM cyto B.
    a. Add 3 ml KRHB/0.25% BSA to a 15-ml conical tube wrapped in aluminum foil.
    b. Vortex the 14 mM cytochalasin B.
    c. Add 140 µl 14 mM cytochalasin B.
    d. Vortex.
    e. Keep on ice.
8. Make incubation solutions:
    a. NOTE: Concentrations are calculated based on insulin with a specific activity of 27 U/mg (Sigma I5523, Lot 12K1881)
    b. Add 10 ml of KRHB/0.25% BSA to each of the 15-ml conical tubes labeled “max ins inc”, “submax ins inc”“cyto b inc”, and “bas inc”.

c. Max insulin solution (KRHB/0.25% BSA, 12.8 nM insulin):
    i. Add 20 µL 1 U/ml insulin to the max ins inc tube.
    ii. Cap and invert several times to mix.
d. Submax insulin solution (KRHB/0.25% BSA, 0.6 nM insulin):
    i. Add 94.5 µl 10 mU/ml insulin to the submax ins inc tube.
    ii. Cap and invert several times to mix.
e. Cyto b solution (KRHB/0.25% BSA, 70 µM cytochalasin B):
    i. Add 50 µL 14 mM cytochalasin B to the control inc tube.
    ii. Cap and invert several times to mix.
f. Add 290 µl of each incubation solution to the appropriate 6-ml scintillation vial.
g. Cap the vials and place them in the 37˚ C water bath.

9. Prepare radio-KRHB (concentration at this point is 45 µCi/ml [^{3}H]2-DOG and 6 mM 2-DOG):
    a. In the tube containing 18 µl of dried down [^{3}H]2-deoxyglucose, add 388 µl of KRHB/0.25% BSA.
    b. Add 12 µl of 0.2 M 2-DOG stock.
    c. Cap and vortex.
    d. Spin briefly at max revolutions.
10. Prepare radio-KRHB for scintillation counting:
    a. Add 50 µl of radio-KRHB to each of the 2 tubes labeled “fat inc”.
    b. Cap, vortex, and leave in the rack in the radioactive area.
11. Place the remaining KRHB/0.25% BSA in 37˚ C water bath.

12. Sacrifice the animals, remove the fat pad(s), and isolate the adipocytes according to the protocol.
13. Aliquot 40-80 µl of fat cake into the appropriate incubation vial at 10-second intervals within each sample. Do not re-cap the vials. (For samples that are limited, it is possible to use 40 µL, but if possible it is desirable to use 60-80 µL)
14. Incubate at 37° C for 45 minutes.
15. Add 10 µl of radio-KRHB to each vial; incubate 3 more minutes.
16. Add 300 µl of ice-cold 500 µM cytochalasin B (final concentration=250 µM).
17. Using a wide-orifice P-1000 (set pipette at 450 µl), transfer the entire contents of the vial to the appropriate 1.5-ml tube with the dp oil. Cap.
18. Separate isolated adipocytes from incubation medium and prepare for scintillation counting.
    a. Spin at 3,000 *g* for 6 seconds (Program #14).
    b. With the P200 pipette set at 175 µl, aspirate the infranatant with a gel-loading tip. It will require three tips to aspirate all of the medium.
    c. Add 150 µl of KRHB/0.25% BSA, squirting the solution down the side of tube and not directly onto the cells (wash #1).
    d. Spin at 3,000 *g* for 6 seconds (Program #14).
    e. Using the P200 pipette set at 175 µl, aspirate the infranatant with a gel-loading tip.

f. Add 150 µl of KRHB/0.25% BSA, squirting the solution down the side of tube and not directly onto the cells (wash #2).

g. Spin at 3,000 *g* for 6 seconds (Program #14).

h. Using the P200 pipette set at 175 µl, aspirate the infranatant with a gel-loading tip.

i. Spin at 3,000 *g* for 6 seconds (Program #14).

j. Alternatives for transferring cell-associated radioactivity into scintillation vial:

    i. Alternative #1: Holding the tube so that the bottom portion rests inside the appropriate 7-ml scintillation vial, cut the tube through the line, allowing the bottom portion of the tube to drop into the vial. Discard the top of the tube into the unwanted radioactive material. This is the method used in the main experiment, but it does provide more variability.

    ii. Alternative #2: Add 200 µL heptane to the tube. Cap the tube and vortex it. Transfer all of the solution in the tube to a scintillation vial. This is the preferred method.

k. Add 5 ml BioSafe II (Research Products International 111195) scintillation fluid. Cap and shake vigorously 15 times.

19. Add 50 µl from each “inc count” tube to 7-ml scintillation vials in duplicate. Add 5 ml of BioSafe II.

20. Count on scintillation counter.

Solutions

0.2 M 2-DOG STOCK

1. Place ~ 8 ml H_2O in a 15-ml conical tube.
2. Add 0.3284 g 2-deoxyglucose (Sigma D3179).
3. Cap and vortex until completely dissolved.
4. Bring to final volume 10 ml with H_2O.
5. Filter through a 0.22-µm filter into a fresh 15-ml conical tube.
6. Using a repeat pipetter, aliquot into sterile 500-µl microcentrifuge tubes in 30 µl aliquots.
7. Store at -20˚ C.

14 MM CYTOCHALASIN B STOCK

1. To a 5 mg stock vial of cytochalasin B (Sigma C6762), add 744.5 µL of 100% ethanol.
2. Cap and vortex until completely dissolved.
3. Using a repeat pipetter, aliquot into sterile 500-µL amber microcentrifuge tubes in 20 µL aliquots.
4. Store at -20° C.

100 U/ML INSULIN STOCK

1. NOTE: The calculations for this protocol are based on insulin with an activity of 27 U/mg. Adjust the volume of glacial acetic acid used depending on the activity of the lot.

2. If needed, make 1% glacial acetic acid solution.
    a. Add 10 ml H_2O to a 15-ml conical tube.
    b. Add 100 µl glacial acetic acid (Fisher A38).
    c. Cap and vortex.
3. Add 2.7 ml of 1% glacial acetic acid to a 10 mg stock vial of insulin (Sigma I5523).
4. Cap and then vortex for 1 minute.
5. Keep solution on ice.
6. Using a repeat pipetter, aliquot 25 µl into sterile 500-µl amber microcentrifuge tubes. Occasionally re-vortex the sample to ensure a homogeneous solution.
7. Store at -20° C.
8. NOTE: These are single-use aliquots only. Do not subject to re-freezing once it is thawed.

2 M SODIUM PYRUVATE

1. Put ~60 ml H_2O in a 150-ml beaker with a stir bar.
2. While stirring at a moderately high speed, add 22.0 g sodium pyruvate (pyruvic acid sodium salt; Sigma 15990).
3. Stir until completely dissolved.
4. Bring to final volume of 100 ml in a graduated cylinder.
5. Using a repeat pipetter, aliquot into sterile 500-µl microcentrifuge tubes in 400 µl aliquots.

6. Store at -20˚ C.

KREBS-RINGER-HEPES BUFFER STOCK I (10X)

1. To a 1-L beaker with a stir bar, add ~800 ml H_2O.
2. Add 75.97 g NaCl (EM Science SX0420-3).
3. Add 3.50 g KCl (Sigma P3911).
4. Add 1.63 g KH_2PO_4 (Sigma P0662).
5. Add 23.83 g HEPES (Sigma H4034).
6. Stir until completely dissolved.
7. Bring to final volume of 1 L with H_2O in a graduated cylinder.
8. Filter through a 022-µm filter into an autoclaved glass bottle.
9. Store at 4˚ C.

KREBS-RINGER-HEPES BUFFER STOCK II (10X)

1. To a 1-L beaker with a stir bar, add ~800 ml H_2O.
2. Add 1.47 g $CaCl_2 \cdot 2H_2O$ (Sigma C3881).
3. Add 2.96 g $MgSO_4 \cdot 7H_2O$ (Sigma M9397).
4. Stir until completely dissolved.
5. Bring to final volume of 1 L with H_2O in a graduated cylinder.
6. Filter through a 022-µm filter into an autoclaved glass bottle.
7. Store at 4˚ C.

CELLULARITY PROTOCOL FOR ISOLATED ADIPOCYTES

Protocol on day of sacrifice

1. NOTE: Perform all steps using osmium tetroxide under a hood unless sample is being stored.
2. Have ready:
    a. 3 X 7-ml glass scintillation vials (Fisher 03-337-26)/sample, labeled.
    b. Under the hood, add 300 µl of adipose tissue fixative to each vial and cap the vial.
3. Sacrifice animals and isolated adipocytes according to the protocol.
4. Add 20-100 µl (dependent upon size of rats and fat pads) of packed cells in triplicate to the vials with fixative.
5. Cap and leave at room temperature for 2 days.
6. Transfer vials to 4˚ C for no more than 30 days.

Preparation of the sample for counting and sizing

7. Preparation for remaining steps:
    a. Set up filtration device with 43-mm circles of 20-µm nylon mesh (Sefar America 03-20/14) on the screen and a 12-cm square of 250-µm nylon mesh (Sefar America 03-250/20) over the top of the glass cup, secured in place with a rubber band. The flask should be labeled: 75% NaCl, 17% corn oil, 8% (120 mM osmium

tetroxide/50 mM 2,4,6 trimethylpyridine), 0.025% Triton X-100. Any time the flask needs to be emptied, the waste bottle it is emptied into should be similarly labeled. Also, 50 ml corn oil (can be purchased at a retail store) should be added to the flask upon emptying.

b. Have ready:
    i. Wash bottle with 0.9% NaCl/0.1% Triton X-100.
    ii. Wash bottle with adipocyte cell counting solution.

8. Pre-wet the 250-µm nylon mesh with distilled water under the tap and assemble it on the filtration device.
9. Turn on the vacuum
10. Flick the vial containing the sample. Carefully pour the contents of the vial on the 250-µm nylon mesh.
11. Rinse the vial with 0.9% NaCl/0.1% Triton X-100 and drain remainder onto the mesh.
12. Re-cap the vial and dispose in biohazard waste.
13. Rinse with 0.9% NaCl/0.1% Triton X-100 through the nylon screen.
14. Turn off vacuum.
15. Remove the glass cup from the filtration device and rinse the mesh with distilled water.
16. Using forceps, take the 20-µm nylon mesh with the collected cells and place on the inside of the appropriate 400-ml beaker under the rim.

17. Rinse the cells off the mesh into the beaker with adipocyte cell counting solution. If needed forceps can be used to hold the mesh in place.
18. Dispose of the mesh in biohazard waste.
19. For the next sample, place a fresh circle of 20-µm nylon mesh on the screen, re-assemble the filtration device, and repeat steps 9-18.
20. Count on Coulter counter according to the protocol.

Solutions

ADIPOSE TISSUE FIXATIVE (0.12 M OSMIUM TETROXIDE, 50 MM 2,4,6-TRIMETHYLPYRIDINE, 0.9% NACL)

1. Place a stir bar in an autoclaved 50- or 100-ml glass bottle.
2. Add 32.8 ml of 0.9% NaCl.
3. Under the hood, add 220 µl of 2,4,6-trimethylpyridine (Sigma 142387).
4. Put on a face mask for the next step.
5. Under the hood, carefully break a glass ampule containing 1 g of osmium tetroxide (Sigma 201030) into the bottle.
6. Tighten the lid on the bottle.
7. Cover with aluminum foil.
8. Stir at moderately high speed for one hour.
9. Using forceps, remove the stir bar.
10. Wash the forceps and the stir bar thoroughly.
11. Store at 4˚ C.

0.9% NaCl/0.1% Triton X-100

1. To 1 L of 0.9% NaCl, add 1 ml of Triton X-100 (Sigma T8787). NOTE: The 0.9% NaCl should be room temperature or the detergent will not go into solution.
2. Cap and invert ~10 times to mix.
3. Filter through 0.22-µm filter into an autoclaved glass bottle.

Adipocyte Cell Counting Solution (20 L)

1. To a car boy with a large stir bar, add 18 L of Isoton II (Beckman-Coulter 6102037).
2. Add ~2 L of glycerol (Sigma G5150).
3. Invert back and forth ~20 times.
4. Spin on a stir plate 1 hour.

COULTER COUNTER PROTOCOL FOR COUNTING AND SIZING FIXED ADIPOCYTES

Protocol

Preparation:

- 2 3.5" floppy disks.
- Samples in beakers.
- Pen and paper for note-taking.
- Bottle of Isoton II.

- 2 empty 400-ml beakers, labeled “Isoton II” and “adipocyte cell counting solution”.
- Paper towel.
- Adipocyte counting solution (Isoton II/10% glycerol).
- Funnel.
- Waste bottle(s). If new bottles are needed, label with a biohazard sticker with the following information for contents: 90% Isoton II (Beckman-Coulter proprietary electrolyte solution), 10% glycerol, 0.02% adipocytes fixed in osmium tetroxide, 0.0025% corn oil. Add 10 ml of corn oil (can buy from retail store) to the bottle.
- 400-µm aperture tube.
- Gloves.
- Kimwipes.
- Wash bottle with H_2O.

Use of the Coulter counter

1. With the sample stand main power turned *off*:
    a. Make sure supply reservoir (on right) is filled ~3/4 full with Isoton II (Beckman-Coulter 6102037).
    b. On the sample stand, replace the vial containing Isoton II with the empty 400-ml beaker labeled “Isoton II”.
    c. Remove the pipette tip from the waste reservoir (on the left).
    d. Turn RESET/COUNT stopcock to RESET position.

e. Turn FILL/CLOSE stopcock to FILL position.

f. Allow the aperture tube (100-µm) to drain into the beaker.

g. Remove the beaker and set aside.

h. Remove the 100-µm aperture tube, rinse it three times with distilled H_2O, and place it gently on paper towel with the aperture opening facing up in a protected area.

i. Take the 400-µm aperture tube from the canister.

j. Place the 100-µm aperture tube into the canister.

k. If needed, lightly place some low vacuum grease on the inside rim of the 400-µm aperture tube. (Low vacuum grease is available from Beckman-Coulter, #306812.)

l. Fit the 400-µm aperture tube onto the sample stand; ensure an airtight seal.

m. Secure the aperture tube with the spring.

n. Clean the aperture with the camel hair brush.

o. Place a fresh 400-ml beaker with adipocyte counting solution under the aperture tube and submerge the tube into the solution.

p. Close the door.

q. Replace the pipette tip into position on the waste reservoir.

r. Turn RESET/COUNT stopcock to COUNT position.

s. Turn FILL/CLOSE stopcock to CLOSE position.

t. Turn on the sample stand.

u. Turn FILL/CLOSE stopcock to FILL position.

v. Slowly turn RESET/COUNT stopcock to RESET position.

w. Allow the tube to fill until solution runs into the waste reservoir; if there are bubbles in the vacuum tube, turn dial back and forth rapidly between fill and close several times or repeat steps 1l-1v.

x. Turn the FILL/CLOSE stopcock to CLOSE position.

y. Turn the RESET/COUNT stopcock to COUNT position.

2. Turn on the MultiSizer II (MSII) and computer monitor.

3. On the MII:

    a. Enter the date.

    b. For Orifice Diameter, enter 400.

    c. Do not change the orifice length (it should = 300 after diameter has been entered).

    d. Enter Setup = Manual.

    e. Press SETUP.

    f. Enter Instrument Control = Time.

    g. Enter Time = 15 seconds.

    h. Press SETUP three times.

    i. Enter Setup = Automatic

    j. Enter Calibration = Recall

    k. Press CAL. Kd should read 4010.3; Size should read 42.49E.

4. Wait 10 minutes.

5. While waiting, the sample beakers can be filled with adipocyte cell counting solution to ~ the 300-ml mark.

6. On sample stand, turn RESET/COUNT dial to RESET and manometer control to OUT position.
7. On MII, push RESET, then FULL.
8. After autocalibration is complete (screen will change), ensure that the RESET/COUNT dial is set to COUNT position.
9. Counting protocol:
    a. On the MII, push RESET.
    b. Remove the beaker from the sample stand.
    c. Empty the waste reservoir and replace.
    d. To the beaker containing the next sample to be counted, add adipocyte counting solution (Isoton II/10% glycerol) to an approximate final volume of 300 ml.
    e. Using the camel hair brush, gently clean the aperture.
    f. Load sample on sample stand, positioning stirrer below the aperture tube in the center of the beaker.
    g. Turn stirrer to 5.
    h. Turn sample stand RESET/COUNT stopcock to RESET position.
    i. When ready, push START on the MSII; observe the accumulation of particles/cells and note if there is a rapid increase in the counting.
    j. When done counting, RESET/COUNT stopcock to COUNT position.
    k. Turn off stirrer and lower the beaker.

l. Repeat steps 9d-9j 2 more times (until accumulated time listed on the MSII = 45 seconds).

m. On computer:

    i. On the Acquire menu, select New Sample. Enter the name of the sample.

    ii. On the Acquire menu, select Collect from Multisizer.

n. On the MII, press PRINT to send the data to the computer.

o. On the computer, enter the sample identification name as the file name. On the first sample, change the drive to the floppy drive (NOTE: On future samples, the floppy drive will be the default drive and only the file name will need to be entered.):

    i. Click on Directory.

    ii. Click on A:.

    iii. Click on Change.

    iv. Enter the file name (name of sample).

    v. Click Save.

    vi. Close the file.

10. To start the next sample, press RESET on the MII, then repeat the counting protocol (step 9).

11. When complete:

    a. On the computer:

        i. On the Acquire menu, select New Sample.

        ii. Click OK.

iii. On the Acquire menu, select Collect from Multisizer.

b. On the MII, press PRINT.

c. On the computer:

i. Click on Directory.

ii. Click on C:.

iii. Click on Change.

iv. Click on OK.

v. Click Cancel. This will return the computer default to the hard drive.

vi. Close all windows; do no save the last window which is untitled.

d. On the MII:

i. Press SETUP.

ii. For Orifice Diameter, enter 100.

iii. Do not change the Orifice Length (it should = 75.00 after diameter has been entered).

iv. Enter Setup = Manual.

v. Press SETUP.

vi. Enter Instrument Control = Siphon.

vii. Press SETUP three times.

viii. Enter Setup = Automatic

ix. Enter Calibration = Recall

x. Press CAL. Kd should read 958.03.

e. Turn the sample stand manometer to 500.

f. Turn off all instrumentation.

g. Move the stirrer out of the way.

h. Replace the 100-µm aperture tube.

    i. Place one of the used sample beakers under the 400-µm aperture tube.

    ii. Remove the pipette tip from the waste reservoir (on the left).

    iii. Turn RESET/COUNT dial to RESET.

    iv. Turn FILL/CLOSE dial to FILL.

    v. Allow the aperture tube (400-µm) to drain into the beaker.

    vi. Empty the beaker into the sink.

    vii. Remove the 400-µm aperture tube, rinse it three times with distilled H_2O, and place it gently on paper towel in a protected area with the orifice facing upward.

    viii. Wipe the inner tube, electrode, and stirrer with a Kimwipe.

    ix. Take the 100-µm aperture tube from the canister.

    x. Place the 400-µm aperture tube into the canister.

    xi. If needed, lightly place some low vacuum grease on the inside rim of the 100-µm aperture tube.

    xii. Fit the 100-µm aperture tube onto the sample stand; ensure an airtight seal.

    xiii. Secure the aperture tube with the spring.

xiv. Place a fresh 400-ml beaker with Isoton II under the aperture tube and submerge the tube into the solution.

xv. Replace the pipette tip into position on the waste reservoir.

xvi. Turn RESET/COUNT dial to COUNT .

xvii. Turn FILL/CLOSE dial to CLOSE .

xviii. Turn the sample stand back on.

xix. Turn FILL/CLOSE dial to FILL.

xx. Slowly turn RESET/COUNT dial to RESET.

xxi. If there are bubbles in the vacuum tube, turn FILL/CLOSE dial back and forth rapidly between FILL and CLOSE several times or repeat steps i-xx.

xxii. Turn the FILL/CLOSE dial to CLOSE .

xxiii. Turn the RESET/COUNT dial to COUNT .

xxiv. Clean the aperture with the camel hair brush.

xxv. Place the aperture in a vial of Isoton II.

xxvi. Turn off the sample stand.

i. Empty the waste reservoir.

12. Clean up any messes.

13. Gather up all materials; make sure to get the diskettes.

14. Upon returning to the lab:

a. Get all beakers washed.

b. Soak the aperture tube overnight in concentrated nitric acid.

c. Rinse the aperture tube several times with H_2O.

d. Using a Pasteur pipette hooked to an air valve, dry the aperture tube.

Solutions

ADIPOCYTE CELL COUNTING SOLUTION (20 L: 90% ISOTON II, 10% GLYCEROL)

5. To a car boy with a large stir bar, add 18 L of Isoton II (Beckman-Coulter 6102037).
6. Add ~2 L of glycerol (Sigma G5150).
7. Invert back and forth ~20 times.
8. Spin on a stir plate 1 hour.

COULTER COUNTER DATA ANALYSIS

1. If samples have been performed in duplicate or triplicate, the data must first be merged together:
    a. Open AccuComp.
    b. Click on the File menu.
    c. Click on Average.
    d. Open the directory where the files are stored.
    e. Double-click on each file for the sample.
    f. Click OK.
2. Subtract the background:
    a. Open the file for the sample. For files that have been merged (Step #1), this is the merged file.

b. Click on Analyze.

c. Click on Subtract Background.

d. Double-click the file where the background data is stored.

3. Get a printout and analysis of the sample:

    a. On the View menu, click on the desired parameter to be analyzed (Diameter, Volume, or Area.

    b. On the Distribution menu, click on and Number and Differential.

    c. On the graph, click on the dashed line and drag it to the 239.2 µm position (with Diameter set as the View setting). While holding down the Shift key, drag the left-most dashed line to the 24.45 µm position.

    d. Click on View.

    e. Click on Zoom In.

    f. Click on RunFile.

    g. Click on Save. Save with a new file name, preferably in a new directory to avoid confusion.

    h. Click on RunFile.

    i. Click on Print Report.

4. The printed report will contain the data, a graph, and a hard copy of the number of cells counted in each channel.

5. Close the file.

6. To determine the percent of cells in each size range:

    a. Open Excel.

b. Click on the Open icon.

c. On the drop-down menu for file type, click “All Files”.

d. Go to the directory where the Coulter counter data is stored.

e. Single-click on the file to open.

f. Click Open.

g. Click Next.

h. In the space next to “Tab”, click it off.

i. In the space next to “Space”, click it on.

j. Click Finish.

k. The file will open up in Excel. Starting on about line 68 will be the counts of cells in each channel. The first column contains the channel number, and the second column contains the average number of cells counted in that channel. The number of cells from channel 24 through 227 may be copied and pasted into the template for Coulter counter cell size distribution calculations.

LIPID CONTENT PROTOCOL

Protocol

1. Label and weigh 7-ml glass scintillation vials (Fisher 03-337-26) (3/sample) and record the mass.
2. Label 15-ml conical tubes, 3/sample.
3. To each tube, add:

a. 1.35 ml Dole solution.

b. 900 µl heptane.

c. 500 µl water.

4. Cap the tube.
5. Isolate adipocytes according to the protocol.
6. Add 60 µl of packed cells to the conical tubes in triplicate. (NOTE: An additional 60 µl is added to adipocyte fixative solution in triplicate according the protocol for Cellularity of Isolated Adipocytes in order to determine the cell number in the sample.)
7. Cap, vortex, and let sit 30-60 minutes.
8. Vortex.
9. Centrifuge at 450 *g* (program #8) for 5 minutes.
10. Take 2 ml of the upper phase (total of 2.6 ml) and place in the appropriate glass scintillation vial.
11. Place under the hood for 2 days.
12. Re-weigh the tube and calculate the lipid content/cell.

Solutions

DOLE SOLUTION (1 L)

1. NOTE: All steps should be performed under a ventilated hood.
2. To a 1-L glass bottle, add:
    a. 800 ml isopropanol.
    b. 200 ml heptane.

c. 5 ml 1 N H_2SO_4.

3. Cap and invert several times to mix.
4. Store under hood.

1 N H_2SO_4

1. To a 100-ml glass bottle, add 100 ml of H_2O.
2. Add 2.890 ml of concentrated sulfuric acid (35.6 N; EM Science SX1244-PC).
3. Cap and invert several times to mix.
4. Store under hood.

HOMOGENIZATION OF FAT

Protocol

1. Have ready:
    a. Autoclaved glass homogenization tubes (#20 tubes may be used for up to 500 mg of tissue; #21 tubes should be used for larger amounts).
    b. Ice bucket with ice.
    c. 2 1.5-ml microcentrifuge tubes/sample, labeled.
    d. If samples are pre-weighed, determine how much fat homogenization buffer is needed for each sample at 1.5 ml buffer/g tissue.
    e. 1-ml syringes.

f. 1-ml syringes with 22-gauge needles.

g. Make sure that the Heraeus centrifuge is pre-cooled to 4° C.

2. Prepare the fat homogenization buffer (50 mM Tris-HCl, 225 mM sucrose, 1 mM EDTA·Na_4, pH 7.4, 1 mM benzamidine, 1 µg/ml pepstatin, 1 µg/ml leupeptin, 1 µg/ml aprotinin, 1 mM activated Na_3VO_4).

    a. Determine volume of buffer needed.

    b. Add the determined volume to a conical tube.

    c. Add protease inhibitors in the following amounts per ml of buffer:

        i. 1.49 µl of 0.67 M benzamidine.

        ii. 2.0 µl of 1 mg/ml pepstatin.

        iii. 0.2 µl of 10 mg/ml leupeptin.

        iv. 1.25 µl of aprotinin (Sigma A6279, 1.6 mg/ml).

        v. 5 µl 200 mM activated Na_3VO_4.

    d. Vortex thoroughly.

    e. Keep on ice.

3. Place a glass homogenization tube on ice.

4. If samples have not yet been weighed:

    a. On dry ice, cut off the size of sample to be homogenized.

    b. Quickly weigh it, record the weight, and add it to the homogenization tube.

5. If samples have already been weighed, add the sample to the homogenization tube.

6. Add 1.5 ml of fat homogenization buffer/g tissue mass. NOTE: For small amounts of fat, use 3.0 ml buffer/g or there will be too much volume loss. For fat from larger or obese animals, use 1.0 ml of buffer/g to keep the protein concentration from being too low.
7. Homogenize with 5-10 strokes of the glass rod.
8. Using a 1-ml syringe (no needle), transfer the homogenate to the appropriately labeled 1.5-ml microcentrifuge tube. For smaller volumes (i.e. ~325 µl or less), a 22-gauge needle may be used to assist in retrieving as much volume as possible. If using #21 glass tubes, it will be necessary to use a 1.5-inch 22-gauge needle to aspirate the homogenate.
9. Leave on ice until all samples have been homogenized.
10. Spin samples at 1,000 *g* for 10 minutes at 4° C (Program #17 on Marathon 21000R).
11. Using a 1-ml syringe with a 22-gauge needle, transfer the infranatant below the fat cake but above the pellet to a fresh 1.5-ml microcentrifuge tube (see below for an alternative protocol with the fat cake).
12. Run the CB-X protein assay on the homogenate, performing each sample in at least duplicate, repeating any that have >10% CV.
13. The sample may be flash frozen in liquid nitrogen, aliquotting into smaller amounts if desired.

Alternative fat cake protocol

1. Some proteins are associated with the fat cake under different conditions. To assay these proteins, perform this protocol. NOTE: Protocol may be performed immediately or the fat cake may be stored at -80° C then thawed on ice 30 minutes prior starting the protocol.
2. Have 2 1.5-ml microcentrifuge tubes/sample ready.
3. Transfer the fat cake to a fresh 1.5-ml microcentrifuge tube (fat cake may be scraped out using a pipette tip or other similar instrument.
4. Add 500 µl of fat homogenization buffer to the tube.
5. Spin samples at 16,000 *g* (13,000 rpm on the Heraeus) for 10 minutes at 4° C.
6. Aspirate the infranatant.
7. Spin samples at 16,000 *g* (13,000 rpm on the Heraeus) for 10 minutes at 4° C.
8. Aspirate the infranatant.
9. Leave samples at room temperature for 15 minutes.
10. Add 100 µl of high-SDS sample buffer.
11. Vortex 10 seconds.
12. Spin samples at 16,000 *g* (13,000 rpm on the Heraeus) for 10 minutes at 4° C.
13. Using a 1-ml syringe with a 22-gauge needle, transfer the infranatant containing the protein extract to a fresh 1.5-ml microcentrifuge tube.

14. Run the CB-X protein assay on the sample, performing each sample in triplicate.
15. Freeze the sample in liquid nitrogen.
16. When loading on a gel, 2 µL of 0.05% bromophenol blue can be added to each lane.

Solutions

FAT HOMOGENIZATION BUFFER

1. Add ~80 ml of H_2O to a glass beaker with a stir bar.
2. Add 0.788 g of Tris-HCl (Chempure 423-398).
3. Add 7.702 g of sucrose (Sigma S0389).
4. Add 200 µl of 500 mM EDTA·Na_4.
5. Adjust pH to 7.4.
6. Bring to final volume of 100 ml with H_2O in a graduated cylinder.
7. Filter through a 0.22-µm filter and store in an autoclaved glass bottle at 4º C.

0.67 M BENZAMIDINE

1. Weigh 0.2098 g of benzamidine hydrochloride hydrate (Sigma B6506) into a 2-ml microcentrifuge tube.
2. Add 1.5 ml of H_2O.
3. Cap and vortex.
4. Using a 2-ml pipette, draw up the solution and determine the volume.

5. Return solution to the tube.
6. Calculate the remaining volume needed to bring the solution to a final volume of 2 ml.
7. Add H_2O to a final volume of 2 ml.
8. Cap and vortex.
9. Aliquot into sterile 500-µL amber microcentrifuge tubes in 100-µL aliquots.
10. Store at -20° C.

1 MG/ML (1.46 MM) PEPSTATIN

1. Add 10 ml dimethylsulfoxide (Sigma D8479) to a 10 mg stock vial of pepstatin A (Sigma P5318).
2. Vortex.
3. Aliquot into sterile 1.5-ml microcentrifuge tubes.
4. Store at -20° C.

10 MG/ML (21 MM) LEUPEPTIN

1. Add 5 ml of H_2O to a 50 mg stock vial of leupeptin hemisulfate (Sigma L2884).
2. Cap and vortex.
3. Aliquot into sterile 500-µL amber microcentrifuge tubes in 120-µL aliquots.
4. Store at -20° C.

Aprotinin solution may also be made instead of purchased from Sigma. Adjust added volumes appropriately for the reduced concentration:

150 µM (1 MG/ML) APROTININ

1. Add 1.026 ml H_2O to a 1 mg stock vial of aprotinin (Sigma A4529).
2. Vortex.
3. Aliquot into sterile 500-µL amber microcentrifuge tubes in 120-µL aliquots.
4. Store at -20° C.

200 MM ACTIVATED Na_3VO_4

1. Add ~450 ml H_2O to a 1-L beaker with a stir bar.
2. Add 18.39 g sodium orthovanadate (Sigma S6508).
3. Spin 1 hour at room temperature.
4. Adjust the pH to 10.0 using either concentrated NaOH or concentrated HCl. The starting pH of the Na_3VO_4 solution may vary with different lots of the chemical. At pH 10.0, the solution will be yellow.
5. Boil the solution in the microwave until it turns colorless (~10 min).
6. Cool to room temperature.
7. Readjust the pH to 10.0 and repeat steps 3-4 until the solution remains colorless and the pH stabilizes at 10.0.
8. Bring to final volume 500 ml using H_2O in a graduated cylinder.
9. Aliquot into sterile 1.5-ml microcentrifuge tubes in 1-ml aliquots.
10. Store at -20° C.

500 MM EDTA·Na_4

1. If needed, make 100 ml of 1 M NaOH.
    f. Under a hood, add ~80 ml of H_2O to a 250-ml beaker with a stir bar.

g. Add ~4 g sodium hydroxide (Fisher S318).

h. Stir until completely dissolved.

i. Bring to final volume 100 ml with H_2O in a graduated cylinder.

j. Store in a glass bottle and room temperature.

2. Put ~7.5 ml 1 M NaOH in a 15-ml conical tube.
3. Add 2.081 g ethylenediaminetetraacetic acid tetrasodium dihydrate (Sigma ED4SS).
4. Cap and vortex until completely dissolved.
5. Bring to final volume 10 ml with H_2O in a graduated cylinder.
6. Pour into a 25-ml beaker.
7. Filter through a 0.22-µm filter into a sterile 15-ml conical tube.
8. Store at 4° C.

HIGH-SDS SAMPLE BUFFER (62.5 MM TRIS, PH 6.8, 20% GLYCEROL, 20% SDS, 5% B-MERCAPTOETHANOL

1. Add ~60 ml H_2O to a glass beaker with a stir bar.
2. Add 0.985 g of Tris base (Fisher BP152).
3. Adjust pH to 6.8.
4. Add 20 ml glycerol (Fisher G33).
5. Stir until completely dissolved.
6. Add 20 g of sodium dodecyl sulfate (Fisher BP166).
7. Stir until completely dissolved.
8. Add 5 ml β-mercaptoethanol (Sigma M7154).

9. Mix thoroughly.
10. Bring to final volume of 100 ml with H_2O in a graduated cylinder.
11. Store in 1-ml aliquots at -20º C.

0.5% BROMOPHENOL BLUE

1. Add ~0.100 g bromophenol blue (Sigma B8026) to a 15-ml conical tube.
2. Add 10 ml H_2O/100 mg bromophenol blue.
3. Vortex until completely dissolved.
4. Store at room temperature.

CB-X PROTEIN ASSAY

1. The CB-X protein assay kit is purchased through Genotech (786-12X).
2. Add 5 µL of sample to a 1.5-ml microcentrifuge tube.
3. Add 500 µl CB-X pre-chilled at -20º C.
4. Vortex.
5. Centrifuge at 16,000 *g* (13,000 rpm on Heraeus) for 5 minutes.
6. Empty the supernatant from the tube without disturbing the pellet.
7. Add 25 µL of CB-X Solubilization Buffer I.
8. Add 25 µL of CB-X Solubilization Buffer II.
9. Vortex 3 seconds to dissolve the protein pellet.
10. Allow to sit for 10 minutes, re-vortexing for 3 seconds after 3-5 minutes.
11. Add 500 µl of CB-X Assay Dye.
12. Vortex briefly.

13. Incubate 5 minutes at room temperature.
14. Transfer 500 µl to a pre-labeled 1-ml cuvette.
15. Read the absorbance at 595 nm, using deionized water as a blank.
16. Use the CB-X table to calculate the amount of protein in the sample. Make sure that the calculations used are appropriate for the lot of CB-X protein assay kit, as it varies from lot to lot.

PALMITIC ACID INCORPORATION INTO TRIACYLGLYCEROL

Protocol

1. Preparation:
    a. Dilute 50 µg of sample protein in homogenization buffer to a concentration of 2 µg/µL.
    b. Turn water bath on to 37º C.
    c. Label 4 13 X 100 mm glass culture tubes (Fisher 14-961-27) per sample.
    d. Label 4 13 X 100 mm glass culture tubes per blank (usually three blanks for determination of background).
    e. For each sample, label one 1.5-ml screw-cap microcentrifuge tube on the side of the tube.
    f. Need 2 glass beakers (250 ml). Label "isoprop/heptane/H_2O" and "NaOH/EtOH/H_2O".

2. Place 2 µg protein/µL homogenized samples on ice.
3. Calculate volume of assay buffer needed (180 µL/sample + 1.3 ml). Hereafter, the volume needed will be referred to as “ABV” for “assay buffer volume”.
4. Transfer 819.51 µL/ml ABV of assay buffer stock solution to a 15-ml conical tube and leave at room temperature.
5. Place the following on ice:
    a. Glycerol-3-phosphate 50 mg/ml stock solution (G3P).
    b. Coenzyme A 50 mg/ml stock solution (CoA).
    c. Adenosine triphosphate 50 mg/ml stock solution (ATP).
    d. Homogenization buffer (50 mM Tris-HCl, 225 mM sucrose, 1 mM EDTA·Na_4, pH 7.4, 1 mM benzamidine, 1 µg/ml pepstatin, 1 µg/ml leupeptin, 1 µg/ml aprotinin, 1 mM activated Na_3VO_4).
    e. Palmitic acid 100 mM stock solution.
    f. Cysteine 1 M stock solution.
6. When sample is close to being completely thawed:
    a. Place the tube of 100 mM palmitic acid at room temperature.
    b. Place the tube of 1 M cysteine at room temperature.
7. Prepare the assay buffer (final composition when added to sample = 42 mM K_2HPO_4, 7 mM cysteine, 2 mM $MgCl_2$, 42 mM NaF, 1 mg/ml free fatty acid-free BSA, 15 mM glycerol-3-phosphate, 0.8 mM coenzyme A, 12 mM ATP, 50 µM palmitic acid (1 µCi/ml), pH 7.4). To the 15-ml conical tube containing the assay buffer stock solution, add:

a. 97.232 µL /ml ABV of G3P.

b. 13.644 µL /ml ABV of CoA.

c. 37.322 µL /ml ABV of ATP.

d. 7.778 µL/ml ABV of cysteine.

e. 0.5556 µL/ml ABV of the palmitic acid.

f. 22.844 µL of H_2O.

g. Return above stock solutions to freezer.

h. Vortex at least 10 seconds or until palmitic acid dissolves.

i. 1.111 µL/ml [^{3}H]palmitic acid (Sigma P1076).

j. Leave solution at room temperature.

8. When sample is completely thawed, place one set of culture tubes on ice.
9. Add 20 µL (40 µg protein) of sample to the appropriate tube.
10. Add 20 µL of homogenization buffer to the “blank” tubes.
11. Return homogenization buffer to freezer.
12. Place tubes in a rack at room temperature.
13. At 10-second intervals:

    a. Add 180 µL of the prepared assay buffer, starting the timer immediately upon adding the buffer to the first sample.

    b. Cap tubes.

    c. Vortex.

    d. Transfer tube to 37 º C water bath.

14. Incubate the tubes for 45 minutes. During this time, turn on the Speed Vac.

15. During the last 5 minutes, remove the tube caps.
16. Pour isopropanol:heptane:H_2O (80:20:2, v:v) into the appropriately labeled glass beaker.
17. Stop the enzymatic reactions by adding 1.5 ml (750 µL X 2) of isopropanol:heptane:H_2O (80:20:2, v:v). Be sure to eject onto the side of the tube and not directly onto the sample, as the force will cause it to spray up. This applies to addition of all other solutions as well. Transfer the tube to a rack at room temperature.
18. After 10 minutes, add 1 ml of heptane to each tube. After the heptane is added, it is no longer necessary to time each sample.
19. Add 500 µL H_2O to each tube.
20. Add 10 µL of [^{14}C] glyceryl trioleate (~0.001 µCi; 1 X 10^{-4} µCi/µL in 0.1 mg/ml solution in chloroform).
21. Cap the tubes.
22. Vortex each sample for 3 seconds.
23. Centrifuge at 450 *g* for 2 minutes (Program 8).
24. Remove caps.
25. Transfer the heptane layer to a new tube (1.3 ml; 650 µL X 2).
26. Pour 1 N NaOH:ethanol:H_2O (5:50:45, v:v) into the appropriately labeled glass beaker and draw solution into the repeat pipetter (set to 4 for 2-ml dispensing).
27. Add 2 ml of 1 N NaOH:ethanol:H_2O (5:50:45, v:v).
28. Re-cap the tubes.

29. Vortex each sample for 3 seconds.
30. Centrifuge at 450 *g* for 2 minutes (Program 8).
31. Remove caps.
32. Transfer the heptane layer to a new tube (1.0 ml).
33. Using the repeat pipetter, add 2 ml of 1 N NaOH:ethanol:H_2O (5:50:45, v:v).
34. Re-cap the tubes.
35. Vortex each sample for 3 seconds.
36. Centrifuge at 450 *g* for 2 minutes (Program 8).
37. Remove caps.
38. Transfer the heptane layer to a new tube (800 µL).
39. Using the repeat pipetter, add 2 ml of 1 N NaOH:ethanol:H_2O (5:50:45, v:v).
40. Re-cap the tubes.
41. Vortex each sample for 3 seconds.
42. Centrifuge at 450 *g* for 2 minutes (Program 8).
43. Transfer 600 µL of the heptane layer to the appropriately labeled 1.5-ml screw-cap microcentrifuge tube.
44. Dry down in the Speed Vac 30 minutes at 35º C.
45. While samples are drying:
    a. Using a dull pencil, mark the chromatography plates at 7 cm from the point of origin. Label each lane above the mark. (Use of high

performance-thin layer chromatography plates permits maximum separation and resolution of the samples; Whatman 4806-411.)

b. Apply 2 µL of 5 mg/ml glyceryl tripalmitate to each lane.

46. Add 50 ml of hexane:ethyl ether:glacial acetic acid (80:20:2, v:v:v) to the chromatography developing tank. Place the lid on the tank.
47. Re-constitute the sample in 10 µL chloroform.
48. With the pipette set at 12 µL, add sample to the appropriate lane on the chromatography plate.
49. Place the plate in the developing tank, replace the lid, and develop to the 7 cm mark.
50. Remove plate and allow it to dry 5 minutes in the hood.
51. Spray the plate with 0.01% primulin (w:v) in acetone:H_2O (80:20, v:v).
52. Allow to dry 10 minutes in the hood.
53. Mark the triglyceride band under a UV light.
54. Scrape the marked area onto wax paper and empty into a scintillation vial.
55. Add 100 µL of the incubation medium in triplicate to a scintillation vial.
56. Add 5 ml of BioSafe II to each vial.
57. Cap the vials and shake vigorously.
58. Count in the scintillation counter, using Program 8 for dual scintillation counting of ^{14}C and ^{3}H. Use ^{14}C to determine the % recovery of triacylglycerol on the TLC plate and use this in subsequent calculations. Subtract the average blank numbers (background) from the calculations.

Solutions

ASSAY BUFFER STOCK FOR FATTY ACID INCORPORATION INTO TRIACYLGLYCEROL (~1.36 X)

1. Add ~450 ml H_2O to a beaker with a stir bar.
2. Add 4.959 g K_2HPO_4 (Fisher BP363).
3. Add 0.2756 g $MgCl_2 \cdot 6H_2O$ (Fisher BP214).
4. Add 1.1955 g NaF (Sigma S7290).
5. Add 0.6799 g free fatty acid-free BSA (Sigma A7030).
6. Adjust pH to 7.4.
7. Bring final volume to 500 ml with H_2O.
8. Filter through a 0.22-µm filter into an autoclaved glass bottle.
9. Store at 4º C.

FAT HOMOGENIZATION BUFFER (50 MM TRIS-HCL, 225 MM SUCROSE, 1 MM EDTA·NA_4, PH 7.4, 1 MM BENZAMIDINE, 1 MG/ML PEPSTATIN, 1 MG/ML LEUPEPTIN, 1 MG/ML APROTININ, 1 MM ACTIVATED NA_3VO_4)

1. Add ~80 ml of H_2O to a glass beaker with a stir bar.
2. Add 0.788 g of Tris-HCl (Chempure 423-398).
3. Add 7.702 g of sucrose (Sigma S0389).
4. Add 200 µl of 500 mM EDTA·Na_4.
5. Adjust pH to 7.4.
6. Bring to final volume of 100 ml with H_2O in a graduated cylinder.

7. Filter through a 0.22-µm filter and store in an autoclaved glass bottle at 4º C.
8. Add fresh on day of use per ml of buffer:
    a. 1.49 µl of 0.67 M benzamidine.
    b. 2.0 µl of 1 mg/ml pepstatin.
    c. 0.2 µl of 10 mg/ml leupeptin.
    d. 1.25 µl of aprotinin (Sigma A6279, 1.6 mg/ml).
    e. 5 µl 200 mM activated Na_3VO_4.

500 mM EDTA·Na_4

1. If needed, make 100 ml of 1 M NaOH.
    k. Under a hood, add ~80 ml of H_2O to a 250-ml beaker with a stir bar.
    l. Add ~4 g sodium hydroxide (Fisher S318).
    m. Stir until completely dissolved.
    n. Bring to final volume 100 ml with H_2O in a graduated cylinder.
    o. Store in a glass bottle and room temperature.
2. Put ~7.5 ml 1 M NaOH in a 15-ml conical tube.
3. Add 2.081 g ethylenediaminetetraacetic acid tetrasodium dihydrate (Sigma ED4SS).
4. Cap and vortex until completely dissolved.
5. Bring to final volume 10 ml with H_2O in a graduated cylinder.
6. Pour into a 25-ml beaker.
7. Filter through a 0.22-µm filter into a sterile 15-ml conical tube.

8. Store at 4° C.

670 mM BENZAMIDINE

1. Weigh 0.2098 g of benzamidine hydrochloride hydrate (Sigma B6506) into a 2-ml microcentrifuge tube.
2. Add 1.5 ml of H_2O.
3. Cap and vortex.
4. Using a 2-ml pipette, draw up the solution and determine the volume.
5. Return solution to the tube.
6. Calculate the remaining volume needed to bring the solution to a final volume of 2 ml.
7. Add H_2O to a final volume of 2 ml.
8. Cap and vortex.
9. Aliquot into sterile 500-µL amber microcentrifuge tubes in 175-µL aliquots.
10. Store at -20° C.

1 MG/ML (1.46 MM) PEPSTATIN

1. Add 10 ml dimethylsulfoxide (Sigma D8479) to a 10 mg stock vial of pepstatin A (Sigma P5318).
2. Vortex.
3. Aliquot into sterile 1.5-ml microcentrifuge tubes.
4. Store at -20° C.

10 MG/ML (21 MM) LEUPEPTIN

1. Add 5 ml of H_2O to a 50 mg stock vial of leupeptin hemisulfate (Sigma L2884).
2. Cap and vortex.
3. Aliquot into sterile 500-µL amber microcentrifuge tubes in 120-µL aliquots.
4. Store at -20° C.

200 MM ACTIVATED Na_3VO_4

1. Add ~450 ml H_2O to a 1-L beaker with a stir bar.
2. Add 18.39 g sodium orthovanadate (Sigma S6508).
3. Spin 1 hour at room temperature.
4. Bring to final volume 500 ml using H_2O in a graduated cylinder.
5. Adjust the pH to 10.0 using either 1 N NaOH or 1 N HCl. The starting pH of the Na_3VO_4 solution may vary with different lots of the chemical. At pH 10.0, the solution will be yellow.
6. Boil the solution in the microwave until it turns colorless (~10 min).
7. Cool to room temperature.
8. Readjust the pH to 10.0 and repeat steps 3-4 until the solution remains colorless and the pH stabilizes at 10.0.
9. Aliquot into sterile 1.5-ml microcentrifuge tubes in 1-ml aliquots.
10. Store at -20° C.

50 MG/ML GLYCEROL-3-PHOSPHATE

1. Add 10 ml H_2O to a 15-ml conical tube.

2. Add 0.5 g of rac-glycerol-3-phosphate (Sigma G2138).
3. Vortex until completely dissolved.
4. Store in aliquots at -20º C.

50 MG/ML COENZYME A

1. Add 2 ml H_2O to a 15-ml conical tube.
2. Add 100 mg of coenzyme A hydrate (Sigma C4282).
3. Vortex until completely dissolved.
4. Store in aliquots at -20º C.

50 MG/ML ADENOSINE TRIPHOSPHATE

1. Add 2 ml H_2O to a 15-ml conical tube.
2. Add 0.1 g adenosine 5'-triphosphate (Sigma A2383).
3. Vortex until completely dissolved.
4. Store in aliquots at -20º C.

100 MM PALMITIC ACID

1. Add 10 ml ethanol to a 15-ml conical tube.
2. Add 0.2564 g of palmitic acid (Sigma P5585).
3. Vortex until completely dissolved.
4. Store in aliquots at -20º C.

1 M CYSTEINE

1. Add 10 ml H_2O to a 15-ml conical tube.
2. Add 1.21 g cysteine (Sigma C7352).

3. Vortex until completely dissolved.
4. Store in aliquots at -20º C.

ISOPROPANOL:HEPTANE:H_2O (80:20:2, V:V:V)

1. To a 1-L glass bottle, add:
    a. 800 ml isopropanol (Fisher A416).
    b. 200 ml heptane (Sigma 27051-2).
    c. 20 ml H_2O.
2. Cap and mix thoroughly.

[^{14}C] GLYCERYL TRIOLEATE

1. If needed, make 50 mg/ml glyceryl trioleate:
    a. Add 10 ml chloroform (EM Science 67-663) to a glass tube.
    b. Add 500 mg of glyceryl trioleate (Sigma T7140).
    c. Vortex until completely dissolved.
    d. Store in the dark at -20º C.
2. If needed, make 5 mg/ml glyceryl trioleate:
    a. To a 1.5-ml amber microcentrifuge tube, add:
        i. 900 µL chloroform.
        ii. 100 µL 50 mg/ml glyceryl trioleate.
    b. Vortex thoroughly.
    c. Store in the dark at -20º C.
3. To a 1.5-ml amber microcentrifuge tube, add:
    a. 1.176 ml chloroform.

b. 24 µL 5 mg/ml glyceryl trioleate.

c. Vortex thoroughly.

d. Add 1.8 µL of [^{14}C]glyceryl trioleate (American Radiolabeled Chemicals ARC-291).

e. Vortex thoroughly.

f. Final composition = 0.1 mg/ml glyceryl trioleate (1 nCi/µL)

4. Check the activity of the solution:

    a. Dry down triplicate 50-µL aliquots 2 hours at 35º C in the SpeedVac.

    b. Re-constitute the pellet in 100 µL of heptane (Sigma 27051-2).

    c. Add the heptane to a scintillation vial and count in the scintillation counter.

    d. Calculate the dpm/µL of chloroform in the 0.1 mg/ml solution (should be ~2,200 dpm/µL) for use in calculations of % recovery on the TLC plate.

1 N NaOH:ethanol:H_2O (5:50:45, v:v:v)

1. If needed, make 1 N NaOH:

    a. Add 400 ml H_2O to a beaker with a stir bar.

    b. Add 20.0 g NaOH (Fisher S318).

    c. Stir until completely dissolved.

    d. Bring to final volume 500 ml with H_2O.

    e. Store at room temperature.

2. To a 2-L glass bottle, add:
    a. 100 ml 1 N NaOH.
    b. 1 L ethanol.
    c. 900 ml H_2O.
3. Cap and mix thoroughly.

5 MG/ML GLYCERYL TRIPALMITATE

1. If needed, make 50 mg/ml glyceryl tripalmitate:
    a. Add 2 ml chloroform to a glass tube.
    b. Add 100 mg glyceryl tripalmitate (Sigma T5888).
    c. Vortex until completely dissolved.
    d. Store at -20º C.
2. To a 1.5-ml microcentrifuge tube, add:
    a. 900 µL chloroform.
    b. 100 µL glyceryl tripalmitate.
3. Store at -20º C.

HEXANE:ETHYL ETHER:GLACIAL ACETIC ACID (80:20:2, V:V:V)

1. CAUTION: All steps involving ether **must** be performed under a hood!
2. To a 2-L glass bottle, add:
    a. 1.6 L of hexane (Fisher H302).
    b. 400 ml ethyl ether (Fisher E134).
    c. 40 ml glacial acetic acid (Fisher A38).
3. Cap and mix thoroughly.

0.01% PRIMULIN IN ACETONE:H_2O (80:20, V:V)

1. Add 100 ml H_2O to a 500-ml glass bottle.
2. Add 0.01 g primulin (MP Biomedicals 8064-60-6, can be ordered through Fisher).
3. Cap and mix until completely dissolved.
4. Add 400 ml acetone (Fisher A924).
5. Cap and mix thoroughly.

Aprotinin solution may also be made instead of purchased from Sigma. Adjust added volumes appropriately for the reduced concentration:

150 µM (1 MG/ML) APROTININ

1. Add 1.026 ml H_2O to a 1 mg stock vial of aprotinin (Sigma A4529).
2. Vortex.
3. Aliquot into sterile 500-µL amber microcentrifuge tubes in 120-µL aliquots.
4. Store at -20° C.

GLYCEROL-3-PHOSPHATE ACYLTRANSFERASE ACTIVITY

Protocol

1. Preparation:
    a. Dilute at least 200 µg of sample protein in homogenization buffer to a concentration of 2 µg/µL.

b. Turn water bath on to 30º C.

c. Label 2 13 X 100 mm glass culture tubes (Fisher 14-961-27) per sample. One tube will be used for determination of GPAT activity in the absence of NEM (total activity); the other will be used for activity in the presence of NEM (mitochondrial GPAT activity. Microsomal activity is the difference between the total and mitochondrial.

d. Label 2 13 X 100 mm glass culture tubes per blank (usually three blanks for determination of background). One set of tubes is for no NEM, the other for with NEM, as explained in the previous step.

e. For each sample, label one 1.5-ml screw-cap microcentrifuge tube on the side of the tube.

f. Need 2 glass beakers (250 ml). Label “chl:MeOH 1:2” and “10% TCA”.

2. Place 2 µg protein/µL homogenized samples on ice.
3. Calculate volume of assay buffer needed (720 µL/sample + 3 ml). Hereafter, the volume needed will be referred to as “ABV” for “assay buffer volume”. NOTE: The calculations include two tubes for each sample (with and without NEM).
4. Transfer 888.89 µL/ml ABV of assay buffer stock solution to a 15-ml conical tube and leave at room temperature.
5. Place the following on ice:

    g. Glycerol-3-phosphate 50 mg/ml stock solution (G3P).

h. Palmitoyl coenzyme A 20 mM stock solution (PCoA).

i. Homogenization buffer (50 mM Tris-HCl, 225 mM sucrose, 1 mM EDTA·Na_4, pH 7.4, 1 mM benzamidine, 1 µg/ml pepstatin, 1 µg/ml leupeptin, 1 µg/ml aprotinin, 1 mM activated Na_3VO_4).

6. When sample is close to being completely thawed, place the tube of 20 mM palmitoyl coenzyme A at room temperature.

7. Prepare the assay buffer (final composition when added to sample = 75 mM Tris-HCl, 4 mM $MgCl_2$, 2 mg/ml free fatty acid-free BSA, 8 mM NaF, pH 7.4, 50 µM palmitoyl CoA, 300 µM glycerol-3-phosphate (5 µCi/ml), with or without 2 mM NEM). To the 15-ml conical tube containing the assay buffer stock solution, add:

   j. 2.150 µL/ml ABV of G3P.

   k. 3.086 µL/ml ABV of PCoA.

   l. 100.31 µL/ml ABV of H_2O.

   m. Return above stock solutions to freezer.

   n. 5.556 µL/ml ABV L-[2-^{3}H(N)]glycerol-3-phosphate (American Radiolabeled Chemicals ART-219).

   o. Vortex and leave solution at room temperature.

   p. Transfer approximately one-half of the buffer to a separate tube. The original tube should be labeled “no NEM”, the new tube should be labeled “2 mM NEM”.

   q. To the tube labeled “no NEM”, add 2.222 µl/ml ABV of ethanol.

r. To the tube labeled “2 mM NEM”, add 2.222 µl/ml ABV of 1 M NEM.

8. When sample is completely thawed, place one set of culture tubes on ice.
9. Add 40 µL (80 µg protein) of sample to the appropriate tube.
10. Add 40 µL of homogenization buffer to the “blank” tubes.
11. Return homogenization buffer to freezer.
12. Place tubes in a rack at room temperature.
13. At 10-second intervals:
    s. Add 360 µL of the prepared assay buffer, starting the timer immediately upon adding the buffer to the first sample. Make sure the appropriate buffer (with or without NEM) is added to the proper tube so that each sample is incubated in each buffer.
    t. Cap tubes.
    u. Vortex.
    v. Transfer tube to 30º C water bath.
14. Incubate the tubes for 15 minutes. During this time, turn on the Speed Vac.
15. During the last 5 minutes, remove the tube caps.
16. Pour chloroform:methanol (1:2, v:v) and 10% TCA into the appropriately labeled glass beakers.
17. Stop the enzymatic reactions by adding 3 ml of chloroform:methanol (1:2, v:v) and 600 µl of 10% TCA. Be sure to eject onto the side of the tube and not directly onto the sample, as the force will cause it to spray up. This

applies to addition of all other solutions as well. Transfer the tube to a rack at room temperature.

18. After 10 minutes, add 500 µl of chloroform and 500 µl of 10% TCA to each tube.
19. Cap the tubes.
20. Vortex each sample for 3 seconds.
21. Centrifuge at 450 *g* for 2 minutes (Program 8).
22. Remove caps.
23. Transfer the upper layer to an appropriately labeled bottle for used radioactive material.
24. Add 2 ml of 10% TCA.
25. Re-cap the tubes.
26. Vortex each sample for 3 seconds.
27. Centrifuge at 450 *g* for 2 minutes (Program 8).
28. Repeat steps 22-27 three more times for a total of 4 washes.
29. After the last spin, transfer 1 ml of the lower chloroform layer to the appropriately labeled 1.5-ml screw-cap microcentrifuge tube.
30. Evaporate 3 hours at 35° C in the SpeedVac.
31. While samples are drying:
    w. Using a dull pencil, mark the chromatography plates (Whatman 4866-820) at 8 cm and 16 cm from the point of origin. Label each lane above the mark.

x. Apply 5 µl of 5 mg/ml lysophosphatidic acid to each lane. (If needed, 5 µl of 5 mg/ml phosphatidic acid, diacylglycerol, and glyceryl tripalmitate may also be applied to each lane if it is necessary to identify these bands.)

32. Add 50 ml of chloroform:methanol:H_2O (65:25:4, v:v:v) to one chromatography developing tank and 50 ml of hexane:ethyl ether:glacial acetic acid (80:20:2, v:v:v) to the other tank. Place the lids on the tanks.
33. Re-constitute the samples in 10 µL chloroform/5% acetic acid.
34. With the pipette set at 15 µL, add sample to the appropriate lane on the chromatography plate.
35. Place the plate in the developing tank containing chloroform:methanol:H_2O (65:25:4, v:v:v), replace the lid, and develop to the 8 cm mark.
36. Remove plate and allow it to dry 5 minutes in the hood.
37. Place the plate in the developing tank containing hexane:ethyl ether:glacial acetic acid (80:20:2, v:v:v), replace the lid, and develop to the 16 cm mark.
38. Remove plate and allow it to dry 5 minutes in the hood.
39. Spray the plate with 0.01% primulin (w:v) in acetone:H_2O (80:20, v:v).
40. Allow to dry 10 minutes in the hood.
41. Mark the lysophosphatidic acid band under a UV light.
42. Scrape the marked area onto wax paper and empty into a scintillation vial.
43. Add 100 µL of the incubation medium in triplicate to a scintillation vial.

44. Add 5 ml of BioSafe II to each vial.
45. Cap the vials and shake vigorously.
46. Count in the scintillation counter, using Program 9. Subtract the average blank numbers (background) from the calculations.

Solutions

GPAT ACTIVITY ASSAY BUFFER STOCK SOLUTION

1. Add ~350 ml H_2O to a beaker with a stir bar.
2. Add 5.91 g Tris-HCl (Chempure 423-398).
3. Add 0.4066 g $MgCl_2 \cdot 6H_2O$ (Fisher BP214).
4. Add 0.1680 g NaF (Sigma S7290).
5. Add 1.25 g free fatty acid-free BSA (Sigma A7030).
6. Adjust pH to 7.4.
7. Bring final volume to 400 ml with H_2O.
8. Filter through a 0.22-µm filter into an autoclaved glass bottle.
9. Store at 4º C.

FAT HOMOGENIZATION BUFFER (50 MM TRIS-HCL, 225 MM SUCROSE, 1 MM EDTA·Na_4, PH 7.4, 1 MM BENZAMIDINE, 1 MG/ML PEPSTATIN, 1 MG/ML LEUPEPTIN, 1 MG/ML APROTININ, 1 MM ACTIVATED Na_3VO_4)

1. Add ~80 ml of H_2O to a glass beaker with a stir bar.
2. Add 0.788 g of Tris-HCl (Chempure 423-398).
3. Add 7.702 g of sucrose (Sigma S0389).
4. Add 200 µl of 500 mM EDTA·Na_4.

5. Adjust pH to 7.4.
6. Bring to final volume of 100 ml with H_2O in a graduated cylinder.
7. Filter through a 0.22-µm filter and store in an autoclaved glass bottle at 4º C.
8. Add fresh on day of use per ml of buffer:
    f. 1.49 µl of 0.67 M benzamidine.
    g. 2.0 µl of 1 mg/ml pepstatin.
    h. 0.2 µl of 10 mg/ml leupeptin.
    i. 1.25 µl of aprotinin (Sigma A6279, 1.6 mg/ml).
    j. 5 µl 200 mM activated Na_3VO_4.

500 mM EDTA·Na_4

1. If needed, make 100 ml of 1 M NaOH.
    p. Under a hood, add ~80 ml of H_2O to a 250-ml beaker with a stir bar.
    q. Add ~4 g sodium hydroxide (Fisher S318).
    r. Stir until completely dissolved.
    s. Bring to final volume 100 ml with H_2O in a graduated cylinder.
    t. Store in a glass bottle and room temperature.
2. Put ~7.5 ml 1 M NaOH in a 15-ml conical tube.
3. Add 2.081 g ethylenediaminetetraacetic acid tetrasodium dihydrate (Sigma ED4SS).
4. Cap and vortex until completely dissolved.
5. Bring to final volume 10 ml with H_2O in a graduated cylinder.

6. Pour into a 25-ml beaker.
7. Filter through a 0.22-µm filter into a sterile 15-ml conical tube.
8. Store at 4° C.

670 mM BENZAMIDINE

1. Weigh 0.2098 g of benzamidine hydrochloride hydrate (Sigma B6506) into a 2-ml microcentrifuge tube.
2. Add 1.5 ml of H_2O.
3. Cap and vortex.
4. Using a 2-ml pipette, draw up the solution and determine the volume.
5. Return solution to the tube.
6. Calculate the remaining volume needed to bring the solution to a final volume of 2 ml.
7. Add H_2O to a final volume of 2 ml.
8. Cap and vortex.
9. Aliquot into sterile 500-µL amber microcentrifuge tubes in 175-µL aliquots.
10. Store at -20° C.

1 MG/ML (1.46 MM) PEPSTATIN

1. Add 10 ml dimethylsulfoxide (Sigma D8479) to a 10 mg stock vial of pepstatin A (Sigma P5318).
2. Vortex.
3. Aliquot into sterile 1.5-ml microcentrifuge tubes.
4. Store at -20° C.

10 MG/ML (21 MM) LEUPEPTIN

1. Add 5 ml of H_2O to a 50 mg stock vial of leupeptin hemisulfate (Sigma L2884).
2. Cap and vortex.
3. Aliquot into sterile 500-µL amber microcentrifuge tubes in 120-µL aliquots.
4. Store at -20° C.

200 MM ACTIVATED Na_3VO_4

1. Add ~450 ml H_2O to a 1-L beaker with a stir bar.
2. Add 18.39 g sodium orthovanadate (Sigma S6508).
3. Spin 1 hour at room temperature.
4. Bring to final volume 500 ml using H_2O in a graduated cylinder.
5. Adjust the pH to 10.0 using either 1 N NaOH or 1 N HCl. The starting pH of the Na_3VO_4 solution may vary with different lots of the chemical. At pH 10.0, the solution will be yellow.
6. Boil the solution in the microwave until it turns colorless (~10 min).
7. Cool to room temperature.
8. Readjust the pH to 10.0 and repeat steps 3-4 until the solution remains colorless and the pH stabilizes at 10.0.
9. Aliquot into sterile 1.5-ml microcentrifuge tubes in 1-ml aliquots.
10. Store at -20° C.

50 MG/ML GLYCEROL-3-PHOSPHATE

1. Add 10 ml H_2O to a 15-ml conical tube.

2. Add 0.5 g of rac-glycerol-3-phosphate (Sigma G2138).
3. Vortex until completely dissolved.
4. Store in aliquots at -20º C.

20 mM PALMITOYL CoA

1. Make 0.01 M sodium acetate (pH 5.2):ethanol (1:1, v:v):
    a. To 20 ml of H_2O, add 83.3 µl of 3 M sodium acetate (Sigma 71196).
    b. Adjust pH to 5.2.
    c. Bring volume to 25 ml with H_2O.
    d. Add 25 ml of ethanol.
2. To a 5 mg vial of palmitoyl coenzyme A (Sigma P9716), add 248.5 µl of 0.01 M sodium acetate (pH 5.2):ethanol (1:1, v:v).
3. Vortex until completely dissolved.
4. Transfer to a 500-µl microcentrifuge tube and store at -20º C.

2 mM NEM

1. Add 10 ml of ethanol to a 15-ml conical tube wrapped in aluminum foil.
2. Add 1.25 g N-ethylmaleimide (Sigma E3876).
3. Vortex until completely dissolved.
4. Store in the dark at 4° C.

5 MG/ML LYSOPHOSPHATIDIC ACID

1. Make chloroform:methanol:H_2O (100:1.2:0.6, v:v:v): In a 50-ml conical tube, combine 50 ml of chloroform (Fisher), 600 µl of methanol, and 300 µl of H_2O, vortexing and shaking until thoroughly mixed.
2. Add 50 ml of chloroform:methanol:H_2O (100:1.2:0.6, v:v:v) to a 25-mg vial of 1-palmitoyl 2-hydroxy-sn-glycerol-3-phosphate sodium salt (Avanti Lipids 857123P).
3. Shake and vortex until thoroughly mixed.
4. Store in aliquots at -20° C.

5 MG/ML PHOSPHATIDIC ACID

1. To a 25 mg vial of 1,2-dipalmitoyl-sn-glycerol-3-phosphate sodium salt (Sigma P4013), add 50 ml of chloroform/5% acetic acid.
2. Shake and vortex until thoroughly mixed.
3. Store in aliquots at -20° C.

5 MG/ML DIACYLGLYCEROL

1. To a 10 mg vial of dioleoylglycerol (Sigma D0138), add 2 µl of chloroform.
2. Vortex until completely dissolved.
3. Transfer to a 15-ml conical tube and store at -20º C.

5 MG/ML GLYCERYL TRIPALMITATE

1. If needed, make 50 mg/ml glyceryl tripalmitate:
    a. Add 2 ml chloroform to a glass tube.

b. Add 100 mg glyceryl tripalmitate (Sigma T5888).

c. Vortex until completely dissolved.

d. Store at -20º C.

2. To a 1.5-ml microcentrifuge tube, add:

e. 900 µL chloroform.

f. 100 µL glyceryl tripalmitate.

3. Store at -20º C.

10% TCA

1. Dilute 100 ml of 100% trichloroacetic acid (Sigma 490-10) into 900 ml of H_2O in a glass bottle.

CHLOROFORM/5% ACETIC ACID

1. To a 100-ml glass bottle, add 95 ml chloroform and 5 ml of glacial acetic acid (Fisher A38).
2. Mix thoroughly.

CHLOROFORM:METHANOL:H_2O (65:25:4, V:V:V)

1. To a 2-L glass bottle, add:

a. 1.3 L of chloroform (Acros Organics 268320025, available through Fisher).

b. 500 ml of methanol (Fisher A454).

c. 8 ml of H_2O.

2. Cap and mix thoroughly.

HEXANE:ETHYL ETHER:GLACIAL ACETIC ACID (80:20:2, V:V:V)

1. CAUTION: All steps involving ether **must** be performed under a hood!
2. To a 2-L glass bottle, add:
    a. 1.6 L of hexane (Fisher H302).
    b. 400 ml ethyl ether (Fisher E134).
    c. 40 ml glacial acetic acid (Fisher A38).
3. Cap and mix thoroughly.

0.01% PRIMULIN IN ACETONE:H_2O (80:20, V:V)

1. Add 100 ml H_2O to a 500-ml glass bottle.
2. Add 0.01 g primulin (MP Biomedicals 8064-60-6, can be ordered through Fisher).
3. Cap and mix until completely dissolved.
4. Add 400 ml acetone (Fisher A924).
5. Cap and mix thoroughly.

Aprotinin solution may also be made instead of purchased from Sigma. Adjust added volumes appropriately for the reduced concentration:

150 µM (1 MG/ML) APROTININ

1. Add 1.026 ml H_2O to a 1 mg stock vial of aprotinin (Sigma A4529).
2. Vortex.
3. Aliquot into sterile 500-µL amber microcentrifuge tubes in 120-µL aliquots.
4. Store at -20° C.

DIACYLGLYCEROL ACYLTRANSFERASE ACTIVITY

Protocol

1. Preparation:
    y. Dilute sample protein in homogenization buffer to a concentration of 2 µg/µL.
    z. Turn water bath on to 37º C.
    aa. Label 4 13 X 100 mm glass culture tubes (Fisher 14-961-27) per sample.
    bb. Label 4 13 X 100 mm glass culture tubes per blank (usually three blanks for determination of background).
    cc. For each sample, label one 1.5-ml screw-cap microcentrifuge tube on the side of the tube.
    dd. Need 2 glass beakers (250 ml). Label "isoprop/heptane/H_2O" and "NaOH/EtOH/H_2O".
2. Place 2 µg protein/µL homogenized samples on ice.
3. Calculate volume of assay buffer needed (180 µL/sample + 1.3 ml). Hereafter, the volume needed will be referred to as "ABV" for "assay buffer volume".
4. Transfer 857 µL/ml ABV of assay buffer stock solution to a 15-ml conical tube and leave at room temperature.
5. Place the following on ice:
    ee. 20 mM palmitoyl CoA stock solution.

ff. Homogenization buffer (50 mM Tris-HCl, 225 mM sucrose, 1 mM EDTA·Na_4, pH 7.4, 1 mM benzamidine, 1 µg/ml pepstatin, 1 µg/ml leupeptin, 1 µg/ml aprotinin, 1 mM activated Na_3VO_4).

6. Dry down 24.8 µl/ml ABV diacylglycerol stock solution (5 mg/ml) 15 minutes in a SpeedVac. Re-constitute in the same volume of ethanol. Keep at room temperature.
7. When sample is close to being completely thawed, place the tube of palmitoyl CoA stock solution at room temperature.
8. Prepare the assay buffer (final composition when added to sample = 175 mM Tris-HCl, 8 mM $MgCl_2$, 1 mg/ml free fatty acid-free BSA, pH 8.0, 200 µM dioleoylglycerol, 30 mM palmitoyl coenzyme A (1 µCi/ml). To the 15-ml conical tube containing the assay buffer stock solution, add:
    gg. 1.8 µL/ml ABV of palmitoyl CoA.
    hh. 24.8 µL/ml ABV of diacylglycerol in ethanol.
    ii. 115.29 µL of H_2O.
    jj. 1.111 µL/ml [9,10-^{3}H]palmitoyl CoA (American Radiolabeled Chemicals ART-339).
    kk. Leave solution at room temperature.
9. When sample is completely thawed, place one set of culture tubes on ice.
10. Add 20 µL (40 µg protein) of sample to the appropriate tube.
11. Add 20 µL of homogenization buffer to the “blank” tubes.
12. Return homogenization buffer to freezer.
13. Place tubes in a rack at room temperature.

14. At 10-second intervals:

    ll. Add 180 µL of the prepared assay buffer, starting the timer immediately upon adding the buffer to the first sample.

    mm. Cap tubes.

    nn. Vortex.

    oo. Transfer tube to 37 º C water bath.

15. Incubate the tubes for 30 minutes. During this time, turn on the Speed Vac.

16. During the last 5 minutes, remove the tube caps.

17. Pour isopropanol:heptane:H_2O (80:20:2, v:v) into the appropriately labeled glass beaker.

18. Stop the enzymatic reactions by adding 1.5 ml (750 µL X 2) of isopropanol:heptane:H_2O (80:20:2, v:v). Be sure to eject onto the side of the tube and not directly onto the sample, as the force will cause it to spray up. This applies to addition of all other solutions as well. Transfer the tube to a rack at room temperature.

19. After 10 minutes, add 1 ml of heptane to each tube. After the heptane is added, it is no longer necessary to time each sample.

20. Add 500 µL H_2O to each tube.

21. Add 10 µL of [^{14}C] glyceryl trioleate (~0.001 µCi; 1 X 10^{-4} µCi/µL in 0.1 mg/ml solution in chloroform).

22. Cap the tubes.

23. Vortex each sample for 3 seconds.

24. Centrifuge at 450 *g* for 2 minutes (Program 8).
25. Remove caps.
26. Transfer the heptane layer to a new tube (1.3 ml; 650 µL X 2).
27. Pour 1 N NaOH:ethanol:H_2O (5:50:45, v:v) into the appropriately labeled glass beaker and draw solution into the repeat pipetter (set to 4 for 2-ml dispensing).
28. Add 2 ml of 1 N NaOH:ethanol:H_2O (5:50:45, v:v).
29. Re-cap the tubes.
30. Vortex each sample for 3 seconds.
31. Centrifuge at 450 *g* for 2 minutes (Program 8).
32. Remove caps.
33. Transfer the heptane layer to a new tube (1.0 ml).
34. Using the repeat pipetter, add 2 ml of 1 N NaOH:ethanol:H_2O (5:50:45, v:v).
35. Re-cap the tubes.
36. Vortex each sample for 3 seconds.
37. Centrifuge at 450 *g* for 2 minutes (Program 8).
38. Remove caps.
39. Transfer the heptane layer to a new tube (800 µL).
40. Using the repeat pipetter, add 2 ml of 1 N NaOH:ethanol:H_2O (5:50:45, v:v).
41. Re-cap the tubes.
42. Vortex each sample for 3 seconds.

43. Centrifuge at 450 *g* for 2 minutes (Program 8).
44. Transfer 600 µL of the heptane layer to the appropriately labeled 1.5-ml screw-cap microcentrifuge tube.
45. Dry down in the Speed Vac 30 minutes at 35º C.
46. While samples are drying:
    pp. Using a dull pencil, mark the chromatography plates at 7 cm from the point of origin. Label each lane above the mark. (Use of high performance-thin layer chromatography plates permits maximum separation and resolution of the samples; Whatman 4806-411.)
    qq. Apply 2 µL of 5 mg/ml glyceryl tripalmitate to each lane.
47. Add 50 ml of hexane:ethyl ether:glacial acetic acid (80:20:2, v:v:v) to the chromatography developing tank. Place the lid on the tank.
48. Re-constitute the sample in 10 µL chloroform.
49. With the pipette set at 12 µL, add sample to the appropriate lane on the chromatography plate.
50. Place the plate in the developing tank, replace the lid, and develop to the 7 cm mark.
51. Remove plate and allow it to dry 5 minutes in the hood.
52. Spray the plate with 0.01% primulin (w:v) in acetone:H_2O (80:20, v:v).
53. Allow to dry 10 minutes in the hood.
54. Mark the triglyceride band under a UV light.
55. Scrape the marked area onto wax paper and empty into a scintillation vial.
56. Add 100 µL of the incubation medium in triplicate to a scintillation vial.

57. Add 5 ml of BioSafe II to each vial.
58. Cap the vials and shake vigorously.
59. Count in the scintillation counter, using Program 8 for dual scintillation counting of ^{14}C and ^{3}H. Use ^{14}C to determine the % recovery of triacylglycerol on the TLC plate and use this in subsequent calculations. Subtract the average blank numbers (background) from the calculations.

Solutions

DIACYLGLYCEROL ACTIVITY ASSAY BUFFER STOCK SOLUTION

1. Add ~450 ml H_2O to a beaker with a stir bar.
2. Add 19.306 g Tris-HCl (Chempure 423-398).
3. Add 1.1385 g $MgCl_2 \cdot 6H_2O$ (Fisher BP214).
4. Add 0.700 g free fatty acid-free BSA (Sigma A7030).
5. Adjust pH to 8.0.
6. Bring final volume to 500 ml with H_2O.
7. Filter through a 0.22-µm filter into an autoclaved glass bottle.
8. Store at 4º C.

FAT HOMOGENIZATION BUFFER (50 MM TRIS-HCL, 225 MM SUCROSE, 1 MM EDTA·NA_4, PH 7.4, 1 MM BENZAMIDINE, 1 MG/ML PEPSTATIN, 1 MG/ML LEUPEPTIN, 1 MG/ML APROTININ, 1 MM ACTIVATED NA_3VO_4)

1. Add ~80 ml of H_2O to a glass beaker with a stir bar.
2. Add 0.788 g of Tris-HCl (Chempure 423-398).
3. Add 7.702 g of sucrose (Sigma S0389).

4. Add 200 µl of 500 mM EDTA·Na_4.
5. Adjust pH to 7.4.
6. Bring to final volume of 100 ml with H_2O in a graduated cylinder.
7. Filter through a 0.22-µm filter and store in an autoclaved glass bottle at 4° C.
8. Add fresh on day of use per ml of buffer:
    k. 1.49 µl of 0.67 M benzamidine.
    l. 2.0 µl of 1 mg/ml pepstatin.
    m. 0.2 µl of 10 mg/ml leupeptin.
    n. 1.25 µl of aprotinin (Sigma A6279, 1.6 mg/ml).
    o. 5 µl 200 mM activated Na_3VO_4.

500 mM EDTA·Na_4

1. If needed, make 100 ml of 1 M NaOH.
    u. Under a hood, add ~80 ml of H_2O to a 250-ml beaker with a stir bar.
    v. Add ~4 g sodium hydroxide (Fisher S318).
    w. Stir until completely dissolved.
    x. Bring to final volume 100 ml with H_2O in a graduated cylinder.
    y. Store in a glass bottle and room temperature.
2. Put ~7.5 ml 1 M NaOH in a 15-ml conical tube.
3. Add 2.081 g ethylenediaminetetraacetic acid tetrasodium dihydrate (Sigma ED4SS).
4. Cap and vortex until completely dissolved.

5. Bring to final volume 10 ml with H_2O in a graduated cylinder.
6. Pour into a 25-ml beaker.
7. Filter through a 0.22-µm filter into a sterile 15-ml conical tube.
8. Store at 4° C.

670 mM BENZAMIDINE

1. Weigh 0.2098 g of benzamidine hydrochloride hydrate (Sigma B6506) into a 2-ml microcentrifuge tube.
2. Add 1.5 ml of H_2O.
3. Cap and vortex.
4. Using a 2-ml pipette, draw up the solution and determine the volume.
5. Return solution to the tube.
6. Calculate the remaining volume needed to bring the solution to a final volume of 2 ml.
7. Add H_2O to a final volume of 2 ml.
8. Cap and vortex.
9. Aliquot into sterile 500-µL amber microcentrifuge tubes in 175-µL aliquots.
10. Store at -20° C.

1 MG/ML (1.46 MM) PEPSTATIN

1. Add 10 ml dimethylsulfoxide (Sigma D8479) to a 10 mg stock vial of pepstatin A (Sigma P5318).
2. Vortex.
3. Aliquot into sterile 1.5-ml microcentrifuge tubes.

4. Store at -20° C.

10 MG/ML (21 MM) LEUPEPTIN

1. Add 5 ml of H_2O to a 50 mg stock vial of leupeptin hemisulfate (Sigma L2884).
2. Cap and vortex.
3. Aliquot into sterile 500-µL amber microcentrifuge tubes in 120-µL aliquots.
4. Store at -20° C.

200 MM ACTIVATED Na_3VO_4

1. Add ~450 ml H_2O to a 1-L beaker with a stir bar.
2. Add 18.39 g sodium orthovanadate (Sigma S6508).
3. Spin 1 hour at room temperature.
4. Bring to final volume 500 ml using H_2O in a graduated cylinder.
5. Adjust the pH to 10.0 using either 1 N NaOH or 1 N HCl. The starting pH of the Na_3VO_4 solution may vary with different lots of the chemical. At pH 10.0, the solution will be yellow.
6. Boil the solution in the microwave until it turns colorless (~10 min).
7. Cool to room temperature.
8. Readjust the pH to 10.0 and repeat steps 3-4 until the solution remains colorless and the pH stabilizes at 10.0.
9. Aliquot into sterile 1.5-ml microcentrifuge tubes in 1-ml aliquots.
10. Store at -20° C.

20 mM palmitoyl CoA

1. Make 0.01 M sodium acetate (pH 5.2):ethanol (1:1, v:v):
    e. To 20 ml of H_2O, add 83.3 µl of 3 M sodium acetate (Sigma 71196).
    f. Adjust pH to 5.2.
    g. Bring volume to 25 ml with H_2O.
    h. Add 25 ml of ethanol.
2. To a 5 mg vial of palmitoyl coenzyme A (Sigma P9716), add 248.5 µl of 0.01 M sodium acetate (pH 5.2):ethanol (1:1, v:v).
3. Vortex until completely dissolved.
4. Transfer to a 500-µl microcentrifuge tube and store at -20º C.

5 mg/ml diacylglycerol

1. To a 10 mg vial of dioleoylglycerol (Sigma D0138), add 2 µl of chloroform .
2. Vortex until completely dissolved.
3. Transfer to a 15-ml conical tube and store at -20º C.

Isopropanol:heptane:H_2O (80:20:2, v:v:v)

1. To a 1-L glass bottle, add:
    a. 800 ml isopropanol (Fisher A416).
    b. 200 ml heptane (Sigma 27051-2).
    c. 20 ml H_2O.
2. Cap and mix thoroughly.

[^{14}C] GLYCERYL TRIOLEATE

1. If needed, make 50 mg/ml glyceryl trioleate:
    e. Add 10 ml chloroform (EM Science 67-663) to a glass tube.
    f. Add 500 mg of glyceryl trioleate (Sigma T7140).
    g. Vortex until completely dissolved.
    h. Store in the dark at -20º C.
2. If needed, make 5 mg/ml glyceryl trioleate:
    i. To a 1.5-ml amber microcentrifuge tube, add:
        i. 900 µL chloroform.
        ii. 100 µL 50 mg/ml glyceryl trioleate.
    j. Vortex thoroughly.
    k. Store in the dark at -20º C.
3. To a 1.5-ml amber microcentrifuge tube, add:
    l. 1.176 ml chloroform.
    m. 24 µL 5 mg/ml glyceryl trioleate.
    n. Vortex thoroughly.
    o. Add 1.8 µL of [^{14}C]glyceryl trioleate (American Radiolabeled Chemicals ARC-291).
    p. Vortex thoroughly.
    q. Final composition = 0.1 mg/ml glyceryl trioleate (1 nCi/µL)
4. Check the activity of the solution:
    r. Dry down triplicate 50-µL aliquots 2 hours at 35º C in the SpeedVac.

s. Re-constitute the pellet in 100 µL of heptane (Sigma 27051-2).

t. Add the heptane to a scintillation vial and count in the scintillation counter.

u. Calculate the dpm/µL of chloroform in the 0.1 mg/ml solution (should be ~2,200 dpm/µL) for use in calculations of % recovery on the TLC plate.

1 N NaOH:ethanol:H_2O (5:50:45, v:v:v)

1. If needed, make 1 N NaOH:
    a. Add 400 ml H_2O to a beaker with a stir bar.
    b. Add 20.0 g NaOH (Fisher S318).
    c. Stir until completely dissolved.
    d. Bring to final volume 500 ml with H_2O.
    e. Store at room temperature.
2. To a 2-L glass bottle, add:
    f. 100 ml 1 N NaOH.
    g. 1 L ethanol.
    h. 900 ml H_2O.
3. Cap and mix thoroughly.

5 mg/ml glyceryl tripalmitate

1. If needed, make 50 mg/ml glyceryl tripalmitate:
    g. Add 2 ml chloroform to a glass tube.
    h. Add 100 mg glyceryl tripalmitate (Sigma T5888).

i. Vortex until completely dissolved.

j. Store at -20º C.

2. To a 1.5-ml microcentrifuge tube, add:

k. 900 µL chloroform.

l. 100 µL glyceryl tripalmitate.

3. Store at -20º C.

HEXANE:ETHYL ETHER:GLACIAL ACETIC ACID (80:20:2, V:V:V)

1. CAUTION: All steps involving ether **must** be performed under a hood!
2. To a 2-L glass bottle, add:

d. 1.6 L of hexane (Fisher H302).

e. 400 ml ethyl ether (Fisher E134).

f. 40 ml glacial acetic acid (Fisher A38).

3. Cap and mix thoroughly.

0.01% PRIMULIN IN ACETONE:H_2O (80:20, V:V)

1. Add 100 ml H_2O to a 500-ml glass bottle.
2. Add 0.01 g primulin (MP Biomedicals 8064-60-6, can be ordered through Fisher).
3. Cap and mix until completely dissolved.
4. Add 400 ml acetone (Fisher A924).
5. Cap and mix thoroughly.

Aprotinin solution may also be made instead of purchased from Sigma. Adjust added volumes appropriately for the reduced concentration:

150 μM (1 MG/ML) APROTININ

1. Add 1.026 ml H_2O to a 1 mg stock vial of aprotinin (Sigma A4529).
2. Vortex.
3. Aliquot into sterile 500-μL amber microcentrifuge tubes in 120-μL aliquots.
4. Store at -20° C.

CONDITIONING MEDIA WITH ADIPOSE TISSUE FRAGMENTS

Protocol

1. Have ready:
    a. Sterile gauze.
    b. 15-ml sterile conical tubes, 2/sample.
    c. 5-ml syringes.
    d. 22-gauge, 1.5-inch syringe needles.
    e. Squares of 500-μm nylon mesh (Tetko 3-500/49), cut so they will fit over a 100-ml beaker, autoclaved.
    f. Autoclaved 100-ml glass beaker.
    g. 20-ml scintillation vials (1/sample; Fisher 03-337-23), autoclaved.
    h. #0 or #1 rubber stoppers, autoclaved.
2. Pre-heat KRHB/5 mM glucose to 37º C. Maintain the buffer at this temperature throughout the experiment.

3. Add 3 ml of KRHB/5 mM glucose to one of the 15-ml conical tubes for each sample. Keep tubes at 37º C.
4. Add 2 ml of KRHB/5 mM glucose to the 20-ml scintillation vial. Seal with a rubber stopper and keep at 37º C.
5. Place the 500-µm nylon mesh over the 100-ml beaker.
6. Extract fat pads from the anesthetized animal, rinse in sterile PBS (Gibco 14190-144) and blot on sterile gauze.
7. Using scissors, mince 250 mg of tissue into 1- to 3-mm fragments.
8. Add fragments to 15-ml conical containing the 3 ml of KRHB/5 mM glucose.
9. Wash 5 times for 5 minutes each by:
    a. Incubate the tube with light shaking in the horizontal position.
    b. Centrifuge at 100 *g* for 30 seconds.
    c. Using a 5-ml syringe with a 1.5-inch 22-gauge needle, aspirate the media from underneath the tissue fragments. The media can be disposed of into a bleach solution.
    d. Add 3 ml of fresh 37º C KRHB/5 mM glucose.
    e. Repeat.
10. After the last wash, do not aspirate the media. Instead, pour the contents of the tube over the piece of 500-µm nylon mesh so that the media goes into the beaker. The tissue fragments will be retained on the mesh.
11. Using forceps, scrape the fragments into the scintillation vial containing the 2 ml of KRHB/5 mM glucose. Seal with the same stopper.

12. Incubate for 20 hours in a 37º C shaking water bath at 30 rpm.
13. Carefully pour the contents of the vial into the remaining 15-ml conical tube and centrifuge at 100 *g* for 30 seconds.
14. Slowly aspirate the conditioned media from underneath the tissue fragments using a 5-ml syringe with a 1.5-inch 22-gauge needle.
15. Remove the needle and attach a 25-mm 0.22-µm syringe filter (Nalgene 190-2520, available through Fisher).
16. Filter the media into sterile 1.5-ml microcentrifuge tubes.
17. Store at -80º C.

Solutions

KREBS-RINGER-HEPES BUFFER STOCK I (10X)

1. To a 1-L beaker with a stir bar, add ~800 ml H_2O.
2. Add 75.97 g NaCl (EM Science SX0420-3).
3. Add 3.50 g KCl (Sigma P3911).
4. Add 1.63 g KH_2PO_4 (Sigma P0662).
5. Add 23.83 g HEPES (Sigma H4034).
6. Stir until completely dissolved.
7. Bring to final volume of 1 L with H_2O in a graduated cylinder.
8. Filter through a 022-µm filter into an autoclaved glass bottle.
9. Store at 4˚ C.

KREBS-RINGER-HEPES BUFFER STOCK II (10X)

1. To a 1-L beaker with a stir bar, add ~800 ml H_2O.
2. Add 1.47 g $CaCl_2 \cdot 2H_2O$ (Sigma C3881).
3. Add 2.96 g $MgSO_4 \cdot 7H_2O$ (Sigma M9397).
4. Stir until completely dissolved.
5. Bring to final volume of 1 L with H_2O in a graduated cylinder.
6. Filter through a 022-µm filter into an autoclaved glass bottle.
7. Store at 4˚ C.

KREBS-RINGER-HEPES BUFFER (KRHB: 130 MM NACL, 4.7 MM KCL, 1.2 MM KH_2PO_4, 1 MM $CaCl_2$, 1.2 MM $MgSO_4$, PH 7.4)/5 MM GLUCOSE

1. To an autoclaved beaker with a stir bar, add 800 ml of H_2O.
2. Add 100 ml of KRHB Stock I.
3. Add 100 ml of KRHB Stock II.
4. Add 0.901 g glucose (Sigma G7528).
5. Stir until completely dissolved.
6. Bring solution to 37º C in a water bath.
7. Adjust pH to 7.4.
8. Filter through a 0.22-µm filter into an autoclaved glass bottle.
9. Store at 4º C.

CONDITIONING MEDIA WITH MUSCLE

Protocol

1. Have ready (all items should be sterile if possible):
    a. 5 20-ml scintillation vials (Fisher 03-337-23) per sample, autoclaved.
    b. Sterile gauze.
    c. 3- and/or 5-ml syringes.
    d. 1.5-ml microcentrifuge tubes.
2. Prepare KHB (0.116 M NaCl, 4.6 mM KCl, 1.16 mM KH_2PO_4, 25.3 mM $NaHCO_3$, 2.5 mM $CaCl_2$, 1.16 mM $MgSO_4$, pH 7.4)/5 mM glucose/35 mM mannitol:
    a. NOTE: This must always be made fresh on the day of the experiment. Ca^{2+} and Mg^{2+} form insoluble carbonates at alkaline pH (i.e. at the pH of ungassed medium containing HCO_3^-). Thus the HCO_3^- is kept separate from the Ca^{2+} and Mg^{2+} before use.
    b. To the 500-ml glass bottle (33-mm neck) labeled “KHB”, add 400 ml H_2O. Add 50 ml 10X Krebs-Henseleit Buffer Stock I. Gas with 95% O_2/5% CO_2 at 4 psi under paraffin on ice for 20 minutes to equilibrate the pH. Add 50 ml 10X Krebs-Henseleit Buffer Stock II and gas for 10 more minutes. Check pH using standard pH paper (Sigma P3536); the pH should be ~7.0-7.2. (NOTE: pH will change to 7.4 after solution warms to 37˚ C.) After solutions have

been gassed, keep them on ice under paraffin as much as possible. Otherwise, CO_2 will exit the solution, pH will become alkaline, and insoluble carbonates will form.

c. Add 0.4505 g glucose (Sigma G7528) and 3.1885 g mannitol (Sigma M4125) and stir gently until dissolved.

d. Filter through a 0.22-µm filter into an autoclaved glass bottle.

e. Gas with 95% O_2/5% CO_2 for 30 minutes. Re-check the pH.

3. Isolate epitrochlearis or soleus muscle from anesthetized rat. Rinse in sterile PBS (Gibco 14190-144), then blot on sterile gauze. For the epitrochlearis, trim any extraneous tissue from the muscle, always handling the muscle very gently. For the soleus, split the muscle longitudinally by cutting into the proximal tendon with a scalpel and gently pulling apart to the distal end using forceps, then trim any extraneous tissue from the muscle.
4. Weigh the muscle and record the mass.
5. Wash the muscle 4 times for 10 minutes each in 5 ml of KHB/5 mM glucose/35 mM mannitol at 37º C under constant gas phase of 95% O_2/5% CO_2 in a shaking water bath at 30 rpm in sterile 20-ml scintillation vials.
6. Transfer the muscle to the last vial and incubate for 4 hours in 50 ml/g muscle KHB/5 mM glucose/35 mM mannitol at 37º C under constant gas phase of 95% O_2/5% CO_2 in a shaking water bath at 30 rpm in sterile 20-ml scintillation vials.

7. Remove the muscle and dispose of it.
8. Using a 3-ml (for epitrochlearis) or 5-ml syringe (for soleus), aspirate the conditioned media.
9. Filter the media through a 25-mm 0.22-µm syringe filter (Nalgene 190-2520, available through Fisher) into sterile 1.5-ml microcentrifuge tubes.
10. Store at -80º C.

Solutions

KREBS-HENSELEIT BUFFER STOCK I (10X):

1. In a 1-L beaker with a stir bar, add ~800 ml H_2O.
2. Add 67.79 g NaCl (EM Science SX0420-3).
3. Add 3.430 g KCl (Sigma P3911).
4. Add 1.578 g KH_2PO_4 (Sigma P0662).
5. Add 21.25 g $NaHCO_3$ (Sigma S7277).
6. Stir until dissolved.
7. Bring to pH to 7.4.
8. Bring final volume to 1 L in with H_2O in a graduated cylinder.
9. Filter through a 0.22-µm filter into an autoclaved glass bottle.
10. Store at 4˚ C.

KREBS-HENSELEIT BUFFER STOCK II (10X):

1. In a 1-L beaker with a stir bar, add ~800 ml H_2O.
2. Add 3.675 g $CaCl_2 \cdot 2H_2O$ (Sigma C3881).

3. Add 2.859 g $MgSO_4 \cdot 7H_2O$ (Sigma M9397).
4. Stir until dissolved.
5. Bring to pH to 7.4.
6. Bring final volume to 1 L in with H_2O in a graduated cylinder.
7. Filter through a 0.22-µm filter into an autoclaved glass bottle.
8. Store at 4˚ C.

LDH ACTIVITY (TYPE H)

Protocol

1. Have ready:
    a. 1 1-ml cuvette/sample + 1 for a blank, labeled.
    b. 1 conical tube.
    c. Calculate volume of sample needed for 50 µg of protein (for adipose tissue homogenates).
    d. Calculate volume of homogenization buffer needed to bring each sample to a final volume of 25 µL.
    e. Turn on the visible light on the spectrophotometer.
2. NOTE: Do 5 samples at a time. The same blank may be used repeatedly.
3. To each cuvette labeled for samples, add 50 µg of homogenate protein or 25 µL of conditioned media.

4. Add volume of homogenization buffer (50 mM Tris-HCl, 225 mM sucrose, 1 mM EDTA·Na_4, pH 7.4, 1 mM benzamidine, 1 µg/ml pepstatin, 1 µg/ml leupeptin, 1 µg/ml aprotinin, 1 mM activated Na_3VO_4) needed to bring each sample to a final volume of 25 µL.
5. Add 900 µL of HBS to the blank cuvette.
6. Add 25 µL of homogenization buffer to the blank cuvette.
7. Make assay buffer (HBS, 20 mM pyruvate, 30 µM NADH):
    a. To a conical tube, add 1 ml of HBS/sample.
    b. Add 10.16 µL of 2 M pyruvate/ml HBS.
    c. Add 6.096 µL of 5 mM NADH/ml HBS.
    d. Vortex thoroughly.
8. Add 900 µL of assay buffer to each sample cuvette.
9. Vortex all cuvettes.
10. Read the absorbance at 340 nm on the spectrophotometer over 4 minutes:
    a. Click on “Kinetics/Time”.
    b. Make sure the method is set to A:\LDH_ACT
    c. Make sure factor entered is:
        i. 3215.4 for adipose tissue homogenates (50 µg protein; using mM extinction coefficient for NADH of 6.22).
        ii. 1607.7 for adipocyte-conditioned media (25 µL).
    d. Place in sampler for spectrophotometer (the blank is always loaded in the first well).

e. Zero the blank.

f. Click on “Read Samples”. Samples will be read at 15-second intervals over the next 4 minutes. During this time, start to prepare the next samples. Print out the data when done, being sure to label the samples on the printout.

Solutions

FAT HOMOGENIZATION BUFFER

1. Add ~80 ml of H_2O to a glass beaker with a stir bar.
2. Add 0.788 g of Tris-HCl (Chempure 423-398).
3. Add 7.702 g of sucrose (Sigma S0389).
4. Add 200 µl of 500 mM EDTA·Na_4.
5. Adjust pH to 7.4.
6. Bring to final volume of 100 ml with H_2O in a graduated cylinder.
7. Filter through a 0.22-µm filter and store in an autoclaved glass bottle at 4º C.
8. Add fresh on day of use per ml of buffer:
    p. 1.49 µl of 0.67 M benzamidine.
    q. 2.0 µl of 1 mg/ml pepstatin.
    r. 0.2 µl of 10 mg/ml leupeptin.
    s. 1.25 µl of aprotinin (Sigma A6279, 1.6 mg/ml).
    t. 5 µl 200 mM activated Na_3VO_4.

10X HBS (HEPES-BUFFERED SALINE; 1X: 0.14 M NACL, 20 MM NA-HEPES, 2.5 MM $MgSO_4$, 1 MM $CaCl_2$, 5 MM KCL)

1. Add ~700 ml H_2O to a 1-L beaker containing a stir bar.
2. Weigh out and add each of the following:
    a. 81.816 g NaCl (sodium chloride, EM Science SX0420-3).
    b. 52.06 g Na-HEPES (HEPES sodium salt, Sigma H3784).
    c. 61.1625 g $MgSO_4 \cdot 7H_2O$ (magnesium sulfate heptahydrate, Sigma M9397).
    d. 1.47 g $CaCl_2 \cdot 2H_2O$ (calcium chloride dihydrate, Sigma C3881).
    e. 3.7275 g KCl (potassium chloride, P4504).
3. Stir until completely dissolved.
4. Bring to pH 7.4 with 12 N HCl (Fisher A-144S).
5. Bring to final volume 1 L in a graduated cylinder.
6. Filter through a 0.22-µm filter into two autoclaved 500-ml glass bottles.
7. Store at 4° C.

2 M SODIUM PYRUVATE

1. Put ~60 ml H_2O in a 150-ml beaker with a stir bar.
2. While stirring at a moderately high speed, add 22.0 g sodium pyruvate (pyruvic acid sodium salt; Sigma 15990).
3. Stir until completely dissolved.
4. Bring to final volume of 100 ml in a graduated cylinder.

5. Using a repeat pipetter, aliquot into sterile 500-µl microcentrifuge tubes in 400 µl aliquots.
6. Store at -20˚ C.

5 mM NADH

1. Make 0.01 M NaOH in HBS:
    a. Add 50 ml of HBS to a beaker with a stir bar.
    b. Add 0.5 g of NaOH (Fisher S318).
    c. Stir until completely dissolved.
2. To a 50 mg vial of β-nicotinamide adenine dinucleotide, reduced form (NADH, Sigma N8129), add 1.410 ml of 0.01M NaOH in HBS.
3. Cap and shake vigorously to dissolve.
4. Store in amber microcentrifuge tubes in single-use aliquots at -80º C.

LDH ACTIVITY (TYPE M)

Protocol

1. Have ready:
    g. 1 1-ml cuvette/sample + 1 for a blank, labeled.
    h. 1 conical tube.
    i. Calculate volume of sample needed for 50 µg of protein (for skeletal muscle homogenates).

j. Calculate volume of homogenization buffer (50 mM HEPES, pH 7.4, 4 mM EGTA, 10 mM EDTA, 15 mM $Na_4P_2O_7$, 100 mM β-glycerophosphate, 25 mM NaF, 5 mM activated Na_3VO_4, 1% Igepal CA630 and 50 µg/ml each of leupeptin, pepstatin, and aprotinin) needed to bring each sample to a final volume of 25 µL.

k. Turn on the visible light on the spectrophotometer.

2. NOTE: Do 5 samples at a time. The same blank may be used repeatedly.
3. To each cuvette labeled for samples, add 50 µg of homogenate protein or 25 µL of conditioned media.
4. Add volume of homogenization buffer needed to bring each sample to a final volume of 25 µL.
5. Add 900 µL of HBS to the blank cuvette.
6. Add 25 µL of homogenization buffer to the blank cuvette.
7. Make assay buffer (HBS; 20 mM lactate; 50 µM NAD^+):
    l. To a conical tube, add 1 ml of HBS/sample.
    m. Add 20.5 µL of 1 M lactate/ml HBS.
    n. Add 102.5 µL of 50 mM NAD^+/ml HBS.
    o. Vortex thoroughly.
8. Add 900 µL of assay buffer to each sample cuvette.
9. Vortex all cuvettes.
10. Read the absorbance at 340 nm on the spectrophotometer over 4 minutes:

p. Click on “Kinetics/Time”.

q. Make sure the method is set to A:\LDH_ACT

r. Make sure factor entered is:

   i. 3215.4 for skeletal muscle homogenates (50 µg protein; using mM extinction coefficient for NADH of 6.22).

   ii. 1607.7 for muscle-conditioned media (25 µL).

s. Place in sampler for spectrophotometer (the blank is always loaded in the first well).

t. Zero the blank.

u. Click on “Read Samples”. Samples will be read at 15-second intervals over the next 4 minutes. During this time, start to prepare the next samples. Print out the data when done, being sure to label the samples on the printout.

Solutions

MUSCLE HOMOGENIZATION BUFFER

See muscle homogenization protocol for the recipe. Protease inhibitors should be added fresh and the buffer then stored in aliquots at -20º C. Thaw on ice just prior to use.

10X HBS (HEPES-BUFFERED SALINE; 1X: 0.14 M NACL, 20 MM NA-HEPES, 2.5 MM $MgSO_4$, 1 MM $CaCl_2$, 5 MM KCL)

1. Add ~700 ml H_2O to a 1-L beaker containing a stir bar.
2. Weigh out and add each of the following:

a. 81.816 g NaCl (sodium chloride, EM Science SX0420-3).
b. 52.06 g Na-HEPES (HEPES sodium salt, Sigma H3784).
c. 61.1625 g $MgSO_4 \cdot 7H_2O$ (magnesium sulfate heptahydrate, Sigma M9397).
d. 1.47 g $CaCl_2 \cdot 2H_2O$ (calcium chloride dihydrate, Sigma C3881).
e. 3.7275 g KCl (potassium chloride, P4504).

3. Stir until completely dissolved.
4. Bring to pH 7.4 with 12 N HCl (Fisher A-144S).
5. Bring to final volume 1 L in a graduated cylinder.
6. Filter through a 0.22-µm filter into two autoclaved 500-ml glass bottles.
7. Store at 4° C.

1 M LACTATE

1. To a 1-g vial of lactic acid (Sigma L6402), add 11.1 ml of HBS.
2. Cap and vortex to dissolve.
3. Store in aliquots at -20° C.

50 MM NAD^+

1. Add ~50 ml of HBS to a beaker with a stir bar.
2. Adjust the pH to 5.0 with HCl (CAUTION: It does not take much!).
3. Add 7.537 ml of HBS, pH 5.0 to a 250-mg vial of β-nicotinamide dinucleotide (N1511).
4. Cap and vortex thoroughly.
5. Store in amber microcentrifuge tubes in single-use aliquots at -80º C.

PREPARATION OF PLASMA OR SERUM

1. Pre-cool the centrifuge to 4˚ C (Program #3 on Fisher Marathon 21000 R).
2. Pre-label 5 500-µl microcentrifuge tubes/sample with the sample number and the letter “P” for plasma or “S” for serum.
3. Using a 5-ml syringe fitted with a 22-gauge, 1-inch needle (Becton-Dickinson 309630, can be ordered from Fisher), extract as much blood as possible via a cardiac puncture to the left ventricle.
4. Keep on ice until able to centrifuge (no more than 30 minutes).
5. Remove the needle and distribute the blood equally between 2 plasma (green cap; Fisher 22-040-117) or serum (red cap; Fisher 22-040-153) gel tubes.
6. Spin down the blood at 1,500 *g* for 10 minutes at 4˚ C (Program #3 on Fisher Marathon 21000R).
7. Keep on ice until able to aliquot.
8. Using a P200 set to 200 µl, distribute the plasma or serum equally between the tubes.
9. Place tubes in -20˚ C freezer until all samples have been collected.
10. Transfer tubes to the -80˚ C freezer until analysis.

PLASMA TRIACYLGLYCEROL AND GLYCEROL

1. Prepare the reagents:

a. Free glycerol reagent: Re-constitute the free glycerol reagent (Sigma F6428) by adding 40 ml of H_2O to the vial, re-capping the vial, and inverting several times to mix. DO NOT VORTEX.
b. Triglyceride reagent: Re-constitute the triglyceride reagent (Sigma T2449) by adding 10 ml of H_2O to the vial, re-capping the vial, and inverting several times to mix. DO NOT VORTEX.
c. Both reagents should be stored in amber bottles at 4° C.

2. Turn on the spectrophotometer and set the wavelength to 540 nm.
3. Warm the free glycerol and triglyceride reagents to room temperature.
4. Label 1-ml cuvettes: 1 for a blank, 1 for a standard, and 1 per sample.
5. Pipette 800 µl of free glycerol reagent into each cuvette.
6. Add 10 µl of H_2O to the blank cuvette.
7. Add 10 µl of glycerol standard (2.5 mg/ml; Sigma G7793) to the standard cuvette.
8. Add 10 µl of plasma (may also use serum) to the appropriately labeled sample cuvette.
9. Cap each cuvette (available from Fisher 402364)
10. Mix by gentle inversion.
11. Incubate for 15 minutes at room temperature.
12. Zero the spectrophotometer using H_2O.
13. Measure the initial absorbance (IA) of each cuvette.
14. Add 200 µl of triglyceride reagent to each cuvette.

15. Mix each cuvette by gentle inversion (can place Parafilm over the top to invert).
16. Incubate for 15 minutes at room temperature.
17. Measure the final absorbance (FA) of each cuvette.
18. Calculate the total triacylglycerol concentration (in mM): $[(FA_{SAMPLE} - FA_{BLANK})/(FA_{STANDARD} - FA_{BLANK})] \times 2.5 \times 1.13$
19. Calculate the glycerol concentration (in mM): $[(IA_{SAMPLE} - IA_{BLANK})/(IA_{STANDARD} - IA_{BLANK})] \times 2.5 \times 1.13$
20. Calculate the true triacylglycerol concentration (in mM): $[(FA_{SAMPLE} - [IA_{SAMPLE} \times (0.81/1.01)])/(FA_{STANDARD} - [IA_{BLANK} \times (0.81/1.01)])] \times 2.5 \times 1.13$

PLASMA GLUCOSE

1. Re-constitute the glucose (HK) assay reagent (Sigma G3293) with 20 ml of H_2O. Mix several times by gentle inversion. Store at 4º C.
2. Turn on spectrophotometer and set the wavelength to 340 nm.
3. Label cuvettes (1 for reagent blank, and 2 for each sample: sample blank and sample).
4. Pipette 1 ml of the re-constituted glucose (HK) assay reagent into the reagent blank cuvette and each sample cuvette (but not the sample blanks).
5. Pipette 1 ml of H_2O into each sample blank cuvette.
6. Pipette 10 µL of each sample into each sample blank and sample cuvette.
7. Gently vortex to mix and incubate for 15 minutes at room temperature.

8. Zero the spectrophotometer with H_2O.
9. Read the cuvettes at 340 nm.
10. Calculations:
    a. $Abs_{total\ blank} = Abs_{sample\ blank} + Abs_{reagent\ blank}$
    b. $\Delta Abs = Abs_{sample} - Abs_{total\ blank}$
    c. Glucose concentration in mg/ml = [(ΔAbs)(TV)(Glucose molecular mass)]/[(ε)(d)(SV)(1000 μg/mg)]
    d. TV = total assay volume, or 1.01 ml
    e. Glucose molecular mass = 180.2 g/mole
    f. ε = millimolar extinction coefficient for NADH at 340 nm (6.22/mM/cm)
    g. d = cuvette light pat length = 1 cm

PLASMA FREE FATTY ACIDS

1. Procedure utilizes kit from Wako Chemicals (NEFA C).
2. Turn water bath on and set temperature to 37º C.
3. Turn on the spectrophotometer and set lightpath to 550 nm.
4. Label a series of glass test tubes as follows:
    a. Reagent blank = B.
    b. Standard = Std.
    c. Sample = Sample #.
    d. Sample blank = Sample # + “B”.
5. Pipette 25 μl of H_2O into the reagent blank tube.

6. Pipette 25 µl of 1 mM standard into the Std tube.
7. Pipette 25 µl of sample into each appropriately labeled sample tube. Do not pipette anything into the sample blank tube at this time.
8. Add 500 µl of Color Reagent A solution into all test tubes.
9. Gently vortex each tube and place in 37º water bath for 10 minutes.
10. Pipette 1 ml of Color Reagent B solution into all test tubes.
11. Pipette 25 µl of sample into each of the sample blank tubes.
12. Gently vortex and incubate for 10 minutes at 37º C in the water bath.
13. Remove the test tubes from the water bath and allow to sit at room temperature for 5 minutes.
14. While tubes are sitting at room temperature, pipette 1 ml from each tube into a cuvette.
15. Zero the spectrophotometer with H_2O.
16. At 5 minutes, read each cuvette at 550 nm on the spectrophotometer.
17. Calculations: Concentration (in mM) = $(Abs_{sample} – Abs_{sample\ blank})/Abs_{Std}$ X 1 mM

PLASMA INSULIN

1. Assay is based on a kit from Linco Research (SRI-13K)
2. Thaw all materials.
3. Label tubes numbered as follows: 1-2 total count tubes (TC), 3-4 non-specific binding (NSB), 5-6 total binding tubes (TB), 7-18 standards, 19-22 quality control, 23+ samples (best in duplicate).

4. Day 1:
    a. Pipette assay buffer into each tube in the following amounts:
        i. 1-2 none
        ii. 3-4 300 µl
        iii. 5-6 200 µl
        iv. All other tubes (7+) 100 µl
    b. Pipette 100 µl of each of the following into the appropriate tube:
        i. 0.02 ng/ml standard into 7-8
        ii. 0.05 ng/ml standard into 9-10
        iii. 0.1 ng/ml standard into 11-12
        iv. 0.2 ng/ml standard into 13-14
        v. 0.5 ng/ml standard into 15-16
        vi. 1.0 ng/ml standard into 17-18
        vii. QC1 into 19-20
        viii. QC2 into 21-22
    c. Pipette 10 µl of sample into the appropriately labeled tube (23+). Pipette 90 µl of assay buffer into each sample tube.
    d. Pipette 100 µl of Sensitive Rat Insulin antibody to all tubes except TC tubes (1-2) and NSB tubes (3-4).
    e. Vortex, cover with paraffin, and incubate 20-24 hours at 4º C.
5. Day 2:
    a. Re-constitute lyophilized ^{125}I-insulin with Label Hydrating Buffer and let it sit at room temperature for 30 minutes.

b. Add 100 µl of the re-constituted ^{125}I-insulin to all tubes.

c. Vortex, cover with paraffin, and incubate 20-24 hours at 4º C.

6. Day 3:

a. Add 1 ml of cold precipitating reagent to all tubes except TC tubes (1-2).

b. Vortex and incubate 20 minutes at 4º C.

c. Centrifuge at 3,000 *g* for 20 minutes at 4º C.

d. Decant tubes for 45 seconds.

e. While still holding tube upside-down, blot the remaining liquid from the lip of the tubes using a Kimwipe.

f. Count tubes in gamma counter.

VITA

David Kump was born February 24, 1967 in Twin Falls, Idaho to Mac and Anna Kump, and attended public schools in Idaho Falls, Idaho, where he graduated from Idaho Falls High School in 1985. After serving a two-year mission in Japan for The Church of Jesus Christ of Latter-Day Saints, he has earned the following degrees: Associates Degree in Arts and Sciences from Ricks College in Rexburg, Idaho (1989); B.A. in Japanese from Brigham Young University in Provo, Utah (1993); M.S. in exercise physiology from Benedictine University in Lisle, Illinois (1997); Ph.D. in physiology from the University of Missouri in Columbia, Missouri (2005). David worked for the Boeing Company in their health and fitness programs from 1996-1999. He married the former Jennifer Moss on June 17, 1994 in the Idaho Falls L.D.S. temple, and they are the parents of four children. He has accepted a postdoctoral position to study with Dr. Robert Kesterson in the Department of Genetics at the University of Alabama at Birmingham.